Energy and Sustainability Research Division, Faculty of Engineering

MICROWAVE PROCESSING OF VERMICULITE

OLAOSEBIKAN FOLORUNSO MSc

Thesis submitted to the University of Nottingham
for the degree of Doctor of Philosophy

20/03/2015

ABSTRACT

Vermiculite is a clay mineral that is generally used for a wide range of applications such as in agricultural, horticultural and construction industries. This is due to its various properties which include high porosity, lightweight, thermo-insulating, non-toxic and good absorption capacity when exfoliated. The objective of this research was to critically evaluate the fundamental interaction of electromagnetic waves with vermiculite from different source locations and to understand the mechanism of exfoliation in an applied microwave field. When vermiculite minerals are placed under the influence of high electric fields, they expand due to the rapid heating of their interlayer water, which subsequently builds up pressure that pushes apart the silicate structure. The degree of exfoliation is directly related to the intensity of the applied electric field. The principal areas covered in this thesis include: a detailed review of the fundamentals of microwave processing and issues surrounding scale up; a critical literature review of vermiculite mineralogy, and previous methods of vermiculite processing and their limitations; understanding the interaction of microwave energy with vermiculite by carrying out mineralogical and dielectric characterisation; microwave exfoliation tests of vermiculite minerals from different source locations and a comparative energy and life cycle analysis of microwave and conventional exfoliation of vermiculite.

A detailed review of the literature revealed that conventional exfoliation of vermiculite by gas or oil fuelled furnaces has significant limitations such as emissions of greenhouse gases, high-energy requirements (greater than 1 GJ/t), health and safety issues and poor process control. All work reported so far on microwave exfoliation of vermiculite has been limited to laboratory scale using domestic microwave ovens (2.45 GHz, power below 1200 W) and the route to scale up the process to industrial capacity has not given due consideration. Mineralogical characterisation of vermiculite from different geographical locations (Australia, Brazil, China and South Africa) revealed that only the sample from Brazil is a pure form of vermiculite while the other samples are predominantly hydrobiotite. All the samples have varying degrees of hydration with the Brazilian sample having the

highest total water content. The presence of water in any form in a material influences its dielectric response and ultimately the microwave absorbing properties. The dielectric characterisation carried out on the different vermiculite samples shows that the vermiculite mineral structure is effectively transparent to microwave energy, but it is possible to selectively heat microwave absorber, which is the interlayer water in the vermiculite structure.

The continuous microwave exfoliation tests carried out at both pilot scale at 53-126 kg/h and the scaled up system at 300-860 kg/h demonstrated that microwave energy can be used for the industrial exfoliation of vermiculite at high throughputs and is able to produce products below the specified product bulk densities standard required by The Vermiculite Association (TVA). The degree of vermiculite exfoliation depends on factors such as power density, feedstock throughput, energy input, interlayer water content, particle size of the feedstock, and vermiculite mineralogy. The highest degree of exfoliation was recorded for the Brazilian sample, which also had the highest water content.

Life cycle analysis (LCA) frameworks by the International Organisation for Standardisation (The ISO 14040: principles and framework and ISO 14044: Requirements and guidelines) and British standards institution (PAS2050) were used to carry out comparative life cycle analysis of vermiculite exfoliation using microwave heating and conventional (industrial and Torbed) heating systems. The results showed that the microwave system potentially can give an energy saving of about 80 % and 75 % over industrial and Torbed Exfoliators respectively, and a carbon footprint saving potential of about 66 % and 65 %. It can be concluded that the reduced dust emission and noise from the microwave system would improve the working conditions, health and safety.

Furthermore, the methodology discussed in this project can be used to understand the fundamental of microwave interaction with perlite and expanded clay, which are minerals with similar physical and chemical compositions as vermiculite.

ACKNOWLEDGEMENTS

I would like to express my sincere appreciation to my supervisors: Professor Sam Kingman, Dr Chris Dodds and Dr Juliano Katrib for their immense support, guidance and professional advice throughout the whole period of my study. My thanks also go to Dr Georgio Dimitrakis who carried out the design and simulations of the microwave cavity and choke systems.

I would like to acknowledge all the members of the National Centre for Industrial Microwave Processing that supported me during my study. Special thanks to Dr Andrew Batchelor, Dr Aled Jones, Dr Paula Palade and Dr Ofonime Udodo for their helpful support during my experimental work. This acknowledgement will not be complete without appreciating the University of Nottingham that gave me a scholarship for my PhD program.

I would also like to appreciate my parents and all my friends for the support given to me.

All Glory be to Almighty God

DEDICATION

I dedicate this thesis to my lovely wife, Adeola

TABLE OF CONTENTS

LIST OF FIGURES

LIST OF TABLES

LIST OF SYMBOLS

E electric field, Vm^{-1}

B magnetic field, Tesla

C_p specific heat capacity, J/kgK

d interatomic or d-spacing

D_p penetration depth of the wave (m)

EIO extended interaction oscillator

f frequency, Hz

c speed of light, m/s

J joules

MUT material under test

P_o polarisation

Q quality factor

Å angstrom, $1.0x10^{-10}$ m

TE transverse electric

TM transverse magnetic

TWT travelling wave tube

V_c volume of cavity (m^3)

V_s volume of sample (m^3)

VNA vector network analyser

P_v Power density (W)

Tan δ loss tangent

Greek Symbols

λ wavelength of the radiation (m)

ε* complex permittivity (F/m)

ε' dielectric constant (F/m)

ε'' loss factor

σ conductivity (S/m)

Θ diffraction angle

LIST OF PUBLICATIONS

1. FOLORUNSO, O., DODDS, C., DIMITRAKIS, G. & KINGMAN, S. 2012. Continuous energy efficient exfoliation of vermiculite through microwave heating. International Journal of Mineral Processing, 114–117**,** 69-79.

2. UDODO, O., FOLORUNSO, O., DODDS, C., KINGMAN, S., & URE, A. 2015. Understanding the Performance of a Pilot Vermiculite Exfoliation Systems through Process Mineralogy. Minerals Engineering.

3. Improving the Design of Industrial Microwave Processing Systems through Prediction of Complex Multilayer Materials (Submitted to the Journal of Material Science, January 2015

CHAPTER ONE
INTRODUCTION AND JUSTIFICATION FOR THE RESEARCH

1.1 Introduction

The world population has experienced dramatic increase from 1.6 billion in 1900 to over 7 billion in 2012 (Berck et al., 2012), and according to the United Nations, world population could reach 9.6 billion by 2050 (United Nations, 2013). Due to this explosion in the world population and enormous growth of industrialisation, there is an increase in the global demand for minerals. The high pressure on the demand for minerals to sustain the increasing population has led to higher production of most mineral commodities such as clay minerals, copper and aluminium (Wills and Napier-Munn, 2006, Richard C. Ferrero et al., 2013). Most mineral processing industries depend on energy from fossil fuel, which is expensive for their operations; and this negatively influences climatic change because the emission of greenhouse gases that lead to global warming (Hammond, 2004, Evans et al., 2009, McLellan et al., 2009).

Global warming and reduction of carbon emission is the world top priority for environmental management (IPCC, 2007). The focus of the United Nations climate change conferences held in Rio de Janeiro in 1992, Kyoto in 1997 and Bali climate change conference in 2007 were the design and implementation of industrial processing techniques, which are sustainable in terms of the three dimensions of sustainable development. These are environmental (reduction of carbon footprint and hazardous wastes), social (improvement of health and safety issues and improvement of process efficiency) and economic (reduction of energy consumption) (Carrera and Mack, 2010, McLellan et al., 2009). In order to implement a sustainable approach to mineral processing and also meet the increasing demand for minerals and mineral products at an affordable cost, the mining and the mineral processing industries are under increased pressure to reduce their energy consumption, improve the occupational health and safety, and finally reduce greenhouse gases emissions (Sterling, 2013, Norgate and Haque, 2010). These factors can only be achieved by shifting to a new concept of engineering

known as green engineering, in which health, safety, process efficiency and environmental issues are integral parts of the design. Thus, the focus of the mineral processing industries and that of research and development institutes has shifted to how to design processing systems that will reduce the amount and cost of energy consumed, processing time, space requirement, carbon footprint and also improve the health and safety of their workforce (McLellan et al., 2009, Kirchhoff, 2003).

Vermiculite is the name of a group of 2.1 phyllosilicates, which contain layers of water molecules within their internal structure (Walker, 1961, Grim, 1968). Vermiculite has been widely exploited for over 50 years in the expanded form for use in horticulture and agriculture, construction, insulation and as an asbestos substitute (Bergaya et al., 2006, Muiambo et al., 2010). Vermiculite exfoliation or expansion occurs when the interlayer water molecules within the structure are transformed into steam when heated to a very high temperature between 870-1100 °C, followed by the mechanical separation of the silicate layers (Hillier et al., 2013, Marcos and Rodríguez, 2010b). Chemical and conventional thermal exfoliation techniques are the two prominent exfoliation methodologies. The chemical exfoliation method, which uses chemicals such as H_2O_2, weak acids and some electrolytes is limited to laboratory research work and there are no reports of such techniques being used for exfoliation on a commercial scale (Obut and Girgin, 2002, Erol Ucgul and Girgin, 2002).

The thermal conventional exfoliation of vermiculite is usually carried out by gas or oil fuelled furnaces and the process requires a significant amount of energy often greater than 1 GJ/t (Andronova, 2007, Torbed Service Limited., 1997) due to its low thermal capacity. In addition to the high energy requirement, other challenges of this exfoliation technique are large over reliance on fossil fuel, emission of greenhouse gases, large space requirements, and emissions of dust and particulate matter (PM<10μm) and poor process control (Strand and Stewart, 1983, Marinshaw, 1995). Due to the sustainability challenges of conventional thermal exfoliation techniques in terms of energy consumption, environmental impact and occupational health and safety issues, designing a more sustainable methodology

for vermiculite exfoliation is vital to the future competitiveness of the vermiculite processing industry. In addition to the improvements in occupational health and safety (OHS), the introduction of green engineering for the processing of vermiculite will maximise the energy savings, process efficiency and profitability, and reduces ultimate environmental impact.

Microwave heating utilises the interaction of electromagnetic energy with the material for selective heating of the microwave absorbing component(s), which may be polar, ionic or electronic features within the material matrix. In this technique the microwave energy is transported as electromagnetic waves of a certain frequency range (normally between 300MHz to 300GHz) to bring about selective and volumetric heating (Schubert and Regier, 2005, Meredith, 1998). This heating technique is attracting much interest for industrial processing of a wide variety of materials such as food and agricultural products (Datta and Anantheswaran, 2001, Shaheen et al., 2012), electronic devices (Vaidhyanathan et al., 2010a, Vaidhyanathan et al., 2010b, Qi et al., 2013), ceramic and composite materials (Huanga et al., 2009, Sutton, 1992), copper ore (Mondal et al., 2009, Vorster et al., 2001) and polymers (Lewis et al., 1988). It has also been used for the remediation of contaminated soil, waste treatment (Robinson et al., 2012, Robinson et al., 2009, Robinson et al., 2010), ore grinding (Kingman et al., 2000) and treatment of coal (Sahoo et al., 2011). This is due to its various advantages over conventional heating, which depend upon conduction, radiation and convection for heat transfer. Key advantages of microwave processes are claimed to include reduced processing time and emission of greenhouse gases, improved process control and the product quality (Clark et al., 2000, Jones et al., 2002, Kingman and Rowson, 1998).

Microwave heating has been used by some researchers to investigate vermiculite exfoliation, due to the presence of interlayer water in vermiculite structure (Zhao et al., 2010, Marcos and Rodríguez, 2010a). Most of these previous studies used domestic microwave ovens (2.45 GHz, power below 1200 W), which produce heterogeneous distribution of electric field, uneven heating of the feedstock due to the creation of multiple hotspots and low power density (Meredith, 1998). Few

attempts have ever been made to scale up microwave processing of vermiculite, this may be due to the little understanding about the interaction of microwave energy with such minerals, and few concepts are developed to process materials at large scale.

The principal aim of this work is to critically investigate the fundamental interaction of electromagnetic waves with vermiculite from different source locations and understand the mechanism of microwave exfoliation. This work will also present the design and quantify the operational performance of an energy-efficient microwave system for vermiculite exfoliation. Specific objectives to be achieved by the research include:

1. To understand the fundamental interaction of microwave energy with vermiculite from different source locations. The factors that influence the degree of vermiculite exfoliation will also be investigated.
2. To understand the relationship between the chemical composition of vermiculite and microwave induced exfoliation. The mineralogical characterisation of the different vermiculite samples will be carried out in order to achieve this objective.
3. To carry out comparative energy assessments and life cycle analysis (LCA) of conventional and microwave exfoliation techniques using LCA protocols designed by the International Organisation for Standardization (ISO 14040 and ISO 14044) and the British Standard Institution (PA 2050). This will give a quantitative assessment of the environmental performance of both conventional and microwave exfoliation techniques and will also give an understanding of the major hotspots of carbon emission in each process for system improvement.

1.2 Thesis Outline

This thesis is structured into eight chapters. This introductory chapter is followed by Chapter 2, which presents a critical literature survey on vermiculite mineralogy, applications of vermiculite and methods of vermiculite exfoliation. The fundamentals of microwave heating and the issues around its safe use are presented

in Chapter 3. In Chapter 3, the dielectric property measurement techniques used in this work are discussed and the factors affecting scale up of microwave heating of mineral reviewed. In Chapter 4, the experimental results of an in-depth mineralogical study and the results of the measurement of the dielectric properties of vermiculite using both cavity perturbation and waveguide techniques are presented and discussed. Also discussed in Chapter 4 is the relationship between the dielectric properties of milled vermiculite and bulk density. In addition, Chapter 4 also presents the prediction of the dielectric properties of solid vermiculite from that of its pulverised sample using mixing rules. The methodologies used in designing the pilot scale and the scale up of the microwave exfoliator systems are discussed in Chapter 5 and the performances of these systems for different feedstock is presented. A comparative energy and carbon footprint analysis of conventional and microwave exfoliation of vermiculite was carried out and discussed in Chapter 6. Finally, Chapter 7 gives a summary of the findings obtained in this research and the future work required.

CHAPTER TWO
INTRODUCTION TO VERMICULITE AND ITS PROCESSING

2.1 Introduction

Vermiculite is the name of a group of 2.1 phyllosilicate minerals composed of hydrated magnesium-aluminium-iron sheet silicates, which contain water molecules within their layered structure (Walker, 1961, Grim, 1968). They are made of one octahedral sheet lies in between two tetrahedral sheets (Velde, 1992). When heated rapidly to between 870 and 1100 °C, the interlayer water is turned to steam and the pressure generated within the structure disrupts the vermiculite silicate layer by a process known as exfoliation (Obut and Girgin, 2002, Marcos and Rodríguez, 2010a). Because of this process, its volume expands to more than eight times that of the unprocessed crude (Justo et al., 1989, Basset, 1963). Exfoliated vermiculite is lightweight with thermo-insulating properties. It is also highly porous, insoluble in water and organic solvent, non-toxic and has good absorption properties (Suquet et al., 1991, Mysore et al., 2005). These physical properties enable its use across a wide range of applications (Muiambo et al., 2010, Mouzdahir et al., 2009, Bergaya et al., 2006).

Due to its poor transfer of thermal energy, vermiculite has a low specific heat capacity and therefore requires a significant amount of energy (greater than 1GJ/t) for its exfoliation (Torbed Service Limited., 1997, Andronova, 2007). The high-energy requirement for its exfoliation using either rotary or vertical furnaces fuelled by oil or natural gas is one of the problems limiting the industrial processing of vermiculite using conventional thermal methodology. Apart from the high consumption, other limitations of the of the conventional method of exfoliation are large space requirements, emission of hazardous gases such as carbon monoxide (CO); carbon dioxide (CO_2); oxides of nitrogen (NO_X) and oxides of sulphur (SO_X), massive emissions of dust and particulate matter (PM < 10 μm), poor process control, and over reliance on fossil fuels. The products also come out at very high temperature (700 °C) and take several hours to cool down. This slows down the marketing and distribution process (Strand and Stewart, 1983, Marinshaw, 1995).

Therefore, this is a process with several challenges and opportunities for improvement.

2.1.1 Vermiculite Characterisation and Physical Properties

Raw vermiculite is characterised into five different grades (micron, superfine, fine, medium and large grades) according to their different particle sizes range. The different grades and the associated particle size and bulk density of raw vermiculite are given in the Table 2-1. It shows that the size of all the vermiculite grades range from 0.250 to 8.00 mm while the loose bulk density varies between 700-1050 mm.

Table 2-1: The different raw vermiculite grades, particle size distribution and bulk density for Palabora vermiculite (Palabora Europe., 2009, The Vermiculite Association, 2011)

Grade	Raw vermiculite		Exfoliated vermiculite	
	Particle size distribution (mm)	Loose bulk density (kg/m^3)	Product bulk density (kg/m^3)	Specific surface area (m^2/g)
Micron	0.250-0.710	700-850	90-160	6.4
Superfine	0.355-1.000	800-950	80-144	5.4
Fine	0.710-2.000	850-1050	75-112	4.4
Medium	1.40-4.00	850-1050	72-90	4.0
Large	2.80-8.00	850-1050	64-85	3.8

Also given in Table 2-1 is The Vermiculite Association (TVA) standard for bulk density and specific surface area of exfoliated vermiculite (The Vermiculite Association, 2011). The TVA is the international vermiculite industry trade association and therefore set the industry standards. Vermiculite processing plants aim to produce an exfoliated vermiculite product with a bulk density within the TVA standard and any exfoliated product outside this density ranges may not be commercially acceptable for industrial applications. The lower the bulk density, the better the quality of exfoliated vermiculite product because most of the applications of vermiculite rely on this property (The Vermiculite Association, 2011). Other typical physical properties of vermiculite are fusion point of between 1200 °C to 1320 °C and sintering temperature between 1150 °C to 1250 °C.

2.1.2 Applications of Raw and Exfoliated Vermiculite

Raw vermiculite has only limited applications such as, for circulation in drilling mud, fillers for fire-resistant wallboard and in the annealing of steel. Thus, the markets for un-exfoliated vermiculite are limited (Strand and Stewart, 1983). Figure 2-1 shows the raw and exfoliate form of medium grade vermiculite obtained from Brazil.

Figure 2-1: The raw and exfoliated form of medium grade of Brazilian vermiculite

The bulk density of the processed crude vermiculite reduced from the range of 640 to 1120 kg/m^3 to the range of 64 to 160 kg/m^3 when exfoliated, depending on the retention time in the furnace, furnace temperature and the furnace efficiency. Mineralogy and the degree of alteration of the parent biotite and phlogopite also influence the degree of exfoliation (Kogel et al., 2006, Justo et al., 1989). The resulting lightweight material has low density, is chemically inert and has a highly porous structure together with exceptional thermal, acoustic, adsorbent and fire resistant properties (Marcos et al., 2009, Muiambo et al., 2010, The Vermiculite Association, 2011, Obut and Girgin, 2002). These properties make vermiculite suitable to be widely used for various industrial applications, such as in the construction, agriculture, horticulture, medicine and cosmetic industries (Muiambo et al., 2010, The Vermiculite Association, 2011, Bergaya et al., 2006).

Table 2-2 highlights the main industrial applications of exfoliated vermiculite. For agricultural and horticultural purposes, it is used as a medium for improving soil

aeration and moisture retention. It is also used for animal feedstuffs, and as a carrier in fertilizer for soil conditioning, herbicides and insecticide (The Vermiculite Association, 2011, Marwa et al., 2009).

Table 2-2: Various uses of vermiculite (Chemical Mine World., 2004)

Industrial	Absorbent packing	**Horticultural**	Blocking mixes
	Brake pads/ brake shoes		Sowing composts
	Drilling mud		Seed germination
	Fire proof safes		Potting mixes
	Furnaces		Seed wedge mix
	Paints		Micro propagation
	Insulation (high and low temperature)		Twin scaling bulbs
Agricultural	Animal feed	**Construction**	Acoustic finishes
	Anti-caking material		Air setting binder
	Bulking agent		Gypsum plaster
	Pesticide		Floor and roof screed
	Soil conditioner		Board
	Fertilizer		Loft insulation

In construction and lightweight aggregate applications, vermiculite is used for lightweight concrete and screeds, building boards, fireproof plaster boards, and refractory board (The Vermiculite Association, 2011, Mackinnon et al., 1989). Cementing mixture of exfoliated vermiculite and binders, such as gypsum and plasters, are also applied as structural steel members in building construction (Government of India, 2012). For applications as an insulating material, exfoliated vermiculite is used for loose fill insulation, fire protection, and refractory and high temperature insulation (tanner, 2013). Other applications of exfoliated vermiculite include, recovery of metallic ions from water and as an absorbent medium for water purification (Seaborn and Jameson, 1976, Malandrino et al., 2006, Giacomino et al.,

2010). Finer grades of exfoliated vermiculite are used for brake lining and brake pad in automobile industry and also as swimming pool liners (The Vermiculite Association, 2011).

2.1.3 Vermiculite Structure and Chemical Composition

Vermiculite minerals are formed through the hydration of either biotite or phlogopite under the influence of weathering or hydrothermal alteration (Basset, 1963, Grim, 1968). This process involves the alteration of the parent biotite or phlogopite by the reaction of hydrothermal fluid (mostly hot water). During this process of vermiculite formation from mica minerals (biotite and phlogopite), which are bound together by strong assemblage of bonds and have low moisture content, there is a slight rearrangement of the atoms (cationic exchange) within the crystal lattice layers followed by the introduction of water molecules into the interlayer space (Bergaya et al., 2006). The interlayer potassium ions (K^+) of the parent mica are replaced by other cations such as Mg^{2+}, or combination of Mg^{2+} and Ca^{2+} ions. Vermiculite produced from this process has hydrated interlayer space and is bound together by a weak Van der Walls bonds. The weaker bond and presence of water in vermiculite interlayer space causes its ability to swell and exfoliate. Following is the general molecular formula for trioctahedral vermiculite (Grim, 1968, Bergaya et al., 2006, Deer et al., 1966).

$$(OH)_4(Mg.Ca)_X(Si_{8-X}.Al_X)(Mg.Fe)_6O_{20}.yH_2O$$

The atoms in the second parenthesis represent an exchangeable interlayer cation surrounded by water molecules, the third parenthesis denotes the tetrahedral layer while the atoms in the fourth parenthesis correspond to the octahedral layer cations (Bergaya et al., 2006, Velde, 1992). Figure 2-2 represents the vermiculite structural diagram with the octahedral, tetrahedral and the hydrated interlayer cations. The interlayer space is occupied by hydrated interlayer cations, which are magnesium when there is a complete vermiculite formation. The degree of hydration and type of interlayer cations has a significant impact on its physical and chemical behaviour, and therefore affects its exfoliation property and applications.

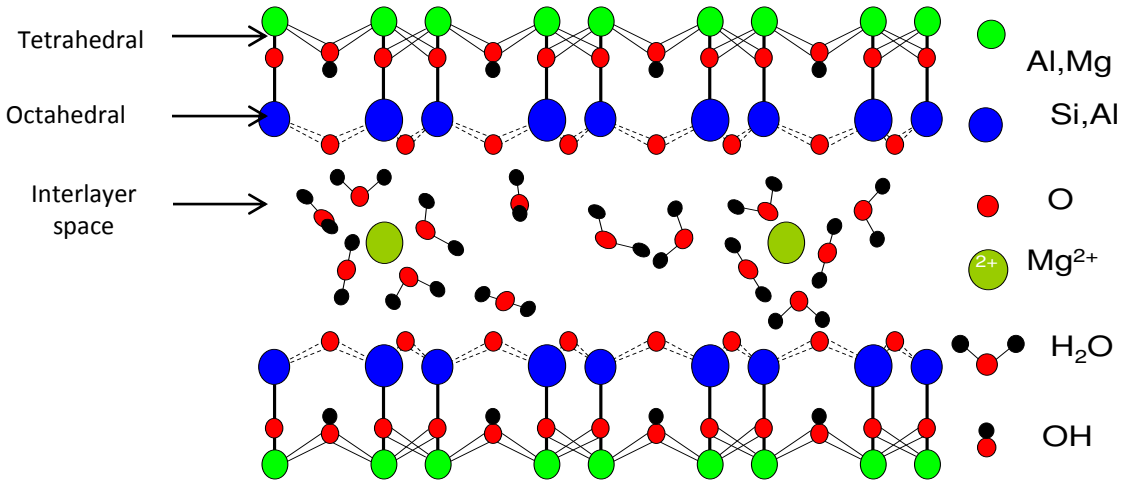

Figure 2-2: The vermiculite structural diagram. Adapted from (Reeves et al., 2006)

Numerous researchers have worked on the analysis of chemical composition of vermiculite from different mine locations, by using different analysis techniques such as, atomic absorption spectroscopy (Justo et al., 1989), electron microprobe (Marcos et al., 2009, Marcos and Rodríguez, 2010b, Harraz and Hamdy, 2010, Marcos et al., 2003), and X-ray fluorescence analysis (Obut and Girgin, 2002, Mouzdahir et al., 2009, Obut et al., 2003). Chemical composition analyses carried out by various authors on vermiculite minerals from different geological mine locations are shown in Table 2-3.

Table 2-3: Chemical composition of vermiculite from various mines

Source	SiO_2	TiO	Al_2O_3	Cr_2O_3	Fe_2O_3	FeO	MnO	MgO	NiO	CaO	Na_2O	K_2O
Madagascar[1]	44.50	0.69	14.70		2.69	-	0.07	33.7	-	-	-	-
Colombia[2]	45.40	0.73	13.06	-	6.91	1.24	0.11	24.1	-	2.88	0.26	0.6
Palabora [3]	38.00	1.12	9.46	-	2.94	-	-	27.9	-	0.74	-	4.42
Piaui, Brazil[4]	39.94	1.13	9.27	0.06	-	6.69	0.04	25.48	0.02	0.2	0.04	3.54
Goias Brazil[4]	40.67	0.79	11.51	0.01	-	9.58	0.08	18.05	0.01	0.03	0.12	1.07
China West[4]	43.22	1.01	11.87	0.16	-	4.28	0.01	24.27	0.04	0.4	0.71	7.48
China East[4]	36.61	1.16	13.91	0.03	-	14.29	0.12	14.75	0.06	1.17	0.6	6.49
Egypt[5]	39.15	1.21	12.20	0.25	1.54	8.36	-	22.06	-	0.53	-	10.3

[1]:(Graf et al., 1994), [2]:(Campos et al., 2009), [3]:(Obut and Girgin, 2002), [4]:(Marcos et al., 2009), [5]:(Harraz and Hamdy, 2010),

The results show similar chemical compositions in the different samples tested, but in different proportions. The variation in the quantity of different chemical compositions of vermiculite from different geological areas may be due to different modes of formation, parent mica and degree of alteration. The presence of high K_2O and low MgO contents in some samples suggests the possibility of having a mixed layer of mica-vermiculite due to an incomplete vermiculite formation alteration process since pure vermiculite has little or no potassium ion (Justo et al., 1989, Bergaya et al., 2006). There is a possibility that they are hydrobiotite or hydrophlogopite, which are intermediate products of the vermiculite formation process (Gruner, 1934b, Ruthruff, 1967).

2.1.4 Interstratification in Vermiculite

The extensive work by Weaver (1956) on 6000 clay mineral samples revealed that about 70% of the samples are mixed–layered or have interstratification of two or more different clay minerals and are therefore not pure vermiculite. Interstratified phyllosilicates are clay mineral compositions made up of two or more different components stacked together along the unit cell (Grim, 1968, Bergaya et al., 2006, Essington, 2004). The interstratification may be regular or irregular. In regular stratification, the stacking of two or more clay minerals follows a regular or periodic repetition (example: chlorite-vermiculite) while the stacking is not well ordered in irregular stratification (example: illite-chlorite). There is possibility that mixed layer interstratifications of clay minerals may have significant importance on its applications and engineering processing because this has a significant influence on its structure and physical properties, such as layer charge, moisture content and exfoliation property (Bergaya et al., 2006, Grim, 1968).

Generally, minerals such as, hydrobiotite and hydrophlogopite that expand when heated or treated with chemical such as H_2O_2 and NH_4Cl are collectively grouped as vermiculite minerals (Walker, 1961, Justo et al., 1989). They are not pure vermiculite but rather mixed-layer interstratification of mica-vermiculite, due to the incomplete process of vermiculite formation (Muiambo et al., 2010, Marcos and Rodríguez, 2010b, Grim, 1968, Basset, 1963, Schoeman, 1989). It is possible the

name vermiculite was adopted for these minerals probably for commercial reasons, since they all possess exfoliation characteristics that give vermiculite its high economic value compared to other non-expendable clay minerals. However, there is tendency that these minerals will behave differently during exfoliation compared to pure vermiculite, due to different structural, physical and chemical compositions (Justo et al., 1989, Muiambo et al., 2010).

Gruner (1934a), used X-ray diffraction data and chemical composition to characterise twelve vermiculite specimens. Only seven of the twelve specimens showed X-ray diffraction peaks the same as pure vermiculite and the remaining samples were classified as hydrobiotite. It was reported that upon heating to 750°C, appreciable exfoliation was only observed in the specimens classified as hydrobiotite. No explanation was given by the author for the higher degree of exfoliation in hydrobiotite compared to pure vermiculite but it may be due to the exfoliation mechanism and the vermiculite structure.

Midgley and Midgley (1960) studied sixteen commercial vermiculite samples to understand the mineralogy of commercially exfoliable minerals. Their findings showed that six samples closest to pure vermiculite were identified as mixed layer vermiculite-chlorite minerals, while two samples were pure hydrobiotite and remaining were mixed layer of vermiculite-hydrobiotite. Similar to the work of Gruner (1934a), the expansion tests showed that greatest degree of expansion was recorded by the samples with a layered hydrobiotite structure while the lowest expansion was recorded in the mixed layer vermiculite-chlorite regarded as pure vermiculite. Gruner (1934a) and Midgley and Midgley (1960) did not explain the relationship between the mineralogy and exfoliation degree of vermiculite samples studied. However, it was also reported in the most recent studies by Justo et al., (1993) and (Hillier et al., 2013), that a vermiculite sample with mica interstratification exfoliates with greater expansion ratio even at lower temperature than pure vermiculite. Most of the authors that reported this result used conventional heating system for their exfoliation process and it can be concluded that the degree

of vermiculite may be associated to many factors that include the specific details of the exfoliation process such as temperature.

2.1.5 Vermiculite Water Network

In phyllosilicate minerals, the water content consists of water adsorbed on external and internal surfaces (bound water) by electromolecular and molecular surface forces. The other form of water is due to the balancing of the excess negative ions in the structure by exchangeable interlayer cation and water (free water) that occupy the interlayer space. The later form of water is held in the interlayer by weakly hydrogen bond and can move and escape at relatively low temperature (between 100 °C to 150 °C) because of the large interlayer space and weak binding force (Foldvari, 1991, Grim, 1968, Boyarskii et al., 2002).

The exfoliation property of vermiculite minerals has been attributed to its water content by different authors (Hayes and Palatine, 1958, Zhao et al., 2010, Justo et al., 1989). Various researchers using vermiculite samples from different geological locations have studied the structure and relationship to water layer hydration states (WLHS) (Basset, 1963, Brindley, 1951, Bassett 1959, Brown, 1961, Hendrick and Jefferson, 1938, Walker and Garrett, 1967). The WLHS is defined as the number of water layers in the mineral interlayer space (Suzuki et al., 1987, Harraz and Hamdy, 2010, Marcos et al., 2009). According to Suzuki et al (1987), vermiculite WLHS are denoted as 0, 1 and 2 water layers and these are related to the interlayer cations, relative humidity, and temperature (Graf et al., 1994, Beyer and Reichenbach, 2002).

Walker (1961) and Ferrage et al (2005) agreed that the nature of the exchangeable interlayer cations plays a major role in the state of the vermiculite interlayer water, since different cations possess different hydrated ionic radii and water layer hydration states (WLHS). As shown in Table 2-4, Mg^{2+} and Ca^{2+} have thicker water layers and higher water content than Ba^{2+}, Na^{+}, K^{+} and NH^{4+} due to their higher hydrated ionic potential.

Table 2-4: Relationship between water layers and interlayer cations in vermiculite (Grim, 1968)

Interlayer cation	Hydrated ionic radius (Å)	WLHS	Water layer thickness (Å)	Basal Distance	Water content (mol/ion)
Mg^{2+}	1.08	2	0.51	1.38-1.44	4.00-4.71
		1	N/A	1.15-1.16	1.57-1.88
		0	N/A	0.93-1.00	0.00-0.51
Ca^{2+}	0.96	2	0.58	1.47-1.59	4.59-5.39
		1	N/A	1.18-1.19	1.23-1.83
		0	N/A	0.95-0.98	0.00-0.21
Ba^{2+}	0.88	1	0.34	1.24	2.36-2.53
		0	N/A	0.99-1.00	0.00-0.50
Na^{+}	0.56	2	N/A	1.48	5.6-6.0
		1	0.56	1.18	2
		0	N/A	N/A	N/A
K^{+}	0.38	0	~0.15	1.06	N/A
NH^{4+}	0.537	0	~0.13	1.08	N/A

Sanz et al (2006) studied the mobility of water in hydrated vermiculite using proton nuclear magnetic resonance (^{1}H NMR) spectroscopy. They observed that Ca vermiculite has the highest water content followed by the Mg-vermiculite. The conclusion of their work was that interlayer water mobility depends on the quantity of water in the interlayer space, because of the water content dependence of relaxation time required for water rotation. This is likely to influence the degree of exfoliation of the vermiculite since its exfoliation involves rapid heating of the interlayer water. Therefore, there is possibility that the Ca-vermiculite will exfoliate to a higher degree than other vermiculite structures followed by Mg-vermiculite due to their higher moisture content.

Suzuki et al., (1987) investigated the distribution of the Gibbs free energy for the water adsorption process in vermiculite. They reported that WLHS of vermiculite, the interlayer and the intra-layer structure of exchangeable cations depend on some forces. These forces are the effective electrostatic interaction between cations and the negative layer charges; hydration energy which is made up of hydrogen bond between the hydrogen atom in the water molecule and the surface oxygen of the silicate; and lastly a weak van-der-Waals attraction between the silicate layers. The effect of van der Waals attraction is insignificant with respect to the electrostatic attraction.

The relationship between electrostatic interaction between the hydrated cations and the negative charge of the silicate is given by Equation 2-1 (Hougardy et al., 1970, Suzuki et al., 1987). Where 2x is the separation of the silicate unit layer, σ is the charge density and ε' is the dielectric constant.

$$n_C = \frac{2\pi\sigma^2 2x(i)}{\varepsilon'} \qquad \text{Equation 2-1}$$

Equation 3-1 shows that the higher the dielectric constant of vermiculite the lower the electrostatic attraction between the interlayer cations and the negative layer charge of the silicate. This implies that lower energy will be required to break the influence of the electrostatic attraction in vermiculite with high value of dielectric constant compared to the one with low value of dielectric constant. This is significant to this project as water has a relatively high dielectric constant and is a good microwave absorber (Metaxas and Meredith, 1983, Gupta and Eugene, 2007, Marcos and Rodríguez, 2010a). However, the authors did not consider the effect of collision between the water molecules.

2.1.6 Dehydration State of Vermiculite

Many researchers categorised the vermiculite water content into different categories, and associated temperature ranges were obtained for the stepwise removal of these waters (Grim, 1968, Reichenbach H. Graf v. and Beyer, 1994, Walker, 1949). The disagreement in the results of the different authors is due to the variability in the mineral composition of different vermiculite samples used for the thermogravimetric analyses (TGA) and differential thermal analysis (DTA) (Grim, 1968).

Most authors grouped the vermiculite moisture content into three types as adsorbed, interlayer water (bounded and unbounded to cations), and high temperature hydroxyl water (Walker, 1949, Deer et al., 1966, Grim, 1968, Gillott .J.E., 1987). The adsorbed water is not chemically bound to the vermiculite structure and released from the surface below 115^{o}C. Low energy interlayer water (bound water) is removed by heating to temperature between 200-300^{o}C while the removal of the

high temperature hydroxyl (H_20^+) water, which its removal causes permanent decomposition of vermiculite structure starts at 500^{o}C and is completely removed at temperature higher than 800^{o}C (Deer et al., 1964, Grim, 1968, Marcos et al., 2009, Gillott .J.E., 1987, Mouzdahir et al., 2009). However, the exfoliation of vermiculite does not take place when it is gently heated to a temperature less than 200°C (Grim, 1968) due to the insufficient internal pressure requires for exfoliation. Therefore, it may be concluded that vermiculite exfoliation requires rapid heating of the interlayer and all the interlayer water must be removed for exfoliation to takes place.

2.2 Previous Laboratory Work on Conventional Exfoliation

Chemical and thermal heating of vermiculite are the two principal exfoliation methodologies. Various researchers have worked on the exfoliation of vermiculite. Some used chemicals such as Hydrogen peroxide, weak acid and some electrolyte for vermiculite exfoliation, some investigated the exfoliation behaviour of vermiculite under conventional thermal energy, while some used the combinations of both techniques for improved exfoliation (Erol Ucgul and Girgin, 2002, Walker and Garrett, 1967, Mouzdahir et al., 2009, Obut and Girgin, 2002, Muiambo et al., 2010, Zhao et al., 2010).

This section reviews the two principal conventional exfoliation techniques, chemical and thermal exfoliation using oil and gas fuelled furnaces. Their limitations in terms of the cost of energy and environmental impacts are also discussed.

2.2.1 Conventional Thermal Exfoliation

This is the most common exfoliation technique and it is used by most of the current exfoliation industry (Elliot, 2011). The application of the thermal exfoliation for industrial exfoliation of vermiculite will be considered in section 3.4. Therefore, many researchers have studied its mechanism and the behaviour of vermiculite minerals from different geological locations to thermal energy (Muiambo et al., 2010, Justo et al., 1993, Mouzdahir et al., 2009).

In order to understand the effect of mineral composition on the degree of vermiculite exfoliation, Justo et al (1989) investigated the thermal behaviour of pure vermiculite obtained from vermiculite mines in Ojen and Santa Olalla (both in Spain) and vermiculite samples with mica or mica/vermiculite interstratification obtained from Kovdor, Russia. The authors used electric muffle furnace heated at 600°C and 900°C for about 15 minutes for the thermal treatment. Higher expansion was obtained in vermiculite samples with mica or mica/vermiculite interstratification compared to the pure vermiculite despite its higher moisture content. The authors concluded that no single explanation was enough to explain the exfoliation mechanism of vermiculite from different geological regions. Vermiculite exfoliation is generally related to the removal of the interlayer water, However, others factors such as chemical composition, loss of OH groups, mineralogical composition, interlayer cations and particle size may also influence exfoliation.

Muiambo et al., (2010) investigated the effect of sodium ion exchange on the exfoliation properties of Palabora vermiculite by using scanning electron microscopy, X-ray diffraction (XRD), inductively coupled plasma mass spectroscopy (ICP-MS) and thermo-mechanical analysis. Their results showed that the expansion of unaltered vermiculite commenced at higher temperature (420 °C) than that of sodium-exchanged vermiculite where the vermiculite onset temperature was reduced to 300 °C. Authors did not report the reason for this observation. A similar result was obtained in the elaborate studies carried out by Muiambo and Focke (2013) when Palabora vermiculite was modified by exchanging the interlayer cations of the neat vermiculite with ammonium (NH_4^+), alkali metal ions (K^+, Na^+) and alkaline earth metal ions (Ba^{2+}, Mg^{2+} and Ca^{2+}). Sodium, potassium and ammonium ions exchanged samples were observed to lower the exfoliation onset temperature (220 °C-250 °C) while the temperature was 420 °C in a pure vermiculite. In addition, samples with alkali metal ion exchanged interlayer cations had a higher expansion ratio with the highest observed in sodium ion (Na^+) exchanged vermiculite sample. The reason for this difference was given to be the presence of monomolecular layer of water in alkali metal exchanged samples, which lowers the ionic potential of the interlayer cations and allows easy removal of

interlayer water, especially at lower temperature. This explanation did not satisfactorily explained their observations as it may be argued that easy removal of interlayer water, may not allow building up of sufficient interlayer pressure required for vermiculite exfoliation when heated. It is necessary to compare the work of these authors to that carried out by others that used vermiculite samples from another source other than Palabora. This will give a better conclusion whether their observation is peculiar to Palabora vermiculite or is a general property of vermiculite.

Huo et al., (2012) also investigated the effect of the interlayer cations on the exfoliation properties of vermiculite, by using vermiculite samples obtained from Qeganbulak, Yuli, and Xinjian vermiculite deposits in China. The vermiculite samples were heated in a muffle furnace for 3 minutes at fixed temperatures of 500 °C, 600 °C, 700 °C, 800 °C and 900 °C. In each of the three samples used, the original vermiculite ore was intercalated with new interlayer cations (Mg^{2+}, Ca^{2+} and Na^{+}) and mineralogy tests showed that Na-vermiculite has monomolecular layer of water while Ca-vermiculite and Mg-vermiculite have two monomolecular layer of water. This suggests that Na-vermiculite has smaller interlayer spacing than the other two vermiculites. Ca-vermiculite was found to have higher interlayer spacing than Mg-vermiculite due to higher ionic radius of Ca compared to Mg. it was speculated by the author that expansion capacity of as-received crude vermiculite is mainly influenced by the mixed-layer mineral content of vermiculite as higher expansion was produced by vermiculite sample with higher amount of mixed layer minerals. In the case of modified vermiculite with Na, Ca and Mg cations, similar trends were noticed in the three different vermiculite samples. Na-vermiculite produced the highest expansion ratio at low temperature (500 °C) compared to Mg, and Ca exchanged vermiculite. This indicates that Na exchanged vermiculite lower the exfoliation onset temperature, and their results agreed with that of Muiambo et al. (2010) and Muiambo and Focke (2013). In contrast to the work of Muiambo et al. (2010) and Muiambo and Focke (2013), higher exfoliation ratio was observed in Mg and Ca vermiculite at high temperature (80 °C-100 °C). The reason for this difference might be due to the different heating rate used by the authors as Muiambo

et al. (2010) and Muiambo and Focke (2013) followed a stepwise heating of the samples up to the high temperatures while Huo et al. (2012) heated the samples rapidly for 3 minutes at a fixed temperature. The author attributed the higher expansion capacity of Ca-vermiculite and Mg-vermiculite to high electrostatic attraction force between the cations (Ca and Mg) and interlayer water.

2.2.2 Chemical Exfoliation

Chemicals such as hydrogen peroxide solution (H_2O_2), sulphuric acid, nitric acid, hydrochloric acid and phosphoric acid can be used for one-dimensional swelling of vermiculite, perpendicular to the silicate layer planes, at temperatures below 100 °C (Walker and Garrett, 1967, Obut and Girgin, 2002). It has been proven that Mn and Fe oxides located in the mineral interlayer space can also catalyse the process (Mikutta et al., 2005).

Expansion by hydrogen peroxide solution is the most effective form of chemical exfoliation in terms of expansion ratio. Many authors proposed that the mechanism of chemical exfoliation by H_2O_2 is by the decomposition of hydrogen peroxide into H_2O and O_2 gas, which diffuses into the interlayer spaces of vermiculite. The evolved gas then causes the disruption of the equilibrium between the individual silicate layer and the interlayer cations (Huo et al., 2012, Erol Ucgul and Girgin, 2002, Walker and Garrett, 1967, Kehal et al., 2010, Obut and Girgin, 2002).

Recently, Obut and Girgin (2002) extended the work of Erol and Girgin (2002) by comparing the chemical exfoliation properties of Karakoc phlogopite (Turkey) earlier investigated by the former authors, to South African phlogopite and vermiculite, by using H_2O_2 solution (1-50 wt.%) and reaction time between 1-30 hours. Their results showed that Karakoc sample has a higher expansion ratio especially at concentration below 30% H_2O_2. The Palabora phlogopite and vermiculite samples showed a stepwise increase in expansion ratio above 30 % H_2O_2 concentration. The maximum expansion ratios obtained at 50 % H_2O_2 concentration in 30 h for Karakoc phlogopite, Palabora phlogopite and Phalaborwa vermiculite are 103, 90 and 118 fold respectively. These results contradict that of

Drosdoff and Miles (2013) that reported that mica minerals exhibit higher exfoliation degree than pure vermiculite.

Erol and Girgin (2002) investigated the chemical exfoliation properties of phlogopite sample obtained from Sivas-Yildizeli-Karakos (Turkey), under varying concentrations of H_2SO_4, HCl, HNO_3, H_3PO_4 and H_2O_2. Their work revealed that H_2O_2 gives the highest degree of exfoliation amongst all the chemical substances used. This is due to the higher oxidizing power of H_2O_2 compared to that of other chemical substances used for vermiculite exfoliation. It was also observed that the degree of exfoliation was influenced by factors such as, hydrogen peroxide concentration, reaction time, and temperature, but the solid to liquid ratio had no significant effect. The exfoliation rate increases with an increase in H_2O_2 concentration. A maximum expansion ratio of 49-fold was obtained for 30 % H_2O_2 in 30 hours and at room temperature. The reaction time was reduced to 70 minutes after heating to 60 °C and the decomposition of the vermiculite structure was observed above 60 °C. Currently, this method is not used for commercial exfoliation because of the high retention time required for the maximum exfoliation at room temperature and elevated temperature. The process also requires high amount of chemical for exfoliating a tonne of vermiculite.

2.3 World Vermiculite Production and Applications

2.3.1 Distribution of Vermiculite Deposits and Production

The major world primary deposits of vermiculite are in USA, South Africa, Zimbabwe, Russia, Australia, China and Brazil (Elliot, 2011). The annual production of vermiculite is estimated to be 570 tonnes in 2012, and the global vermiculite reserves were estimated to be 60 million tonnes (tanner, 2013). The global vermiculite production from 2000 to 2011 is shown in Figure 2-3, with South Africa having the highest production from 2000-2011. The figure excludes production by countries for which data are not available while the total productions for Argentina, Australia, Bulgaria, Egypt, India, Japan and Uganda are grouped as others (Brown et al., 2013, tanner, 2013, Cordier, 2010). The price of vermiculite

varies with factors such as applications, size grade, source of raw vermiculite and demand (Elliot, 2011).

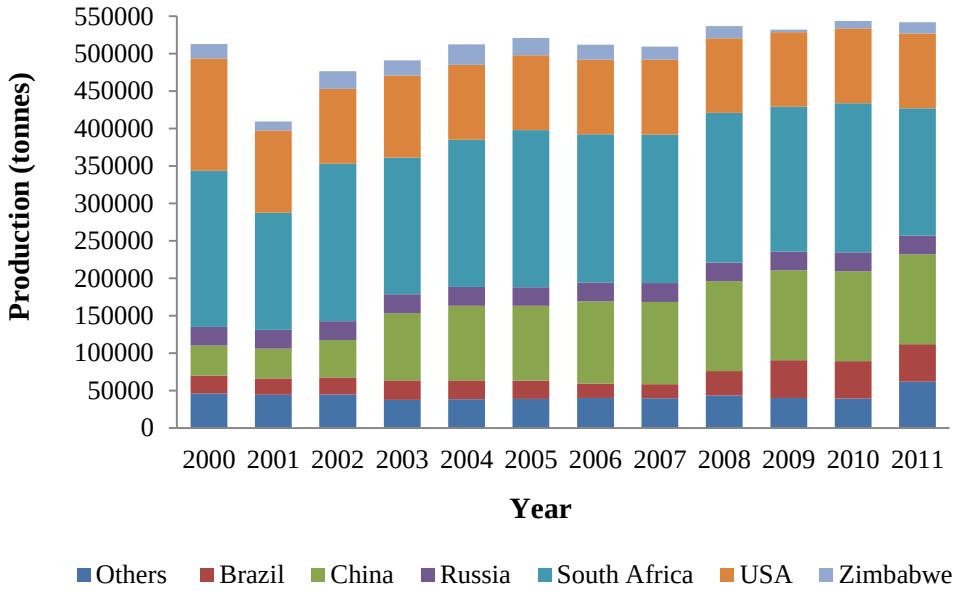

Figure 2-3: Global Vermiculite production, 2000-2011 (Brown et al., 2013, tanner, 2013, Cordier, 2010)

Vermiculite is commercially mined by using the open-pit mining technique because it is typically near the surface (Bergaya et al., 2006, The Vermiculite Association, 2011, Kennedy, 1990, Marinshaw, 1995). The vermiculite deposits in China and Russia have been shown to exhibit poor exfoliation property compared to the South African and USA vermiculite which has been showed to exfoliate to a higher degree (Crowson, 2001). Crowson (2001) also reported that there is a poor understanding of the reason for the different thermal behaviour of vermiculite from different mine locations, but the recent investigations of the physical and chemical behaviour of Chinese vermiculites indicates that they are not pure vermiculite material but biotic or phlogopitic materials (Marcos and Rodríguez, 2010b, Marcos et al., 2009). This may have contributed to their poor exfoliation behaviour.

In 2011, there were about 18 vermiculite exfoliation plants in 11 states, in the United States. These plants thermally exfoliate vermiculite by using oil and gas fuelled furnaces, and this process is energy intensive with high greenhouse gasses emissions. (Marinshaw, 1995, NPI, 1999). About 36 % of the exfoliated vermiculite

in the United States of America is used for lightweight concrete aggregates, 43 % for agriculture/horticulture, 7 % for insulation and 14 % for other usage. Apart from the higher demand and lower supply of coarser grades vermiculite, which have caused an increase in its price, fluctuations in the price of the oil and natural gas and the high cost of transporting exfoliated vermiculite due to its high volume, also affects the prices of exfoliated vermiculite (tanner, 2013).

2.4 Industrial Exfoliation of Vermiculite

2.4.1 Conventional Thermal Exfoliation

Vertical, inclined, rotary and fluidised bed furnaces are some of the conventional thermal methods used industrially for exfoliating vermiculite materials (Strand and Stewart, 1983, The Vermiculite Association, 2011). Figure 3-4 shows the schematic section of the vertical type furnace system used for vermiculite exfoliation.

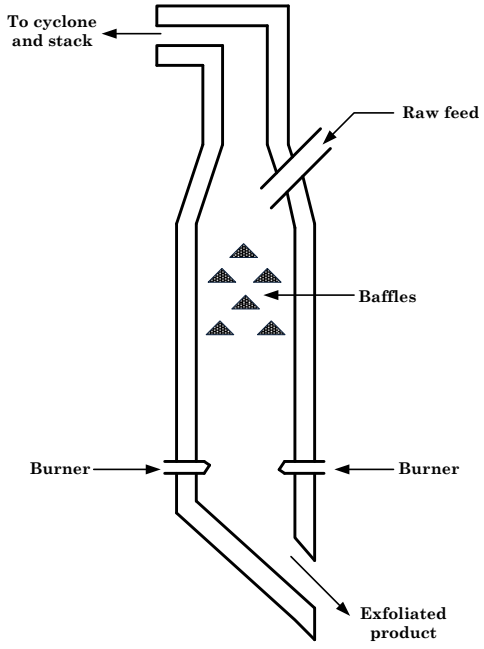

Figure 2-4: Schematic section of vertical-type vermiculite exfoliator (Mackinnon et al., 1989)

During the exfoliation process, the raw material is conveyed into the furnace by means of bucket elevator, and the ore is spread internally within the furnace by means of baffles and heated to a temperature between 850 °C and 1100 °C for a

period up to 8 seconds (NPI, 1999, Marinshaw, 1995, Kogel et al., 2006). The exfoliated product is rapidly removed from the furnace by an incorporated suction fan.

The Torbed vermiculite exfoliator (Torbed 400 and 1000) designed by Torftech Limited, UK, incorporates fluidised bed and cyclone technologies. This system operates by the continuous contact between hot gas heated by flames (1250 °C) and vermiculite ore. Torbed Ltd designed two exfoliation reactors, Torbed 400 (max 0.25 t/h) and Torbed 1000 (max 2 t/h) for exfoliating vermiculite. Both reactors operate by the burning of either oil or natural gas. Torftech claimed that the systems has a compact design, good control facilities and high energy transfer, thereby reducing the processing time (Torbed Service Limited., 1997). Since vermiculite ore has a low thermal capacity, its thermal exfoliation requires a high amount of energy transfer (greater than 1 MWh/t) from the silicate surface into the interlayer water in the interlayer space by process of conduction and radiation (Andronova, 2007).

2.4.2 Limitations of Conventional Exfoliation

Several methods for vermiculite exfoliation have been patented since the US Patent application by Hayes in 1958 (Hayes and Palatine, 1958, Michael Windsor Symons., 1997, Caplain et al., 2009, George, 1960). Most of the patented works detailed pre-treatment of vermiculite ore by intercalated agents such as hydrogen peroxide, ammonia solution and hydrochloric acid. No literature was available showing the commercial use of these technologies and this may be related to the flowsheet complexity and safety issues due to the high amount of chemicals required and the cost of chemicals. Apart from the high-energy consumption required by the thermal exfoliation, the products also come out at over 700 ^{O}C and take many hours to cool down, therefore requiring storage and slowing the bagging and distribution process. Another disadvantages of this exfoliation technique is the potential emission of greenhouse gases and other hazardous waste (Strand and Stewart, 1983, Marinshaw, 1995).

2.4.3 Previous Works on Microwave Exfoliation of Vermiculite

Microwave energy has potential applications in industrial processing of minerals due to its advantage of selectively heating the microwave susceptible phases within the minerals structure (Chen et al., 1984a). Vermiculite sheet silicates are transparent to microwave because of their structure and this is confirmed by their low dielectric properties. As discussed in Section 3.15, vermiculite contains free, bound, and high temperature hydroxyl water. Free water within the vermiculite interlayer space has high dielectric properties compared to the surrounding silicate layers (e.g. distilled water ε'=76.7 and ε'' =12.2 at 25 °C) (Metaxas and Meredith, 1983). The presence of this interlayer water, which is a good microwave absorber within vermiculite structure, creates a potential opportunity to selectively heat the interlayer water in order to exfoliate the vermiculite. Due to the selective heating of the interlayer water, which is about 5-15% of the vermiculite mass to create steam and thus causes exfoliation, there is a potential to reduce the energy requirement compared to conventional heating whereby 100 % of the material is heated to the required temperature.

The concept of using microwave energy to exfoliate vermiculite is not new. For example US Patent 3758415 (Wada and Osaka, 1973) reported pre-treatment of vermiculite ore with polar molecules (one end of the molecule is positively charged while the other end is negatively charged) such as H_2O_2 before microwave exfoliation. Wada and Osaka (1973) described that less energy is needed for microwave exfoliation when compared to the conventional thermal heating, and the products have improved quality such as high water retention and cation exchange capacity.

PCT application WO 2006/127025 by Sklyarevich and Shevelev (2006) suggested using 83 GHz microwave energy with low power density (5 kW/cm^2) for expanding perlite and similar hydrated minerals including vermiculite (Figure 2-5). In this invention, the microwave energy is generated using a gyrotron at 83 GHz, and maximum output power of 15 kW. The microwave beam generated is then focussed on a mirror inclined at an angle to direct microwave energy perpendicular to the

treated material on conveyor system. The microwave energy then heats the moving material and the expanded product drops into the stationed carrier.

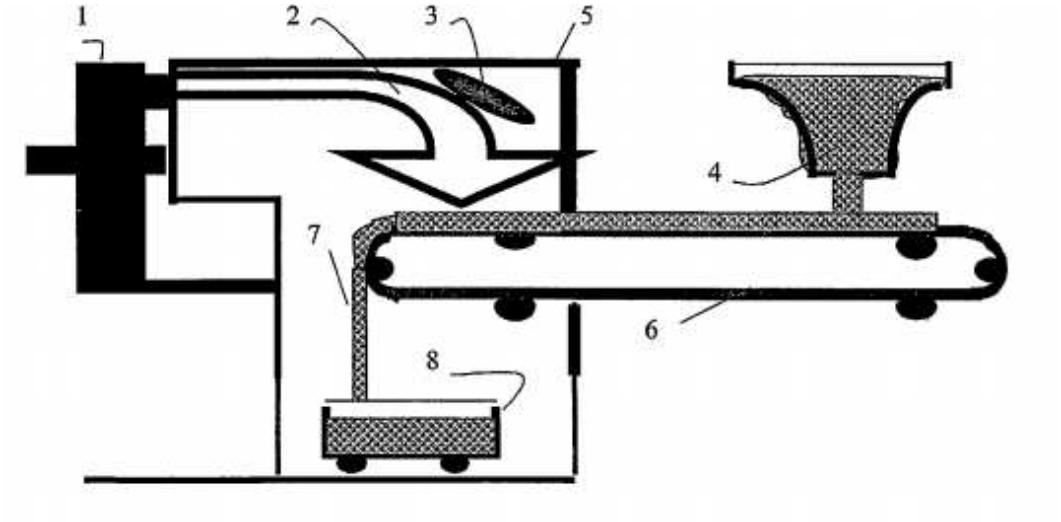

Figure 2-5: Schematic view of the microwave mineral exfoliator operating at 83GHz. (1) Gyrotron, (Harrison et al.) Microwave beam, (3) Focussing mirror, (4) Ore, (5) Microwave chamber, (6) Conveyor, (7) Expanded material and (8) Carrier (Sklyarevich V; and Shevelev M, 2006)

The Inventor reported that the ore size should be close to the wavelength of the microwave frequency used and it was challenging exfoliating fine grades by this equipment. Other potential limitations are the safety challenges and the low product throughput of about 108 kg/h.

Most of the published laboratory investigations of microwave exfoliation of vermiculite to date (Obut et al., 2003, Zhao et al., 2010, Marcos and Rodríguez, 2010a) have been carried out using domestic microwave ovens (kitchen microwaves at 2.45 GHz). Such systems comprise a rectangular cavity that supports a number of resonant modes (multimode applicator) within the frequency range of the magnetron, which generates the microwave energy (Metaxas and Meredith, 1983). Obut et al. (2003) and Zhao et al. (2010) in their studies pre-soaked the vermiculite ore with H_2O_2.

Obut et al (2003) used a domestic white Westinghouse (Model KM-90 VP, 2.4GHz) microwave oven to study the effect of microwave powers of 600, 950 and 1300W (maximum energy of 0.10 kWh/t) on the exfoliation behaviour of phlogopite and

vermiculite already pre-treated (soaked) with water and hydrogen peroxide (10% H_2O_2 and 20% H_2O_2). Similarly, Miao et al (2010) also used the combination of hydrogen peroxide with a concentration between 5%-30% and a domestic microwave oven to study the effect of microwave power, hydrogen peroxide concentration, heating time, and solid immersion time on the degree of exfoliation. These authors agreed that vermiculite exfoliation is interlayer water dependent and the expansion degree is directly proportional to the concentration of H_2O_2. Carrying out such a process at commercial or even at pilot scale will require a complex multiphase plant flowsheet consisting of the operating units for the mixing of vermiculite with H_2O_2 and that of the microwave heating. Other limitations are the high cost of H_2O_2 requires for the processing and the cost of waste disposal. The recent paper by Marcos and Rodríguez (2010b) used a domestic multimode microwave oven (2.45 GHz, 800 W) to compare microwave exfoliation to conventional heating at 1000 °C. The results showed that expansions occurred in the microwave oven at bulk temperatures below 100 °C. It was also reported that microwave exfoliation is slower than that of vacuum dehydration and conventional heating at 1000 °C. This may be due to uneven distribution of electric field and low power density in the domestic microwave oven used. However, the works of these authors give no suggestions of routes to scale up were given, nor were issues of microwave safety, energy balances and the challenges of continuous processing addressed.

The limitations of domestic ovens are the spatial non-uniform distribution of the electric field, which causes uneven heating of materials, the creation of multiple hotspots within the cavity and the low power density (Meredith, 1998). These drawbacks make domestic microwave ovens un-suitable for scientific investigations as the distribution of the electric field may vary considerably between discrete treatment of different samples and it is subsequently impossible to predict the distribution of the electric field in the workload. In addition, the results obtained from the domestic microwave oven do not give any clue about the scale up to commercial throughput since the degree of exfoliation is not linear to the power density and energy input.

Due to the limitations of the existing systems for sustainable processing of vermiculite in terms of energy requirement, environmental impact and product quality, designing an energy efficient method of exfoliating vermiculite ore to give a lower product temperature, lower production costs and minimise the environmental impact while also increasing the product yield and quality is important. Microwave exfoliation, which is a technique that selectively heats the vermiculite interlayer water, which is microwave absorber rather than the whole vermiculite silicate structure that is microwave transparent, has the potential of reducing the energy requirement for vermiculite exfoliation, operating cost and increasing the quality and yield of exfoliated vermiculite. This research will focus on how to use microwave energy for vermiculite exfoliation by rapid and selective heating of the interlayer water.

2.5 Conclusions

Vermiculite has been adopted as a general name for minerals that exhibit exfoliation property. Most of these minerals are not pure vermiculite, but are mixed layer vermiculite-mica and they possess distinct physical and chemical properties, which vary in different vermiculite samples. The variations in the geochemistry of vermiculite samples obtained from different geological locations may be due to the different mode of formations, primary mica minerals and stages of alteration. These influence the behaviour of the different vermiculite samples when undergoing exfoliation.

Water networks have been described as the major factor that gives vermiculite its exfoliating property and hence as minerals of high industrial and economic values. Chlorite minerals that have the same chemical composition as vermiculite, but no interlayer water do not expand like vermiculite. The water content in vermiculite is characterised as free water, bound water, and high temperature hydroxyl water as a function of the temperature required for their removal from the vermiculite structure.

Thermal exfoliation by oil and natural gas fuelled furnaces is the current conventional exfoliation methodology and requires high consumption of energy due to low thermal conductivity of vermiculite. Other factors limiting conventional exfoliation are emission of greenhouse gases and other hazardous pollutants. In addition, the fluctuations of the price of natural gas and oil resulted to the increase in the operating cost of vermiculite furnace and subsequent increase in the price of processed vermiculite.

Microwave heating technique, which has the advantage of giving rise to selective, rapid, uniform and volumetric heating (Metaxas and Meredith, 1983), has been used for vermiculite exfoliation by various researchers mostly at laboratory scale. However, there have been challenges in scaling up the technology to a commercial throughput due to poor understanding of fundamental of microwave interaction with vermiculite, vermiculite geochemistry, and material handling.

CHAPTER THREE
FUNDAMENTALS OF MICROWAVES AND MICROWAVE HEATING

3.1 Introduction

Conventional heating involves the transfer of heat energy to materials by conductive, radiative and convective heat transfer across a temperature gradient, usually from the material surface to the internal region (Carslaw and Jaeger, 1959, Hahn and Ozisik, 2012). The rate of heat flow from a material surface to the interior part is therefore limited by the temperature gradient and thermal diffusivity, which is a function of the thermal conductivity, density and specific heat capacity of the material. The thermal diffusivity dictates the rate of heat transfer in a material, and heat moves rapidly in workload with high thermal diffusivity while its movement is slow in materials with low thermal diffusivity (Carslaw and Jaeger, 1959). Therefore, the application of conventional heating in industrial processing is challenging when selective heating is required. This can result in a slow and high-energy consuming process, especially when non-conducting or insulating materials are to be heated. Other disadvantages of conventional heating are uneven temperature distributions in the workload, poor product quality, difficult process control and environmental pollution (Chandra, 2011, Stuerga and Gaillard, 1996, Metaxas and Meredith, 1983, Thostenson and Chou, 1999).

The limitations of conventional heating processes can be overcome by exploiting microwave heating technology, which delivers high efficiency in converting electricity to electromagnetic energy. This is due to the high efficiency of magnetrons (86 % at 900 MHz and 80 % at 2450 MHz). In the microwave heating, there is no transfer of heat energy within the material in the conventional sense of heating, and from a thermodynamic point view, the material itself acts as the source of heat (Mehdizadeh, 2010, Meredith, 1998). Volumetric and internal heating are some of the important characteristics of microwave heating which distinguish it from conventional heating. This means that microwave energy can be absorbed directly by the heated material and be instantaneously delivered to the whole mass (Guo et al., 2010, Menezes et al., 2007, Zlotorzynski, 1995, Haque, 1999,

Mehdizadeh, 2010). It therefore allows selective, rapid and controlled heating of materials. This concept has been used for many decades as part of a kitchen appliance for faster and efficient heating of food (National Research Council (NRC). 1994, Ku et al., 2001b, Swain et al., 2008), but currently, the technology is receiving a growing interest industrially as an energy efficient heating technique for material processing. These include areas such as, in drying of wood (Vongpradubchai and Rattanadecho, 2009), food engineering for reheating, precooking, cooking, tempering, baking, drying, pasteurization, and sterilization (Datta et al., 2005), ceramic processing (Huanga et al., 2009) remediation of oil contaminated drill cutting (Robinson et al., 2009), pre-treatment of coal (Lester and Kingman, 2004), and treatment of sulphide (Al-Harahsheh et al., 2006b). This chapter considers the fundamentals of microwave heating, discusses issues around their safe use, previous work on its applications for the processing of industrial minerals and the scale up of microwave systems for industrial processing.

3.2 The Electromagnetic Spectrum

It is important to understand electromagnetic waves and the electromagnetic spectrum because the microwaves are electromagnetic waves. Electromagnetic waves are time varying electric (E) and magnetic fields (B), that can travel through an empty space or matter transversely with an associated velocity equal to the speed of light (Meredith, 1998). They possess all the waves' properties such as reflection, refraction, interference, diffraction and absorption. Figure 3-1 shows the orthogonal oscillation of magnetic and electric field during the propagation of electromagnetic waves.

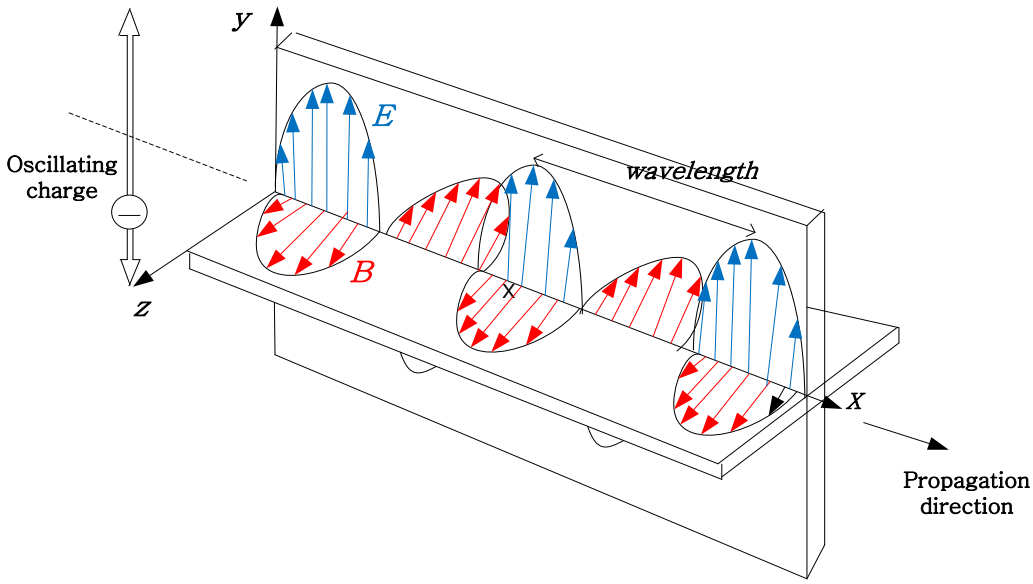

Figure 3-1: Perpendicular oscillations of electric and magnetic fields in electromagnetic waves E-electric field, B-magnetic field (Chan and Reader, 2000)

The Electromagnetic spectrum (Figure 3-2) presents the range of frequencies of electromagnetic energy oscillating with an electric field and magnetic field perpendicular to each other. Waves can be described by any of the following three physical parameter: frequency, wavelength and photon energy, and are arranged from the low frequency electromagnetic waves used for radio communication and heating, to high frequencies infrared, ultraviolet and gamma (Metaxas and Meredith, 1983). The electromagnetic photon energy is directly proportional to the wave frequency as expressed in (Equation 3-1), where E is the energy (J), 'h' is a plank constant ($6.63X10^{-34}$ m^2kg/s), λ is the wavelength, c, the speed of electromagnetic waves and f is the frequency in Hertz (Hz).

$$E = hf = \frac{hc}{\lambda} \qquad \text{Equation 3-1}$$

Equation 3-1 implies that the microwave has higher energy than radio waves, which has a lower oscillating frequency. Electromagnetic waves are divided into two different groups as; ionising radiation that removes electrons from an atom and molecules with the production of harmful free radicals; and non-ionising radiation that does not cause atomic ionisation (Kitchen, 1993).

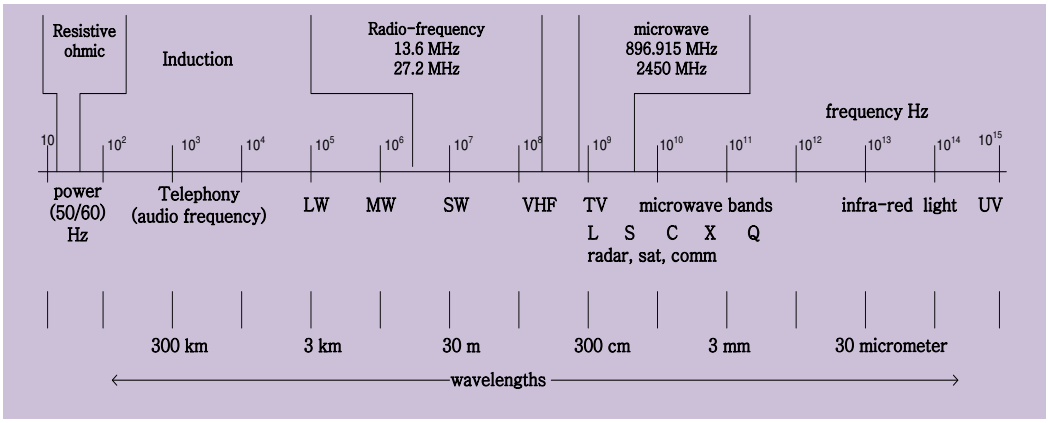

Figure 3-2: The Electromagnetic Spectrum on logarithmic frequency scale (Meredith, 1998)

3.3 Microwave Energy and ISM

Microwaves are a non-ionizing form of electromagnetic energy lying between the radio and infra-red region in the electromagnetic spectrum and within the frequency range of 300 MHz to 300 GHz, with corresponding wavelengths ranging from 1 m to 1 mm respectively (Thostenson and Chou, 1999, Clark et al., 2005). The microwave frequency range is divided into three different frequency bands ranging from the ultrahigh frequency (UHF: 300 MHz to 3 GHz), super-high frequency (SHF: 3 GHz to 30 GHz) and the extremely high frequency (EHF: 30 GHz to 300 GHz) (Ku et al., 2001b, Metaxas and Meredith, 1983). Even though microwave frequencies range from 300 MHz to 300 GHz, governments restrict most of the frequency range for their own use, thereby leaving limited frequencies for domestic, industrial and medical usage. In order to avoid interference with telecommunications and cellular phone frequencies, microwave heating uses the allocated frequency bands known as Industrial Scientific and Medical frequencies (ISM). These allocated frequencies vary slightly in some countries. For example, 896 MHz is used in the United Kingdom while 915 MHz is used in United States for industrial heating applications (Chan and Reader, 2000, Metaxas and Meredith, 1983). The regulatory authorities in different countries strictly follow the international table of frequency allocations designed by The International Telecommunication Union (ITU) for the allocation of certain frequencies for industrial, scientific and medical purposes. Table 3-1 lists the ITU permitted

frequencies for industrial, scientific and medical applications (ISM) applications worldwide.

Table 3-1: Permitted Frequency for ISM Applications (Gupta and Eugene, 2007, Osepchuk, 2002)

ISM frequency	Frequency tolerance	Area permitted
433.92MHz	±0.87MHz	Include Europe and part of Asia
896MHz	±10.0MHz	UK only
915MHz	±13.0MHz	Western Hemisphere
2450MHz	±50.0MHz	Worldwide
5800MHz	±75.0MHz	Worldwide
24125MHz	±12.0MHz	Worldwide
61.25GHz	±250MHz	Worldwide
122.50GHz	±500MHz	Worldwide

3.4 Advantages and Challenges of Microwave Heating Applications

Many factors have justified the application of microwave energy for heating in industrial food processing. These have led to advances in its research, development and application to many other materials processing applications (Clark and Sutton, 1996) in areas such as ceramic sintering (Clark et al., 2005), plastics recycling (Tsintzou et al., 2012, Siddiqui et al., 2012), graphene synthesis (Kumar et al., 2013), gold recovery and treatment (Amankwah and Ofori-Sarpong, 2011, Amankwah et al., 2005), welding of thermoplastics (Yarlagadda and Chuan, 1998) and waste management (Oncu and Balcioglu, 2013).

Unlike conventional heating processes, microwave energy volumetrically heated dielectric materials resulting in rapid and efficient distribution of heat. Likewise, in a multiphase material with each phase having different dielectric properties (microwave absorbing capacity and dissipation as heat); microwave energy selectively interacts more strongly with the microwave absorber in the processed material, and generates heat instantaneously within the material matrix. Therefore, compared to the conventional heating where there is slow heating rates and poor process control, microwave heating is rapid, volumetric and selective, as the

microwave energy interacts with only the microwave absorber. Other advantages stated in the literature are cost and energy savings, environmentally friendly, improved product quality, faster and higher production throughput, less floor space requirement, reduction in heat loss, precise and controlled heating, and rapid heating of thermal insulators (Clark and Sutton, 1996, Clark et al., 2000, Meredith, 1998).

Nevertheless, a number of factors have limited microwave applications at industrial scale processing. Its main source of power is electrical energy, which is more expensive than gas typically and the cost of energy consumption will be affected by the increase in the cost of electricity irrespective of the efficiency of the microwave system (Shaheen et al., 2012). For full-scale utilisation of microwaves, intelligent understanding of the fundamental interaction of microwave energy with materials is required (Thostenson and Chou, 1999, Yoshikawa, 2011). The poor understanding of microwave fundamentals has limited the commercialisation of some of the laboratory breakthroughs as a potential green chemistry and green engineering processing techniques because it requires engagement of multidisciplinary teams for intelligent scale up (Sutton, 1992).

Thermal runaway, which is a thermal instability caused by the interaction of electromagnetic waves with materials is another challenge faced during microwave processing of minerals (Metaxas and Meredith, 1983, Shaheen et al., 2012). This phenomenon causes an uncontrollable increase in the temperature of the workload and subsequent damage. It is interesting to note that the causes of this effect are different under different processing conditions. Lastly, microwave heating is material property dependent. Some materials are good microwave absorbers; some are transparent while others reflect microwave energy without heat generation. Therefore, for the development of any microwave heating process, a key prerequisite is a detailed understanding of microwave fundamentals and an understanding of the interaction of microwave energy with the material to be processed.

3.5 Mechanisms of Microwave Heating

Materials differ in their interaction with microwave energy and nearly all materials interact to a greater or lesser degree, except perfect conductors and insulators. The dielectric heating mechanism may be due to the polarisation of charges or polar molecules in a heated material or direct conduction or migration of ions or charges under the influence of the alternating electric field. Therefore, Ionic conduction and polarisation are the two principal mechanisms responsible for dielectric heating in materials. Various polarisation mechanisms can be induced in dielectric materials including dipole, atomic, electronic and Maxwell-Wagner polarization with each occurring across specific frequency ranges (Metaxas and Meredith, 1983, Taylor et al., 2005, Hippel, 1954). Ionic conduction and dipolar polarisation, which are the two important microwave-heating mechanisms, are described in detail in this section.

3.5.1 Ionic Conduction of Microwave Energy in Dielectrics

When microwave energy is transferred into a conducting solid or liquid material, the charge carriers (ions, electrons, etc.) within the material are set in motion by the influence of the externally applied electric field, E, resulting to the polarisation, P, in the same phase with the electric field (Metaxas and Meredith, 1983). Figure 3-3 shows an ionic conduction heating mechanism in a material. The charged particles in a material are at equilibrium state when there is no applied electric field but ionic movement starts instantaneously when the material is under the influence of electric field. The collision force of the ions converts its kinetic energy into heat within the material volume (Whittaker G., 1994 & 2007).

This mechanism is dominant at low microwave frequencies (<200MHz) and occurs because of the collision of ionic species when they move through the material under the external applied electric field (Komarov et al., 2005a). As the frequency increases, the ionic conduction effect is insignificant because the time required for the ionic movement in the direction of electric field decreases (Clark and Sutton, 1996).

No E Field (E=0) **Local E field (E>0)**

Figure 3-3: Charged Particle following the Electric Field (Lidstrom et al., 2001)

The ionic conduction mechanism generates more heating than dipolar effects, especially for solutions with high amount of ionic species and it is important for the microwave heating of microwave transparent solid or liquid materials, either by the addition of ions or increasing the temperature in order to increase the coupling efficiency of the material to microwave energy (Gupta and Eugene, 2007, Lill et al., 2007, Al-Harahsheh and Kingman, 2004). However, if the heated material is highly conductive, microwave energy will not be able to penetrate the surface of the material and will be reflected back (Metaxas and Meredith, 1983).

3.5.2 Dipolar Polarisation Heating Mechanism in Dielectric Materials

Dipolar polarisation is the most significant of all the microwave-heating mechanisms, especially at frequencies above 1GHz in polar materials with asymmetrical charge distribution and permanent dipole moment (Metaxas and Meredith, 1983, Stuerga, 2006). Water is a typical example of polar liquid with a permanent dipole moment. Its presence in some materials such as organic and inorganic chemical substances, soil and clay minerals contributes to their microwave heating (Meredith, 1998). A water molecule is structurally arranged in such a way that one oxygen atom is bonded to two hydrogen atoms to make an angle of 104.5° with an H-O bond length of 0.958Å (Figure 3-4).

The non-linear structure of a water molecule causes its dipole behaviour by having excess negative charge on the oxygen side and positive charge on the hydrogen side

(Kupfer, 2005). Therefore, It has a high dielectric constant of 80 (microwave absorption capability) at 25°C and 2.45GHz. (Meredith, 1998).

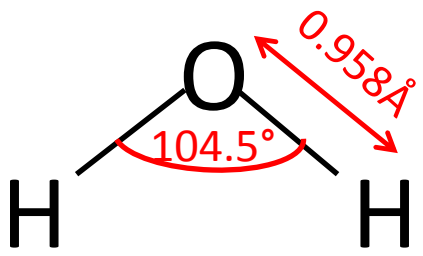

Figure 3-4: Water dipole structure (Boyer, 2002)

When materials containing dipoles are placed in an alternating electric field, for example at 2.45 GHz, the dipoles align themselves about 2.5 billion times per second in the direction of the electric field and also increase the internal energy of the dielectric material (Fernandez et al., 2011). The ability of a dipole to polarise when placed in an electric field varies with the wave frequency and viscosity of the liquid. The rate of alignment of the dipole is more rapid in gases than in liquid because gas molecules are more spaced and the rapid alignment is restricted by other molecules in liquids due to its viscosity (Lidstrom et al., 2001). The large distance between the gas molecules explains why gases are very challenging to heat directly with microwave energy.

The main controlling factor for this mechanism is that the frequency of the time changing electric field should be adequate to produce a good polarisation within the dipolar material such as water, wet clay mineral or soil and water containing organic and inorganic material (Clark and Sutton, 1996, Venkatesh and Raghavan, 2004). At lower frequencies, the dipole rotation is in phase with the oscillating electric field because the reversal of electric field takes longer than the dipole rotation. The molecule gains energy but the energy transfer is so small that the temperature hardly increases. In addition, if the frequency of the externally applied electric field is high, the dipole will not have sufficient time to respond to the rapidly changing electric field. No heating takes place under this condition since there is no

rotation of the dipole (Metaxas and Meredith, 1983, Clark and Sutton, 1996, Lidstrom et al., 2001). When the applied field is within the microwave frequency region, the dipoles have sufficient time to re-orient with the changing electric field and, therefore, rotate. There is a phase lag between the electric field and the dipole, and this generates heat within the heated material by molecular friction and collisions of the dipoles (Mutyala et al., Sateesh et al., 2010).

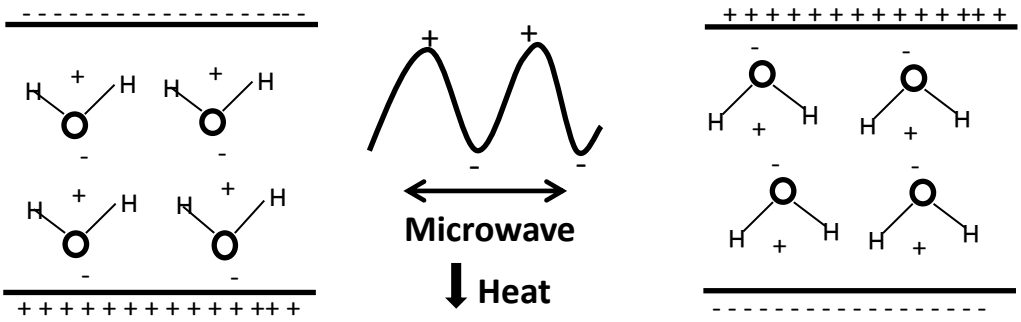

Figure 3-5: Dipolar Molecule Aligning with Electric Field (Tsuji et al., 2005)

Figure 3-5 shows the dipolar polarisation heating mechanism, with the dipoles (e.g. water molecule) in an equilibrium state in the absence of an electric field, but start polarising with the generation of heat within the material structure immediately when an external electric field is applied.

Other polarisation mechanisms are Maxwell-Wagner or interfacial polarisation, electronic and atomic polarisation. The Maxwell-Wagner is specific to heterogeneous materials and is a combination of conduction and dipolar polarisation mechanisms. This mechanism influences the polarisation of heterogeneous mixtures with constituents having different permittivity (microwave absorption capabilities) and electrical conductivity or solid materials with charged particles mobile in an enclosed region, at the lowest frequency band used for industrial heating ($f<5x10^7$Hz) (Metaxas and Meredith, 1983, Zlotorzynski, 1995). For example, this heating mechanism is important in soils and clay minerals such as perlite and montmorillonite because they are mixture of different heterogeneous constituents (solids, liquids and air) with different electrical properties separated by distinct boundaries or interfaces (Chen and Or, 2006, Gupta and Eugene, 2007).

The electronic and atomic polarisation process are dominant at optical and infrared frequency region respectively, and the requirements for these polarisation are higher than what can be produced at microwave region because their polarisations are faster than the field at microwave region (Al-Harahsheh and Kingman, 2004, Murphy and Morgan, 1937, Zlotorzynski, 1995). Therefore, they do not contribute to microwave heating of materials. Detailed discussion of these polarisation mechanisms are given in the literature (Hippel, 1954, Murphy and Morgan, 1937, Gupta and Eugene, 2007).

3.6 Electromagnetic Properties of Materials

As discussed in section 3-5, microwave heating of materials is due to various heating mechanisms, which depend upon the frequency, chemical and structural composition of the material. Therefore, different materials interact and show different heating behaviours when subjected to microwave energy. The reason for this lies in the study of the electromagnetic properties of materials.

The electromagnetic properties of materials are characterised by parameters which include complex permittivity (ε*), complex permeability (μ*) and conductivity (σ) (Chen et al., 2004, Hippel, 1954, Schubert and Regier, 2005). Only the complex permittivity (ε*) and conductivity are significant to this work because vermiculite, which is the material under study, is an insulating material with low electrical conductivity due to its ionic water. Complex permittivity gives information about the energy coupling efficiency of electromagnetic waves with materials and controls microwave applicability for processing wide varieties of non-conductive materials (Schubert and Regier, 2005, Tang et al., 2002). Therefore detailed understanding of the dielectric properties of materials gives important information for predicting a mineral's behaviour under electromagnetic fields, and it also helps the microwave engineer in modelling and designing a suitable microwave applicator and choke systems for material processing (Roebuck and Goldblith, 2006, Metaxas and Meredith, 1983).

3.6.1 Complex Permittivity

Material dielectric properties dictate the response of the material to electromagnetic fields. It can be represented in complex form as the frequency function given as below.

$$\varepsilon^*(\mathrm{w}) = \varepsilon'(\mathrm{w}) - \mathrm{j}\varepsilon''(\mathrm{w}) \qquad \text{Equation 3–2}$$

Where $\varepsilon^*(\mathrm{w})$ is the complex permittivity; the real part, $\varepsilon'(\mathrm{w})$, known as the frequency dependent dielectric constant, is used as an indicative factor of the ability of material to be polarised and store electromagnetic energy. The imaginary part, $\varepsilon''(\mathrm{w})$, known as the loss factor, accounts for the power dissipation, internal loss mechanism, or the efficiency with which electromagnetic waves are converted to heat in the material (Kelleners and Verma, 2010, Fernández et al., 2011). These electrical properties for most materials are independent of electrical field strength (Frohlich, 1958). Generally, a materials' ability to convert microwave energy into heat energy is proportional to the value of its dielectric loss (Metaxas and Meredith, 1983).

The relationship between the real and imaginary parts of the complex permittivity is expressed as the loss tangent (Equation 3-3), expressed mathematically as the ratio of loss factor to the dielectric constant. This signifies a materials' ability to convert electromagnetic energy into heat (Meredith, 1998, Mingos and Baghurst, 1991).

$$\tan\delta = \frac{\varepsilon''}{\varepsilon'} \qquad \text{Equation 3–3}$$

The effective loss factor is the summation of losses due to polarisation and conduction mechanisms as expressed below.

$$\varepsilon''_{\text{effective}} = \varepsilon''_{\mathrm{d}}(\mathrm{w}) + \varepsilon''_{\mathrm{i}}(\mathrm{w}) + \varepsilon''_{\mathrm{a}}(\mathrm{w}) + \varepsilon''_{\mathrm{e}}(\mathrm{w}) + \varepsilon''_{\mathrm{c}}(\mathrm{w}) \qquad \text{Equation 3–4}$$

Where subscripts d, i, a, e and c denote dipole polarisation, interfacial, atomic, electronic, and ionic conduction respectively. Across the industrial microwave frequency range (100 MHz-3G Hz), ionic and dipolar polarisation are the prominent heating mechanisms in moist minerals including soil and clay minerals, while atomic and electronic polarization play no part in dielectric heating, as they cause heating in the high frequency infra-red and optical regions respectively (Metaxas and Meredith, 1983). Loss factor is therefore expressed in Equation 3-5 as the sum of a conduction and dipolar polarisation terms (Hallikainen et al., 1985). Where σ is the conductivity (Sm^{-1}), ε_0 is the permittivity of free space ($8.8542x10^{-12}$ Fm^{-1}) and the second function on the right hand side of the equation is the ionic conduction term.

$$\varepsilon''_{\text{effective}} = \varepsilon''_{\text{dipolar}}(\text{w}) + \frac{\sigma_{\text{c}}}{\omega\varepsilon_0} \qquad \text{Equation 3–5}$$

In this research, dielectric characterisation of vermiculite minerals from different geographical regions at ISM frequencies is required for studying the fundamentals of microwave vermiculite exfoliation, and for modelling and designing continuous microwave heating systems for its processing at industrial scale.

3.6.1.1 Variation of Dielectric Properties of Materials with Frequency

The dielectric properties of minerals are a function of several factors such as, frequency, temperature, moisture content, density, and structural composition of the materials. Understanding the variation in dielectric properties with these factors is vital for an optimum application of microwave energy for mineral processing (Marland et al., 2001, Nelson et al., 1991, Logsdon and Laird, 2003, Meredith, 1998). The dielectric properties of most materials, except that of very low loss materials, vary with the propagating frequency of the applied electric field. (Venkatesh and Raghavan, 2004, Sosa-Morales et al., 2010, Nelson, 1991). Figure 3-6 shows the contribution of ionic conduction, dipolar, atomic and electronic polarisation to the dielectric properties of a hypothetical material as a function of frequency. At low frequencies, near d.c., the dielectric constant has a maximum

value because there is sufficient time for the ionic conduction and all the polarisation mechanisms to follow the changing electric field and contribute significantly to the dielectric constant.

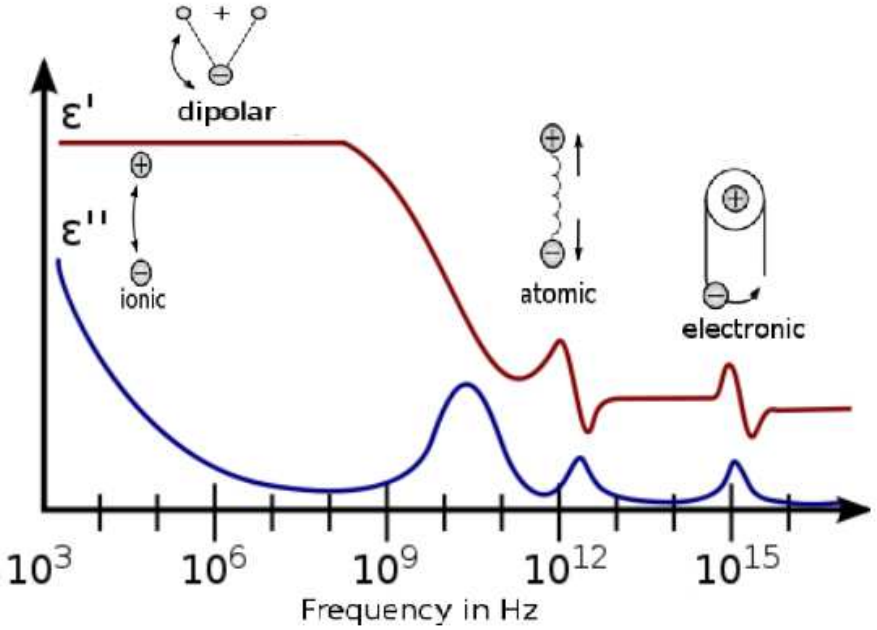

Figure 3-6: Frequency dependence of dielectric properties as a function of microwave heating mechanisms (Metaxas and Meredith, 1983)

With increasing frequency, the dielectric constant begins to fall as the relaxation frequency of the ionic conduction mechanism is below the operating frequency, and the relaxation frequency of dipolar polarisation is being approached. The dielectric constant reaches a minimum as the applied frequency is above the relaxation frequency of dipolar polarisation mechanisms. The dielectric constant then increases again when the relaxation frequencies of atomic and electronic polarisations are reached (Murphy and Morgan, 1937, Metaxas and Meredith, 1983, Venkatesh and Raghavan, 2004, Clark and Sutton, 1996). The sharp decrease of the effective polarisation, results in a fall in dielectric constant and a rise in the loss factor due to the dissipation of stored energy as heat within the material (Figure 3-6).

Table 3-2 shows the dielectric properties of selected clay minerals and soils at microwave frequencies. Feldspar, muscovite and phlogopite, which are examples of clay minerals, have low dielectric constant and loss factor. Both dielectric

constant and loss factor of muscovite and phlogopite decrease with an increase in frequency.

Table 3-2: Dielectric properties of selected clay minerals and soil (Meredith, 1998)

Material	Temp (°C)	ε'		ε''	
		1 GHZ	2.5 GHz	1 GHz	2.5 GHz
Feldspar 1.25 g/cm^3	24	2.61	2.61	0.024	0.020
Muscovite 0.45 g/cm^3	24		1.62	0.006	0.005
Phlogopite 0.7 g/cm^3	24	2.1	2.04	0.014	0.11

3.6.1.2 Variation of Materials Dielectric Properties with Temperature

Industrial minerals have different physical and chemical properties at different temperatures; therefore, the variation of dielectric properties of minerals with varying temperature is an important factor in their processing (Meredith, 1998, Komarov et al., 2005b). Complex permittivity may increase or decrease with temperature depending on the physical and chemical properties, such as moisture content, chemical composition and charge distribution (Venkatesh and Raghavan, 2004, Schubert and Regier, 2005). The temperature dependence of dielectric properties is a function of dielectric relaxation frequency and operating frequency. Thus, an increase in temperature decreases the value of relaxation time and shifts the peak in loss factor to higher frequencies. An increase in temperature of the treated sample increases the dielectric constant in the region of dispersion while loss factor may either increase when the operating frequency is higher than the relaxation frequency or decrease when the operating frequency is lower than the relaxation frequency. Outside the range of dispersion, the dielectric constant of a material decreases with an increase in temperature (Venkatesh and Raghavan, 2004, Nelson, 1994). The loss factor of moist materials generally increases with increasing temperature up to 100 °C at low frequency (<200 MHz) due to the effect of ionic conduction (Guan et al., 2004), but free water dispersion at microwave frequency

(915 MHz and 1.8 GHz) causes a decrease in loss factor with an increase in temperature (Sosa-Morales et al., 2010).

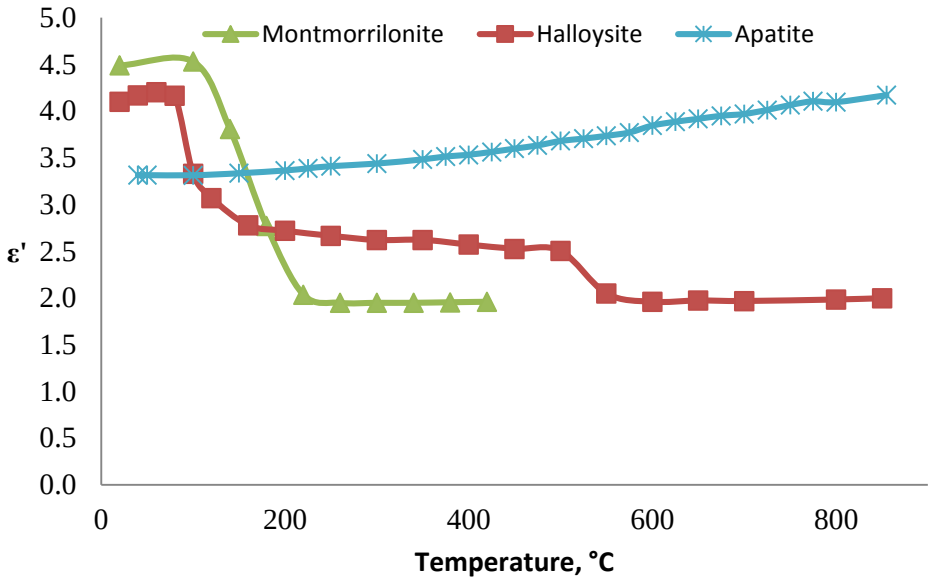

Figure 3-7: Variation of dielectric constant of selected mineral with temperature (Kobusheshe, 2010)

Figure 3-7 and Figure 3-8 show the variation of dielectric constant and loss factor of selected minerals with temperature as reported by Kobusheshe (2010). The result shows that both the dielectric constant and loss factor of montmorillonite and halloysite decreased with an increase in temperature while that of apatite increased with an increase in temperature. Montmorillonite ($Al_2Si_4O_{10}(OH)_2$.nH2O), is a 2:1 dioctahedral smectite with interlayer water sandwiched in its interlayer space. Halloysite is 1:1 phyllosilicate clay mineral with monomolecular water and cation in its interlayer space (Grim, 1968). On dehydrating halloysite by heating, it changes into kaolinite structure due to the removal of its interlayer water (Sakiewicz et al., 2011). The presence of water bearing phases (H_2O and OH) contributes to the decrease in the loss factor in montmorillonite and halloysite due to the dissipation of energy by dipolar polarisation. The increase in the dielectric constant and loss factor of apatite with temperature may be due to the absence of molecular water in its structure and its microwave heating effect may be due to the ionic conduction.

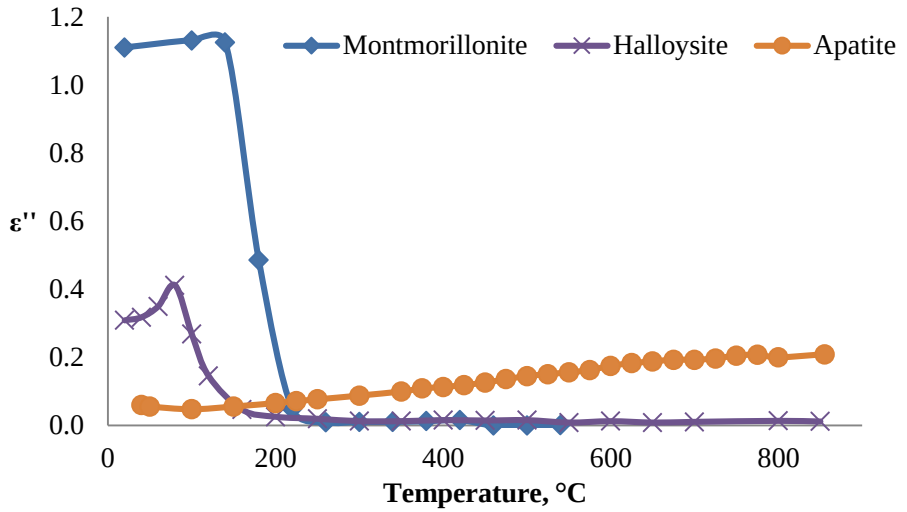

Figure 3-8: Variation of loss factor of selected minerals with temperature (Kobusheshe, 2010)

3.6.1.3 Variation of Materials Dielectric Properties with Moisture Content

Many applications of microwave processing of minerals involve drying or dehydration of the workload through the removal of moisture. This is the main process involved in the exfoliation of vermiculite as the interlayer water in the vermiculite structure is rapidly heated and escapes from the silicate sheets. Therefore, variation in dielectric properties with moisture content plays a significant role in microwave processing of hydrated minerals including vermiculite (Metaxas and Meredith, 1983). Generally, the higher the moisture content of a material, the larger the value of its dielectric properties due to the occurrence of the water molecules. In descending order of mobility, water in dielectric materials can be divided into free water, which exists in capillaries and intercellular space, and multilayer and monolayer bound water, tightly bound to the molecular structure of the material (Metaxas and Meredith, 1983, Komarov et al., 2005a). Dielectric spectroscopy studies of water reveal three relaxation domains of KHz, MHz, and GHz for ice, bound and free water respectively. Relaxation time of ice, τ_{ice} is higher than that of bound water τ_{bw} while that of free water is least ($\tau_{ice} > \tau_{bw} > \tau_{fw}$) (Boyarskii et al., 2002, Hasted, 1973)

As moisture is removed from a hydrated material during microwave processing, the average dielectric properties of the material decrease rapidly until a critical value of moisture content below which the decrease in loss factor is insignificant because of presence of bound water (Komarov et al., 2005a, Metaxas and Meredith, 1983). Dry soil behaves as an insulating material of very low loss factor and high resistivity, but the conductivity and complex permittivity increase with increasing water content at microwave frequencies due to an increase in the percentage of polar material that interacts with the electromagnetic wave. (Ponizovsky et al., 1999, Boyarskii et al., 2002, Cosenza and Tabbagh, 2004). It has been reported that the dielectric constant of soil varies between 2-3 for dry soil and up to 20 depending on the soil moisture content while the loss factor of dry soil is less than 0.5 and increases to greater than 4 as the moisture content increases (Venkatesh and Raghavan, 2004, Hoekstra and Delaney, 1974). Table 3-3 shows the increase in dielectric properties of loamy and sandy soils with increasing moisture content.

Table 3-3: Effects of moisture content on dielectric properties of soil (Meredith, 1998)

Material Soil	Temp. (°C)	$\varepsilon'/\varepsilon''$		
		30MHz	1GHz	2.5GHz
Loamy, 0% H_2O	25	2.48/0.03	2.46/0.008	2.44/0.004
Loamy, 14% H_2O	25	17/10	20/2.5	20/2.5
Sandy, 0% H_2O	25	2.55/0.033	2.55/0.012	2.55/0.007
Sandy, 17% H_2O	25	20/0.3	20/0.3	17/0.3

The increase in the dielectric properties of soil with increasing water content is due to the high values of dielectric properties of water.

3.6.1.4 Variation of Dielectric Properties with Density

A mineral's density has a significant effect on its dielectric properties since the interaction of electromagnetic waves with materials is a function of the interacting mass (Nelson, 1994). This effect is more pronounced in particulate or granular materials, which are multiphase mixtures of air and solids. Results of previous work

on granular materials showed that both dielectric constant and loss factor increase with an increase in the material bulk density due to a reduction in voidage. Different relationships have been developed by various workers to predict the dielectric properties and moisture content of materials using their density relationships (Maron and Maron, 2004, Asami, 2002, Dube and Parshad, 1969, Goncharenko, 2003, Nelson et al., 1991, Nelson S.O and You T.S, 1989, Nelson, 2005, Hilhorst et al., 2000). Figure 3-9 and Figure 3-10 show the positive density dependence of the dielectric properties of phlogopite and muscovite, which are examples of phyllosilicate clay minerals similar to vermiculite being studied in this research project.

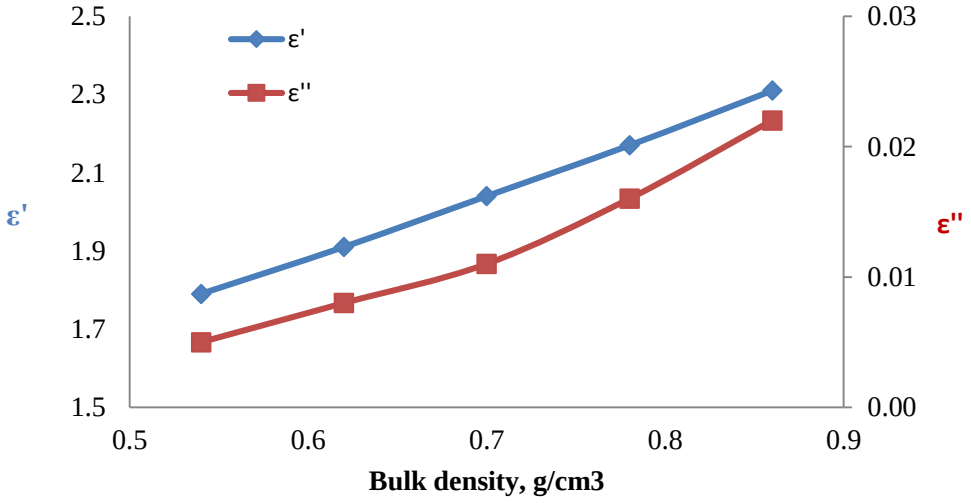

Figure 3-9: Density dependence of dielectric properties of phlogopite (Nelson et al., 1989)

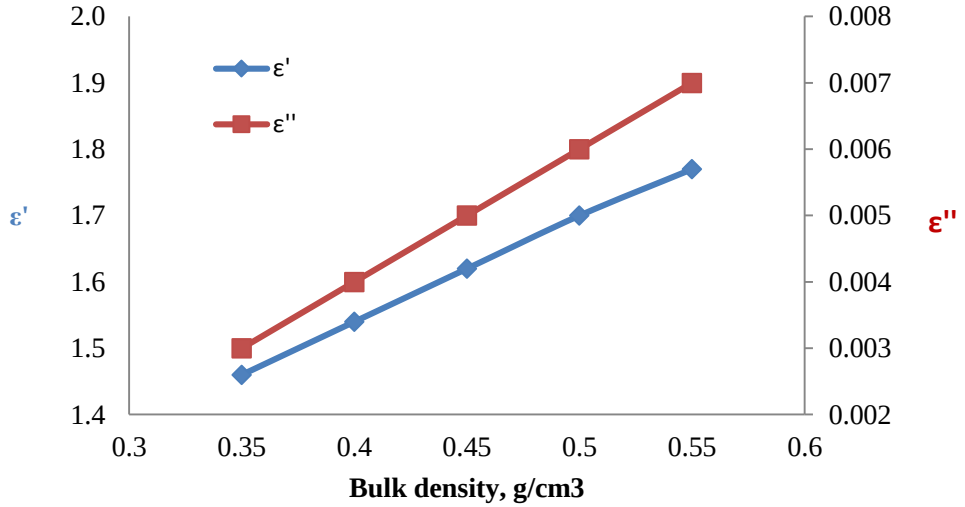

Figure 3-10: Density dependence of dielectric properties of muscovite (Nelson et al., 1989)

3.7 Microwave Interaction with Dielectric Materials

3.7.1 Power Density

Microwave processing of materials involves the conversion of electromagnetic energy to heat within the material heated phase. The rate at which microwave power is absorbed or dissipated as heat in the workload is expressed as a power density. In dielectric materials, which are insulators and non-magnetic, only the losses due to the electric field contribute to the absorbed power as the magnetic losses are negligible. Therefore the power density created in the heated phase is expressed as Equation 3-6, where P_v is the power density (W/m^3) created in the workload, f is the frequency in Hertz (Hz), E is the electric field intensity inside the workload (V/m^{-1}). This equation is suitable for a material with no magnetic constituents where only the effect of electric loss is significant. In a material with magnetic constituents, magnetic losses due to the magnetic field also play significant effect in the heating mechanism.

$$P_v = 2\pi f \varepsilon_0 \varepsilon'' |E|^2 \qquad \text{Equation 3-6}$$

Equation 3-6 shows that the power density is directly proportional to the frequency, loss factor and the square of electric field intensity inside the material. Thus, the higher the frequency the smaller the electric field required for specific power dissipation, assuming a constant loss factor (Gupta and Eugene, 2007, Metaxas and Meredith, 1983, Behari, 2005).

3.7.2 Microwave Penetration Depth into materials

During the interaction of microwave energy with a dielectric material, the amplitude of the incident wave falls due to the absorption of microwave power in the material. In the absence of reflected waves in the material, the power density falls with depth in the material (Hippel, 1954, Meredith, 1998). The microwave penetration depth 'D_p' in meters is defined as the depth into a workload where the electric field intensity and associated power flux drop to e^{-1} (~37%) of its value at the material surface. The general expression of penetration depth is given by Equation 3-7.

Where λ_0 is the wavelength of the electromagnetic wave in meters (m), and ε' and ε'' are dielectric constant and loss factor of material, respectively (Mehdizadeh, 2010, Meredith, 1998).

$$D_p = \frac{\lambda_0}{2\pi\sqrt{2\varepsilon'}} \frac{1}{\sqrt{\left[\left\{1+\left(\frac{\varepsilon''}{\varepsilon'}\right)^2\right\}^{\frac{1}{2}}-1\right]}}$$ Equation 3-7

For low loss materials (ε''<<<ε'), Equation 3-7 becomes Equation 3-8. (Although with approximately 10% error).

$$D_p \approx \frac{\lambda_0\sqrt{\varepsilon'}}{2\pi\varepsilon''}$$ Equation 3-8

From the Equation 3-8, it is shown that the higher the value of the wavelength (lower frequency), the higher the penetration depth. Penetration depth also decreases with an increase in value of loss factor. Materials with a loss factor between limits 0.01-5 are regarded as suitable for microwave heating. Materials with loss factors less than 0.01 would require high electric field to ensure a sufficient temperature rise, while a material with a loss factor higher than five produces a low penetration depth. This is due to the high rate of microwave absorption by the material, with most of incident power being absorbed within the first few millimetres of the material resulting to nonhomogeneous surface heating (Chan and Reader, 2000, Metaxas and Meredith, 1983).

In conductive materials such as copper, aluminium and steel, microwave interaction is limited to the skin depth defined as the distance where the electromagnetic field is attenuated to 1/e of its surface value (Metaxas and Meredith, 1983). Where μ is real part of permeability, σ and ω are electrical conductivity and angular frequency.

$$\delta = \sqrt{\frac{2}{\sigma\omega\mu_o}}$$ Equation 3-9

Skin depth is frequency dependent and decreases with an increase in propagation frequency of electromagnetic waves. Skin depth of copper at 2.45 GHz is 1.3μm

and is difficult to heat bulk sample by microwave energy as incident microwaves energy are attenuated close to the surface, but in the case of powder material the heat induced is very significant because of the high surface area (Mondal et al, , 2009, Sun et al., , 2005b).

3.7.3 Microwave Heating Rate

In high-temperature microwave heating, such as sintering of ceramics, metal and glass, volumetric temperature rise of the heated material is important (Mehdizadeh, 2010, Clark et al., 2005). In thermodynamics, the power required to bring about an increment in the temperature (ΔT) of a unit mass (kg) of material in a period of time (Δt) in seconds is given by:

$$\text{Power} = \frac{mC_p \Delta T}{\Delta t} \qquad \text{Equation 3-10}$$

An expression for the volumetric rate of temperature rise ($\Delta T/\Delta t$) in microwave treated materials is given as Equation 3-11, when the thermodynamic equation is related to microwave heating by combining Equation 3-10 for the power absorbed by the material to Equation 3-6 for the power density in the heated material. Where C_p is the material specific heat capacity (J/kg°C), ρ is the material density (Kg/m^3) and $\Delta T/\Delta t$, is the rate of temperature change of the material.

$$\frac{\Delta T}{\Delta t} = \frac{2\pi f \varepsilon_0 \varepsilon'' |E|^2}{\rho C_p} \qquad \text{Equation 3-11}$$

It is assumed that the electric field distribution is uniform throughout the material and that there is no heat losses from the material surface (Oghbaei and Mirzaee, 2010, Tierney and Lindstrom, 2005). It is shown by Equation 3-11 that the conversion efficiency of microwave energy into heat energy in a workload is directly proportional to the dielectric loss factor and square of electric field strength (Mingos and Baghurst, 1991).

3.8 Measurement Techniques for Dielectric Properties

Microwave processing of foods and minerals has received huge attention in both domestic and industrial applications, and in the academic research environment. A high precision measurement of dielectric properties of materials is vital for exploring these applications. Various dielectric property measurement techniques, which include coaxial probes, cavity perturbation, waveguide, free space, resistivity cell, time domain reflectometry, parallel plate, lumped circuit, and waveguide transmission line, are used for material dielectric property characterisation, and numerous review papers on characterisation of materials electromagnetic properties have been published (Gregory and Clarke, 2006, Hasar, 2010, Sheen et al., 2007, Sheen, 2009, Max Sucher and Fox, 1963, Komarov et al., 2005a, Chao, 1985).

These different measurement techniques are grouped into resonant and non-resonant methods, based on the methods of propagation of electromagnetic waves and measurements of electromagnetic parameters. Each of these techniques has specific advantages and disadvantages, and the choice of a particular technique for dielectric characterisation depends upon the physical properties of the material, the required frequency and temperature ranges, accuracy, cost and availability of the necessary equipment. The dielectric properties measurement techniques used in this project are rectangular waveguide and the cavity perturbation.

3.8.1 Rectangular Waveguide Technique

This is a non-destructive transmission-reflection non-resonant method of measuring both the complex permittivity and complex permeability of completely loaded low, medium and high loss materials. The measured materials may be in solid, liquid or granular form. In contrast to resonant techniques, this method gives details of a materials complex permittivity over a wide range of frequencies and requires less sample preparation (Hasar, 2010, Gregory and Clarke, 2006, Baker-Jarvis et al., 1993, Hippel, 1954). The physics of this method is based on the scattering parameters (S11: reflected signal and S21: transmitted parameter) of the rectangular waveguide filled with a dielectric sample under study and the dielectric properties are determined from the measured reflection coefficient and transmission

coefficient. Unlike the cavity perturbation technique, this method requires rigorous calibration of the system prior to use.

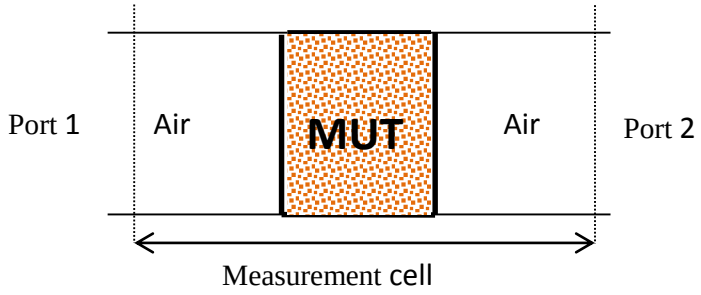

Figure 3-11: Waveguide technique for dielectric measurement

During the measurement, the material under test (MUT) is placed in a waveguide transmission line sample holder known as the waveguide cell as shown in Figure 3-11. When microwave energy is transmitted to the measured sample by means of a vector network analyser (VNA), part of the signal is reflected from the sample while the rest is absorbed by the sample or propagated through it. The S-parameters are measured by the VNA in the frequency domain and can then be used to compute the complex permittivity by using an algorithm with either iterative or non-iterative techniques (Chen et al., 2004, Ebara et al., 2006). The technique has been employed for the measurement of dielectric properties of both solid and liquid materials (Belrhiti et al., 2012, Wang and Afsar, 2003, Ebara et al., 2006).

3.8.2 Cavity Perturbation

Though regarded as the most suitable method for measuring material dielectric properties at frequencies above 100MHz, it is also considered a more accurate and simpler technique for measurements above 600 MHz. It is generally designed for high temperature measurements of dielectric materials (Marland et al., 2001, Greenacre, 1996). The available frequencies of measurement in this method depend on the resonant mode of the cavity used. This also limits the range of frequencies that can be measured (Greenacre, 1996, Chen et al., 2004, Max Sucher and Fox, 1963). The method is generally used for measuring the dielectric properties of low loss solid materials, especially in powder form, and is also used for measurement of low loss liquid substances (Metaxas and Meredith, 1983, Komarov et al., 2005a).

This technique is used in this project to determine the dielectric properties of vermiculite particulate.

The physics of this technique are based on the perturbation of a resonant cavity, when a small volume of sample is introduced into it, followed by the relative analysis of the electromagnetic characteristics of the empty and partially loaded resonance cavity. This is in order to separate the influence of the material on the characteristics of the cavity (Hippel, 1954, Raju, 2003, Venkatesh and Raghavan, 2005, Donovan et al., 1993). Figure 3-12 shows the basic components of a system designed for using the cavity perturbation technique for dielectric property measurement of materials. The system consists of an insulated cylindrical copper cavity placed underneath a conventional furnace, that is capable of supporting heating to temperature up to 1800^{o}C (Tinga and Xi, 1993). A microwave transparent quartz tube and low loss fibreglass act as the sample holder, and are both attached to a computer controlled robotic arm, which moves the measured sample vertically upward and downward into the furnace and cavity respectively. A VNA is used for transmitting energy to the system and for detection and determination of frequency shift and quality factor when the dielectric material inserted is inserted.

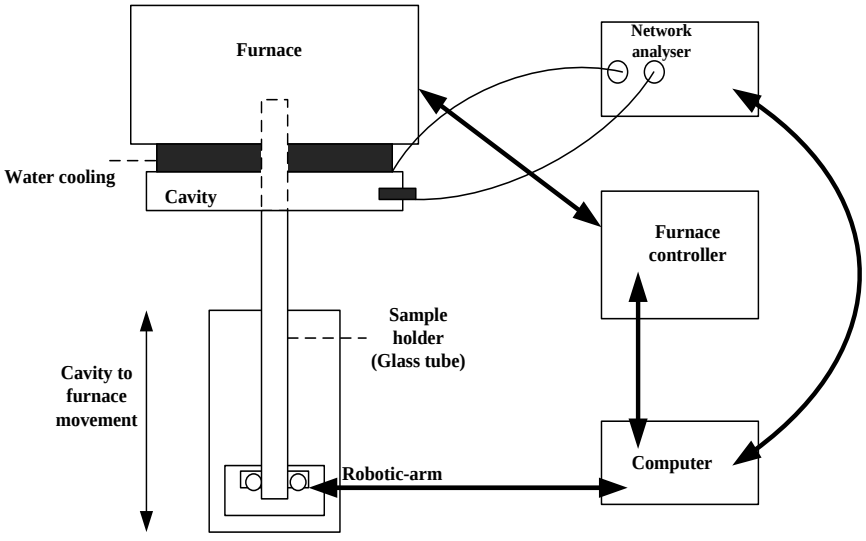

Figure 3-12: Basic components of cavity perturbation technique for measurements of dielectric properties

Dielectric constant and loss factor are computed from the solution of Maxwell's equations, derived from perturbation theory using an appropriate boundary condition corresponding to the cavity dimensions (Venkatesh and Raghavan, 2005, Greenacre, 1996).

$$\varepsilon'' = J_1^2(x_{1,m})\left(\frac{1}{Q_1} - \frac{1}{Q_2}\right)\frac{V_c}{V_s} \qquad \text{Equation 3-12}$$

$$\varepsilon' = 1 + 2J_1^2(x_{1,m})\frac{f_0 - f_1}{f_0}\frac{V_c}{V_s} \qquad \text{Equation 3-13}$$

Where, V_c = Cavity volume (m^3), Vs = volume of sample (m^3), f_0 = Resonant frequency of the empty cavity (Hz), f_1 = Resonant frequency of the cavity with sample (Hz), J_1 = First order Bessel function, Q_1= quality factor of empty cavity, the Q_2= quality factor of the cavity with dielectric material, and $x_{1,m}$ = function of air filled cavity.

3.9 Microwave Processing System Design and Selection

Figure 3-13 shows the block diagram of the main components of microwave system, though this can be modified according to the specific need of the project.

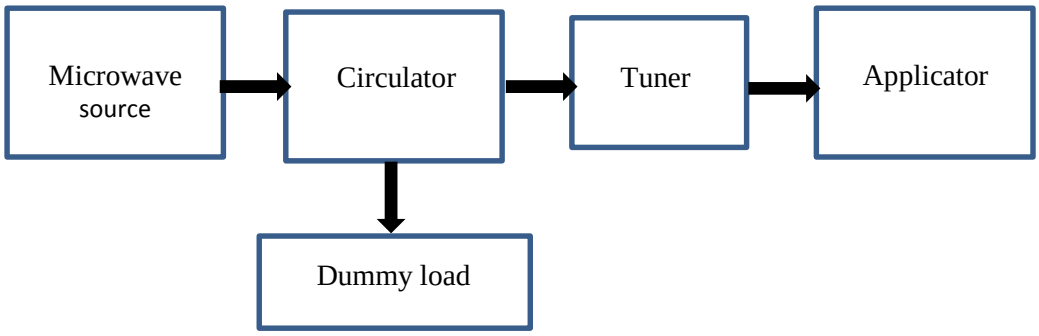

Figure 3-13: Block diagram of microwave processing system

The microwave generating device generates the electromagnetic energy directly incident on the workload (Das et al., 2008). Waveguide is a transmission device which conveys the propagated microwave energy from the source to the applicator, where the energy is absorbed by the material (Das et al., 2008, Thostenson and Chou, 1999). The design of these three main components is governed by complex Maxwell's equations using approximate boundary conditions.

In-between the applicator and the microwave-generating source are the adjustable tuner and circulator. The circulator protects the magnetron by redirecting the excess microwave energy reflected back from the load. The excess microwave energy may be redirected to a dummy load, which is usually water because of its high microwave absorbing capacity. The function of the tuner is to match the impedance (resistance) of the microwave source and the transmission line to that of the load, thereby maximising the microwave absorbed by the workload and minimising the power reflected.

3.9.1 Devices for Generating Microwaves

Microwaves are generated as a result of the movement of electrons accelerating along a large potential difference in an orthogonal magnetic field. This magnetic field causes the oscillation of these electrons in a helical path (Sobby and Chaouki, 2010). Some of the vacuum tubes used for microwave generation are magnetron, klystron, extended interaction oscillator (EIO), permanent magnet gyrotron and travelling wave tubes (TWT). Selection of microwave sources is a function of the cost, efficiency, frequency stability and power (Metaxas A.C; Meredith R.J, 1988). Most domestic, industrial and commercial microwave processing systems use magnetrons as the generating device because of its high power output, higher efficiency, frequency stability and relatively low cost (Metaxas A.C; Meredith R.J, 1988), therefore its operational principle is discussed in this thesis.

Magnetrons, shown in Figure 3-14, are a high vacuum electronic valve consisting electron-emitting cathode surrounded by hollow copper anode. It is the most commonly used microwave source for domestic and industrial microwave heating and Its usage is around about 98% of all installations (Metaxas, 1996).

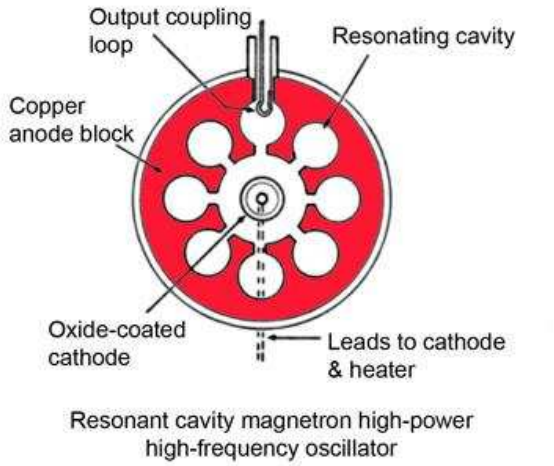

Figure 3-14: travelling wave resonant cavity magnetron

The anode has a set of vanes that project radially inward to form slots, which are approximately $\lambda/4$ between them and therefore resonate at the microwave frequency (Metaxas and Meredith, 1983, Schubert and Regier, 2005). It can generate either continuous or pulsed power up to megawatt and operating frequency between 1-40 GHz. The power efficiency is about 85% with a lifetime close to 5000 hours (Chandra, 2011). Two large pole pieces of magnets produce magnetic field normal to the cavity plane and the anode is at higher potential relative to the cathode. The interaction in magnetron depends on the motion of electrons in an orthogonal electric and magnetic field. Trajectory and velocity of these electrons are determined by the d.c. electric field strength and magnetic field strength in the space between the anode and the cathode. The magnetic field strength or the tube current controls the power output of magnetron and the maximum power is limited by the anode temperature. The 2.45 GHz can achieve maximum power of 1.5 kW and 25 kW for air or water-cooled anodes respectively (Schubert and Regier, 2005, Metaxas, 1996, Thostenson and Chou, 1999).

3.9.2 Microwave Transmission Devices

Transmission line guided the microwave energy generated by the microwave source to the microwave applicator, where the interaction of electromagnetic waves with the materials to be processed takes place. Type of transmission line used depends

on the power of propagated microwave. Coaxial cable can be used to transmit low power microwave, but it produces significant losses at high power and frequency. Therefore, at high microwave power and frequency, waveguide is used for transmission owing to its low losses at high frequency (Thostenson and Chou, 1999, Chan and Reader, 2000). Only the waveguide, which is used in this project for transmitting microwave energy into the cavity, is discussed in this thesis.

Waveguide consists of hollow metallic tubes of constant cross section, which are either rectangular or circular in shape. Transverse electric (TE) and transverse magnetic (TM) are the two possible modes of microwave propagation in waveguides (Chan and Reader, 2000, A.C Metaxas and R.J. Meredith, 1983). Figure 3-15 shows the TE and TM modes in a waveguide system.

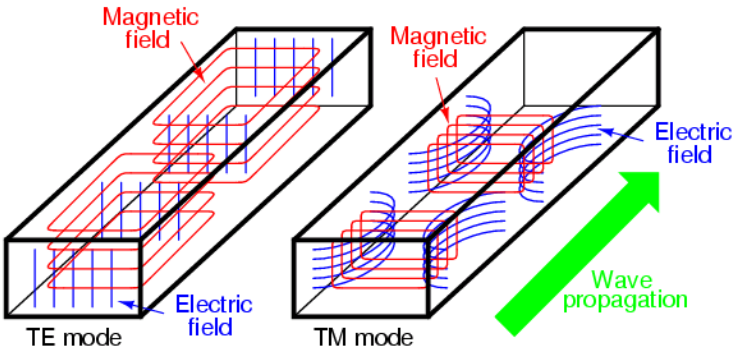

Figure 3-15: Transverse electric (TE) and transverse magnetic (TM) waveguide (http://www.allaboutcircuits.com/vol_2/chpt_14/8.html)

For the TE mode, the electric line of force is perpendicular to the axis of waveguide and the electric field component in the direction of propagation is zero ($E_z = 0$) while for TM mode, the magnetic line of force is perpendicular to the axis of waveguide and the magnetic field component in the direction of propagation is zero ($H_z = 0$) (Meredith, 1998, Chan and Reader, 2000). Energy is carried by the electric and magnetic fields associated with the wave and there is a possibility of having several modes of propagation (Chan and Reader, 2000, Thostenson and Chou, 1999).

3.9.3 Microwave Heating Applicators

Microwave applicators are metallic enclosures where microwave interaction with dielectric materials takes place. The applicator enables coupling of the microwave energy into the workload volume to a level sufficient to causes a temporary or permanent change in the workload property (Mehdizadeh, 2010). Their design is essential to microwave heating since the temperature distribution pattern within the heated material depends on the electric field distribution in the applicator (Thostenson and Chou, 1999, Metaxas and Meredith, 1983). The single mode and multimode microwave heating cavities commonly used for domestic, laboratory research and industrial heating applications are discussed in this section. The types of applicator used for materials processing depends on the processing requirement and electromagnetic properties of materials to be processed (Chan and Reader, 2000, Bradshaw et al., 1998).

3.9.3.1 Single Mode Cavities

This type of cavity supports only one resonant mode and its size is of the order of approximately one wavelength. To support this single resonant mode, it requires a microwave source that has little frequency variation and the size of this type of cavity is within the vicinity of operating wavelength or slightly higher. The electromagnetic field pattern is well defined and can be easily determined by solving Maxwell's equations using suitable boundary conditions either by using analytical or numerical method. Therefore, areas of high and low electromagnetic distributions are well known. The single mode cavity has only one hot spot where electric field intensity is highest and the processed material is placed at this region for optimum heating as shown in Figure 3-16, which is a single mode cavity made of waveguide that is shorted by a short tuner at one end and microwave is fed from the other end (Chan and Reader, 2000, Metaxas and Meredith, 1983, Mehdizadeh, 2010).

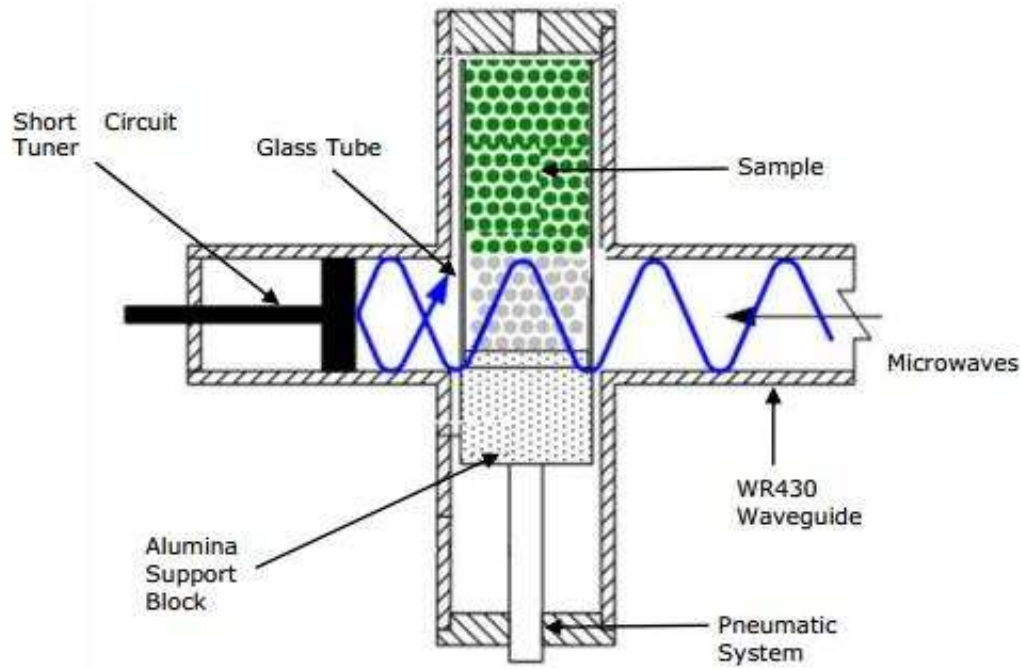

Figure 3-16: Schematic diagram of microwave single mode cavity (Kobusheshe, 2010)

The magnetic field with its maximum located at a position different from that of the electric field is also set up in this type of cavity and this makes it a suitable cavity for processing magnetic materials. Applying the same microwave power, a single mode cavity will produce higher electric field strengths than other form of applicator, and it is, therefore, useful for processing of low loss materials such as ceramics and quartz, which are difficult to heat to high temperatures (Metaxas and Meredith, 1983, Hassler and Johansen, 1988, Huanga et al., 2009, Sutton, 1992).

Some of the advantages of using single mode cavities are ease of design and construction, homogeneity of the electromagnetic field, especially in a targeted zone of the applicator, sensitivity and predictable high field zone. Another advantage is the separation of the location of electric and magnetic field, and this feature has been used by some researchers for the microwave metal sintering (Gupta and Eugene, 2007, Leonelli et al., 2008, Demirskyi et al., 2010). Due to small size and geometry, only small sizes of material can be processed using this cavity even at 915MHz and the cavity requires continuous tuning (Chan and Reader, 2000,

Mehdizadeh, 2010). Other limitations of this type of cavity include high cost per load volume and ease of arcing due to creation of high field zones.

3.9.3.2 Multimode Cavities

Multimode cavities are the most common class of high-frequency applicator used for processing of materials. An example of this class of applicator is the domestic microwave oven, which is essentially a closed metal box with a magnetron for microwave generation with no need for a sophisticated tuning device (Metaxas and Meredith, 1983). It is also used for many low power and high power industrial microwave installations. In principle, multiple resonant modes are supported in a given frequency range in this kind of microwave cavity, owing to multiple superposition of incident and reflected waves, governed by the cavity dimensions and nature of workload (Metaxas and Meredith, 1983, Chan and Reader, 2000). The number of possible resonant modes is proportional to the size of the applicator, and this is usually larger than one wavelength in each dimension. The relationship between the cavity resonant frequency and its geometry is given as Equation 3-14, where f_0 (Hz) is the resonant frequency, a, b and c are the dimensions (meters) in the x, y and z directions respectively, C is the speed of light (m/s) and indices m, n and k represent any integer (zero inclusive).

$$f_0 = \frac{C}{2}\sqrt{\left(\frac{m}{a}\right)^2 + \left(\frac{n}{b}\right)^2 + \left(\frac{k}{c}\right)^2} \qquad \text{Equation 3-14}$$

A typical electric field pattern obtained in the multimode cavity is shown in Figure 3-17. In an empty cavity, a sharp resonance response is given by the obtained modes at a given frequency but the quality factor of each modes is reduced when the cavity is partly filled with workload (Metaxas and Meredith, 1983). The presence of multiple resonant modes gives rise to multiple hotspots within the cavity and resulting in uneven heating of the material to be processed. This non-homogeneous heating effect can be minimised by using turntables as in domestic microwave ovens. The multimode heating cavity is not suitable for heating low loss materials and process that involves high temperature heating because the energy is dissipated over a large volume (Chan and Reader, 2000).

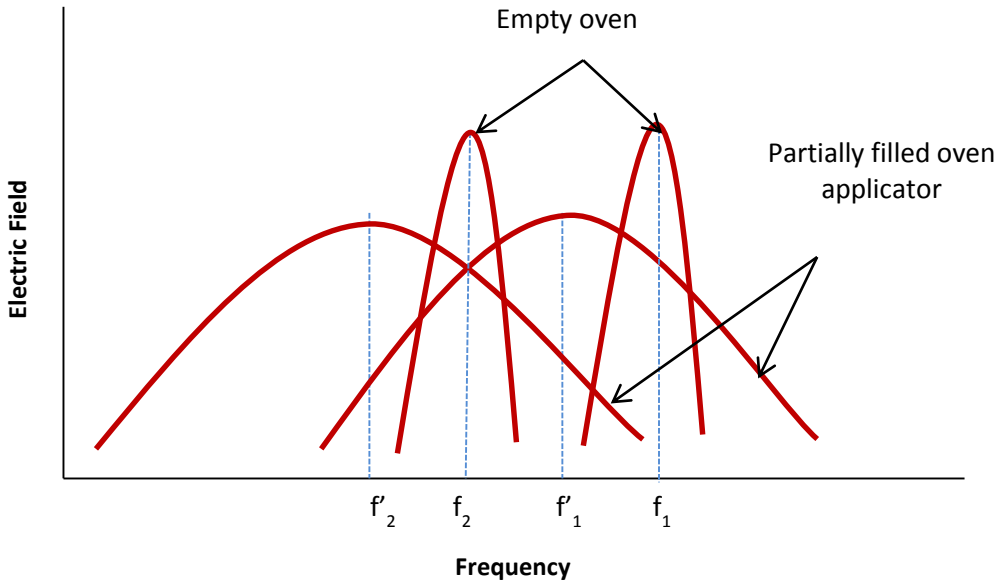

Figure 3-17: Frequency shift and damping of mode patterns due to the loading effect of the dielectric in the multimode oven (Metaxas and Meredith, 1983)

Advantages of this type of cavity are possibility of installing multiple microwave inlets, large dimensions, low cost, and ease of construction (Metaxas and Meredith, 1983, Chan and Reader, 2000, Thostenson and Chou, 1999). This type of applicator is industrially suitable for the processing of food materials and microwave induced chemical reactions (Bows, 2000). Figure 3-18 is a schematic of a multimode oven applicator used for continuous industrial processing of bulk materials.

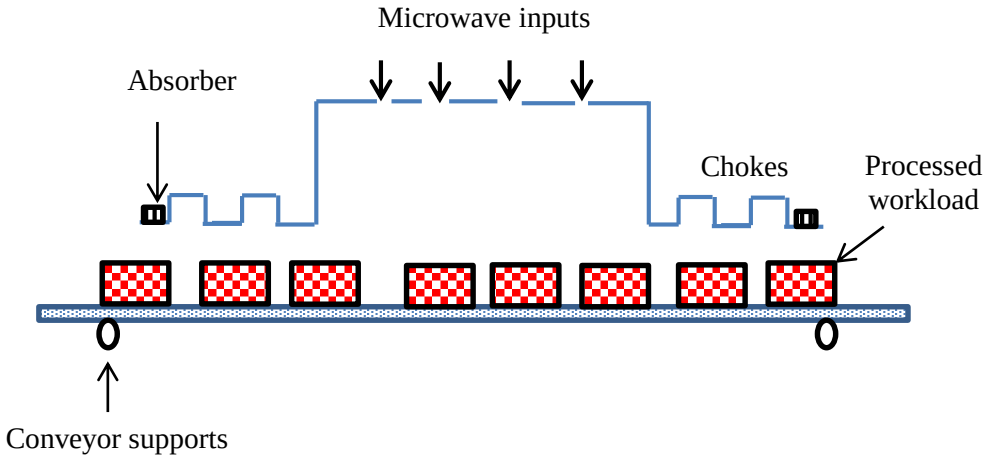

Figure 3-18: Multimode oven applicator for industrial tapering of meat (Metaxas and Meredith, 1983)

It incorporated four magnetrons for microwave generation and microwave leakage is minimised by the absorptive and the reflective choke system (Metaxas and Meredith, 1983).

3.9.4 Other Components in Industrial Microwave Systems

Circulators, directional couplers and tuners are other important components of microwave system. Theoretically, zero reflection of microwave energy from the load occurs when the losses of the load and the cavity walls are equal to the impedance of the waveguide. Interestingly, this may not be possible in reality because the impedance of the heating system may be affected by a slight variation in the characteristics of the heating cavity due to temperature, chemical or phase change (Chan and Reader, 2000). Therefore, a circulator, which is a directionally dependent microwave device, is used to redirect the reflected waves into a dummy load, which is usually water. This is usually installed in a microwave system to prevent the magnetron from damage because of reflected waves. A three-port circulator is the most common type of circulator used. In this device, one port of the circulator is connected to the applicator, another to the microwave source and the third port is connected to a dummy water load, which adsorbs reflected microwave power. This is important, especially when the workload is a poor microwave absorber. A directional coupler can be used to measure the forward and reflected power during microwave heating as these results help researchers to investigate the coupling capability of workload with microwave energy (Thostenson and Chou, 1999, Chan and Reader, 2000, Schubert and Regier, 2005).

3.10 Electromagnetic Compatibility (EMC) and Health and Safety

Industrial microwave heating of materials involves installation of equipment with the potential to increase health and safety risks owing to the possibility of emission of microwave energy to the environment, through the open tunnel or the aperture of the system and also from the use of very high voltages. The potential hazards from the leakage of microwave energy from an applicator or tunnel can be categorised into two groups. The first form of hazard, which falls within the health and safety

regime, relates to the direct hazard to the personnel and the people in the immediate environment. The other form of hazard, termed electromagnetic compatibility (EMC) relates to interference of microwave energy, which has the potential to cause electromagnetic disturbances of radio and telecommunications, or the malfunctioning of electronic components and equipment (Meredith, 1998, Metaxas and Meredith, 1983).

Different regulating bodies enforce exposure standards, which deal with the limits of electromagnetic exposure to human beings. In the United States, exposure limits range from 1 W/m^2 to 1000 W/m^2. The former value is regarded as the safest under all conditions while exposure above the latter figure is considered dangerous (John and Ronald, 2003). In the UK, The National Radiological Protection Board (NRPB) provides advice on limiting the exposure of people to electromagnetic fields, based on the outcome of the research conducted by the International Commission on Non-ionising Radiation Protection (International Commission on Non-Ionizing Radiation Protection (ICNIRP), 1998, ICNIRP, 2009). The unit of measurement by the ICNIRP is specific absorption rate, which is the rate of absorption of electromagnetic energy per unit mass. For controlled (occupational) and uncontrolled (public) environments, limits were set as 0.4 W/kg and 0.08 W/kg (NRPB, 2004). For industrial microwave heating, the accepted levels for microwave energy leakage are below 10 mW/cm^2 and 5 mW/cm^2 at 2450 MHz and 896 MHz respectively, over an exposure time of 6 min for both frequencies measured at a distance of 5 cm from the equipment (NRPB, 2003, Meredith, 1998, NRPB, 2004).

The closeness of the ISM frequencies and those used for communications and telecommunications compels directives and legislation that control electromagnetic compatibility, and limit electromagnetic interference with other devices. The EMC standard requirements are many orders of magnitude stricter than the above limits for health and safety and vary between different continents and often countries. For example in Europe, the accepted level of microwave energy emissions is 47dB (μV/m) at distance of 10m from the equipment between 230MHz to 1GHz. The limits at a distance of 3m from the installation are 76dB (μV/m) and 80dB (μV/m)

for a frequency regime of 1 GHz-3 GHz and 3 GHz-6 GHz respectively (BS EN 55103, 2012).

To ensure that microwave leakage is detected and hence minimised, microwave leakage meters are used. Such devices comprise a thermal sensor (thermistor or thermocouple) which is heated by the microwave flux. The intensity of the temperature change is proportional to the magnitude of the microwave flux, which the device recorded as mW/cm^2. In addition, different types of specialized equipment, collectively termed chokes are used to reduce microwave leakage to acceptable levels. The two types of chokes used are resistive and the reflective chokes, based on the method used to attenuate the escaping microwave energy (Meredith, 1998).

Although, some researchers have carried out extensive work on the design, simulation and construction of microwave chokes and filters (Catalá-Civera et al., 2006, Koughnett and Dunn, 1973, Kusama et al., 2002), but it is dangerous and not advisable to use their results directly in the design of chokes for a new microwave system for the following reasons:

- In designing and commissioning of microwave chokes, accurate verification of the electrical specification of the proposed chokes must be carried out at the operating conditions for comparison with the permissible levels. However, most of the chokes design from the literature did not consider wide range of operating conditions but they are designed considering specific fixed condition.
- The frequency stability of the microwave magnetron is influenced by the load, which infers that that the chokes will behave differently with different processed feedstock (Mehdizadeh, 2010). Nonetheless, many of the chokes discussed in the literature used specific load for verification of the performance. This means that the results will not be suitable for designing chokes for microwave system meant for processing different load.

- Furthermore, most of the chokes discussed in the literature were tested and validated when the microwave system is empty (without load) but the performance will be different when the load is introduced.

Therefore, it is imperative when designing chokes or filters for open waveguide continuous microwave system to work with people with vast knowledge of choke design and electromagnetic theory for the design of special chokes for the system, so as to mitigate the microwave leakage to non-detectable or permissible levels. This is because the impact of dielectric properties of load and manufacturing tolerances can be significant on the performance of the chokes at low margins.

3.11 Scale up Considerations of Microwave System

Previous work by many researchers has shown that microwave processing of numerous industrial minerals and materials is feasible and can result in process advantages such as volumetric heating and reduced energy consumption (Metaxas and Meredith, 1983, Al-Harahsheh and Kingman, 2004, Al-Harahsheh et al., 2006a, Robinson et al., 2010). With many hundreds of publications in the literature detailing applications of microwave energy, it is surprising that most of these investigations have been limited to laboratory and little scale up attempts have been made (Bradshaw et al., 2007). Factors responsible for the failure in scaling up the microwave processing are highlighted below (Bradshaw et al., 2007, Gupta and Eugene, 2007).

- Poor understanding of the microwave heating fundamentals (dielectric properties, optimum frequency of operations and power density)
- Insufficient data and poor electromagnetic modelling and simulations of microwave heating cavities
- Little or no information about the mineralogy or chemistry of the materials
- Poor bulk materials handling

However, the work of some researchers has resulted in scale up of microwave processing systems from laboratory results. Examples of these are in the area of microwave chemistry and microwave assisted organic synthesis (Bowman et al.,

2008, De La Hoz et al., 2011), treatment of contaminated drill cuttings and hydrocarbon contaminated soils (Robinson et al., 2012, Robinson et al., 2010, Lin et al., 2012), ceramics, food processing (Kumar et al., 2008, Coronel et al., 2005, Terigar et al., 2011) and mineral processing (Bradshaw et al., 2007).

In the scale-up of the microwave system for treatment of oil contaminated drill cuttings, Robinson et al., (2010), employed the in-depth understanding of bulk materials handling, electromagnetic simulations and engineering design. The needs for the homogenous high power density eliminate the use of multimode microwave cavities (low power density and high power density distribution) and single mode (high power density but uneven electric field distribution). A special form of applicator named tunnel applicator, which produced both high power density and even electric field distribution was used for this purpose. The microwave energy is perpendicularly fed into the applicator in order to distribute the power density throughout the cavity geometry homogeneously. This system is capable of removing the drill cuttings oil content below the 1% stipulated by UK environmental legislation.

Possible approaches for scaling up microwave enhanced chemistries have been published by many researchers for various chemical reactions (Bowman et al., 2008, Morschhäuser et al., 2012, C. Oliver Kappe, 2012, Hoz et al., 2011, Bertrand Perio, 1998, J. Cleophax, 2000, Fredrik Lehmann, 2003, T. Michael Barnard, 2006, Riina K. Arvela, 2005, Moseley et al., 2007). The scale up possibility of microwave chemical processes is due to the high polarity of most solvents, novel process optimization and good understanding of electromagnetic simulations for designing suitable applicators for the processes. These may either be monomode or multimode cavities (Morschhäuser et al., 2012).

The scale up concept employed is either continuous flow or batch processing depending on the reaction type and nature of reacting mixtures. Researchers have been able to achieve microwave enhanced chemical synthesis at a gram scales using a batch reactor but operating the same at kilogram scales is still challenging

(Moseley et al., 2007, Bowman et al., 2008, Hoz et al., 2011). This may be because of limited penetration depth of only a few centimetres. Safety is another issue in batch processing (sealed or open reaction vessels), as it is challenging to monitor the process at high volume, elevated temperature and pressure. However, it overcomes the challenges of material heterogeneity (Bowman et al., 2008, Morschhäuser et al., 2012, Toma N. Glasnov, 2007). Studies on the scale up approach of continuous flow microwave based chemical processing have shown that high energy efficient microwave enhanced chemical reactions is feasible even at high temperature and pressure process conditions (Morschhäuser et al., 2012, Bergamelli et al., 2010).

Various concessions are made when considering scale-up of microwave system. The chosen frequency of operation within the ISM range directly influences the size of the cavity and the dielectric properties of the materials. In addition, the microwave depth of penetration into the treated minerals is frequency dependent, and the penetration is greater at lower frequencies. The choice of microwave cavity is made by considering the expected throughput, homogeneity of the electric field, power density requirement and the effect of system turndown on the energy consumption, as the overall purpose of scaling up is to maximize the cost benefit over the conventional system of mineral processing (Bradshaw et al., 2007, Metaxas and Meredith, 1983).

3.12 Conclusions

The fundamental principles of microwave heating, and materials interaction with electromagnetic field were discussed. Cavity perturbation and waveguide techniques, which are the two dielectric properties measurement techniques proposed to be used for the measurement of electrical properties of vermiculite, were introduced. The cavity perturbation was proposed for the measurement of dielectric properties of vermiculite particulates because it gives accurate result for the measurement of low loss materials. Waveguide measurements will, however, give a better understanding of bulk dielectric properties of vermiculite.

The magnetron is the most important device used for microwave generation. A waveguide system is used for the transmission of the microwave energy to the applicator, where the efficient interaction of microwave energy with processed materials takes place. The appropriate selection of a suitable applicator is required for energy efficient and homogenous heating of materials.

CHAPTER FOUR
UNDERSTANDING THE INTERACTION OF MICROWAVE ENERGY WITH VERMICULITE

4.1 Introduction

The potential benefits of microwave heating as a tool for industrial processing of minerals were discussed in Chapter 3. The dielectric properties are a material property, which govern how the materials will absorb and dissipate microwave energy as heat. Therefore, there is a need for accurate measurement of the dielectric properties of a material for proper understanding of its behaviour under an applied electromagnetic field. In addition, the dielectric data are used by the microwave engineer for modelling and designing of microwave applicator and choke system (Metaxas and Meredith, 1983, Geyer, 1990)

The dielectric properties of a material depend upon factors such as temperature, frequency, moisture content, and bulk density. Other important factors that influence dielectric properties and the response of a material to microwave energy are the material mineralogy and chemical properties (Sengwa R.J and Soni A., 2008, Salsman J. B; and Holderfield S. P, 1994, Jinkai, 1990, Chen et al., 1984b). Geyer, (1990) classified materials into different categories as a function of the dielectric properties as follows.

- Low dielectric constant, low loss ($\varepsilon' \leq 4$ and $\tan\delta < 0.001$)
- High dielectric constant, low loss ($\varepsilon' \geq 10$ and $\tan\delta < 0.001$)
- Very high dielectric constant, ultra-low loss ($\varepsilon' \geq 100$ and $\tan\delta < 0.0002$)
- Lossy dielectric ($\tan\delta \geq 0.1$)

To investigate the interaction of electromagnetic waves with vermiculite from different source locations (South Africa, China, Australia and Brazil), the cavity perturbation and waveguide measurement techniques discussed earlier in Chapter 3 were employed. The Cavity perturbation technique only allows measurement at limited specific frequencies, which are typically around the ISM frequencies for microwave heating. The waveguide technique was applied to measure dielectric

properties of the bulk vermiculite sample over a broad range of frequencies. The waveguide measurement results could then be used to study the dielectric relaxation of vermiculite sample. Furthermore, the dielectric properties of the vermiculite samples were also measured over a wide range of temperatures in order to quantify their microwave heating ability and this is where the cavity perturbation method was employed.

Minerals such as oxides (goethite), carbonate (calcite and dolomite), and silicates (biotite, montmorillonite and vermiculite) are naturally occurring chemical compounds with varying complex compositions and physical properties (Deer et al., 1966, Grim, 1968). The dielectric properties of the different minerals vary with their chemical compositions as shown in Table 4-1 for sulphides, oxides, hydrides and silicates at 9.37 GHz, with silicates having the lowest dielectric permittivity.

Table 4-1: Results of dielectric properties of minerals (Jinkai, 1990)

Mineral	**ε'**	**ε''**
Sulphides	4.44-60.0	0.02-9.00
Oxides	4.17-15.0	0.02-4.04
Hydrides	5.23-18.08	0.02-0.11
Silicates	3.58-24.8	0.02-0.90

The potential of utilising microwave energy for industrial mineral processing depends on the selective absorption of microwave energy by a microwave absorber in the mineral phase and the transparency of the other constituents (Webb and Church, 1986, Church et al., 1988, Metaxas and Meredith, 1983). Therefore, predicting the rate of material heating in an electromagnetic field requires an understanding of its mineralogy and its dielectric properties. Some authors have studied the relationship between the chemical compositions and microwave heating properties of some minerals and rocks (Jinkai, 1990, Sengwa R.J and Soni A., 2008, Church et al., 1988, Nelson et al., 1989, Sharif, 1995, Ulaby et al., 1990). However, the literature survey shows that no work exists on the chemical composition

dependence of the dielectric properties of vermiculite, and this is investigated in this project for samples from different geological locations for the first time.

Water exists in clay minerals such as hydrated halloysite, montmorillonite and vermiculite as adsorbed, interlayer and lattice OH water, and there is a considerable variation in the moisture content of different clay minerals (Grim, 1968, Deer et al., 1966, Velde, 1992, Bergaya et al., 2006). As discussed in Chapter 2, the adsorbed water in vermiculite is not chemically bound to the vermiculite structure or interlayer cations, and is released from either the surface or the interlayer space as free water below 115 ^{o}C. Low energy interlayer bound water, which forms a geometric structure around interlayer cations, is completely removed by heating up to temperature between 300-400 ^{o}C. The high temperature hydroxyl water, also known as crystalline water is strongly bounded to the vermiculite structure. The release of this water type from the structure starts at 500 ^{o}C and is completely removed at temperature higher than 800 ^{o}C. The removal of the hydroxyl water causes permanent decomposition of the vermiculite structure (Deer et al., 1964, Grim, 1968, Marcos et al., 2009, Gillott .J.E., 1987, Mouzdahir et al., 2009, Velde, 1992).

Kaviratna and Pinnavaia (1996), reported that moisture content has a considerable effect on dielectric properties of clay minerals such as montmorillonite, hectorite and laponite. This is due to the high dielectric constant and loss factor of about 77 and 13 respectively possessed by water at 2.45 GHz (Metaxas and Meredith, 1983). Another factor is the easy polarisation of these water molecules (especially free water held to the mineral by weak Van der Wall force) within the mineral structure, when under influence of alternating electric field (Atomic Energy of Canada Limited, 1990, Metaxas and Meredith, 1983, Meredith, 1998). However, some silicate minerals such as feldspars, muscovite and quartz are transparent to microwave energy because of their low dielectric properties as a result of absence of either adsorbed or bound water (Chen et al., 1984b). Therefore, the effect of the change in the mineral's water network on their dielectric properties when heated to a high temperature is significant in the context of microwave heating.

This chapter presents an experimental study carried out to investigate the microwave heating properties of vermiculite from different geological locations. Also investigated is the effect of vermiculite compositional and mineralogical variations on the microwave heating behaviour. Apart from the cavity perturbation and waveguide techniques used for the dielectric properties metrology, other experimental techniques employed for mineralogical characterisation are, X-ray diffraction (XRD), mineral liberation analysis (MLA), and thermogravimetric analysis (TGA). XRD was used for the identification and classification of the different mineral phases present in the studied vermiculite samples (Moore and Reynold, 1998, Brown, 1961, Dinnebier and Billinge, 2008).

The mineral liberation analyser (MLA) consists of a scanning electron microscope (SEM) incorporated with energy dispersive X-ray spectrometer and computer software for automated mineralogical analysis. It was used in this project for the identification and quantification of the mineral phases present in the vermiculite samples and to determine the grain size distribution of the identified mineral phases in accordance with methodologies by Petruk (2000), Jones (1987) and Fandrich et al (2007) . The vermiculite moisture content, which consists of the adsorbed water, the bound water and the hydroxyl water, was studied using thermogravimetric analysis (TGA) in accordance with methodologies developed by Földvári (2011).

4.2 Geology of the Various Vermiculite Samples

Medium and superfine grades, which are representatives of coarse and fine vermiculite grades in terms of chemical composition, applications and commercial productions, were obtained from four geological locations. The medium grade samples were obtained from Brazil and China, while the superfine grade samples were obtained from Australia and South Africa. Microwave exfoliation of all the samples is studied using the pilot and commercial scale continuous microwave system, and the results of the exfoliation performance of the microwave system are reported in Chapter 5.

4.2.1 South African Vermiculite Deposit

The South African vermiculite deposit is located in the Palabora mine located in the republic of South Africa. This is one of the major vermiculite deposits in the world. This vermiculite deposit is located in ultrabasic igneous rock complex close to rock forming minerals such as serpentine and pyroxenite rocks (Strand and Stewart, 1983). Figure 4-1 shows the three separate open-pit mines of vermiculite; the second is a copper mine with various by-products such as magnetite, apatite, gold, silver, zirconium, uranium, and nickel. The third mine in the Palabora complex is that of phosphate deposit.

The vermiculite formation in this mine has been reported to be due to either weathering or hydrothermal alteration of mica (biotite or phlogopite) or the combination of the two processes (Strand and Stewart, 1983, Schoeman, 1989, Frank and Edmond, 2001). Hydrothermal alteration involves the hydration of mica such as biotite and phlogopite, as a result of the removal of alkali interlayer cation and the diffusion of water.

Figure 4-1: Palabora mine pit complex showing the copper, vermiculite and igneous phosphate pit (Rio Tinto, 2010)

4.2.2 Chinese Vermiculite Deposit

The Chinese vermiculite sample used in this project was from the Qieganbulak vermiculite-apatite deposit in Xinjiang, China (Sun et al., 2005a). This vermiculite mine holds the largest vermiculite deposit in China and second largest vermiculite deposit in the world after the Palabora vermiculite deposit in South Africa. The coarse grade in this vermiculite mine complex is the fourth largest vermiculite deposit in the world following South Africa, U.S.A. and Russia (Ye et al., 2013, Sun et al., 2005a). This vermiculite deposit is reported to have been a product of weathering of mica, especially phlogopite (Pirajno et al., 2011). Only a small amount of information about the geology and mineralisation of this mine is available in English.

4.2.3 Brazilian Vermiculite Deposit

The Brazilian vermiculite deposit operated by Brazil Minerios is situated in the southeastern part of the state of Goias. This mine is located in ultramafic alkaline carbonatite complex also known as ultrabasic rock complex (Tassinari et al., 2001). In addition to the vermiculite deposit in this mine site, it also produces other minerals such as apatite, pyrochlore, anatase, and laterite (Tassinari et al., 2001).

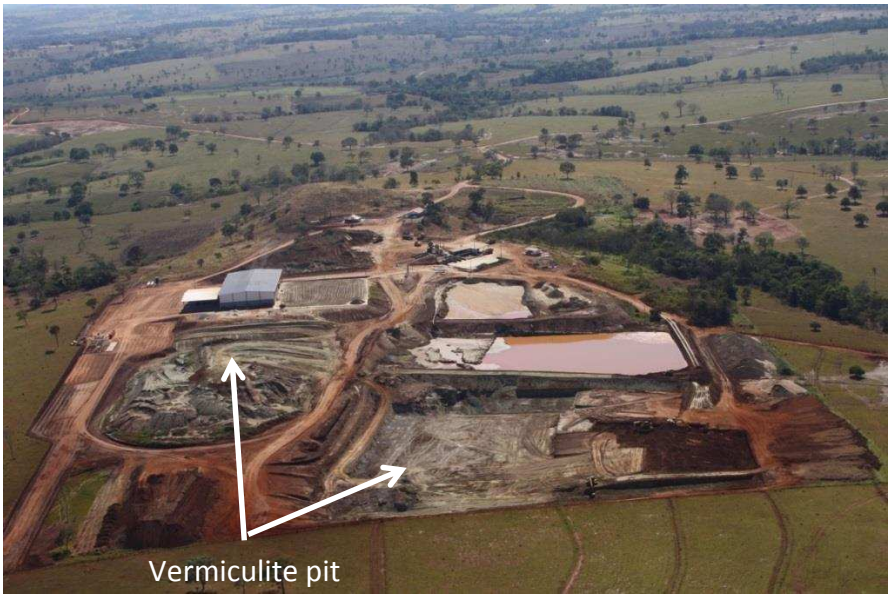

Figure 4-2: Brazil Minerios mine pit complex showing the vermiculite pit (Brazil Minerios, 2011)

Figure 4-2 shows the Brazil Minerios vermiculite open pit mine complex. The open pits for the other associated minerals are not shown in this picture.

4.2.4 Australian Vermiculite Deposit

Imerys operates the Australian vermiculite site known as Mud Tank. The mine is located in the northern part of Alice Springs (Young, 2013). The geology of this mine is that of carbonatite rocks which intervened calsilicate, quatz-feldpar and low pyroxenite formations (Young, 2013, Currie et al., 1992) . The carbonatite complex is made of mafic (silicate mineral and magnesium rock) that have been altered over time to mica rich mineral by hydrothermal process. Therefore, the vermiculite in this mine complex is agreed to have been formed as a result of hydrothermal alteration of phlogopite rich mica (Young, 2013, Currie et al., 1992). The vermiculite is mined by open-pit surface mining.

4.3 Sampling of Vermiculite Ores

Prior to any form of experimental analyses, a sub-sample of the bulk sample needs to be prepared. The accuracy of the experimental analyses carried out depends on the representativeness of the prepared sub-sample used. Previous work shows that most experimental errors are associated with the poor sampling technique rather than errors committed in the course of the experiment (Gy, 1979, Petersen et al., 2005). Therefore, the main goal of a representative sample preparation is to reduce a large volume of bulk material to a small volume that retains the characteristics of the original bulk sample (Petersen et al., 2005, Petersen et al., 2004)

The vermiculite ores used in this work were in the form of granular materials shipped from Australia, Brazil, China and South Africa, mostly in one tonne bags. Therefore, the bulk vermiculite samples need proper sample preparation to obtain a representative specimen suitable for the various experimental procedures. Utilisation of a sophisticated sampling procedure is the first step in all of the experimental methods employed in this work, in order to obtain data exhibiting minimal error attributable to sample heterogeneity.

Various techniques are available for splitting granular materials, but most of these fall within the four categories, namely, coning and quartering, riffling, fractional and alternate shovelling, along with the sectorial divider (Gy, 1979). Results from previous research have shown that both the rotary divider and riffle splitter have good accuracy, with a good level of confidence for splitting granular materials (Wills and Napier-Munn, 2006, Petersen et al., 2005, Schumacher et al., 1990). Therefore, these two techniques were both employed in this work for splitting the bulk vermiculite samples to obtain smaller experimental representative samples. The as-received 1 tonne bags of vermiculite were also noted to contain segregated particle size distributions due to the effect of vibration on the sample bags during loading, shipping and off-loading. This phenomenon of sample segregation whereby the largest particle size goes to the top and lowest particle size settles at the bottom is known as the Brazil nut effect (Ellenberger et al., 2006)

Figure 4-3 shows the rotary sample divider (RSD) used to obtain a homogenous mixture of the sample. The vermiculite sample to be divided is fed from the hopper to the vibratory feeder. The vibratory feeder then uniformly dropped the vermiculite at an equal rate into the four rotating drums placed on turning table. The 1 tonne bags of each vermiculite sample used for the experimental work in this project was first divided into a quarter (primary sample: four parts of 250kg each). Each of the four primary samples obtained were then subdivided into a quarter fractions to obtained sixteen representative samples. One part of each quarter obtained from the splitting of the four primary samples was selected.

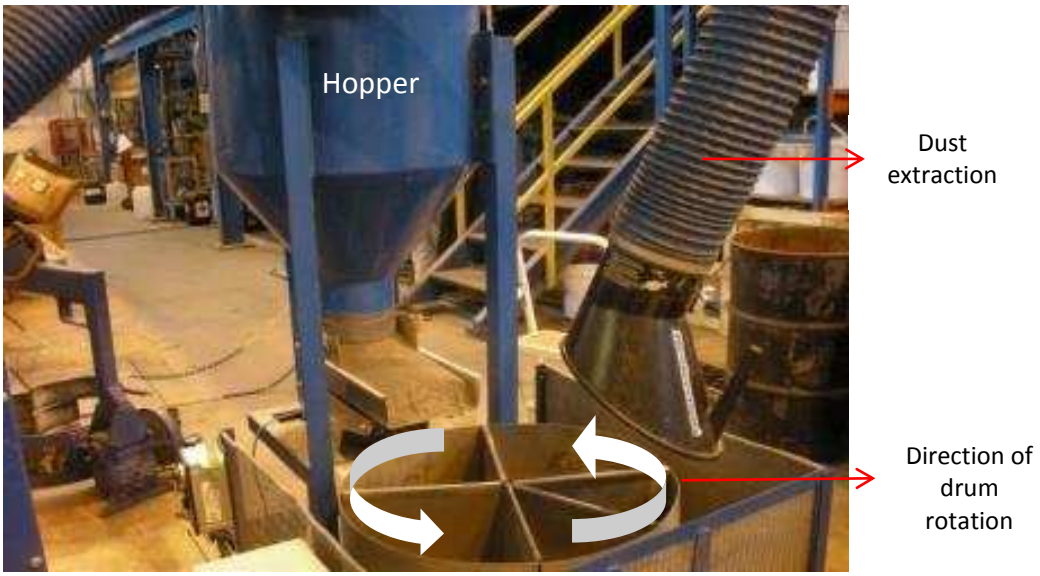

Figure 4-3: Rotary sample divider used for vermiculite homogenisation and size reduction

The selections were randomly made without any bias to ensure that every sample had an equal probability of becoming part of the selection. This was followed by recombination and mixing of the four samples selected to form a secondary sample as shown in Figure 4-4. The same procedure was repeated on the secondary sample to obtain the laboratory sample (about 62.5 kg), which was representative of the original 1 tonne bags.

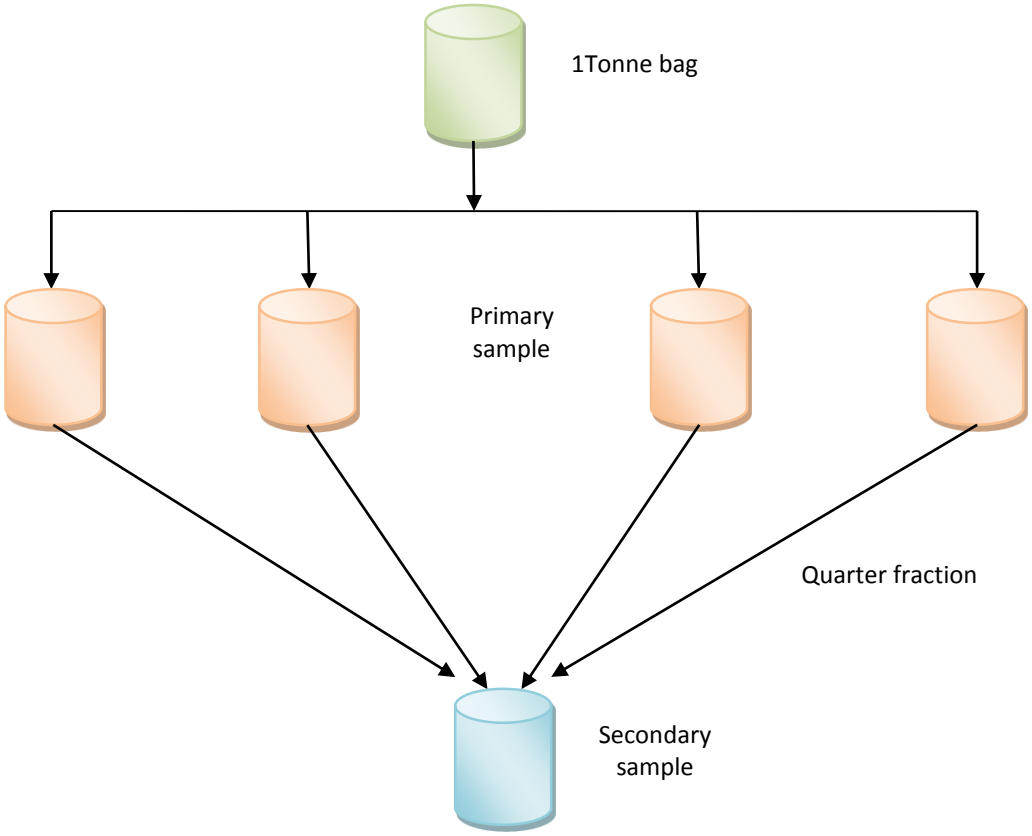

Figure 4-4: Representative sample preparation using rotary sample divider

The riffle splitter also known as a Jones riffle, was then used successively to further split the 62.5 kg vermiculite sample obtained to a size of about 1 kg, from which the specimens required for experimental work were prepared. This also enhances the homogenisation of the vermiculite sample. The riffle splitter is a mechanical method used for sample size reduction and bulk sample homogenisation by sample mixing. This device has an equal number of narrow sloping chutes with alternate chutes discharging the sample in opposite directions into two empty collection pans (Schumacher et al., 1990). For the size reduction, vermiculite sample was passed through the riffle splitter and one of the pans, which contains about one-half of the original volume of the ample, was randomly selected. The sample in the selected pan was then passed through the riffle splitter again to obtain one-quarter of the original sample volume. This process was repeated until the desired sample size (1 kg) was obtained.

4.4 Mineralogical Analysis of Vermiculite Ores

As discussed in section 4.1, mineralogy influences the microwave heating behaviour of minerals. It is, therefore, essential to this project to identify the different mineral phases present in the raw vermiculite samples, as this will provide better understanding of the contributions of the different mineral phases to the dielectric properties of the bulk material mixture. These results will give information about the vermiculite microwave heating mechanisms. In addition, the results could be used for the bulk sample handling, process design and optimisation. This section discusses the different techniques used to conduct mineralogical tests on medium grade vermiculite from Brazil and China, and the superfine grade from Australia and South Africa.

XRD analyses will give information about the different mineral phases present in the different vermiculite ores studied. In addition to the identifications and quantifications of the different mineral phases present in the analysed vermiculite samples, MLA also gives information about the textural analysis of individual grains in the measured samples in terms of grain size distribution, mineral liberations and associations. The thermogravimetric analysis (TGA) performed on the vermiculite flakes provides information about the hydrating state of the different vermiculite samples by measuring the weight loss under controlled heating. The mineralogical results will be used to understand the microwave heating behaviour of the different mineral phases identified and their significant effect on the overall exfoliation performances of the different vermiculite ores, in terms of the bulk density of the exfoliated product. The mineralogical variation of vermiculite samples obtained from the different geological locations will help to understand the variation in their microwave heating behaviour. In addition, these results will be useful for process control and optimisation of the microwave exfoliation system.

4.4.1 X-ray Diffraction (XRD) Analysis

X-ray diffraction (XRD) is a reliable tool used by mineralogists for identifying and characterising different clay minerals. It is a non-destructive analysis technique, which provides information about the compound crystallography and identifies the different mineral phases present in crystalline materials. This method relies on the principle that each crystalline substance has its own characteristics regular atomic structure which scatters X-ray beams at certain angles of incidence (Moore and Reynold, 1998, Brown, 1961). The X-ray radiation is generated by the rapid deceleration of the fast-moving electrons as they strike the metal target in a vacuum X-ray tube. The X-ray diffraction gives a high spectral resolution, but is of lower intensity for a given beam current than energy dispersive X-ray (EDX).

Figure 4-5 shows the schematic representation of XRD by regularly spaced reflection plane obtained from atoms in a crystal.

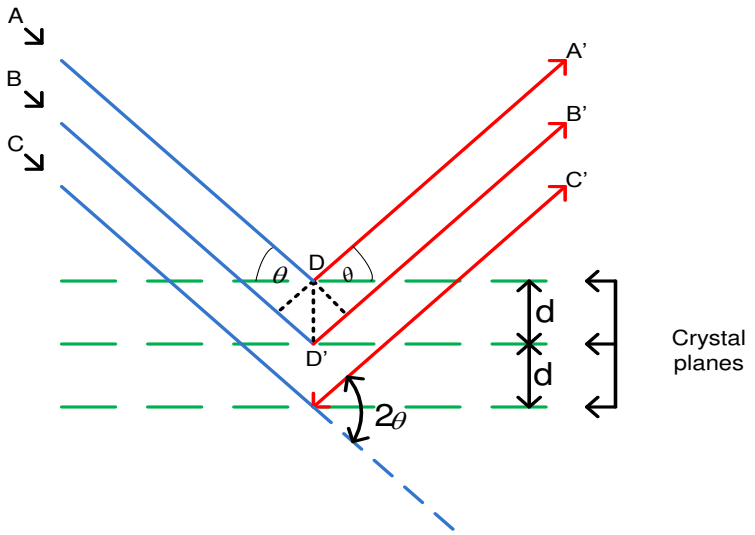

Figure 4-5: Bragg reflection of coherent x-ray from uniformly spaced atomic plane within the crystal

The distance between two successive planes is known as the inter-atomic spacing or interplanar spacing (d-spacing). A relation known as Bragg's law (Equation 4-1) gives the relationship between this inter-atomic spacing, the angle of diffraction (θ) and the wavelength of the incident radiation. The derivation of this equation can be

found in the literature (Brown, 1961, Dinnebier and Billinge, 2008, Pecharsky and Zavalij, 2009).

$$n\lambda = 2d \sin\theta \qquad \text{Equation 4-1}$$

Where,

n = Integer (order of diffracted beam)

λ = wavelength (Å)

d = inter-atomic or d-spacing

θ = Diffraction angle or Bragg's angle (degrees)

When a focused monochromatic X-ray beam interacts with a single crystal mineral or mixture of minerals in powder form, diffraction occurs from the atomic planes in the crystal materials. This occurs when the optical path difference between rays ADA' and BDB' (Figure 4-5) is an integral multiple of the wavelength, leading to the constrictive interference and formations of XRD peaks. The movable detector in the x-ray diffractometer measures the intensity and diffraction pattern, which give information about the structural details of the measured minerals. Details about the theory and the instrumentation of XRD are available in the literature (Brown, 1961, Reed, 2005, Clegg, 1998, Dinnebier and Billinge, 2008, Pecharsky and Zavalij, 2009).

4.4.1.1 Test Minerals and Method for XRD Analysis

Sample preparation is the key factor that determines the quality of data obtained from XRD crystallography. Due to the layered structure of vermiculites, special precautions were taken in this work to ensure that representative samples were presented for measurement in order to obtain accurate results. Fine powder fractions (< 80 μm) of representative samples of vermiculite received from different source locations, and prepared as discussed in section 4.3 were presented for the XRD analysis.

A Hilton Brook diffractometer (Philip PW 1050) available at The University of Nottingham was used for the X-ray analysis at room temperature. The vermiculite powder specimens for measurement were mounted in a sample holder and a glass plate was used to press the powder to obtain a flat surface. The XRD traces were collected by generating the X-ray beam at 40 kV, 20 mA (Cu k_β radiation at λ = 1.5406 Å), and the scan was carried out from 5 to 65° 2θ range using 2θ step scan of 0.05 s. The diffraction angles between 5 to 65° used correspond to that of clay minerals (Brown, 1961). The obtained data were compared and matched with the reflection standards from the JADE software (powder analysis diffraction package) developed by Material Data Incorporation (Jade 6.5, 2003). JADE software is a database that contains a very large set of standard data provided by the International Centre for Diffraction Data (ICDD). It contains digital XRD patterns, both experimental and calculated from about 254,873 known inorganic and organic substances. This software identifies the different mineral phases present in the diffracted sample by search-match and compares the sample pattern obtained (peaks and intensities) with the peaks and relative intensities from that of its database.

4.4.1.2 Analysis of XRD Results of Characterised Vermiculite Ores

The XRD analyses were performed on the four vermiculite samples obtained from four geological settings (Australia, Brazil, China and South Africa). The analyses were carried out for five repeats on the representative specimens of each vermiculite sample. The XRD reflection peaks obtained for each sample are shown in the appendix 1, but the analyses of the reflections pattern are given in this section.

The X-ray pattern for the Brazilian sample shows that this sample has mineralogy that is predominantly of vermiculite with insignificant traces of other silicates. The most intense peak in Brazilian sample is at 14.40 Å. This peak represents the most characteristic reflection of vermiculite. The peaks at 14.40 Å, 2.88 Å, 2.41 Å in this sample indicate it is a Mg-vermiculite that has magnesium as the hydrated interlayer cation (Moore and Reynold, 1998, Grim, 1968) while the peak at 19.2 Å is as a result of a low amount of octahedral iron in this sample (Mouzdahir et al., 2009). The reflection at 1.54 Å also indicates that this sample is a tri-octahedral form of

vermiculite (Campos et al., 2009). The XRD analysis of the South African sample shows a predominant peaks corresponding to hydrobiotite, which is a mixed layer of vermiculite and biotite. The reflections 12.2Å and 8.54Å indicate the presence of regular interstratified vermiculite/biotite mixed layer (Brindley, 1951). It has a weak reflection of 14.26Å at about 6°, and this corresponds to vermiculite characteristic reflection (Grim, 1968, Harraz and Hamdy, 2010). The weak intensity of peak 10.28 Å at 8.6° signifies that the sample has low amount of magnesium in its octahedral sheet (Moore and Reynold, 1998). This is due to the low intensity of vermiculite peaks in this sample. The South African sample also shows peaks peculiar to carbon bearing mineral (calcite), pyroxene (dolomite) and phosphate mineral (Apatite). The XRD pattern obtained in this project for the South African sample is similar to what Muiambo et al (2010) reported for the vermiculite ore obtained from the same mine area.

Similar to the South African sample, the XRD peaks of the Australian vermiculite ore also present a predominant peak, which correspond to that of mixed layer structure of vermiculite/mica (Hydrobiotite). It also has a weak reflection peak of 14.60 Å, which is peculiar to vermiculite (Grim, 1968, Harraz and Hamdy, 2010). Other peaks identified in the Australian sample are that associated with quartz and calcite. Of all the vermiculite samples studied by X-ray diffraction, only the Chinese sample shows crystalline diffraction peaks that are characteristic of pure hydrobiotite with insignificant trace of impurities.

The XRD reflections pattern of all the vermiculite samples characterised shows that only Brazilian sample has a strong peak associated to vermiculite while that of Australian, South African and Chinese samples are predominantly that of hydrobiotite, which is vermiculite/mica inter stratification. Pure vermiculite is different from mica (biotite and phlogopite) and the hydrated form of the micas (hydrobiotite and hydrophlogopite), in terms of the intersilicate layer, chemical composition and water content (Bergaya et al., 2006, Velde, 1992). Vermiculite has hydrated interlayer cation, which is usually magnesium while mica consists of anhydrous potassium ions as the interlayer cation. The mineralogical variations of

the Australian, South African, Brazilian and Chinese samples would have significant impact on their degree of exfoliation (Grim, 1968).

The XRD results were used to determine the hydration state of the vermiculite ore studied in this project. This hydration state is defined by Suzuki et al (1987) as the number of interspacing water-layer hydration states (WLHS). The notations used by Suzuki et al (1987) to describe the water-layer hydration state are 0, 1, 2 water-layer hydration states for dehydrated, 1-WLHS and 2-WLHS respectively. Brazilian sample has a strong intensity peak at 14.40 Å, which corresponds to 2-WLHS as shown in Table 4-2.

Table 4-2: Hydration states observed in samples correspond to pure vermiculite

Sample	**Basal spacing (Å)**		
	2-WLHS	**1-WLHS**	**1/0**
Brazilian	14.40		
Chinese		11.26	10.22
Australian	14.60	11.91	
South African	14.26	11.91	10.28

This is the most intense peak identified in the Brazilian sample when compared to the other vermiculite samples studied. The 1-WLHS and the dehydrated phase 1/0-WLHS are not present in this sample. The presence of a strong reflection peak associated to 2-WLHS in the Brazilian sample implies that this ore has double layers of water in its interlayer space (Suzuki et al., 1987). The 2-WLHS state was not identified in the Chinese sample but has the reflections at 11.26 Å and 10.22 Å as the most intense reflections. These two strong reflections identified represent 1-WLHS and dehydrated phase respectively. The absence of 2-WLHS in the Chinese sample indicates the absence or insignificant vermiculite content; therefore, there is tendency that the Brazilian sample will have higher moisture content than the Chinese sample despite that they are of the same particle size range (1.4 mm-4.0 mm). The XRD pattern for the South African sample shows a 2-WLHS at 14.26 Å with 1-WLHS and dehydrated states 1/0-WLHS at 11.91 Å and 10.28 Å

respectively. The 2-WLHS in this sample is of lower intensity when compared to its 1-WLHS and 1/0 WLHS. Therefore, it has a monolayer of water in its interlayer space. In the case of the Australian sample, 2-WLHS and the 1-WLHS are the two-hydration states identified from the XRD peaks. The reflection of the 2-WLHS is of low intensity compared to that of 1-WLHS, which represent mica or hydrobiotite peak.

4.4.2 Mineral Liberation Analysis of Vermiculite Ore

Most mineral ores including vermiculite exist not as pure minerals, but as a mixture of different mineral phases, with each phase having unique physical and chemical properties. For microwave heating of mineral ores, each of the mineral phases present in the ore heat at a different rate when subjected to microwave energy. Therefore, there is a need to identify and quantify the different mineral phases present in the vermiculite ores. The Investigation of the associations of each mineral phase in the vermiculite ores will allow the determination of the individual and collective contribution of each mineral to the dielectric properties of the bulk vermiculite and the microwave heating mechanism.

The FEI, Quanta 600 (See Figure 4-6), which is made up of scanning electron microscope (SEM) incorporated with energy dispersive X-ray (EDAX) spectrometer and computer software (Genesis 4000) was used for the mineral liberation analysis of vermiculite ores. Mineral quantification is obtain using the Mineral liberation analyser (MLA) software developed at the Julius Kruttschnitt Mineral Research Centre (JKRMC) at The University of Queensland, Australia (Gu, 2003, JKMRC, 2004). The software module in the installation, controls the accelerating electron voltage and magnification of the SEM, backscattered electrons (BSE) brightness and contrast, working distance and spot size (Figueroa et al., 2011). This installation provides automated image analysis and quantitative mineral liberation of minerals (Fandrich et al., 2007).

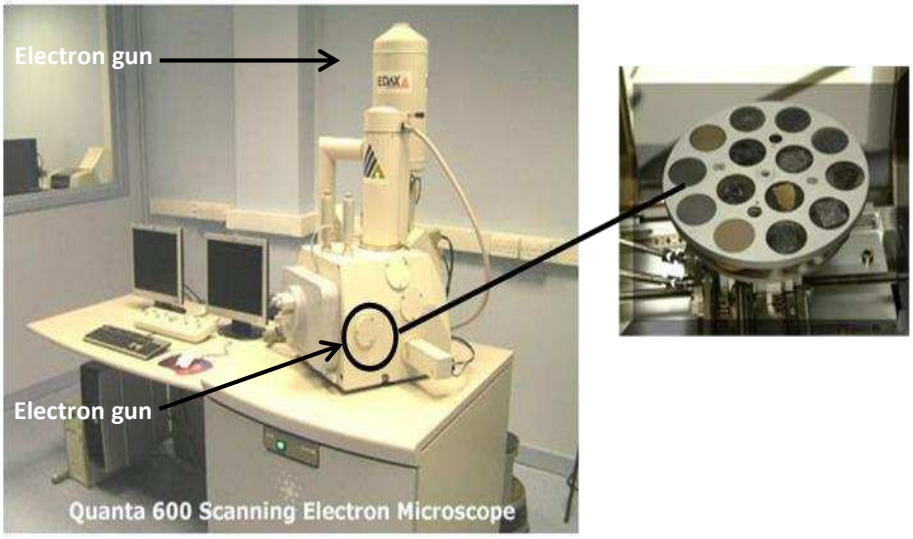

Figure 4-6: Mineral liberation analyser showing the SEM equipment and the sample holder (JKMRC, 2004)

Figure 4-7 shows a typical column of SEM chamber, with an electron gun made of tungsten generating a high-energy monochromatic beam of electrons in a vacuum.

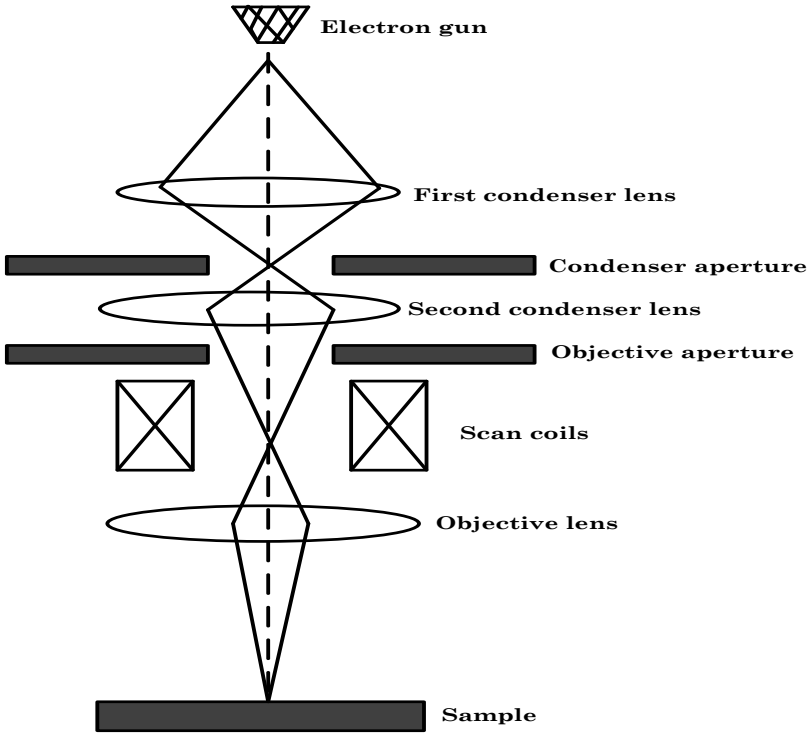

Figure 4-7: A typical column of the Scanning Electron Microscope (Reed, 2005)

The beam of electrons is focused to the prepared polished sample by a series of lenses (condenser and objective) and apertures (Reed, 2005), and the electrons are scanned across the sample surface (frame) to produce information about the surface morphology/image or the sample elemental composition. The interaction of the electron beam with the specimen surface generates signals, which may include backscattered electrons (BSE) and characteristic X-ray.

High-energy Backscattered electrons (BSE) originated from a greater depth within the sample are generated by the deflection of incident electrons at an angle greater than 90 °C or by multiple reflection through a small angle. Backscattered electrons collected by the detector (screen) produce an image. X-rays are produced by the inelastic bombardment of the specimen by electrons to generate either continuous or a characteristic X-ray spectrum, which is the characteristics of the elements present in the tested mineral. The MLA software therefore integrates the collected images and X-rays to gives information about the sample chemical composition and their distribution (Reed, 2005, Fandrich et al., 2007).

4.4.2.1 Sample Preparation and Method

The sample preparation procedure for this measurement follows the MLA System User Operating Manual (JKMRC, 2004). A statistically representative sample of the vermiculite ores prepared as discussed in section 4.3 was pulverised and riffled with a small box riffle to retain the <150 μm size fraction. About 1.5-2 g of the micro-riffled specimens were placed in a 30mm diameter polythene mounting cup and epoxy resin mixed with a hardener in a ratio of 15:2 was carefully added. The mounted specimens were then placed in a Struers Epovac vacuum pump for about 45 minutes to remove all the air from between the ore particles and to ensure that all the pores were filled with resin. The mounts were then cured for 13 hours at 35 °C after which they were removed from the mounting cup.

The specimens surface were subjected to sequential grinding and polishing with abrasive of increasing fineness to 1μm diamond media on a Struers Tegrapol polisher. After polishing, a conductive coating of carbon was then applied to the

polished surfaces to prevent charging of the surface by the primary electron beam. The prepared specimens were then positioned inside the SEM chamber (shown in Figure 4-6) and the EDAX X-ray detector collected representative spectrums of each mineral phase present in the samples. They were then matched to the standard spectra held in the MLA mineral database. The MLA software follows the following steps for the automatic measurement of the sample chemical composition and images (JKMRC, 2004).

1. Capture of multiple frames with BSE imaging.
2. On-line segmentation of the images based on BSE contrast.
3. On-line acquisition of EDX spectra for each segment.
4. The classification of each mineral segment by matching the automatic pattern of the measured spectra by EDX with predetermined standard spectra (from the mineral database) for each mineral in the agglomerated sample.
5. Multiple frames were then merged to produce a classified image of the complete particle.
6. Lastly, the obtained images from measurements were analysed to quantify mineral weight percentages.

For the MLA analyses, the filament of the electronic beam source was operated at 25kV under high vacuum. The MLA software has a number of measurement modes but the Extended Backscattered Electron (XBSE) mode was used for all the test work. In the XBSE mode, the mineral grain boundaries are classified by BSE imaging and a single X-ray analysis are used for mineral identification of each grain (JKMRC, 2004, Gu, 2003).

A part of the MLA software known as Dataview is employed for the examination, processing, presentation and storage of the image and quantitative mineralogical data obtained from the MLA analysis. DataView combines the MLA images

produced, elemental composition and densities of the identified minerals, to generate both graphical and tabular forms of mineralogical data such as modal mineralogy, mineral grade recovery, elemental grade recovery, particle size distribution, mineral grain size distribution, particle density distribution, mineral locking, mineral liberation by particle composition and mineral liberation by free surface. The calculated assay, elemental distribution, mineral association, and phase specific surface area, are presented in tabular form only (JKMRC, 2004, Fandrich et al., 2007, FEI, 2013). The MLA Dataview allows the generated mineralogical data to be exported to other software such as Microsoft Excel and Word.

4.4.2.2 Analysis of MLA Results of Vermiculite Ores

4.4.2.2.1 Mineral Composition

The vermiculite ores from Australia, Brazil, China, and South Africa were presented for the MLA tests for the mineralogical assessment of the different mineral phases present, the association of the different minerals, grain size distribution, and liberation analyses of the minerals of interest. The MLA characterisation was repeated three times for each sample.

Figure 4-8 shows an example of images from MLA analysis of Australian vermiculite. The image shows the different mineral phases identified on measured polished sample frame, in descending order of weight percentage. The legend shows the mineral phases that are greater than 1% while minerals such as quartz, augite, albite and magnetite, which are less than 1%, are grouped as others. The predominant phase in the Australian sample corresponds closely to that of hydrobiotite, which is about 83% of the mineral compositions. This agrees with the result obtained from XRD analysis. Hydrobiotite is a regular 1:1 interstratification of true vermiculite and biotite sheets (Ruthruff, 1967, Grim, 1968). To maintain particle representativeness the total particle counts were approximately 20000 particles.

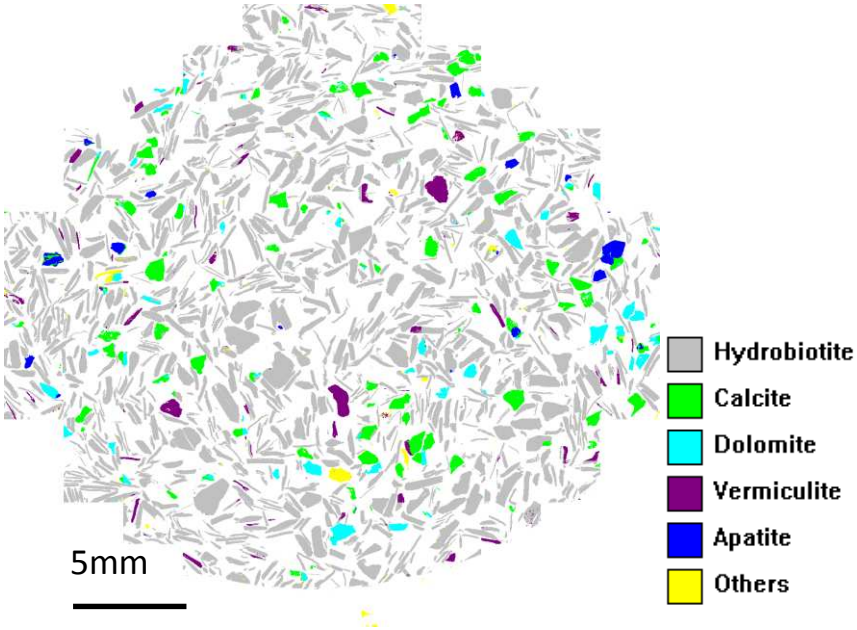

Figure 4-8: Example of MLA images of Australian superfine vermiculite

Similar to vermiculite, hydrobiotite has water network in the structure, but in lower quantity. Chemical analysis of hydrobiotite shows that it has high amount of K_2O due to the potassium interlayer cation while pure vermiculite has high amount of MgO. The higher amount MgO in vermiculite is due to the exchange of potassium interlayer cation in mica (biotite and phlogopite) for magnesium during vermiculite formation. Given below is the structural formula of hydrobiotite with potassium as the interlayer cation.

$[K(Mg,Fe)_3(Al,Fe)Si_3O_{10}(OH,F)_2].[(Mg,Fe,Al)_3(Si,Al)_4O_{10}(OH)_2.4(H_2O)]$ (Grim, 1968).

Apatite, which is a phosphate-bearing mineral and carbon bearing minerals such as dolomite and calcite, are the main impurities present in the sample, with about 1%, 8%, and 3% by weight respectively. Vermiculite, which is an expanded sheet silicate, is also present in small quantity of about 2 %.

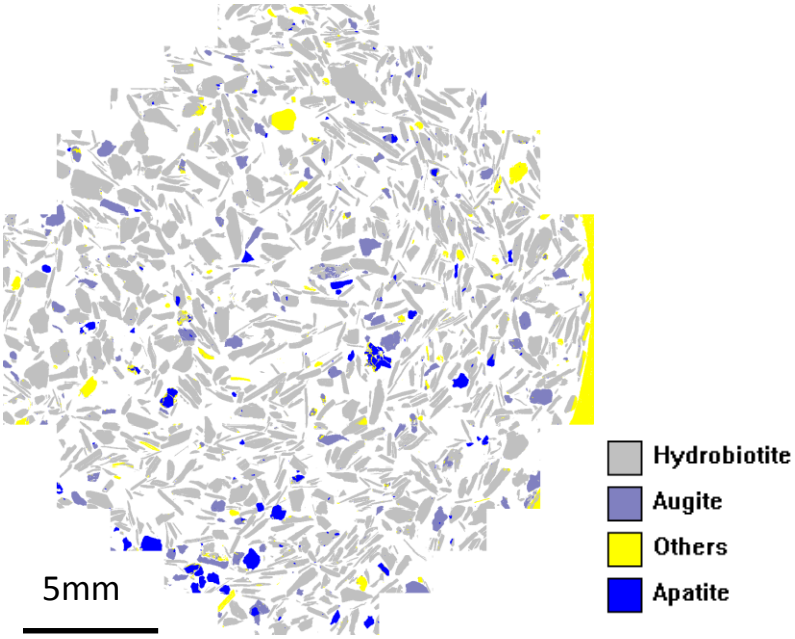

Figure 4-9: Example of MLA images of South African superfine vermiculite

Shown in Figure 4-9 is the MLA image of the South African vermiculite sample. Hydrobiotite is the predominant mineral present (about 84% by weight) in this sample. The yellow stripe down the side of the image is the reflection of the frame used. Apatite, which is a phosphate bearing mineral and augite which is a pyroxenite rock forming mineral are the main impurities present. This is due to the formation of the South African sample from pyroxenite rock. Other identified minerals such as vermiculite, dolomite, calcite, quartz and magnetite are grouped as others because they are less than 1% and are insignificant.

Vermiculite and Hydrobiotite are the significant minerals present in Brazilian vermiculite with average percentage weights of 86 and 12 % respectively (Figure 4-10). Quartz, which is a neo-silicate mineral is the main impurity present in this vermiculite sample. Traces of augite, orthoclase, olivine and magnetic accessories, which are less than 1 % by weight, are also identified in this sample.

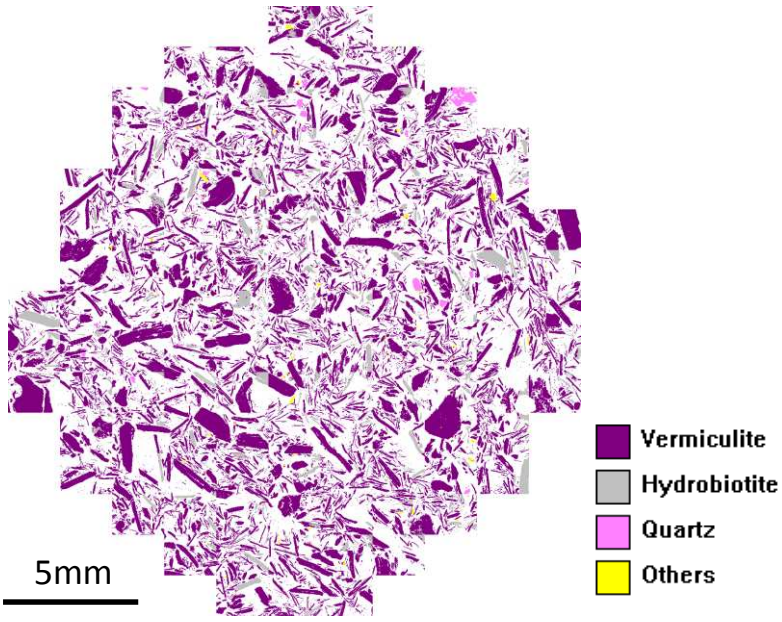

Figure 4-10: Example of MLA image of Brazilian medium vermiculite

Figure 4-11 shows that Hydrobiotite is also the predominant mineral phase in Chinese vermiculite with about an average of 96 % by weight of the ore composition. Trace minerals identified in insignificant quantities (less than 1 %) includes dolomite, augite, magnetic materials, quarts and vermiculite.

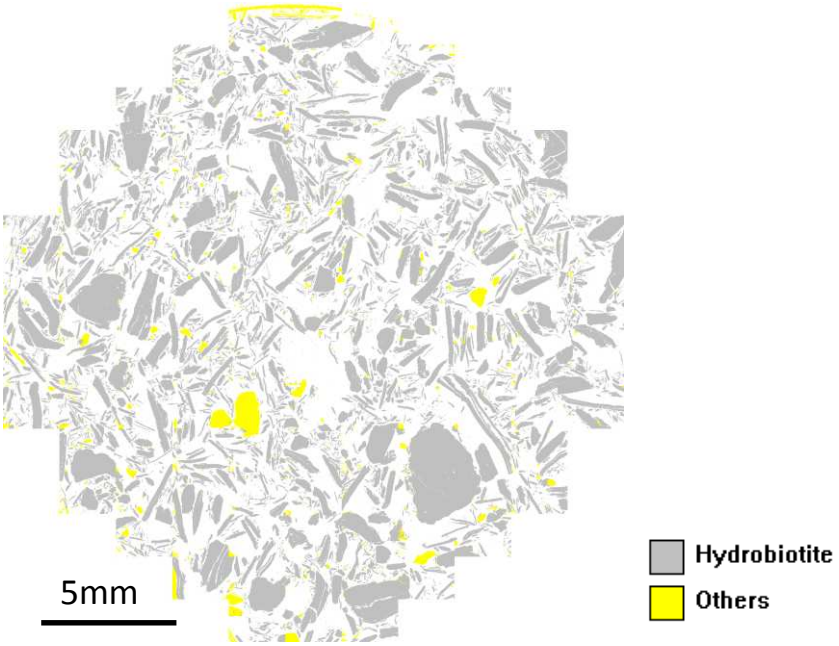

Figure 4-11: Example of MLA images of Chinese medium vermiculite

The complete quantitative assessment of the minerals identified in the four vermiculite ores is presented in Table 4-3.

Table 4-3: Mineral abundance of analysed vermiculite ores (three repeats)

Mineral	Australian	South African	Chinese	Brazilian
Hydrobiotite	82.63	84.39	96.33	12.27
Vermiculite	2.62	1.14	0.17	86.16
Calcite	8.75	0.50	0.53	ND
Dolomite	3.44	0.92	0.44	ND
Apatite	1.43	3.67	0.09	ND
Quartz	0.38	0.20	0.15	1.08
Augite	0.21	7.27	0.31	0.10
Albite	0.12	0.09	0.47	ND
Olivine	ND	0.08	0.31	0.10
Orthoclase	0.04	0.06	0.06	0.22
Fe_Oxide	0.08	0.07	0.08	0.04

ND: Not detected

The Brazilian vermiculite is the most distinct in composition with a significant vermiculite composition compared to the other samples. Accessory minerals (less than 1%) such as quartz, augite, orthoclase and magnetic minerals (Hematite and magnetite), which are present in minute quantities are the impurities common to the four vermiculite ores. Calcite, dolomite and apatite are absent in the Brazilian vermiculite. The results confirmed that Brazilian vermiculite is a pure form of vermiculite in composition when compared to the Australian, Brazilian and the Chinese vermiculite (Hillier et al., 2013).

Table 4-4, Table 4-5, and Table 4-6 summarise the significant mineral phases identified in Australian, South African and Brazilian vermiculite and their individual response to microwave energy. Hydrobiotite is the only abundant mineral in the Chinese vermiculite; other identified minerals are in trace quantities (less than 1 %). Dielectric properties of the pure form of all the identified mineral phases were measured in this project and the results are presented in Appendix 2 but the information about their microwave heating behaviour were obtained from the

literature (Walkiewicz et al., 1988, McGill et al., 1995, Lovás et al., 2011, Koleini and Barani, 2012, Chen et al., 1984b, Hua Yixin. and Chunpeng, 1996).

Table 4-4: Microwave heating response of the most abundant minerals in the Australian vermiculite ore

Mineral	Formula	Microwave heating	Weight %	Reference
Hydrobiotite	$[K(Mg,Fe^{2+})_3(Al,Fe^{3+})Si_3O_{10}(OH,F)_2.(Mg,Fe^{2+},Al)_3(Si,Al)_4O_{10}(OH)_2.4H_2O]$	Heats well, but its response changes with temperature as the water content is reduced.	82.63	(Obut et al., 2003)
Calcite	$CaCO_3$	Does not heat	8.75	(Marland et al., 2001)
Dolomite	$CaMg(CO_3)_2$	Does not heat	3.44	(Marland et al., 2001)
Vermiculite	$(OH)_4(Mg.Ca)_X(Si_{8-X}.Al_X)(Mg.Fe)_6O_{20}.yH_20$	It heats well due to rapid heating of interlayer water to cause structural expansion.	2.62	(Marcos and Rodríguez, 2010a)
Apatite	$Ca_5(PO_4)(OH,F,Cl)$	Does not heat	1.43	(McGill et al., 1995)

Table 4-5: Microwave heating response of most abundant minerals in South African vermiculite ore

Mineral	Formula	Microwave heating	Weight %	Reference
Hydrobiotite	$[K(Mg,Fe^{2+})_3(Al,Fe^{3+})Si_3O_{10}(OH,F)_2.(Mg,Fe^{2+},Al)_3(Si,Al)_4O_{10}(OH)_2.4H_2O]$	Heats well, but its response changes with temperature as the water content is reduced.	84.39	(Obut et al., 2003)
Augite	$(Ca,Na)(Mg,Fe,Al,Ti)(Si,Al)_2O_6$	Does not heat	7.27	(Hua Yixin. and Chunpeng, 1996)
Apatite	$Ca_5(PO_4)(OH,F,Cl)$	Does not heat	3.67	(McGill et al., 1995)

Vermiculite	$(OH)_4(Mg.Ca)_X(Si_{8-X}.Al_X)$ $(Mg.Fe)_6O_{20}.yH_20$	It heats well due to rapid heating of interlayer water to cause structural expansion.	1.14	(Marcos and Rodríguez, 2010a)

Minerals such as calcite, dolomite, apatite, quartz and augite identified as impurities in all the measured vermiculite ores, have been reported by some authors to be microwave transparent (Walkiewicz et al., 1988, McGill et al., 1995, Lovás et al., 2011, Koleini and Barani, 2012, Chen et al., 1984b, Hua Yixin. and Chunpeng, 1996). This is due to their low dielectric properties. The results of the dielectric properties of these minerals are shown in appendix II. Hydrobiotite, which is the most abundant mineral in Australian, Chinese and South African samples, and vermiculite which is the predominant mineral in Brazilian vermiculite ore, have been demonstrated to heat well under microwave energy, with a resultant exfoliation of the hydrobiotite and vermiculite structures (Obut et al., 2003, Zhao et al., 2010, Marcos and Rodríguez, 2010a). The explanation given for this is the rapid and selective heating of vermiculite and hydrobiotite structural interlayer water, which is a good absorber of microwave energy.

Table 4-6: Microwave heating response of most abundant minerals in Brazilian vermiculite ore

Mineral	Formula	Microwave heating	Weight %	Reference
Vermiculite	$(OH)_4(Mg.Ca)_X(Si_{8-X}.Al_X)$ $(Mg.Fe)_6O_{20}.yH_20$	It heats well due to rapid heating of interlayer water to cause structural expansion.	86.16	(Marcos and Rodríguez, 2010a)
Hydrobiotite	$[K(Mg,Fe^{2+})_3(Al,Fe^{3+})Si_3O_{10}(OH,F)_2.$ $(Mg,Fe^{2+},Al)_3(Si,Al)_4O_{10}(OH)_2.4H_2O]$	Heats well, but its response changes with temperature as the water content is reduced.	12.27	(Obut et al., 2003)
Quartz	SiO_2	Does not heat	1.08	(Marland et al., 2001)

4.4.2.2.2 Grain Size Distribution

Size distribution is an important mineralogical parameter used for characterising particle and mineral grains (Petruk, 2000). It plays a significant role in mineral processing for equipment design, bulk sample handling, material processing and system optimisation (Wills and Napier-Munn, 2006, Petruk, 2000). The MLA is used to determine the particle size distribution of the measured vermiculite samples because of its ability to selectively and quantitatively analyse the particle size of minerals or group of minerals (JKMRC, 2004). It has been empirically proven that the size distribution obtained from image analysis techniques such as MLA is approximately the same as the true size distribution, when the powder material presented for polished section has a wide size range less than 4mm (Petruk, 2000). It will be assumed that the particle size distribution of vermiculite obtained from MLA is the true size distribution since polished samples less than 150 μm were presented for the measurement. The particle size distributions of the measured vermiculite samples are generated by using the MLA Dataview.

Figure 4-12 presents the grain size distribution of South African and Australian vermiculite samples while Figure 4-13 shows the grain size distribution of Chinese and Brazilian vermiculite. Figure 4-12 show that the grain sizes of vermiculite in both Australian and South African samples range from 3.4 μm-1 mm. The similarity in the particle size distribution of both South African and Australian vermiculite may be due to the similarity in their chemical composition, mode of formation from ultramafic rock or the use of similar commuinition devices.

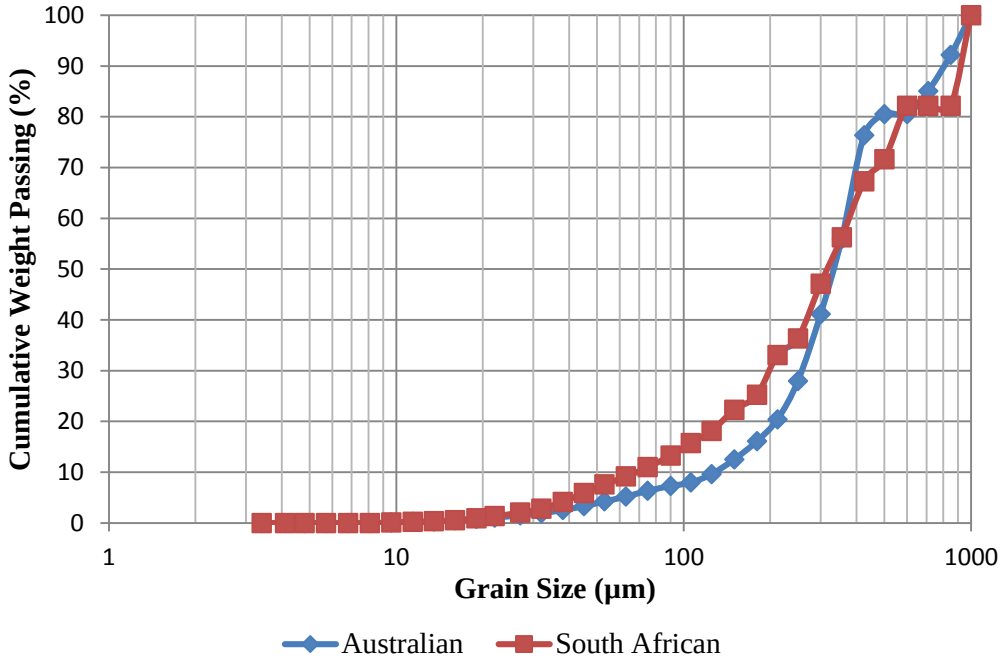

Figure 4-12: Grain size distribution of vermiculite in Australian and South African samples

The d_{25}, d_{50} and d_{75} of the vermiculite grain in the Australian sample are about 230 µm, 320 µm and 400 µm respectively, while the values of d_{25}, d_{50} and d_{75} in the South African sample are about 180 µm, 325 µm and 550 µm respectively.

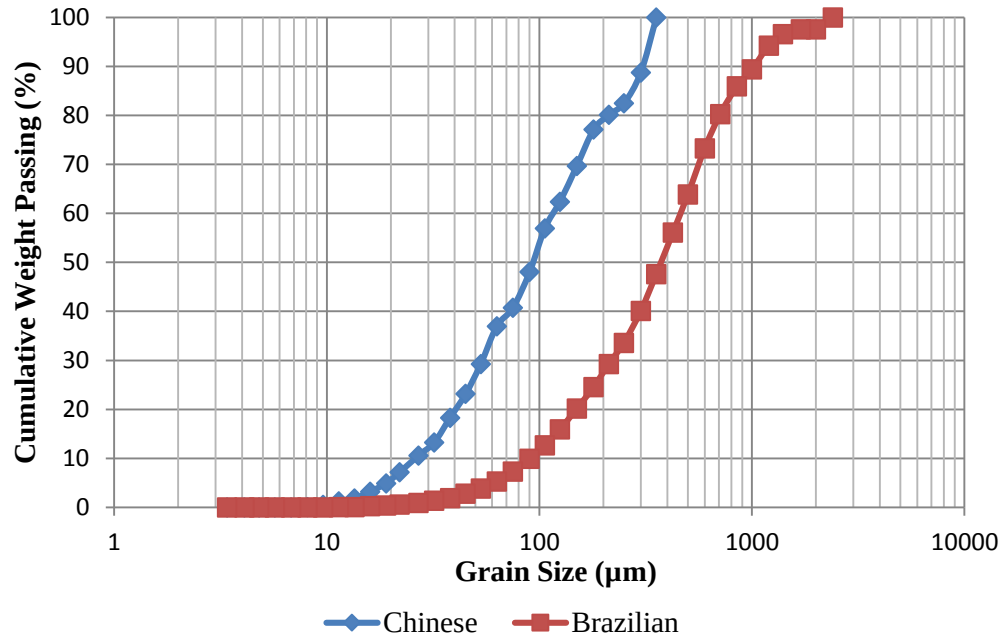

Figure 4-13: Grain size distribution of vermiculite in Chinese and Brazilian samples

Figure 4-13 shows that the grain size distribution in the Chinese vermiculite sample ranges from 3.4 µm-355 µm, but that of Brazilian sample ranges from 3.4 µm - 2.4mm. The d_{25}, d_{50} and d_{75} of the vermiculite grain in the Chinese sample are about 50 µm, 95 µm and 300µm respectively. For the Brazilian sample, the values of d_{25}, d_{50} and d_{75} are 180 µm, 400 µm and 1000 µm respectively.

The MLA Dataview was also used to determine the particle size distribution of hydrobiotite presents in the measured samples. Figure 4-14 shows the grain size distribution of hydrobiotite in Australian and South African vermiculite ores. The hydrobiotite size distribution in the Australian sample ranges from 3.4 µm to 1200 µm respectively, while the hydrobiotite size distribution in the South African sample ranges from 3.4 µm to 1700 µm. The results show that the hydrobiotite grains in the South African sample are slightly coarser than that of Australian sample.

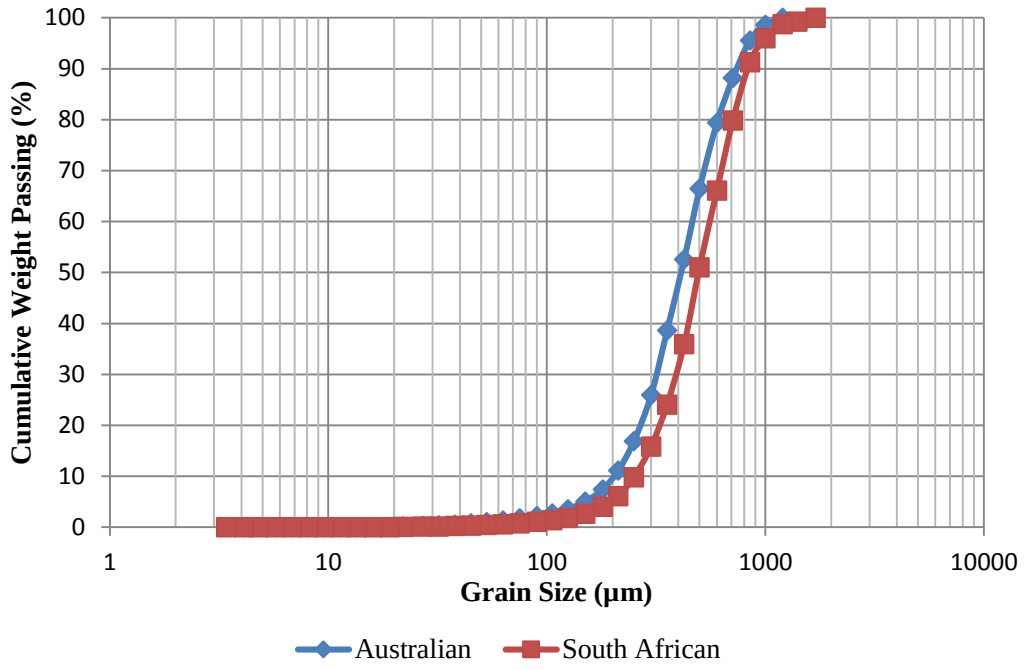

Figure 4-14: Grain size distribution of Hydrobiotite in Australian and South African samples

According to Figure 4-14, the values of d_{25}, d_{50} and d_{75} of the hydrobiotite grains in the Australian sample are 300 µm, 400 µm and 700 µm respectively, while they are about 360 µm, 500 µm and 800 µm respectively in the South African sample.

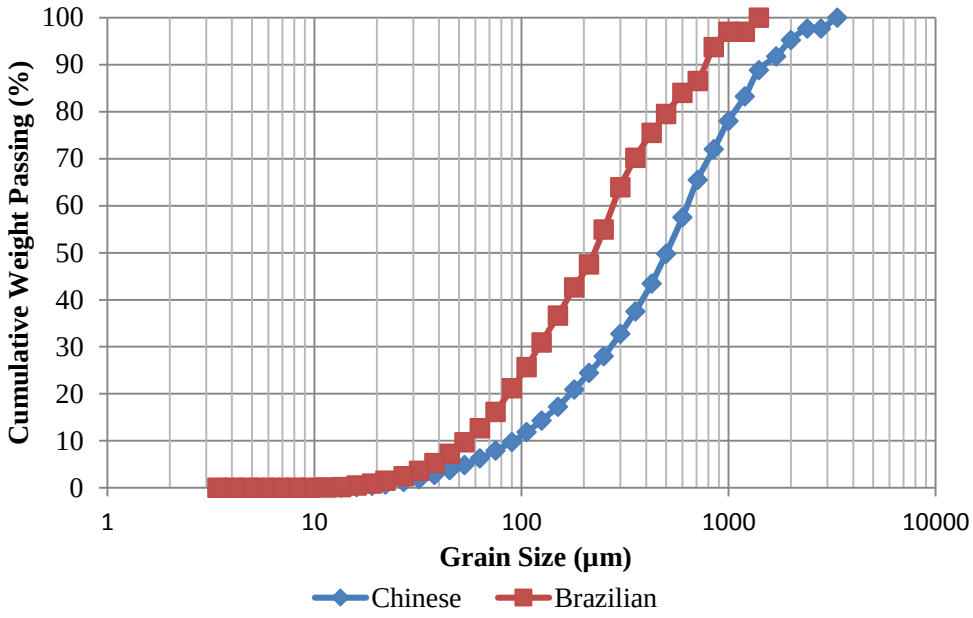

Figure 4-15: Grain size distribution of Hydrobiotite in Chinese and Brazilian samples

Figure 4-15 shows the grain size distributions of hydrobiotite in Chinese and Brazilian vermiculite ores. In the case of Chinese sample, the grain size distribution ranges from 3.4 µm to 3350 µm, while it ranges from 3.4 µm to 1400 µm in the Brazilian sample. The results show that the hydrobiotite grains in the Chinese sample are coarser than that of Brazilian sample. The d_{25}, d_{50} and d_{75} of the hydrobiotite grains in the Chinese sample are about 212 µm, 500 µm and 1700 µm respectively, while they are 106 µm, 212 µm and 800µm respectively in the Brazilian sample. About 50% of hydrobiotite grains in the Chinese sample are coarser than 500 µm, while only 20% are coarser than 500 µm in the Brazilian sample vermiculite. The coarseness of hydrobiotite and vermiculite minerals identified in all the measured samples is dependent on their weight abundance in the measured ores.

4.4.3 Thermo-gravimetric Analysis (TGA)

Thermal exfoliation of vermiculite is due to the rapid heating of interlayer water (Muiambo et al., 2010, Obut et al., 2003). It is, therefore, crucial to understand the water network within vermiculite from different geographical locations. Information on the vermiculite water network will help to understand its

contribution to the exfoliation mechanism. Thermo-gravimetric analysis, which measures the changes in the mass of materials as a function of temperature when heated in a controlled environment, was used in this project to study the moisture content in vermiculite samples from Australia, Brazil, China and South Africa. This method has been used to determine moisture content, study decomposition and ash content of soil and clay minerals by analysing the traces of mass loss with temperature (Grim, 1968).

Previous research has shown that the mass loss in vermiculite when heated under controlled temperatures exhibits 3-4 separate stages associated with the removal of different forms of water. These stages have been associated with the losses of adsorbed, free and bound water and water loss due to the dehydroxylation (loss of water from OH) (Brandley and Serrratosa, 1960, Walker, 1961, Marwa et al., 2009, Mouzdahir et al., 2009, Grim, 1968, Földvári, 2011). The temperature range at which the different forms of water are removed from vermiculite are influenced by factors such as, abundance of the interlayer cation, dipole moment and the dielectric constant of the interlayer water (Grim, 1968).

4.4.3.1 Vermiculite Thermo-gravimetric Analysis

The thermo-gravimetric studies of the four vermiculite samples were performed by using a TA Q500 Thermo-gravimetric analyser. The instrument consists of a precision balance, furnace system and sample holders automatically controlled via a computer system. During the measurement process, the measured samples are held in the furnace to scan through the range of required temperature. The objective of this test is to obtain information about the moisture contents of each vermiculite sample by monitoring the change in weight when the vermiculite flakes are continuously heated in a controlled environment.

The tests were repeated five times for each vermiculite sample and the mean values are presented. Consistent heating rate and sample size were maintained to ensure repeatability. Prior to the thermo-gravimetric tests, the ceramic pans used for holding the sample were cleaned in a methane flame to avoid cross contamination

and were then allowed to cool before the sample loading. Between 10-15 mg of vermiculite flakes obtained from representative sample were pre-weighed and placed in each pan. Prepared samples were then heated in the TGA furnace from 25 °C to 900 °C in a nitrogen atmosphere with a flow-rate of 70 ml/min. A slow heating rate of 10 °C/min was chosen to obtain a slow and uniform heating of the sample and hence results to good detail in the dehydration curves.

4.4.3.2 Analysis of TGA Result of Vermiculite

Figure 4-16 shows the TGA result for the Australian and South African vermiculite samples. It was difficult to show error bars on the TGA curves due to the large data points. The results show the average of five repeats for each test. Due to the small amount of samples used for the measurement, the repeatability of the TGA measurement carried out on all the vermiculite samples was determined in terms of the relative standard deviation using Equation 4-2. Where RSD is the relative standard deviation, s is the standard deviation and $\overline{X}$ is the mean of measurements.

$$\%\,\mathrm{RSD} = \frac{s}{\overline{X}} \times 100 \qquad \text{Equation 4-2}$$

The calculated RSD of Australian and South African samples are between 0.05 %-4.02 % and 0.02 %-2.15 % respectively. The low values of percentage relative standard deviation signify that the measurement is repeatable within the measured conditions.

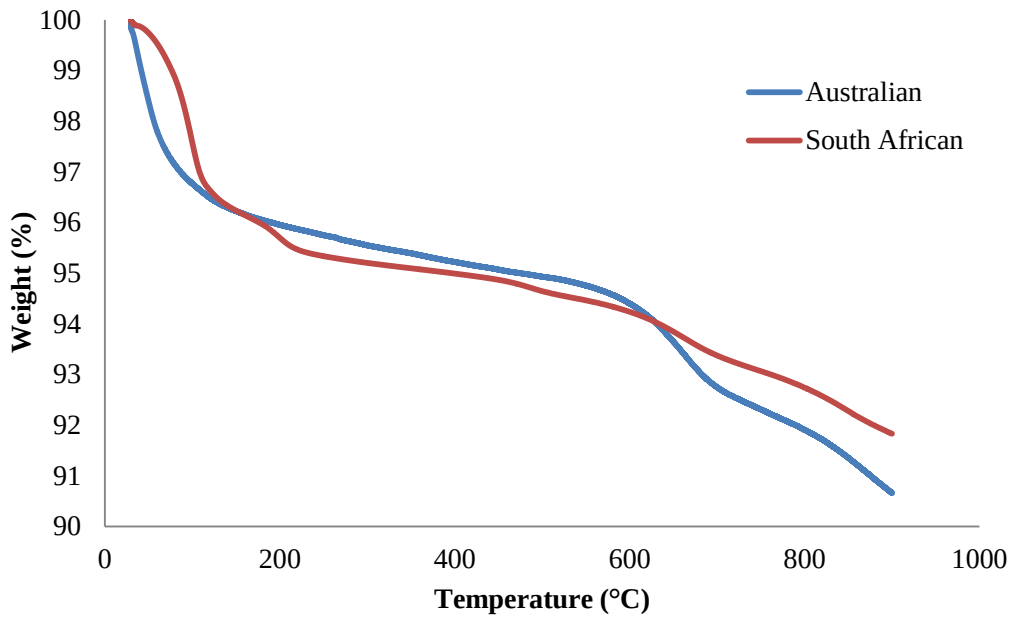

Figure 4-16: Weight change from thermo-gravimetric analysis of Australian and South African vermiculite

The ordinate is the percentage weight change while the abscissa is the controlled temperature. The dehydration curve for Australian vermiculite depicts three steps assumed to be due to the removal of water from the vermiculite structure. This sample shows a weight loss of about 3.53 % below 125 °C, and this is attributed to the complete removal of free interlayer water not in coordination with the interlayer cations. This follows by the average weight change about 1.82 % between 125 °C to a temperature of about 520 °C. This is attributed to the removal of the interlayer bound water. The third step of water removal, starting from 520 °C is due to the gradual loss of OH lattice water (Grim, 1938; Bergaya et al, 2006).

Similarly, South African vermiculite also shows three steps of water removal according to the TGA curves shown in Figure 4-16. The first stage of weight change shown by the TGA curve of South African sample corresponds to the removal of about 4.00 % of free water that is completely removed after about 155 °C. The second dehydration step is assumed to be due to the breakdown of interlayer bound water in coordination with interlayer cations (Grim, 1968). This bound water, which is about 1.77 %, is completely removed by around 500 °C. The last stage of water

removal corresponds to the dehydroxylation of vermiculite. The South African vermiculite ore has higher free water content than Australia vermiculite ore. This may be due to the higher amount of vermiculite mineral in the South African grade compared to Australian grade. The dehydration curve also shows that the Australian vermiculite ore has a higher rate of dehydroxylation than that of the South African vermiculite ore. Figure 4-17 shows the dehydration curves of Chinese and Brazilian vermiculite ores. The % RSD of Brazilian and Chinese samples are between 0.01 %-2.01 % and 0.05 %-4.89 % respectively.

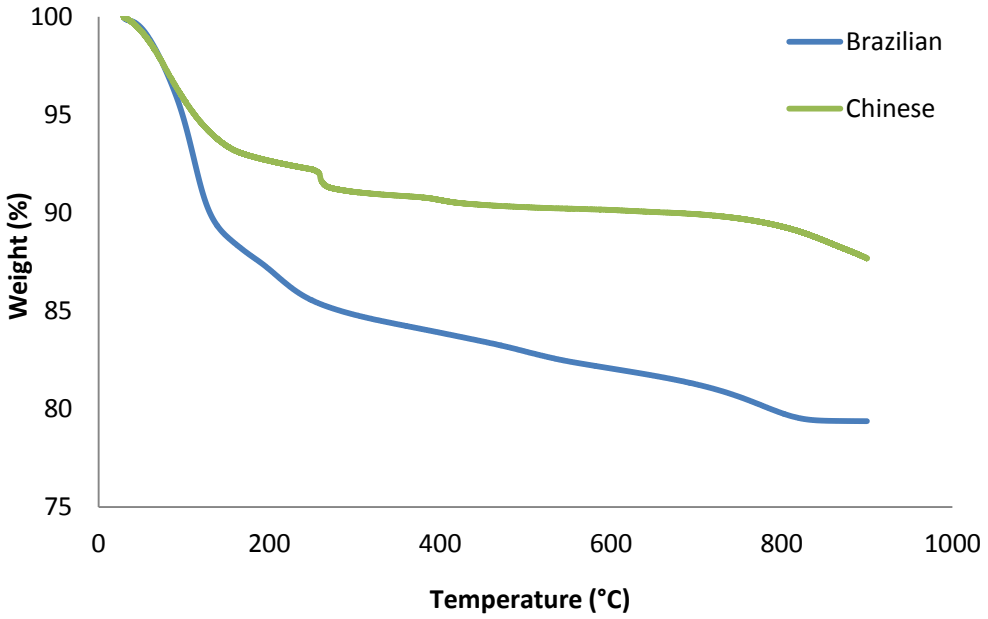

Figure 4-17: Weight change from thermo-gravimetric analysis of Brazilian and Chinese vermiculite

For the Chinese vermiculite ore, the first stage of rapid removal of water from about 30 °C to 150 °C is associated with the removal of 6.65 % of free water (unbounded interlayer water). The second dehydration stage with a weight loss of about 3.27% at temperature range of 150 °C to 620 °C is attributed to the removal of bound water and this is then followed by the dehydroxylation of the vermiculite sample. The TGA curve for Brazilian sample also shows rapid weight loss during the heating process from 35 °C up to about 150°C. About 12.02 % weight loss, which is associated to free water, was recorded during this stage. This is followed by about 6.04 % weight loss from 150 °C up to 500 °C. This second stage of dehydration is

associated to the removal of interlayer bound water. The weight loss observed from 500 °C up to 900 °C is associated to the loss of high temperature hydroxyl (OH) water (Grim, 1938; Bergaya et al, 2006).

A summary of the percentages of free and bound water in the Australian, Brazilian, Chinese and South Africa vermiculites is given in Table 4-7.

Table 4-7: Moisture content analysis of vermiculite ores from four geographical locations (TIWC: total interlayer moisture content).

Grade	Sample	Free water	Bound water	TIWC
Superfine	Australian	3.53	1.82	5.35
	South African	4.00	1.77	5.77
Medium	Chinese	6.65	3.27	9.92
	Brazilian	12.02	6.04	18.06

The free water and the bound water are regarded as interlayer water in the vermiculite structure (Bergaya et al., 2006, Grim, 1968). The thermal exfoliation of vermiculite has been reported to be due to the rapid heating of this interlayer water, which therefore creates enough internal pressure to push apart the vermiculite silicate structure.

Although, Australian and South African vermiculite ores are of the same particle size range between 0.355 mm-1.0 mm (The Vermiculite Association, 2011), there is a slight variation in the quantity of their free water and total interlayer water contents. This is reflected in the variations in their chemical and mineralogical compositions. The effect of variation in chemical compositions is more significant when the moisture content of Chinese and Brazilian samples are compared. The interlayer water in Chinese vermiculite is about half of that in Brazilian sample. The results of XRD and MLA previously discussed in section 4.4.1 and section 4.4.2 show that the Brazilian sample is pure vermiculite when compared to the Chinese

sample, which is predominant hydrobiotite. The XRD analysis indicates that the Brazilian sample has a double layer of water in its interlayer space compared to the Chinese, which has a monomolecular layer of water.

It is also evident from the TGA analysis of Australian, South African, Chinese and Brazilian vermiculite that the water content is a function of the particle size. The Brazilian and Chinese samples, which have a higher particle size range, possess higher moisture contents compared to the South African and Australian sample with lower particle size ranges. It has been demonstrated by various authors that moisture content is one of the factors that influences the degree of vermiculite exfoliation (Brandley and Serrratosa, 1960, Hillier et al., 2013, Huo et al., 2012, Justo et al., 1989). Therefore, the Brazilian sample with higher moisture content would be expected to exfoliate with a higher expansion degree than the Chinese sample. The South African sample would also be expected to exfoliate with a higher expansion degree than Australian vermiculite and this will be examined later in the thesis.

4.5 Dielectric Properties of Vermiculite

A rigorous understanding of the fundamental mechanism through which vermiculite ore heats under microwave energy is crucial to this research. The knowledge of the fundamental mechanism will be used for the process design, development and the improvement. The variations in dielectric properties of materials including vermiculite, with factors such as frequency, density, temperature, moisture content and chemical composition underpin the basis of the engineering modelling, design and construction of either batch or continuous microwave system (Metaxas and Meredith, 1983, Lovás et al., 2011, Chan and Reader, 2000). Therefore, the accurate measurement of dielectric constant (ε') and loss factor (ε'') is required for determining the microwave absorption (power density) in the vermiculite and the penetration depth of the electromagnetic field into the vermiculite structure.

Vermiculite ore is a complex multiphase mineral with high variability in its chemical composition, moisture content and physical properties (Bergaya et al., 2006, Grim, 1968). The mineralogical analysis of vermiculite samples from

different geological locations (Australia, Brazil, China and South Africa) carried out in sections 4.4.1 to 4.4.3, showed mineralogical variations in the vermiculite ores obtained from the different deposits. Therefore, this may also have a significant influence on the dielectric properties of the vermiculites and the resulting microwave interactions.

The objective of this project is to design a microwave heating system suitable for exfoliating all vermiculite grades and other hydrated clay minerals from different geological deposits. Using the limited published data on dielectric properties of vermiculite will not give accurate and complete information about the electromagnetic properties of the different vermiculite samples, and this will lead to insufficient information for the electromagnetic simulation and design of an optimised microwave-heating cavity. Therefore, it is important to carry out measurements of the dielectric properties of vermiculite samples obtained from different geological locations.

Apart from its application for microwave heating, the database of dielectric properties of vermiculite may also be applicable in the mining industry for the dielectric separation of vermiculite from gangue materials during its mining and concentration processes (Ballantyne and Holtham, 2010, Wang H; Lu S, 2003, Andres, 1996). In addition, vermiculite future potential for optical applications may also require accurate knowledge of its detailed dielectric properties (Janek et al., 2010, Marian Janek et al., 2009)

According to the literature survey, only a few studies have been undertaken on the dielectric properties of vermiculite, with the data published in the literature are either limited or not appropriate for a rigorous study of microwave exfoliation (Anjos et al., 2011, Fontgalland et al., 2009, Ruscher and Gall, 1997, Ruscher and Gall, 1995, Marian Janek et al., 2009, Janek et al., 2010). None of the previous investigations measured the dielectric properties of bulk vermiculite at the ISM frequencies, especially at 915 MHz, 896 MHz and 2450MHz, which are the

frequencies allocated for microwave heating (Gupta and Eugene, 2007, Osepchuk, 2002).

Ruscher and Gall (1997) used impedance spectroscopic techniques to measure the conductivity and dielectric constant of iron bearing phyllosilicate (biotite and vermiculite crystals) at low frequencies from 0.1 kHz to 1MHz, and between 290-890°C. Anisotropic measurements were performed on different crystals with the electric field parallel and perpendicular to the (001) planes E||(001) and E $\perp$ (001) modes respectively. Six peaks associated with dehydration of water from the vermiculite interlayer space were observed and the intensity of these peaks was inversely proportional to the applied frequency (intensity decreased with an increase in the frequency). The Phyllosilicate minerals measured (biotite and vermiculite) were reported by the author to be anisotropic in nature and for vermiculite, values of $\approx$ 5 and 40 were recorded for ε'||(001) and ε' $\perp$ (001) respectively at temperatures below 500 °C. The author did report the loss factor (ε'') and loss tangent (tanδ), which are two parameters used in predicting the microwave heating behaviour of materials (Komarov et al., 2005a, Ku et al., 2001a).

Marian et al (2010, 2009) used Terahertz time-domain spectroscopy (THz-TDS) in the far-infrared frequency region (THz) to determine the complex refractive index of layered silicate materials, which include vermiculite, phlogopite, muscovite and biotite. They recorded the lowest value for refractive index and dielectric constants of 2.51 and 6.30 respectively for vermiculite, compared to phlogopite, muscovite and biotite with refractive index of 2.76, 2.73 and 2.82 and dielectric constant of 7.12, 7.45 and 7.95 respectively, despite these minerals having lower moisture contents than vermiculite. The author did not give the reason for this. Fontgalland et al. (2009) proposed the use of time domain reflectometry (TDR) to measure dielectric properties of vermiculite but did not publish the results of their experimental tests. Anjos et al. (2011) used a volumetric water content probe operating at 100 MHz to measure the permittivity of bulk vermiculite and recorded an average value of 4.87 for the dielectric constant. The author did not report the

measured bulk density of vermiculite at which the dielectric constant measurement was performed however.

The limited publications to date on the measurement of dielectric properties of vermiculite may possibly be due to its layered structure, anisotropic nature and the complexity of its multiphase composition. These properties make the accurate measurement of dielectric properties of vermiculite and other phyllosilicate minerals challenging, especially for samples in bulk form (Anjos et al., 2011). The orientation of the vermiculite layer structure to the electric field affects the measurement results (Ruscher and Gall, 1995, Ruscher and Gall, 1997). In addition, it is difficult to obtain suitable vermiculite crystals that can properly fit the available instrumentation for dielectric property measurement. Therefore, theoretical mixing rules and a method based on the density dependence of the dielectric properties of particulate are used in this project to estimate the dielectric properties of solid or vermiculite crystal at the solid density, from the results obtained from measurements carried out in a pulverised or powdered form.

This work includes the dielectric properties of vermiculite ores obtained from Australia, Brazil, China and South Africa. The measurements were conducted at ISM frequencies using cavity perturbation and waveguide techniques. The cavity perturbation was employed for the accurate measurement of the dielectric properties of vermiculite ores in particulate form while the waveguide technique was used to carry out the measurement of the bulk samples of vermiculite.

4.5.1 Cavity Perturbation

As discussed in the Chapter 3, there are many techniques of measuring the dielectric properties of materials at microwave frequencies. These include coaxial probe techniques, waveguide, RF techniques, free space, cavity perturbation and time domain spectroscopy. The cavity perturbation technique employed in this research used a copper resonating cylindrical cavity of TM_{0n0} at frequencies between 400 MHz to 2470 GHz, depending on the cavity dimensions and designs. This method was used for the measurement of dielectric properties of vermiculite, which is a low

loss material, because it is stated as being the most accurate method for measuring dielectric properties of low loss material in pulverised or granular form (Chen et al., 2004, Chao, 1985, Donovan et al., 1993, Sheen, 2009). The method also possesses many other advantages over other dielectric measurement techniques, as it requires no calibration and requires only a small volume of sample.

4.5.1.1 Sample Preparation and Dielectric Properties Measurement Process

The impurities such as stone and magnetic accessory minerals visually identified as non-phyllosilicate minerals in a representative sample of vermiculite ores were hand picked. The samples used for the measurements were then slowly pulverised by hand using an agate mortar and pestle to prevent contamination from milling. The experiment set-up used for the measurements is shown as Figure 4-18. The sample to be measured is auto-mechanically inserted into the cavity region where the measurement takes place by an electric motor. The vector network analyser (VNA) which consists of signal source, a receiver and display units sends electromagnetic signals into the material under test (MUT) in the cavity. The VNA then detects and measures the reflected signal from the MUT and the transmitted signal through it. A furnace is incorporated into the system for high temperature measurements of dielectric properties.

The measurement begins by using the VNA to excite the empty cavity without any foreign bodies present. This is required to determine the resonant frequency and the quality factor of the empty cavity. A 3 mm internal diameter empty quartz tube was inserted into the cavity hole with the aid of movable sample holder incorporated with an actuator. The resonant frequency (f_0) and quality factor (Q_0) of the cavity with the empty glass tube were then measured. The quartz tube was then removed from the cavity, weighed and the mass of the empty tube with fibreglass used as sample stopper was measured and recorded.

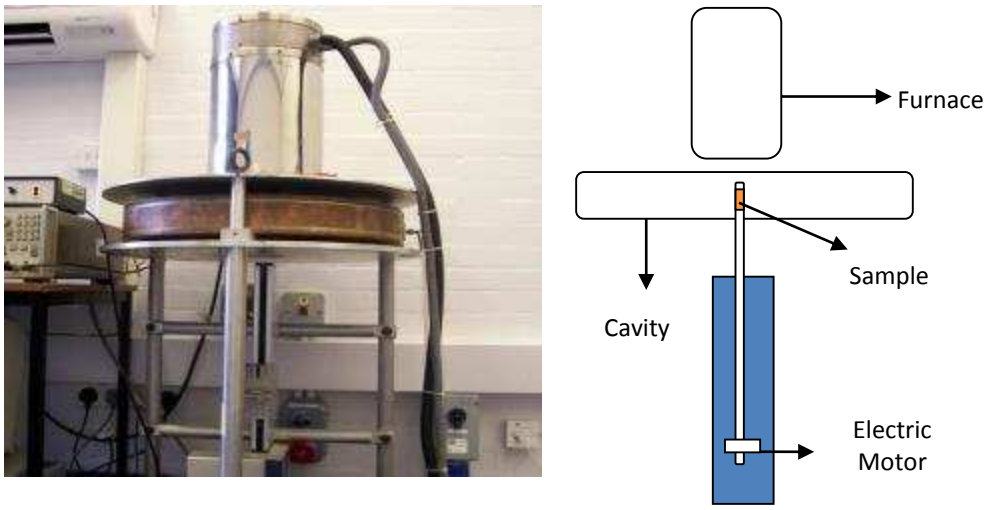

Figure 4-18: Experimental set-up for cavity perturbation

The empty glass tube was filled with the pulverised sample to a height between 15-17 mm and the mass of the sample loaded tube was measured again in order to obtain the sample mass. The loaded sample was compacted by tapping the quartz tube on a wooden block between 30-50 times to obtain the desired packing densities between 0.84 g/cm^3 to 1.42 g/cm^3. A density variation along the sample height was avoided by not applying pressure to the sample surface. The sample was inserted into the cavity until a maximum perturbation was achieved. This was indicated by the VNA as the maximum shifting of the resonant frequency peak. The sample-loaded cavity was then excited to measure the resonant frequency (f_1) and the quality factor (Q_1). Measured quality factor and resonant frequency for both the empty tube and sample-loaded cavity were then inserted into the Equation 3-12 and Equation 3-13 to calculate the loss factor and dielectric constant respectively.

4.5.1.2 Example of Dielectric Properties Calculations

Table 4-8 shows an example of the measurements carried out on South African vermiculite at two frequencies, 934 MHz and 2143 MHz. Both loss factor and dielectric constant are calculated at each frequency using Equation 3-12 and Equation 3-13 respectively. The volume of the cavity and the vermiculite sample in the 3mm tube are 1154430 mm^3 and 13.6 mm^3 respectively.

Table 4-8: Frequency and Q-factor perturbation in a test measurement

	Empty tube		Sample loaded tube	
Modes	Frequency (f_0, MHz)	Q_0-factor	Frequency (f_1, MHz)	Q_1-factor
TM01	933.56	2646.80	933.26	2297.46
TM02	2140.98	2728.50	2139.41	1983.62

Expressed below is the calculation procedure for the TM01 mode measurement at room temperature. The parameters used for the calculation have been defined earlier in Chapter 3.

$$\varepsilon' = 1 + 2 * J_1^2(x_{1,m}) * \frac{V_c}{V_s} * \frac{f_0 - f_1}{f_0} = 1 + 2 * 0.51915^2 * \frac{1154430}{91.43} * \frac{933.56 - 933.26}{933.56} = 3.18$$

4.5.1.3 Validation of Results

As a way of evaluating the accuracy of the measurement technique as well as to consider the results of the measured dielectric properties as a reliable measurement with a high degree of confidence, a validation process is required. This was carried out by measuring the dielectric properties of a known standard material and the obtained results were compared to the results of the National Physical Laboratory (NPL) database. Poly-tetrafluoroethylene (PTFE), a thermoplastic polymer was used as a standard material because it is a low loss material that is cheap and readily available. The results obtained for measurement of the PTFE at room temperature and at 2470 MHz are shown in Table 4-9.

Table 4-9: Dielectric properties of PTFE at 2470 MHz

	Dielectric constant (ε')			Loss factor (ε'')		
PTFE	2.07	2.09	2.09	0.00045	0.00046	0.00048

The average values obtained for dielectric constant and loss factor are 2.08±0.01 and 0.00046±1.53E-05 respectively. These results are in close agreement with that available in the NPL database (2.1 and 0.00042 for dielectric constant and loss factor respectively). This indicates that the available cavity perturbation equipment would accurately measure the dielectric properties of vermiculite, as it is also a low loss material with properties in a similar range of values.

4.5.2 Dielectric Properties Results Measured at Room Temperature by Cavity Perturbation Technique

Dielectric property measurements were carried out on vermiculite ores from Australia, Brazil, China and South Africa, following the procedure described in section 4.5.2.1. It is expedient to state in this section before presenting the dielectric properties results, that the higher the dielectric constant of the material, the greater the capacity and the amount of microwave energy absorbed and stored by this material. In addition, the higher the measured loss factor of material, the greater the tendency of this material to dissipate stored microwave energy as heat (Geyer, 1990, Venkatesh and Raghavan, 2004). The mechanism by which the material dissipates stored microwave energy as heat is the function of the property of the material and the operating frequency. The measurements on Australian and South African samples were carried out at 934 and 2143 MHz over a wide bulk density range. Measurements on Brazilian and Chinese samples were also carried out over a wide bulk density range at five different frequencies (395 MHz, 910 MHz, 1429 MHz, 1949 MHz and 2470 MHz). Measurements were carried out at room temperature on each of the vermiculite samples, each repeated ten times at each frequency and bulk density. The mean values of ε’ and ε’’ were then plotted against the bulk density. A constant volume of the sample was maintained at each bulk density for consistency.

Figure 4-19 to Figure 4-22 showed the relationships between the ε’ and ε’’ and bulk density for the pulverised vermiculite samples from South Africa, Australia, Brazil and China respectively. Figure 4-19 shows the results of dielectric constant and loss factor of South African vermiculite measured at room temperature over a bulk

density ranging from 0.84 g/cm^3 to 1.42 g/cm^3 and microwave frequencies of 934 MHz and 2143 MHz. Both the dielectric constant and loss factor of South African vermiculite sample increased with increasing bulk density. This is due to an increase in interacting mass with electromagnetic field as void ratio is reduced with an increase in bulk density. The dielectric constant of this sample is slightly higher at 934 MHz for all measured bulk densities than the measured values at 2143 MHz. However, higher values of loss factor were obtained at 2143 MHz than at 934 MHz.

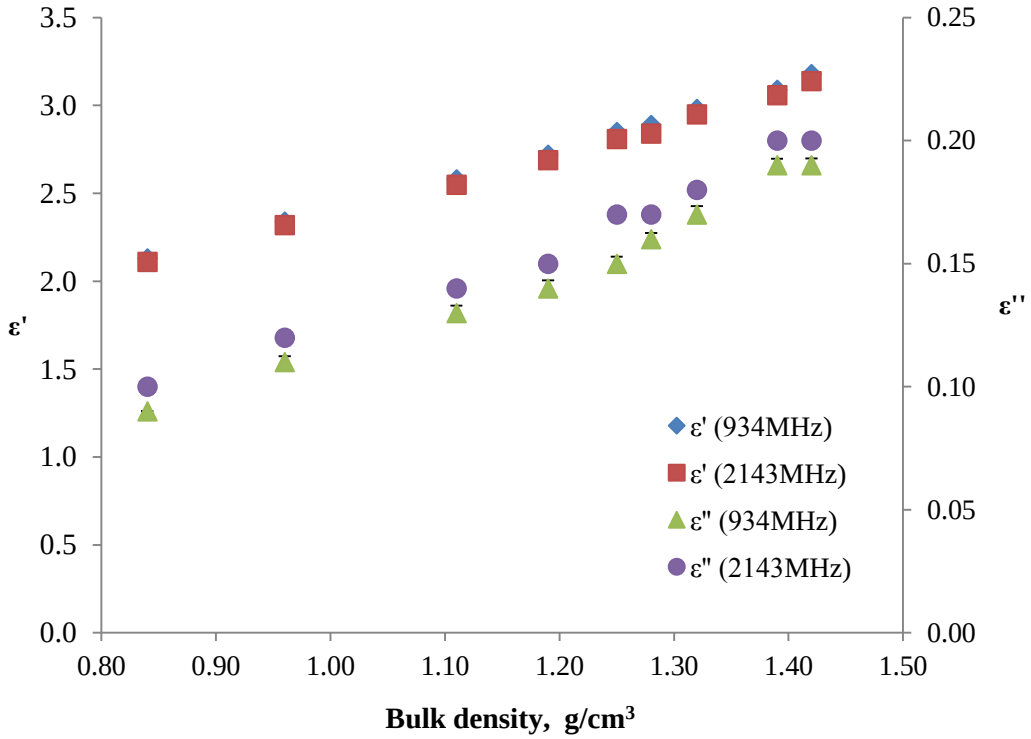

Figure 4-19: Density dependence of dielectric constant and loss factor of South African vermiculite at 934 and 2143 MHz

Figure 4-20 shows the results of dielectric constant and loss factor of the Australian sample against the measured bulk density.

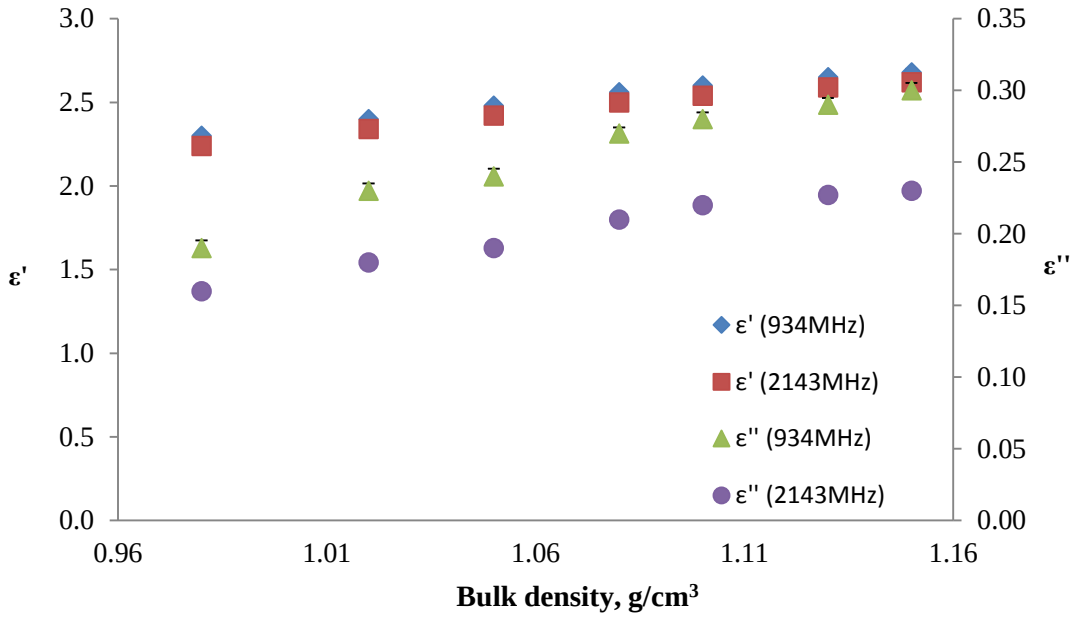

Figure 4-20: Density dependence of dielectric constant and loss factor of Australian vermiculite at 934 and 2143 MHz

The values of ε' obtained at the measured bulk densities were higher at the lower frequency, 934 MHz. In contrast to the results obtained in the South African sample, the results of loss factor in the Australian were higher at the higher frequency, 2143 MHz.

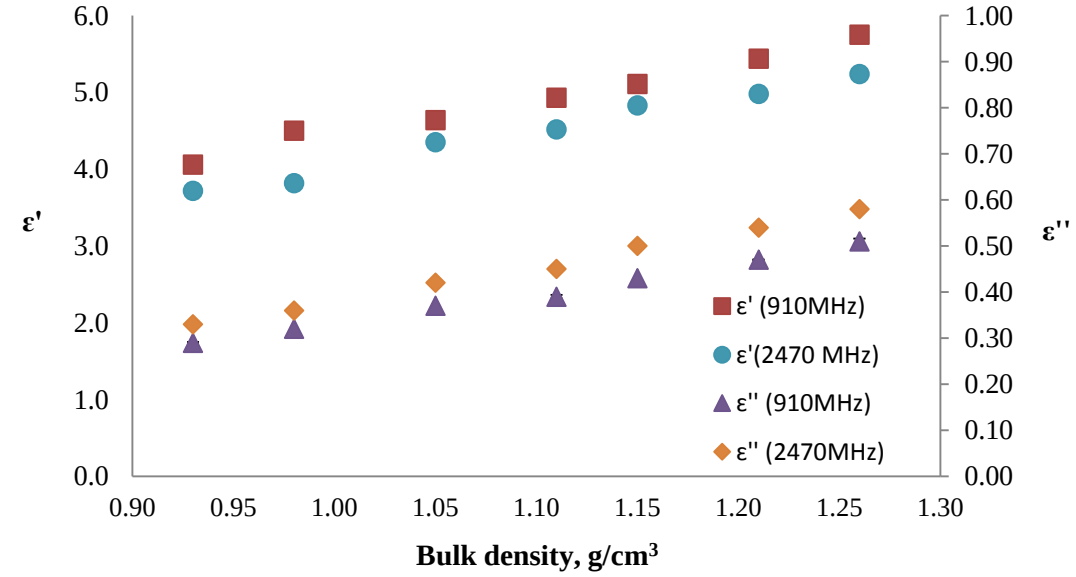

Figure 4-21: Density dependence of dielectric constant and loss factor of Brazilian vermiculite at 910 and 2470 MHz

Figure 4-21 shows the relationship between both ε' and ε'' of the Brazilian vermiculite sample and bulk density at 910 MHz and 2470 MHz. As expected, both dielectric constant and loss factor increase with an increase in the bulk density. The measured dielectric constant over the bulk density range is higher at lower frequency (910 MHz), while the reverse is the case in the measured ε'' as the measured values of ε'' are higher at higher (2470 MHz). The ε' and ε'' trends obtained in the Brazilian sample are similar to that obtained in the South African sample. The results obtained from the dielectric property characterisation of Chinese vermiculite samples are shown in Figure 4-22. Similar to the other measured vermiculite samples, there is a positive correlation between the dielectric properties and density of Chinese vermiculite.

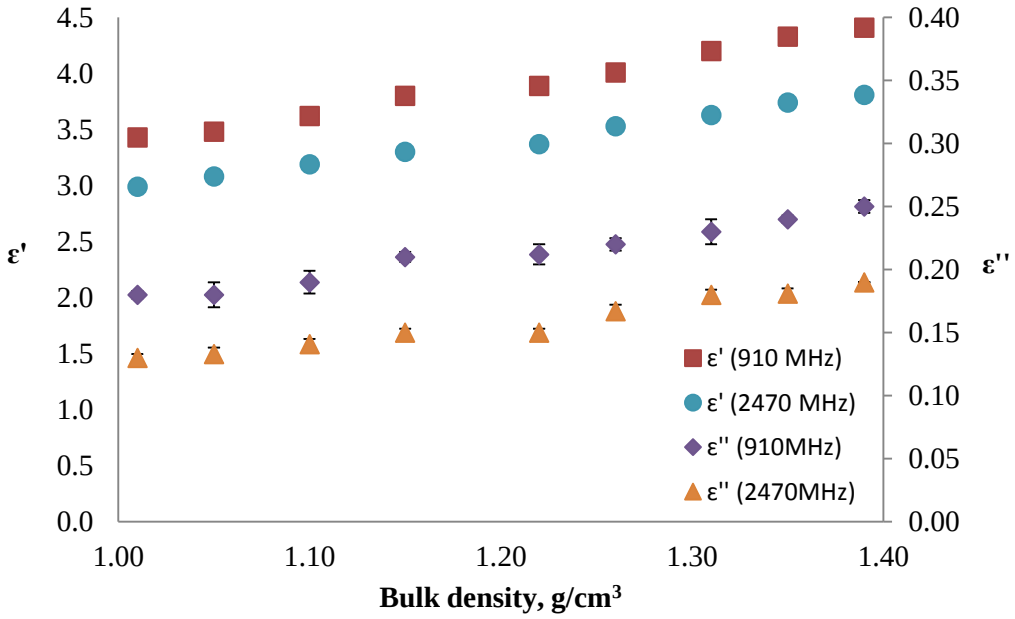

Figure 4-22: Density dependence of dielectric constant and loss factor of Chinese medium vermiculite at 910 and 2470 MHz

The ε' measured over the bulk density range of 1.01 g/cm^3 to 1.4 g/cm^3 is higher at the lower frequency. This is similar to the trend obtained from the ε' of Australian, Brazilian and South African samples. Similarly, the values of loss factor for Chinese sample at lower frequency (910 MHz) are higher than the values obtained at higher frequency (2470 MHz). This is similar to the trend obtained for the loss factor in Australian vermiculite.

A higher dielectric constant at lower frequency in all the measured samples is likely to be due to the effect of both conduction mechanism underpinned by the interlayer cation or ionic water phase and dipolar polarisation of interlayer water, which produces a higher net polarisation effect at lower frequencies. The ionic conduction becomes less significant as frequency increases (Metaxas A.C; Meredith R.J, 1988). The water phase in the vermiculite structure is not pure but contaminated by ions (Grim, 1968), and this significantly contributes to the ionic conduction mechanism at low frequencies (910 MHz and 934 MHz). The higher loss factor recorded at higher frequencies of 2143 MHz and 2470 MHz for South African and Brazilian samples is, therefore, likely to be due to the increase in the rate of polarisation of the free water in the interlayer space. The higher free water content in South African and Brazilian samples when compared to Australian and Chinese samples might have influenced this. This observation agrees with the quantification of the vermiculite water network as described by the XRD analysis in section 4.4.1.3, which shows that Brazilian and South African samples have 2-water layer hydration state (WLHS). In the case of Australian and Chinese vermiculite, the loss factor is higher at lower frequency than at higher frequency. This may be due to the effect of the monomolecular layer of water, the enhanced crystallinity of the interstratified mica/vermiculite structure and a less hydrated potassium cation in the interlayer cation in these two vermiculite samples (Marcos and Rodríguez, 2010b, Marcos et al., 2009). Because of the monomolecular layer of interlayer water in Australian and Chinese samples, they have lower amount of water than the South African and Brazilian samples that contain two layers of water molecules.

4.5.2.1 Effect of Mineralogy on Dielectric Properties of Vermiculite

For the study of the effect of mineralogy on the dielectric properties of vermiculite ore, a superfine grade from South Africa and Australia are compared. Medium grade from Brazil and China are also compared. The results of both dielectric constant and loss factor measured at the same frequency and discrete solid volume fraction are used to study the effect of mineralogy on the dielectric properties of all the four vermiculite samples studied. Figure 4-23 presents the dielectric constant of Brazilian and Chinese samples measured at frequencies of 395 MHz, 910 MHz,

1429 MHz, 1949 MHz and 2470 MHz and at a discrete solid fractional volume of 0.53, which is the highest achieved packing density.

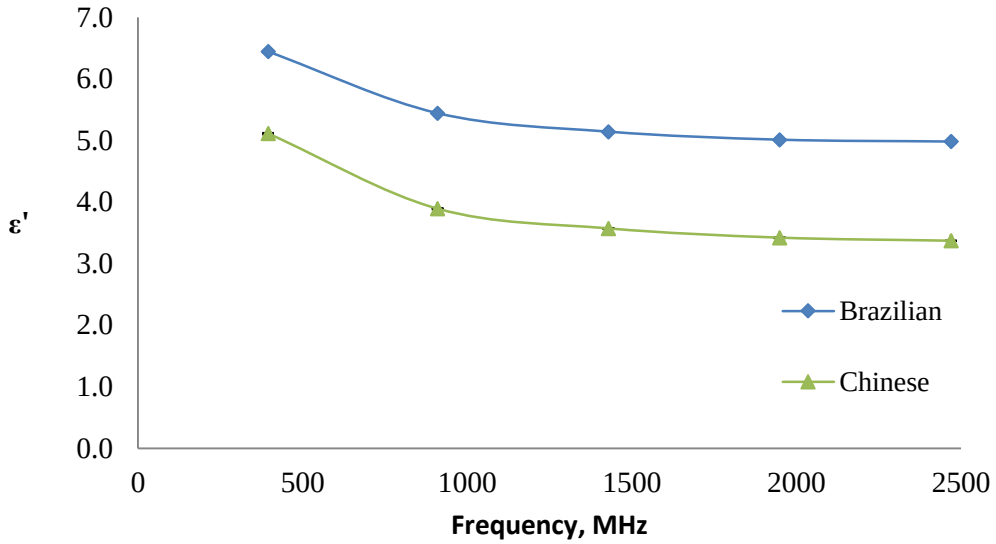

Figure 4-23: Dielectric constant of Brazilian and Chinese samples measured at a discrete solid volume fraction of 0.53 and 395 MHz, 910 MHz, 1429 MHz, 1949 MHz and 2470 MHz.

Figure 4-24 presents the results of the dielectric constant for South African and Australian samples at frequencies of 395 MHz, 910 MHz, 1429 MHz, 1949 MHz and 2470 MHz. The packing of the powder samples was performed to obtain a discrete solid phase volume fraction of 0.53.

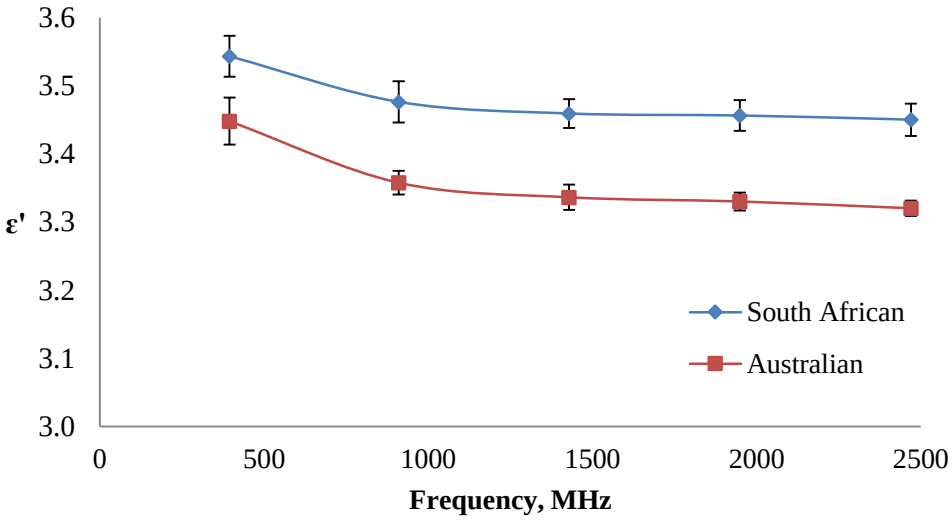

Figure 4-24: Dielectric constant of South African and Australian samples measured at a discrete solid volume fraction of 0.53 and 395 MHz, 910 MHz, 1429 MHz, 1949 MHz and 2470 MHz.

Figure 4-23 shows that the Brazilian sample possesses higher values of dielectric constant at all the measured frequencies than that of Chinese sample. It was also shown by Figure 4-24 that South African sample has higher dielectric constant than the Australian sample at all the measured frequencies. The variation in the dielectric constant of Brazilian and Chinese samples and that of South African and Australian samples can be explained by the variations in their mineralogical composition. The higher ε' recorded for the Brazilian and South African samples when compared to the Chinese and Australian samples respectively, is probably due to the high polarisation of their interlayer water content and the significant effect of ionic conduction mechanism of interlayer cation (Stuerga, 2006). Both Brazilian and South African samples also have higher vermiculite mineral when compared to Chinese and Australian samples respectively and they also possess higher free and total water content as discussed in section 4.4.3.1

Figure 4-25 presents the ε'' of Brazilian and Chinese samples from 395 MHz to 2470 MHz, while Figure 4-26 shows that of South African and Australian samples across the same frequency range.

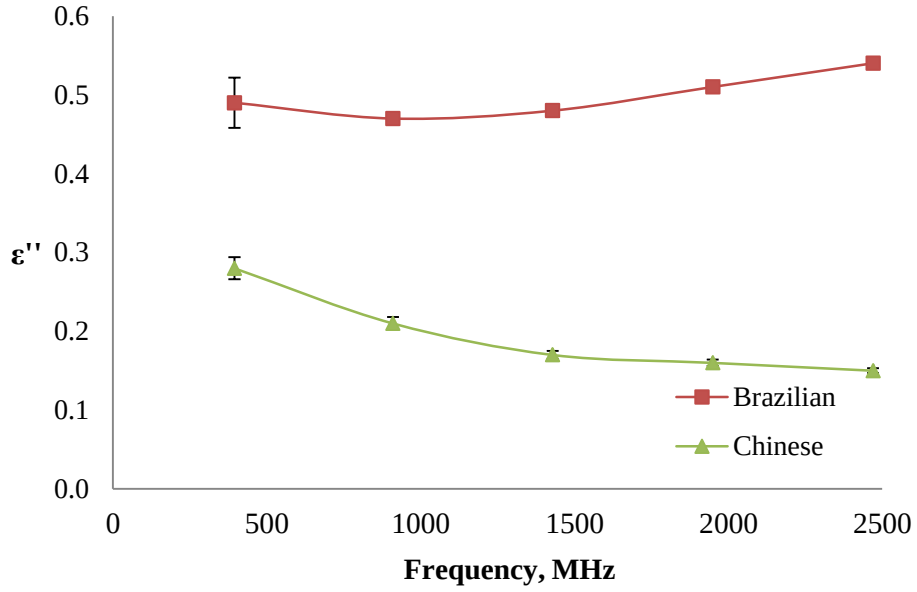

Figure 4-25: Loss factor of Brazilian and Chinese samples measured at a discrete solid volume fraction of 0.53 and 395 MHz, 910 MHz, 1429 MHz, 1949 MHz and 2470 MHz.

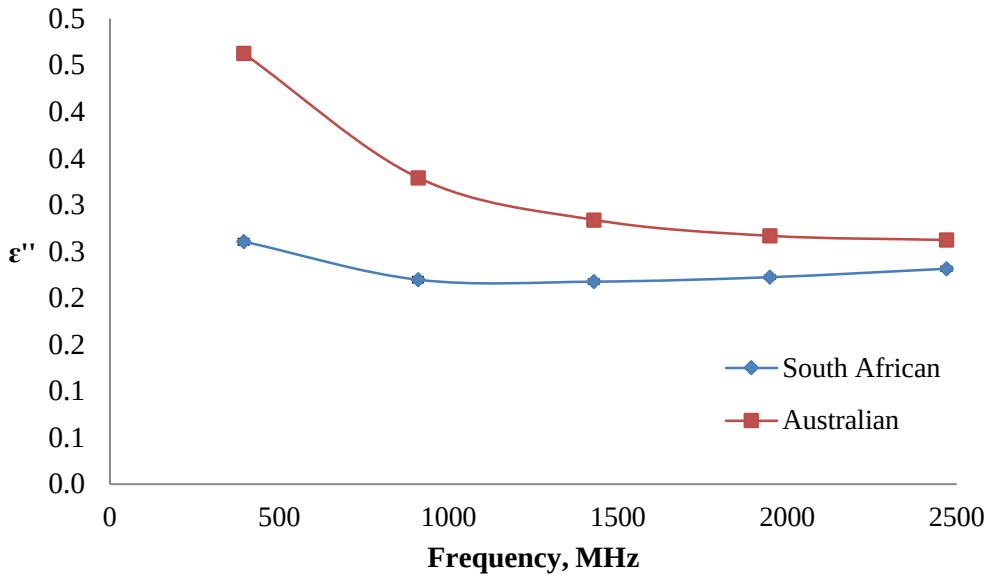

Figure 4-26: Loss factor of South African and Australian samples measured at a discrete solid volume fraction of 0.53 and 395 MHz, 910 MHz, 1429 MHz, 1949 MHz and 2470 MHz

Figure 4-25 shows that the loss factor of the Brazilian sample increases with an increase in microwave frequency, from 395 MHz to 2470 MHz. It increased steadily from 0.49 at 395 MHz to about 0.54 at 2470 MHz. In contrast to the data for loss factor of the Brazilian sample, the loss factor of the Chinese sample decreases with an increase in frequency. The values of ε'' in the Chinese sample were found to decrease from about 0.28 at 395 MHz to about 0.15 at 2470 MHz. It is evident from Figure 4-25 that the ε'' measured at each frequency point in the Brazilian sample is higher than the values obtained for the Chinese sample. The frequency variations of ε'' in both South African and Australian samples as illustrated in Figure 4-26, showed that the ε'' decreased with an increase in microwave frequency from 395 MHz to 2470 MHz. At all the measured frequencies, the values of ε'' recorded are higher in the Australian sample than the South African sample.

According to the theories of dielectric relaxation expressed by Equation 4-3 and Equation 4-4 (Metaxas and Meredith, 1983, Hippel, 1954), both ε' and ε'' should decrease with increasing frequency, assuming the operating frequency is higher than the material relaxation frequency. Parameters ε_0 and ε_∞ are the values of dielectric

constants at d.c. and very high frequencies respectively, and ω and τ are the angular frequency and relaxation time respectively.

$$\varepsilon'(\omega) = \varepsilon_\infty + \frac{(\varepsilon_0 - \varepsilon_\infty)}{1 + \omega^2 \tau^2} \qquad \text{Equation 4–3}$$

$$\varepsilon''(\omega) = \frac{(\varepsilon_0 - \varepsilon_\infty)\omega\tau}{1 + \omega^2 \tau^2} \qquad \text{Equation 4–4}$$

The dielectric constant results of both Brazilian and Chinese samples (Figure 4-23) and that of South African and Australian samples (Figure 4-24) show the expected trend of a decrease in ε' with increasing frequency. This indicates that the microwave absorption capacity of the four measured vermiculite ores reduced with an increase in frequency. The higher dielectric constant reported at low frequencies is due to the combined effect of dipolar polarisation and ionic conduction of interlayer cation since the interlayer water in vermiculite structure is not pure water but water containing dissolved cations (Bergaya et al., 2006, Grim, 1968, Metaxas and Meredith, 1983).

The increase in the loss factor of Brazilian vermiculite with frequency (Figure 4-25) suggests that the frequencies used for the dielectric property measurements are lower than its relaxation frequency, assuming the Brazilian sample is a Debye solid with a single relaxation frequency. In contrast to the Brazilian sample, the values of dielectric loss factor in the other three vermiculite samples decreased with an increase in microwave frequency. This signifies that the ability of South African, Chinese and Australian samples to dissipate microwave energy as heat reduces within the measured frequency range (395 MHz to 2470 MHz). If these three samples are also assumed to be Debye solids, the decrease in the loss factor may suggest that the operating frequencies from 395 MHz to 2470 MHz are higher than the relaxation frequency of these vermiculite samples. Comparative analysis of the dielectric properties of the measured vermiculite ores shows that there is a variation in the electromagnetic properties of these samples. The electromagnetic variations

of these samples could be explained by their mineralogical variations as discussed in section 4.4.

The calculated values of loss tangent for Brazilian and Chinese vermiculites are shown in Figure 4-27, while Figure 4-28 presents the calculated loss tangent of South African and Australian samples. The loss tangent was calculated from the ratio of loss factor to the dielectric constant. The loss tangent is a measure of the degree of dissipation of absorbed microwave energy as heat (Meredith, 1998).

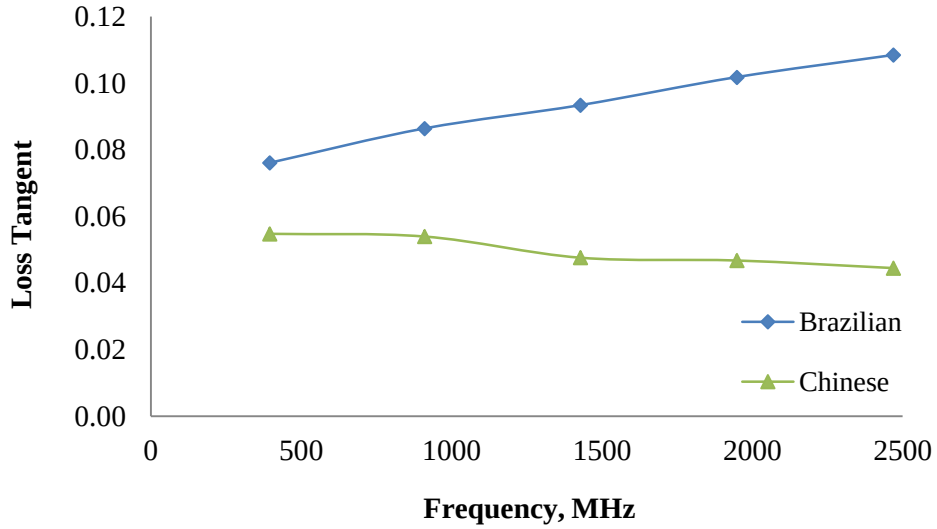

Figure 4-27: Loss tangent of Brazilian and Chinese vermiculite ores

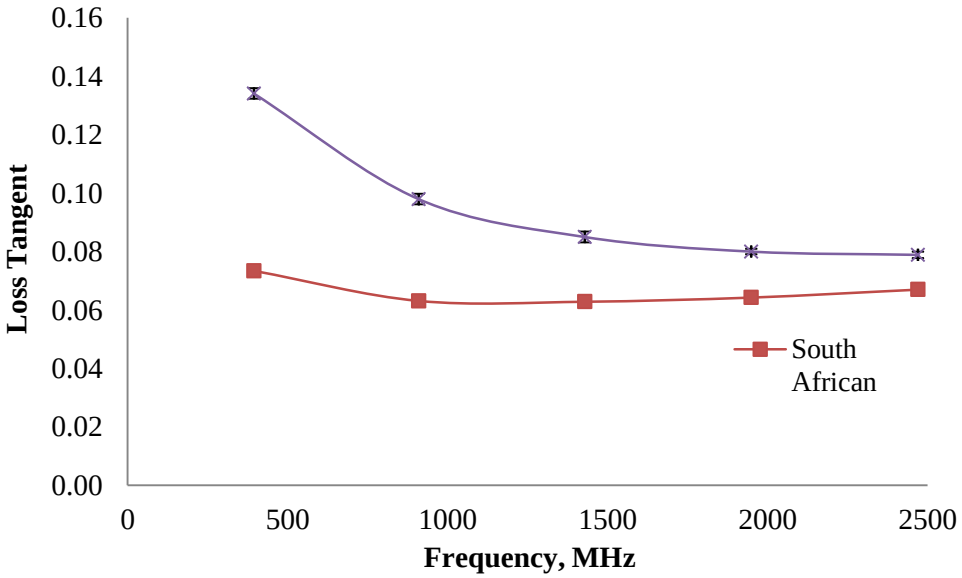

Figure 4-28: Loss tangent of South African and Australian vermiculite ores

Since the loss tangents at each frequency were not measured directly by cavity perturbation, but were calculated from the measured loss factor and dielectric constant, the propagation error of each calculated loss tangent was determined using Equation 4-5.

$$\Delta \mathrm{Tan}\delta = \mathrm{Tan}\delta \times \sqrt{\left(\frac{\Delta\varepsilon''}{\varepsilon''}\right)^2 + \left(\frac{\Delta\varepsilon'}{\varepsilon'}\right)^2} \qquad \text{Equation 4–5}$$

Where ΔTanδ is the uncertainty in the calculated loss tangent and Δε' and Δε'' are the standard deviations of measured dielectric constant and loss factor. The calculated propagation errors are from 0.001 to 0.005 for the Brazilian sample and from 0.001 to 0.003 for the Chinese sample. In both Brazilian and Chinese samples, the highest propagation errors were obtained at the lowest frequency. The calculated propagation errors in the Australian sample range from 0.001 to 0.002 while the propagation error in the South African sample is approximately 0.001.

The loss tangent trends observed in both Brazilian and Chinese samples are similar to the trends obtained for their loss factor. This is because the changes observed in their ε'' as a function of frequency was higher than that of ε'. The loss tangent of Brazilian vermiculite increased with frequency from 0.08 at 395 MHz to about 0.11 at 2470 MHz. The loss tangent of the Chinese sample remains constant at 0.05 from 395 MHz to 1949 MHz before reducing to 0.04 at 2470 MHz. The implication of the higher loss tangent in the Brazilian sample at all the measured frequencies compared to the Chinese sample, is that the degree of dissipation of absorbed microwave energy would be higher in the Brazilian sample. This result is consistent with the higher values of ε' and ε'' in the Brazilian sample. The loss tangent of the Australian sample follows the same trend as its loss factor. Its loss tangent decreases with an increase in frequency from about 0.13 at 395 MHz to about 0.08 at 2470 MHz. In the case of the South African sample, its loss tangent values from 910 MHz to 1949 MHz remains constant at 0.06 while a value of 0.07 was recorded at 395 MHz and 2470 MHz.

The Brazilian sample, which has the highest vermiculite content among the four samples measured, has significantly higher values of ε', ε'' and tan δ at all frequencies compared to the Chinese, Australian and South African samples that are predominantly mixed layers of mica/vermiculite (hydrobiotite). The reason for the higher dielectric properties of the pure vermiculite as found in the Brazilian sample is explained in terms of the mineralogical variations. Apart from the fact that Brazilian sample has a higher free water and total moisture content than the other measured samples, the mica/vermiculite interstratification structure creates a strong opposing force to the polarisation of the free water within the vermiculite structure and this causes a lower value of loss factor (Grim, 1968).

4.5.2.2 Effect of Temperature on Dielectric Properties of Vermiculite

Vermiculite exfoliation either by conventional or microwave heating involves the rapid heating of the interlayer water within the vermiculite structure. The exfoliation takes place at elevated temperatures up to 900 °C in conventional furnace techniques (Marcos and Rodríguez, 2010b, Marwa et al., 2009, Muiambo et al., 2010), but the critical temperature required for microwave exfoliation is lesser than 500 °C (Marcos and Rodríguez, 2010a, Obut et al., 2003). Microwave polarisation processes such as ionic conduction and dipolar polarisation are strongly dependent not only on microwave operating frequency, but also on the operating temperature. Therefore, since the dielectric property of the material, which is the main parameters that dictates its microwave heating is temperature dependent, therefore, it is important to study the effect of temperature on vermiculite dielectric properties. The objective of this is to determine the responsiveness of dielectric constant, loss factor and loss tangent of the vermiculite materials to a change in temperature at constant frequency.

The temperature variations of the dielectric properties of vermiculite were carried out at 910 MHz and 2470 MHz using the cavity perturbation technique. These measurements were complicated by the exfoliation property of vermiculite at high temperature because the cavity perturbation theory depends on the volume of the measured sample. Therefore, small samples of vermiculite were used in order to

minimize exfoliation. The high temperature measurements of dielectric properties of vermiculite were limited to only the medium grade of Brazilian and Chinese samples because each measurement takes a very long time (over 15 hrs) to complete. Measurements were carried out at room temperature (20 °C) for both samples and at successive temperatures of 50 °C up to 800 °C.

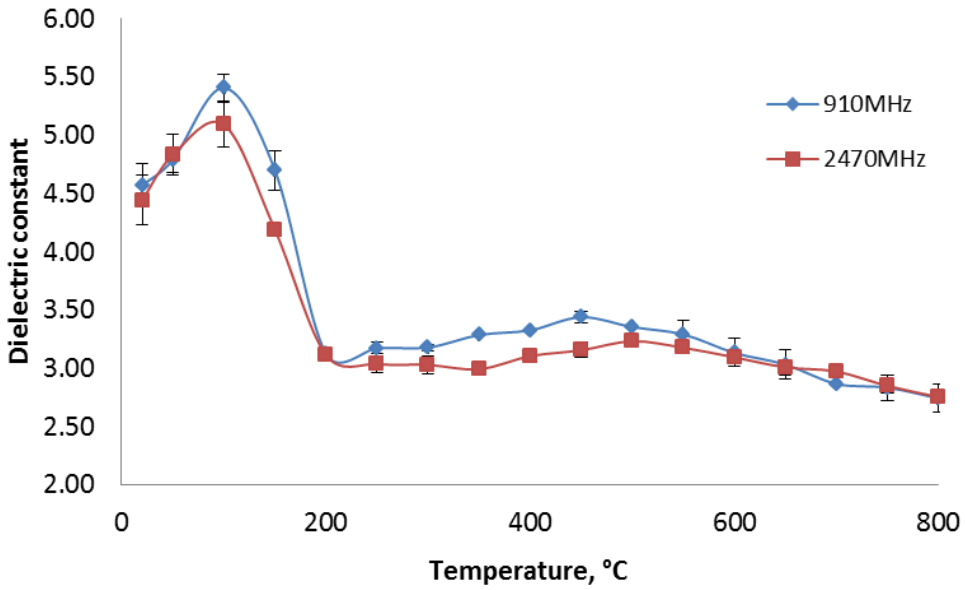

Figure 4-29: Dielectric constant of Brazilian vermiculite as a function of temperature at 910 and 2470 MHz

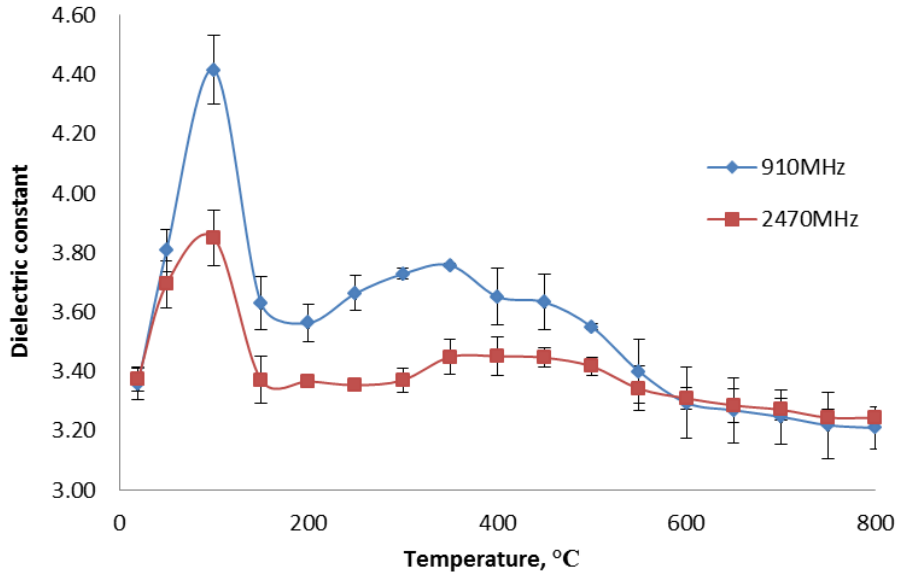

Figure 4-30: Dielectric constant of Chinese vermiculite as a function of temperature at 910 and 2470 MHz

Figure 4-29 and Figure 4-30 show the measured ε' for Brazilian and Chinese samples respectively. The measurements were carried out from the room temperature up to 800 °C, for two distinct frequencies of 910 and 2470 MHz. The plots are average of three repeat measurements. In the Brazilian sample, similar trends in terms of the dielectric profile against temperature were obtained at the two frequencies. The ε' of Brazilian sample shows a significant increase from room temperature up to 100 °C and then decreases rapidly from 100 °C up to 200 °C. In both measured frequencies, the dielectric constant steadily increases from 200 °C up to 450 °C before it starts decreasing up to the 800 °C.

For the ε' results of Chinese sample shown in Figure 4-30, ε' increases rapidly from room temperature up to 100°C, before it starts decreasing. The ε' then increases from 150 °C up to 350 °C, before it starts decreasing up to 800 °C. At the two frequencies under study, the ε' of Brazilian sample is higher than that of Chinese sample. In both samples, two peaks of ε' were observed. These peaks were observed at 100 °C and 450 °C in the Brazilian sample, but they occurred at 100 °C and 350 °C in the Chinese sample. The first peak at 100 °C in both samples is due to the breaking down and removal of free water from the vermiculite structure (Bergman et al., 2000, Ruscher and Gall, 1997). The dehydration of the vermiculite material due to the removal of free water at 100 °C, reduces the dipole-dipole interactions and subsequently increases the dipolar polarisation mechanism (Ruscher and Gall, 1997). The second peak observed in both samples, but at different temperatures, may be due to the combinational effect of the breaking down of the cationic bounded water and the complete removal of the interlayer water. It was observed that the values of ε' and the intensity of these two peak decreases with increasing frequencies. This is because the higher the frequency, the more challenging it become for the dipoles to follow the electric field (Kaur et al., 2012, Metaxas and Meredith, 1983). The higher dielectric constant obtained in the first peak at 100°C compared to the second peak which were observed at 450 °C and 350 °C in Brazilian and Chinese samples respectively agrees with the literature (Boyarskii et al., 2002, Robinson et al., 2002). The gradual decrease in ε' observed from 450 °C up to 800 °C in the Brazilian sample, and from 350 °C up to 800 °C in the Chinese sample, is

due to the dehydroxylation and complete removal of bound water in the form of OH^-. Beyond 350 °C and 450 °C in both Brazilian and Chinese samples, the ability of to absorb microwave energy reduces significantly.

The temperature dependence of ε'' of Brazilian and Chinese samples at 910 MHz and 2470 MHz are presented in Figure 4-31 and Figure 4-32 respectively.

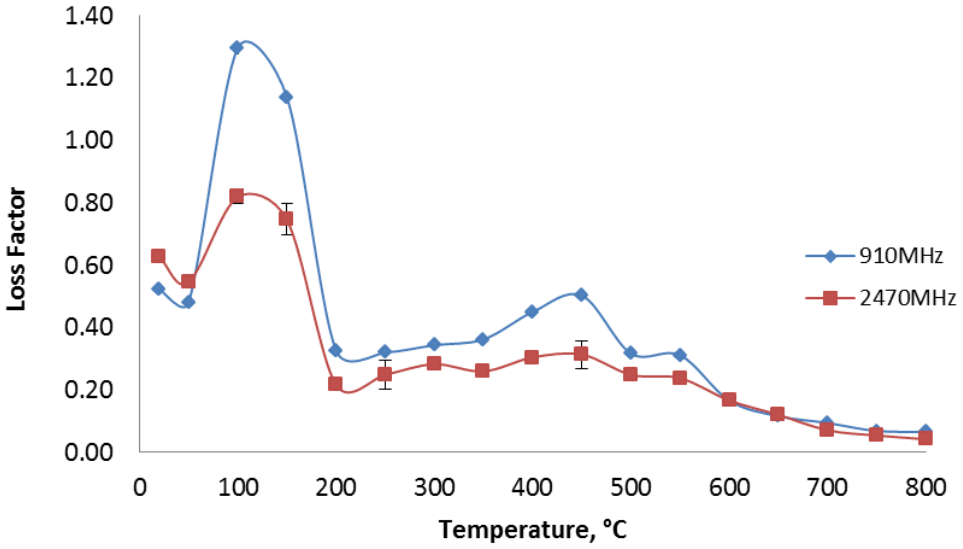

Figure 4-31: Loss factor of Brazilian vermiculite as a function of temperature at 910 and 2470 MHz

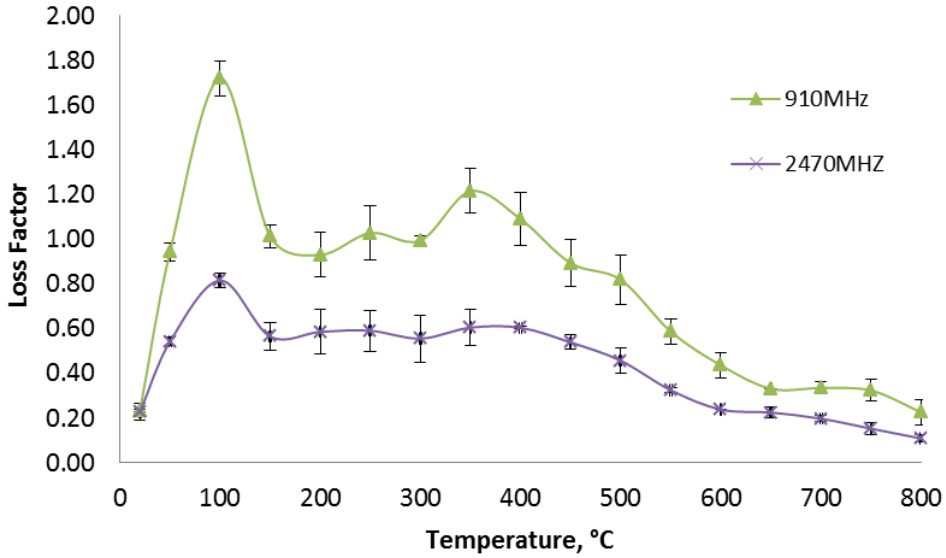

Figure 4-32: Loss factor of Chinese vermiculite as a function of temperature at 910 and 2470 MHz

The ε'' of Brazilian sample shows very strong peaks at about 1.30 and 0.50 at 100 °C and 450 °C respectively (Figure 4-31). Similar to the measured ε' of this sample, its ε'' decreased rapidly by about 75 % and 73 % at 910 MHz and 2470 MHz respectively from 100 °C to a temperature of 200 °C. The loss factor also decreased from the observed peaks at 450 °C, up to a minimum value of about 0.04 at 800 °C.

The loss factor of the Chinese vermiculite sample increased rapidly from room temperature, 20 °C up to 100 °C, where the maximum loss factor was obtained. Another loss factor peak was obtained at 350 °C for the two measured frequencies, but the intensity of these peaks was stronger at 910 MHz.

As already discussed for the maximum values of dielectric constant obtained at 100 °C, the high values of loss factor at 100 °C in both samples is associated with the dissipation due to free water in the vermiculite interlayer space. The loss factor decreases from 100 °C up to 200 °C in Brazilian sample and up to 150 °C in the Chinese. This is due to the complete removal of dissociated free water (Bergman et al., 2000). Most of the interlayer bound water that is in coordination with the interlayer cations (Grim, 1968, Hougardy et al., 1970, Bergaya et al., 2006) is broken down between 250 °C-500 °C. The high loss factor peaks observed at 450 °C and 350 °C in Brazilian and Chinese samples could be explained by the dissipation effect due to the vermiculite lattice's bound water. The steady decrease in loss factor of Brazilian and Chinese samples from 450 °C and 350 °C respectively up to 800 °C in both samples is likely due to the complete removal of interlayer water (free and bound water) and the dehydroxylation of hydroxyl water.

The variation in dielectric properties of vermiculite reveals that its dielectric properties change significantly with increasing temperature, demonstrating that its microwave absorption property change as it is heated. The results demonstrate that the dielectric properties of vermiculite ores irrespective of geological sources are strongly affected by the total water content (free, bound and hydroxyl water). As the water molecule in the vermiculite lattice is removed, their dielectric properties reduced (Ruscher and Gall, 1995, Ruscher and Gall, 1997). The dielectric results

agree with the dehydration profile obtained from the thermogravimetric analysis discussed earlier in section 4.4.3. The increase in ε' and ε'' at 100 °C and between 350 °C and 450 °C is almost certainly due to the breaking down of free water and the bond between the bound water and interlayer cations respectively. The breaking down of these waters reduces their dipole-dipole interactions and, therefore, increases their mobility and ease of polarisation.

4.5.3 Waveguide Measurement of Dielectric Properties of Vermiculite

Measuring dielectric properties of materials over a wide frequency range is one of the limitations of the cavity perturbation technique used for the vermiculite dielectric property measurements, because the method only allows dielectric measurements at limited frequency points (Chen et al., 2004, Donovan et al., 1993). The cavity perturbation technique also has an inherent challenge in measuring a bulk sample of material, as a small volume of sample especially in powdered form is required (Sheen, 2009). In order to obtain the dielectric properties of a bulk sample of vermiculite across a broadband of frequencies, a non-destructive method based on measuring the scattering parameters on the transmission line of a rectangular waveguide system was employed in this project. The waveguide technique was used to carry out measurements of dielectric properties of vermiculite samples from the four geological locations, from 0.8GHz to 1GHz. This was the available waveguide kits during the time of this experiment. This measurement technique is well suitable for measuring solid material but the main limitation of this technique is that it requires a complex calibration procedure, which determines the accuracy of the measurement results (Hasar, 2010, Max Sucher and Fox, 1963, Belrhiti et al., 2012, Ebara et al., 2006, Jenkinst et al., 1989). This method measures material properties in terms of scattering parameters (S-parameter), which are the reflection and transmission coefficient of the material under test (MUT).

4.5.3.1 Experimental Procedure for Waveguide Technique

The experimental setup used for this system is shown in Figure 4-33. It consists of an Agilent 8753 VNA connected to both ports of an open-ended rectangular

waveguide (WR975), with two coax-to-waveguide adapters. The system has a sample holder of 3 litres capacity and it is connected to a computer system that measures, calculates, and stores the measured dielectric properties by using a computer software developed by Andrew Gregory of National Physical Laboratory (NPL). In order to measure the S-parameter of the MUT using the VNA, the waveguide system is calibrated by Thru-Reflect-Line (TRL) calibration, which was first proposed by Engen and Hoer (1979). This calibration procedure was chosen to obtain a high measurements accuracy by correcting the measurement deviations due to VNA and connecting cables fluctuations (Caballero et al., 2013, Engen and Hoer, 1979). After the TRL calibration, prepared vermiculite samples from South Africa, Australia, Brazil and China were placed in the sample holder guided by polytetrafluoro-ethylene (PTFE), and it was ensured that MUT completely filled up the sample holder as shown in Figure 4-33 to prevent air gaps in the sample holder.

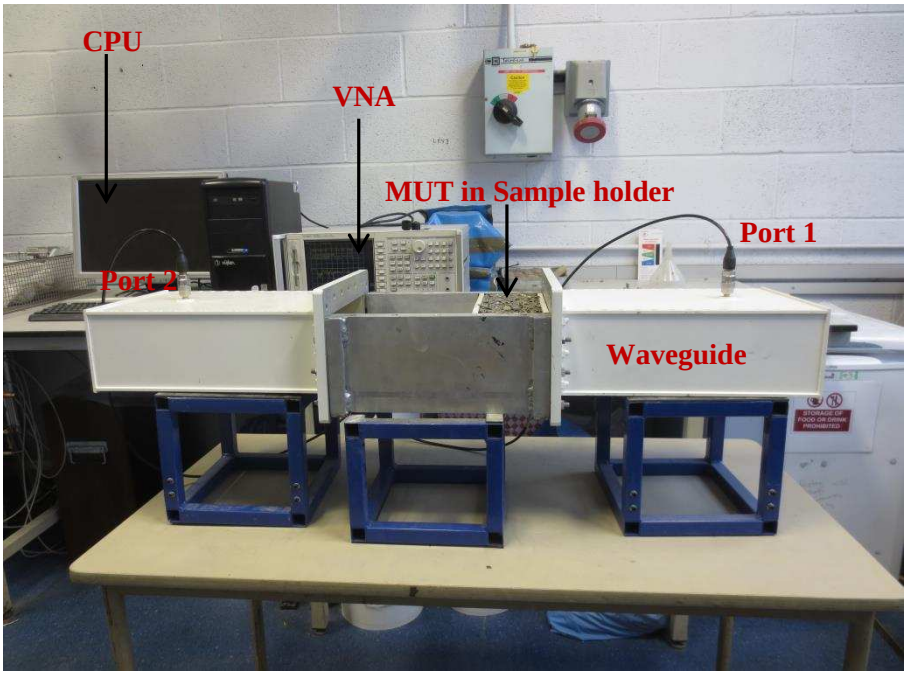

Figure 4-33: Rectangular waveguide loaded with vermiculite bulk sample

The bulk densities of the measured samples were calculated from their masses and volumes. The VNA connected to both ports of waveguides was then used to measure the scattering parameters, that is the transmission coefficient (S_{21} and S_{12}) and reflection coefficient (S_{11}, S_{22}) of the MUT from 0.8 GHz 800MHz to 1 GHz. A

computer connected to the waveguide system, then collects the measured scattering parameter from the VNA. The dielectric properties results (both ε' and ε'') were extracted by using the Newton-Raphson iterative approach that is more accurate than the Nicholson-Ross and the ordinary Newton-Raphson formula (Clarke et al., 2003, Grantt et al., 1989). This iterative calculation of dielectric constant and loss factor values has been reported to be suitable for characterising low loss materials (Jebbor et al., 2013).

4.5.3.2 Results of Waveguide Measurements of Dielectric Properties of Vermiculite

A waveguide technique was used to study the dielectric properties of vermiculite samples from Australia, Brazil, China and South Africa, over a range of frequencies from 0.8 to 1GHz. Each sample was measured at between three to five bulk densities and measurements were repeated for five times at each bulk density. For clarity, only the results obtained at one bulk density for each sample are discussed in this section. However, the comprehensive results of the waveguide measurement are shown in the Appendix 2. The dielectric constant of South African and Australian samples are shown in Figure 4-34, while the dielectric constant of the Brazilian and Chinese samples are presented in Figure 4-35.

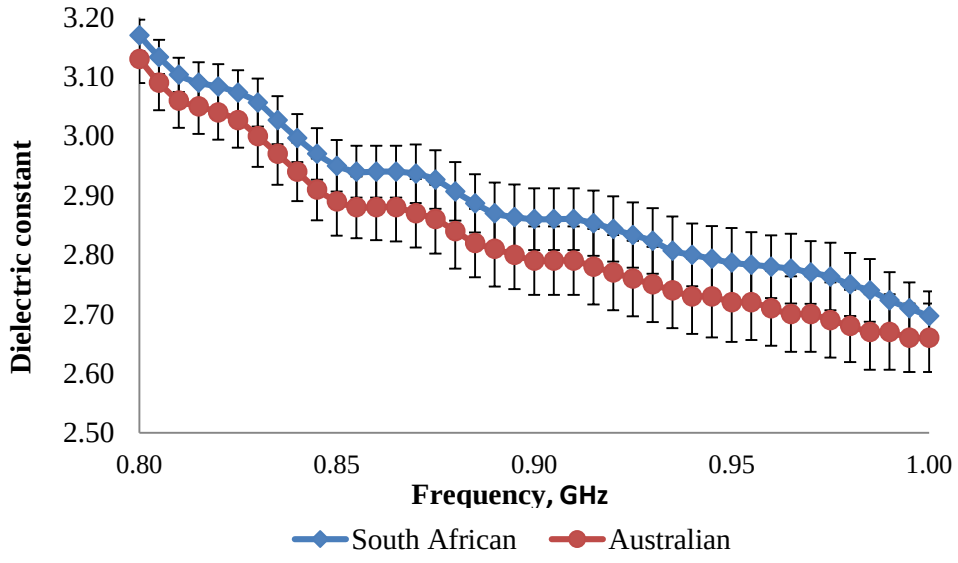

Figure 4-34: Dielectric constant of South African and Australian samples

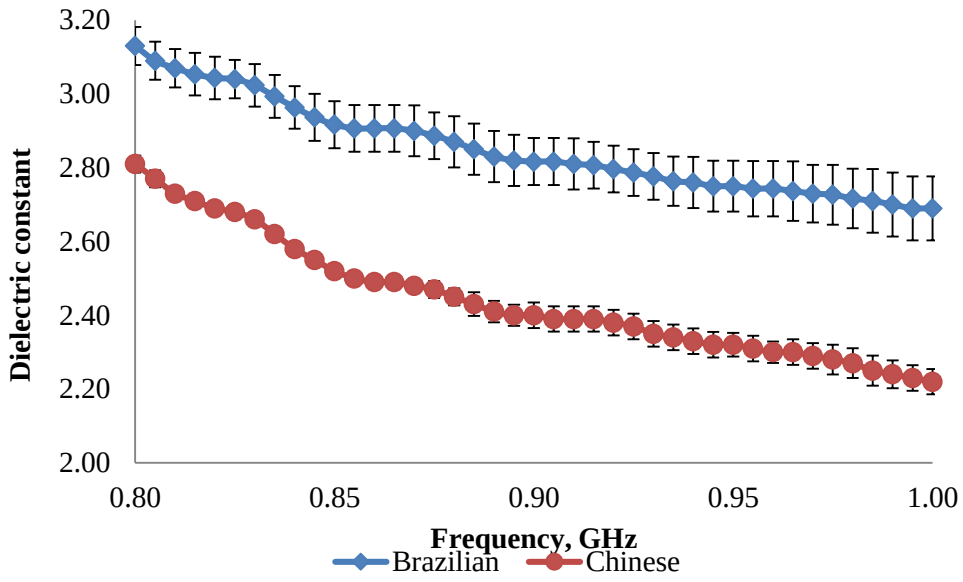

Figure 4-35: Dielectric constant of Brazilian and Chinese samples

The results presented in Figure 4-34 show that the dielectric constant of the South African sample decreases with an increase in frequency from 0.8 GHz to 1 GHz. A similar trend was exhibited for the dielectric constant of Australian sample. At all the measured frequency range, the values of dielectric constant of the South African sample are higher than that of Australian sample.

Figure 4-35 shows that the dielectric constant of the Brazilian sample decreases with an increase in the frequency within the measured frequencies. Likewise, the values of dielectric constant of Chinese sample. The results revealed that the variation between the Brazilian and Chinese samples increased with increasing frequencies. Within the measured frequency range, the dielectric constant of Brazilian sample is higher than that of the Chinese sample by between 10 % to 17 %. The higher difference in the dielectric constant of Brazilian and Chinese samples as the frequency increases indicates that the effect of dipolar polarisation is more significant in the Brazilian sample compared to the Chinese sample that is predominant hydrobiotite.

The values of the measured loss factor of South African and Australian samples are reported in Figure 4-36 while the loss factor of Brazilian and Chinese samples are shown in Figure 4-37.

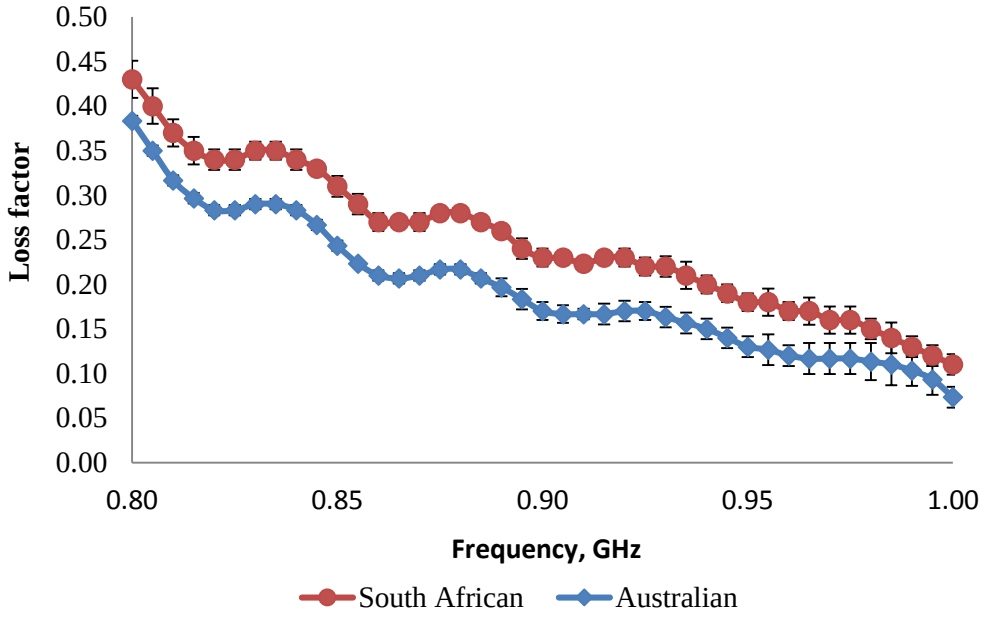

Figure 4-36: Loss factor of South African and Australian samples

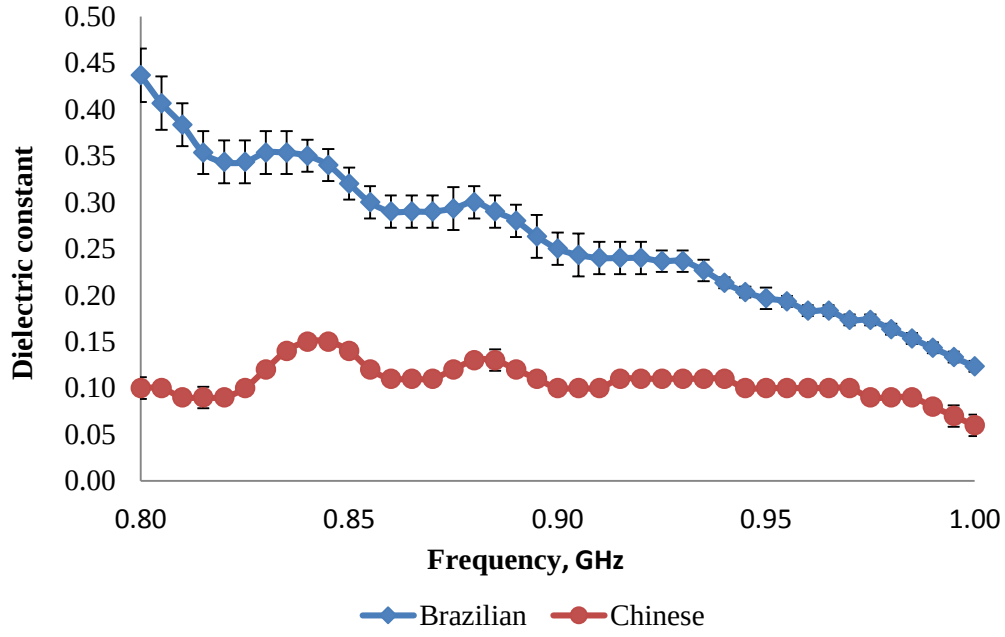

Figure 4-37: Loss factor of Brazilian and Chinese samples

Similar to the trend exhibited by the dielectric constant of the South African sample, the measured loss factor of the South African sample decreases with frequency, from 0.8 GHz to 1 GHz. In addition to the decrease in measured loss factor of the South African sample with frequency, the plot of loss factor against frequency also shows an oscillatory behaviour of more than one peak within the measured frequencies. A similar loss factor trend was shown by the Australian sample, but the values of measured loss factor are higher in the South African sample compared to the Australian sample.

The results of loss factor for the Brazilian sample also show a decrease from 0.8 GHz to 1 GHz. A similar trend was obtained for the Chinese sample, but with a lower rate of decrease compared to the Brazilian sample. Similar to the dielectric constant of both samples, higher values of loss factor were obtained for the Brazilian sample. As discussed earlier, the decrease in the measured dielectric constant and loss factor with an increasing frequency indicates that the polar molecules and the charged particles within the vermiculite structure are inhibited in rapidly following the changing electric field as the microwave frequency increases. The oscillatory trend of loss factor obtained (more than one loss factor peak) in all the measured samples within the measured frequency range, suggests that vermiculite is not a perfect Debye solid or it may consist of more than one dipole in its molecular structure (Mantas, 1999). The effective polarisation effect in vermiculite material could be explained to be due to the dipolar polarisation of the interlayer water and the ionic conduction (ionic drift) of interlayer cation (Camelia et al., 1998). Higher values of dielectric constant and loss factor of Brazilian and South African samples when compared to that of Chinese and Australian samples indicates the possibility of these two samples to absorb and dissipate microwave energy as heat within their structure with higher rate than that of the Chinese and Australian samples respectively.

4.6 Theoretical Estimation of Dielectric Properties of Vermiculite

Often it is challenging to measure the dielectric properties of solid materials typically because of their often irregular shapes. For example, cavity perturbation which is one of the methods used in this project for measuring the dielectric constant and loss factor of vermiculite, requires a small volume of sample usually in a pulverised or powder form (Nelson, 1992a, Dube and Parshad, 1969). Due to the importance of understanding the electromagnetic properties of solid materials at their natural particle density, researchers have devised theoretical techniques based on mixing equations for accurate prediction of dielectric properties of solid materials (Maron and Maron, 2004, Böttcher, 1945, Dube and Parshad, 1969, Sihvola, 2000, Sihvola, 2000 (a), Regalado, 2004). In addition to mixing rules, a simple estimation procedure based on the graphical extrapolation of curves reporting the relationship between the dielectric properties of pulverised material to its bulk densities can be used to estimate both dielectric constant and loss factor of same material (Nelson, 2005, Nelson S.O and You T.S, 1989, Kent, 1977, Klein, 1981, Looyenga, 1965).

Both mixing rules and graphical extrapolations are employed in this project for understanding the theoretical estimation of dielectric properties of vermiculite at different bulk densities up to the particle density. This is due to the challenges of the inherent complex multiphase structure of vermiculite, variation of dielectric properties of material with bulk density and the limitation of obtaining a solid sample that can suitably fit the measuring kits of the available dielectric properties techniques. This will give the knowledge of the value of dielectric properties of the solid materials, which can be used for the accurate modelling and simulations of vermiculite in the cavity, design of microwave cavity and waveguide systems, and may also gain future applications such as for optical electronics and the design of the dielectric separator for mining process. Vermiculite samples from Australia, Brazil, China and South Africa were used in this project for testing the applicability of mixing rules and graphical extrapolations for the estimations of dielectric

properties. Comparative analyses of the results obtained from both methods were also carried out.

4.6.1 Review of Mixing rules used for Theoretical Estimation

Many theoretical mixture equations have been proposed and used for the estimation of dielectric properties of both homogenous and heterogeneous solid materials from measurements of materials in a pulverised form (Sihvola, 2000 (a), Sihvola, 2000, Nelson, 1994, Sheen and Hong, 2010, Hilhorst et al., 2000). However, they are often derived from first principles using different assumptions and experimental data, and therefore, produce differing degrees of precision in terms of the calculated values of dielectric properties for materials of varying geometry and composition (Sihvola, 2000 (a), Sihvola, 2000, Goncharenko, 2003, Maron and Maron, 2004).

Only those mixing rules used in this project are described in this section. An in-depth critical review of the fundamental theories, derivations and theoretical assumptions used can be found in the literature (Sihvola, 2000, Sihvola, 2000 (a), Reynolds J.A and Mough J.M, 1957, Knoll, 1996). Lichtenecker and Rother (1931) proposed a general power law from which most volumetric mixing models are derived (Knoll, 1996, Regalado, 2004).

$$\varepsilon_m^{\alpha} = \sum_{i}^{n} V_i \varepsilon_i^{\alpha} \qquad \text{Equation 4-6}$$

Where ε_m and ε_i represent the complex permittivity of the measured mixture and its components respectively. V_i is the fractional volume of each phases and this sum up to unity. The constant, 'α' is a geometric factor called depolarisation constant (Sihvola, 2000, Hilhorst et al., 2000). This constant ranges from -1 to 1 and relates to the direction of the layering of the individual constituents to that of the direction of the applied electric field.

The complex refractive index model (CRIM) expressed as Equation 4-7, is obtained when α is 0.5 (Regalado, 2004, Brichak et al., 1974, Asami, 2002). Where v_a and

v_s are the fractional volume occupied by air and the solid particle in air-particle mixture. The fractional volume of the solid material, v_s, in the particle-air mixture is calculated from the ratio of the bulk density of the measured vermiculite to its particle density. ε_a and ε_s represent the dielectric properties of air and solid materials respectively in a two-phase mixture of air and particle such as powdered or pulverised material.

$$(\varepsilon_m)^{1/2} = v_a(\varepsilon_a)^{1/2} + v_s(\varepsilon_s)^{1/2} \quad \text{Equation 4-7}$$

Looyenga (1965) proposed a theoretical relationship which fitted well with experimental data for ordered spherical inclusions and randomly oriented ellipsoids (Looyenga, 1965). Landau and Lifshitz (1960) derived this same relation, but in a more rigorous way. They imposed a boundary of application to this equation but Looyenga (1965) claimed it had general applicability. The proposed value of α is 1/3 (Regalado, 2004, Looyenga, 1965).

$$(\varepsilon_m)^{1/3} = v_a(\varepsilon_a)^{1/3} + v_s(\varepsilon_s)^{1/3} \quad \text{Equation 4-8}$$

The surprising thing about this equation in its derivation is the simultaneous assumption of random and ordered inclusion, and this might affect its prediction accuracy and sensitivity. In this project, this mixing rule is referred to as the Landau, Lifshitz and Looyenga equation.

The logarithmic form of Lichtenecker and Rother's equation (1931) used for homogenous and isotropic mixtures is expressed as Equation 4-9 (Regalado, 2004, Maron and Maron, 2004). An assumption was made in its derivation that the dielectric system is a random spatial distribution of particles in an embedded medium.

$$\log\varepsilon_m = v_a \log\varepsilon_a + v_s \log\varepsilon_s \quad \text{Equation 4-9}$$

A further mixture equation used in this project is the Böttcher equation. This equation gives a good approximation for the dielectric properties of low loss crystalline materials (Dube and Parshad, , 1969).

$$\frac{\varepsilon_m - \varepsilon_a}{3\varepsilon_m} = v_s \frac{\varepsilon_s - \varepsilon_a}{\varepsilon_s + 2\varepsilon_m}$$ Equation 4-10

Goldschmidt proposed a theoretical equation (Equation 4-11) for predicting the effective permittivity of fibrous and layered materials.

$$\varepsilon_m = \frac{\varepsilon_a \left\{\varepsilon_a + (\varepsilon_s - \varepsilon_a)(v_s + fv_a)\right\}}{\varepsilon_a + fv_a(\varepsilon_s - \varepsilon_a)} \quad 0 \le f \le 1 \qquad f = 0.11$$ Equation 4-11

Where f is a constant, which relates the orientation of the material's molecular structure to the direction of the applied electric field (Raju, 2003). This method takes values of 0, 0.5 and 1 for parallel, cylindrical and series inclusions respectively. Since vermiculite is a layered material, it is assumed in the present project that the constant f in the Goldschmidt equation is close to zero.

Also used in this project is the Bruggeman-Hanai equation (Equation 4-12), which is based on electrostatics of low dielectric dispersion materials. The derivation of this equation considers the interactions of the dispersed particles in the medium (Sihvola, 2000 (a)).

$$\frac{\varepsilon_m - \varepsilon_s}{\varepsilon_a - \varepsilon_s}\left(\frac{\varepsilon_a}{\varepsilon_m}\right)^{1/3} = 1 - v_s$$ Equation 4-12

These six mixing equations and the modified form of Bruggeman-Hanai (when depolarisation constant, α, is equal to 1/6) are used in this project to estimate the dielectric properties of solid forms of vermiculite at its natural particle density from the data obtained from the measurements of its pulverised form. The dielectric constant and loss factor of air are 1 and 0 respectively, and these values are inserted into the mixing rules to express the corresponding equations for estimating the dielectric properties of solid material.

4.6.2 Density Dependence of Dielectric Properties of Particulates

The relationship between the dielectric properties of a powder or pulverised material could be used for estimating the dielectric properties of the solid form of the same

material. This method has been previously used by some researchers for predicting the dielectric properties of bulk solid materials of coal, limestone, wheat flour and fish (Nelson, 1992b, Nelson S.O and You T.S, 1989, Kent, 1977, Klein, 1981). However, this method has not been used for predicting the dielectric properties of vermiculite. This project therefore, employs these routes for the theoretical estimation of vermiculite's dielectric properties.

Kent (1977) expressed the permittivity of a fish meal sample as a quadratic function of density as expressed in Equation 4-13 and Equation 4-14. Where ∂, α and δ are constants specific to the measured material.

$$\varepsilon' = \partial\rho^2 + \beta\rho + 1 \qquad \text{Equation 4-13}$$

$$\varepsilon'' = \alpha\rho^2 + \delta\rho + 0 \qquad \text{Equation 4-14}$$

Klein (1981) reported a linear relationship between the square root of the dielectric constant ($\sqrt{\varepsilon'}$) and the bulk densities of coal (Equation 4-15). Where "m" is a constant for a given material and the slope of the graph of the dielectric properties of the material against the bulk density, while the intercept '1' is the dielectric constant of air at zero density.

$$\sqrt{\varepsilon'} = \mathrm{m}\rho + 1 \qquad \text{Equation 4-15}$$

Likewise, Nelson and You (1989) used the same relationship to estimate the dielectric properties of materials such as plastics, coal, limestone, wheat and flour. Comparison of the second order polynomial function (Equation 4-13) and the linear relationship between $\sqrt{\varepsilon'}$ and bulk density described in Equation 4-15, shows that the constants ∂ and β in Equation 4-13 are equal to "m^2" and "2m" respectively. If this relationship holds for any material, it is possible to estimate its dielectric constant at any known bulk density up to the material particle density, which signifies the dielectric properties of the solid form of the material.

In order to estimate the loss factor of a solid material, Nelson (1992b) obtained a linear relationship between the measured loss factor of pulverised materials and bulk density, by completing the square of Equation 4-14 to obtain Equation 4-16.

$$\sqrt{\varepsilon'' + \frac{\delta^2}{4\alpha}} = \sqrt{\alpha}\rho + \sqrt{\frac{\delta^2}{4\alpha}} \qquad \text{Equation 4-16}$$

This relationship can be used to estimate the loss factor of a material at any density provided the loss factor at a minimum of two bulk densities is known. For the theoretical estimation of the dielectric properties of solid vermiculite carried out in this research, the mean values of dielectric constant and loss factor obtained from the different mixture rules are compared to the values obtained from the extrapolation method.

4.6.3 Processing of Measured Permittivity data for Theoretical Estimation

Four vermiculite samples from Australia, Brazil, China and South Africa were used to study how the relationship between complex permittivity of pulverised vermiculite and bulk density can be used to calculate the complex permittivity of the solid form. Plots of dielectric constant and loss factor for each pulverised sample versus bulk density were used for the graphical extrapolation of both dielectric constant and loss factor for the solid form of vermiculite. The plots of dielectric properties against the bulk densities are shown in appendix 3 for measurements taken at 934 MHz and 2143 MHZ on pulverised samples of Australian and South African vermiculite. The results of dielectric properties of the Chinese and Brazilian samples were shown at 910 MHz and 2470 MHz. Table A:3-1 to A:3-4 in appendix 3 present the regression coefficient and empirical equations relating both dielectric constant and loss factor of Australian, Brazilian, Chinese and South African vermiculite samples to bulk density. These empirical equations were then used to estimate the dielectric constant and loss factor of solid forms of vermiculite using their particle density.

Table 4-10 illustrates the estimated values of dielectric constant and loss factor of the four studied samples.

Table 4-10: Estimated ε' and ε'' of solid vermiculite from graphical extrapolations

Sample	Freq. (GHz)	Particle density (g/cm^3)	Estimated ε' of solid			Estimated ε'' of solid		
			Polyno. Function	$(\varepsilon')^{1/2}$	$(\varepsilon')^{1/3}$	Polyno. Function	$(\varepsilon''+e)^{1/2}$	$(\varepsilon'')^{1/2}$
South Africa	0.934	2.71±0.02	6.35	6.19	6.55	0.73	0.52	0.54
	2.143	2.71±0.02	6.42	6.08	6.44	0.67	0.53	0.55
Australia	0.934	2.41±0.02	6.81	5.41	5.97	1.77	0.85	0.82
	2.143	2.41±0.02	6.87	5.22	5.73	1.18	1.04	1.02
Brazil	0.910	2.28±0.01	12.12	12.38	14.54	1.69	0.63	0.61
	2.470	2.28±0.01	12.08	11.08	12.88	1.66	1.82	1.92
China	0.910	2.71±0.03	11.00	10.06	11.72	0.68	0.51	0.58
	2.470	2.71±0.03	8.37	8.29	9.47	0.76	0.46	0.49

For each vermiculite sample, the calculated values of dielectric constant and loss factor of the solid vermiculite from the second order polynomial regression are higher than the values obtained from other regression models used.

4.6.4 Applications of Mixing rules for Theoretical Estimations of ε' and ε'' of vermiculite

The dielectric constant and loss factor of the pulverised vermiculite samples from South Africa, Australia, Brazil and China, measured at different bulk densities, were used as the input into Equation 4-7 to Equation 4-12 to estimate the effective dielectric constant and loss factor of the solid form. The notations discussed in section 4.6.1 were used throughout the mixture equations. Table 4-11 shows the estimated value of dielectric constant and loss factor of solid forms. The results for both South African and Australian samples were for the measurements at 934 MHz and 2143 MHz, while that of both Brazilian and Chinese samples were for the measurements carried out at 910 MHz and 2470 MHz.

Sample	Freq. (GHz)	CRIM		LLLM		Goldschmidt		Böttcher		Lichtenecker		Bruggeman-Hanai		Modified Bruggeman -Hanai	
		ε’	ε’’	ε’	ε’’	ε’	ε’’	ε’	ε’’	ε’	ε’’	ε’	ε’’	ε’	ε’’
South Africa	0.9340	6.17	0.50	6.91	0.61	6.18	0.57	7.05	0.63	9.84	1.20	9.04	1.25	6.13	0.52
	0.2143	6.06	0.53	6.78	0.66	6.05	0.61	6.91	0.69	9.57	1.28	8.76	1.29	6.02	0.56
Australia	0.9340	5.37	0.84	5.91	1.02	5.28	0.92	5.96	1.03	7.86	1.81	7.06	1.68	5.29	0.86
	0.2143	5.20	0.66	5.69	0.79	5.69	0.54	6.27	0.59	7.49	1.39	7.70	1.02	5.57	0.50
Brazil	0.9100	12.41	1.30	14.71	1.70	15.81	2.79	14.42	1.61	27.23	4.58	34.57	12.59	13.04	1.55
	0.2470	10.97	1.46	12.71	1.89	12.97	2.65	12.63	1.80	22.24	4.70	23.96	8.22	11.34	1.69
Chinese	0.9100	10.18	0.78	12.08	1.02	11.82	1.33	12.30	1.05	21.66	2.71	25.69	6.14	10.62	0.91
	0.2470	8.41	0.56	9.73	0.72	9.05	0.79	9.90	0.74	15.85	1.67	16.04	2.35	8.55	0.62

Table 4-11*: Estimated ε’ and ε’’ for solid vermiculite materials from mixture rules*

4.6.5 Discussion and Comparison of Estimations from Extrapolation and Mixture Equations

Comparative analyses of the estimated dielectric constant and loss factor using graphical extrapolations and mixing rules were carried out. For all of the vermiculite samples tested, the estimated values of both dielectric constant and loss factor by a second order polynomial function are higher than the estimated values obtained from the relationships of the square root and cube root of dielectric constant and loss factor (Table 4-10). The curves of the square root relationship produce the y-axis intercept closest to 1 and 0 for both dielectric constant and loss factor, respectively (Table A:3-1 to A:3-4 in appendix 3).

Statistically, this implies that the square root relationships will give more accurate estimations of dielectric constant and loss factor than the polynomial regression and cubic root function. Therefore, the square root relationship can be used with high level of confidence in estimating the complex permittivity of solid vermiculite from that of the measured pulverised sample. It is interesting that the loss factor extrapolated by the linear relationship curves of square root of the measured loss factor of pulverised vermiculite and $(\varepsilon'' + e)^{1/2}$ against bulk density gives statistically close results for all the studied samples.

There are significant variations in the estimated values of dielectric constant and loss factor obtained from the different dielectric mixture equations. This may be due to their dependence on the particle size, micro-geometry and shape of the pulverised sample (Nelson, 1992b, Nelson S.O and You T.S, 1989). Comparative analysis of the estimated dielectric constant and loss factor from the mixture rules (Table 4-11), and graphical extrapolations shown in Table 4-10, shows that the dielectric constant and loss factor estimated by the CRIM, Goldschmidt and modified Bruggeman-Hanai equation are within 1-9 % deviation from the estimated value from the square root relationship. A deviation of less than 2 % was recorded between CRIM and the square root relationship for the estimated ε'. There is also a deviation of less than 6% between the Landau, Lifshitz and Loyenaga equation (LLL) and the cube root relationship. The consistencies between the results of CRIM and the square root relationship and between the results of Landau, Lifshitz and Looyenga and cube root function

are similar to published results in the literature (Nelson S.O and You T.S, 1989, Nelson, 1992b, Sengwa R.J and Soni A., 2008).

The estimated values from the Landau, Lifshitz and Loyenaga equation (LLL) and Böttcher equation are very close, but they overestimated the dielectric constant and loss factor compared to the results obtained from the square root relationship. LLL and Böttcher both overestimated dielectric constant with deviations of between 9-20 % and 10-22 %, respectively, while both mixing rules give deviation above 25 % for ε'' estimations.

The Lichtenecker and Bruggeman-Hanai models also overestimated both dielectric constant and loss factor with even higher deviations than that obtained by LLL and Böttcher. These two mixing rules give a deviation of over 50% for estimating dielectric constant and loss factor. This may be due to the oversimplification of the material microstructure in their derivations and they are, therefore, probably more suitable for heterogeneous materials while vermiculite is assumed homogenous. There is a close correlation between the estimated dielectric constant and loss factor of solid vermiculite from extrapolations of the linear relationships of $(\varepsilon')^{1/2}$, $(\varepsilon'')^{1/2}$ and $(\varepsilon''+e)^{1/2}$ versus bulk density and from that obtained from the CRIM, Goldschmidt and modified form of Bruggeman-Hanai equations. The CRIM, Goldschmidt and the modified form of Bruggeman-Hanai equations are, therefore, suitable and could be confidently used for estimating the dielectric properties of solid vermiculite. This information together with the literature stating that Goldschmidt is good for layered materials suggests that the three mixing equations may also be suitable for other layered materials; however, this would require further verification.

4.7 Conclusions

Vermiculite samples from South Africa, Australia, Brazil and China were presented for mineralogy test using X-ray diffraction analysis (XRD) and Mineral Liberation Analysis (MLA). These tests were carried out to determine the different mineral phases present in the different vermiculite ores. The XRD analysis of the four vermiculite samples presented for mineral identification

shows the presence of different mineral phases. Hydrobiotite, which is hydrated mica, was observed to be the predominant mineral phase in the South African, Chinese and the Australian samples. Of all the four samples presented for XRD analysis, the Brazilian sample has the most distinct mineral composition with significant vermiculite composition when compared to the other samples.

The quantitative analysis of the mineral composition by MLA reveals that the Chinese sample demonstrates the highest hydrobiotite composition when compared to the South African and Australian sample with hydrobiotite as the dominant mineral constituents, while the Brazilian sample has the highest vermiculite composition. TGA was used to determine the moisture contents of the four vermiculite ores and it identified free water, bound water and the high temperature hydroxyl water as the three different types of water network in the ore structures. The temperature for the removal of these phases is a function of the mineralogy of the vermiculite ore. The Brazilian sample has the highest interlayer water (both free and bound water) content followed by the South African sample.

The dielectric property characterisation of samples studied demonstrated that both dielectric constant and loss factor of vermiculite ores are a function of bulk density, temperature, mineralogy and frequency. All the samples show a decrease in dielectric constant with frequency as a result of the lagging of the interlayer molecules (interlayer water and cations) behind the applied electric field. There is a positive correlation between measured dielectric properties (both ε' and ε'') and bulk density. Dipolar polarisation and ionic conduction are believed to be the dominant polarisation mechanisms in the samples. The effect of the ionic conduction is highly significant at the lower frequencies, and this can be explained by the excitation of the interlayer cations. The Brazilian sample was found to have a loss tangent of about 0.11 at 2.47GHz, but the other samples all exhibited lower values.

A method based on the linear functions of the dielectric constant and loss factor against bulk density of air-particle mixtures, was introduced in this project to estimate the complex permittivity (ε' and ε'') of the solid vermiculite from the measurements of ε' and ε'' of the pulverised form over a range of bulk density.

The linear relationship of $\sqrt{\varepsilon'}$ against the bulk density is consistent with the CRIM mixing equation and the linear relationship of $\sqrt[3]{\varepsilon'}$ against the bulk density is consistent with the LLL mixing equation. The linear relationship of $\sqrt{\varepsilon'}$ against density gives a reasonable estimation of the dielectric constant of the solid vermiculite. For all the vermiculite samples tested, the estimated values of ε' obtained from the linear relationship of $\sqrt{\varepsilon'}$ are close to the estimated values obtained from the CRIM, Goldschmidt and modified Bruggeman-Hanai mixing rules. For the loss factor estimation, the linear relationships of $(\varepsilon'')^{1/2}$ and $(\varepsilon''+e)^{1/2}$ give a closer estimation than the loss factor estimation obtained from the second order polynomial function of loss factor. The values of loss factor estimated by the linear relationships of $(\varepsilon'')^{1/2}$ and $(\varepsilon''+e)^{1/2}$ are consistent with the results obtained for loss factor using the CRIM, Goldschmidt and modified Bruggeman-Hanai mixing rules. There is an agreement between the results of Böttcher and LLLM, but these models give higher estimations than of the CRIM, Goldschmidt and modified Bruggeman-Hanai mixing rules. The Lichtenecker and Bruggeman-Hanai equations overestimate the values for both dielectric constant and loss factor and they are not suitable for estimating the complex permittivity of vermiculite.

CHAPTER FIVE
MICROWAVE EXFOLIATION OF VERMICULITE

5.1 Introduction

Microwave energy, which selectively heats the interlayer water molecules within the vermiculite mineral has been suggested to be an efficient method for exfoliating vermiculite minerals in terms of energy savings, reduced processing time and lower exfoliation temperature (Vorster, 2001, Obut et al., 2003, Zhao et al., 2010, Marcos and Rodríguez, 2010b, Marcos and Rodríguez, 2014). Dodds et al. (2010) demonstrated that microwave power densities (described in chapter 3) of greater than $2x10^8$ W/m^3 in the heated phase were required to successfully exfoliate all size classifications of vermiculite, though the required power density depended upon the grade being processed, bed thickness (Dodds, et al 2010) or mass of material in the cavity.

A microwave applicator or cavity is a device that supports an electric field pattern, which when applied to a material volume brings about either a permanent or temporary change to a material property or parameter (Mehdizadeh, 2010, Chan and Reader, 2000). The main requirement of a microwave cavity is to maximise the transfer of microwave energy to the workload. Its performance depends on shape, geometry, microwave input (feed), electrical properties and volume of the workload (Metaxas and Meredith, 1983, Chan and Reader, 2000, Milovanović et al., 2004). This device is an essential component of a microwave system, and the choice of applicator used determines the efficiency and effectiveness of microwave processing. In designing a microwave system for vermiculite exfoliation, the cavity must be designed and simulated to achieve a high power density, sufficient for rapid heating of the interlayer water in vermiculite structure.

As expressed by Equation 3-6, the power density in a material is directly proportional to the square of the electric field within the material, the loss factor of the workload and the operating frequency (Gupta and Eugene, 2007, Metaxas and Meredith, 1983). This implies that an increase in the value of frequency, loss factor and electric field intensity within the workload will bring about an increase in the power density available for microwave heating within the workload. Therefore, it is important to design an applicator that supports an

electric field strength above that which is required by the feedstock for achieving the required level of exfoliation. The treatment of material in an applicator with an electric field intensity, which creates a power density far below the critical power density required in the vermiculite-heated phase, will result in poor quality products in terms of bulk density.

Multimode cavities provide the largest cavity volume when compared to other cavity types, but there are drawbacks as discussed in Chapter 3, which make them unsuitable for scientific investigations of vermiculite exfoliation. Therefore, the results obtained from investigations of microwave exfoliation using this type of cavity fail to provide the information and operating parameters required for the design of pilot scale or commercial scale up systems, because they do not allow prediction of the distribution of electric field in the workload. Single mode cavities have the potential to deliver a high microwave power density to the workload, however its use for the design of a microwave vermiculite exfoliator was rejected early on because the electric field distribution is not homogeneous (Chan and Reader, 2000, Meredith, 1998). The electric field in a single mode applicator varies from maximum at the centre of the cavity to zero at the cavity walls. The implication of the uneven electric field distribution in the single mode is the uneven treatment of the workload at different regions in the cavity. In eliminating the variation of electric field in the cavity, a resonant tunnel cavity was used in the design of the microwave exfoliator. The resonant tunnel cavity can sustain an electric field and therefore power density that is high and homogenous throughout a well-defined treatment region. A specific requirement of the microwave exfoliator is the design of a microwave-heating cavity that can supply a maximum electric field required for rapid heating of the interlayer water phase.

The aim of this chapter is to use a continuous microwave system, which has the potential of exfoliating vermiculite from different source locations to process two size classifications of vermiculite from Australia, Brazil, China and South Africa. The methodologies for designing an energy efficient and safe continuous microwave system with operating frequencies of 2.45 GHz for the pilot scale and 896 MHz for the commercial scale up system are presented in this chapter.

The mechanism of vermiculite exfoliation using the microwave system is compared to that of the conventional system. Furthermore, the effects of throughput and mineralogy of vermiculite samples on the degree of exfoliation were discussed.

5.2 Microwave Applicator for Continuous Pilot Scale Treatment of Vermiculite at 2.45 GHz

Designing a continuous microwave system requires knowledge of bulk materials handling, material mineralogy and an understanding of the electromagnetic properties of the feedstock. The results of mineralogical composition and dielectric property measurements on vermiculite from Australia, Brazil, China and South Africa were discussed in Chapter 4 of this thesis. Dielectric property data is used in this project for the design and electromagnetic simulation of the microwave heating cavity and choking structures(Venkatesh and Raghavan, 2005, Mehdizadeh, 2010).

Finite element method (FEM) and the finite difference time domain (FDTD) are two methods used for the computational analysis and simulation of electromagnetic field distributions within microwave applicators, the workload and for the simulation and design of microwave chokes (Sundberg et al., 1996, Datta and Anantheswaran, 2001, Sullivan, 2000, Liu et al., 2013). These methods have been used for designing applicators for different applications such as for processing of fish (Liu et al., 2014b), sintering of ceramics (Mehdizadeh, 2010), and food processing (Liu et al., 2013, Liu et al., 2014a) . FDTD was chosen for simulation of the applicators and choke systems in this project because of its flexibility, accuracy, suitability for large scale simulation, performance when undertaking broadband simulations and efficiency of its programming and algorithm (Dibben and Metaxas, 1996, Sullivan, 2000). However, FDTD is slow for simulating small devices and not efficient for highly resonant devices. Unlike FDTD, FEM requires a matrix solve for complex mesh and therefore requires large amount of computer memory. In the FDTD computational technique, the entire region is divided into 2 cubic meshes offset from each other. One of them is used to model the electric field while the other is used for modelling the magnetic field (Dibben, 1995). The time dependent

Maxwell's equations are solved alternately for both electric and magnetic field components. The electric field component at time t is used to solve the magnetic field at time $t+\Delta t/2$, and this is then used to determine the electric field component at time $t+\Delta t$ and so on (Datta and Anantheswaran, 2001, Sullivan, 2000). The electromagnetic simulations and designs of the microwave system (applicator and chokes) for both the pilot scale and scaled up vermiculite exfoliator discussed in this chapter were carried out by electromagnetic experts at the National Centre for Industrial Microwave Processing (NCIMP) and not by the author. The microwave applicator for the pilot scale system, which operates at 2.45 GHz, was designed focused upon achieving a well-defined electric field distribution and high power density sufficient for maximum vermiculite exfoliation.

The microwave exfoliator designed in this project has two apertures that allow a microwave transparent conveyor belt, which conveys the feedstock to pass through the high electric field zone. All the simulations of the electromagnetic field distribution in the pilot scale cavity and the workload were carried out using Concerto software supplied by COBHAM (Concerto, 2006). This software is used for the simulation of high frequency electromagnetic field and it is based upon FDTD as described above (Taflove et al., 2005, Jokovic et al., 2014). Since the focus is to develop a continuous system with an open end at the entrance and exit of the tunnel, and a conveyor belt conveying the workload through the cavity, the dielectric properties of vermiculite and belt material were used for the simulation. A vermiculite feed bed depth of 5 mm was used for the simulation. The reader is asked to note that these simulations were not performed by the authors of this thesis, but by other members of the NCIMP.

The time and the frequency domain technique requires the meshing of the entire computational domain (Chan and Reader, 2000). Therefore, in order to implement the FDTD method, a model of the applicator shown in Figure 5-1 was created and the electrical properties of all the materials (vermiculite and conveyor belt) and boundaries specified. The boundaries used are the walls of the cavity, which is assumed as a perfect electric conductor (conductivity, σ=infinity). This means that on the wall of the cavity, the tangential component

of the electric field is set to zero. Then a fine cubic mesh was applied over the entire volume of the cavity by dividing the model into small cubic cells. The automatic mesh generator in the Concerto was used for this purpose.

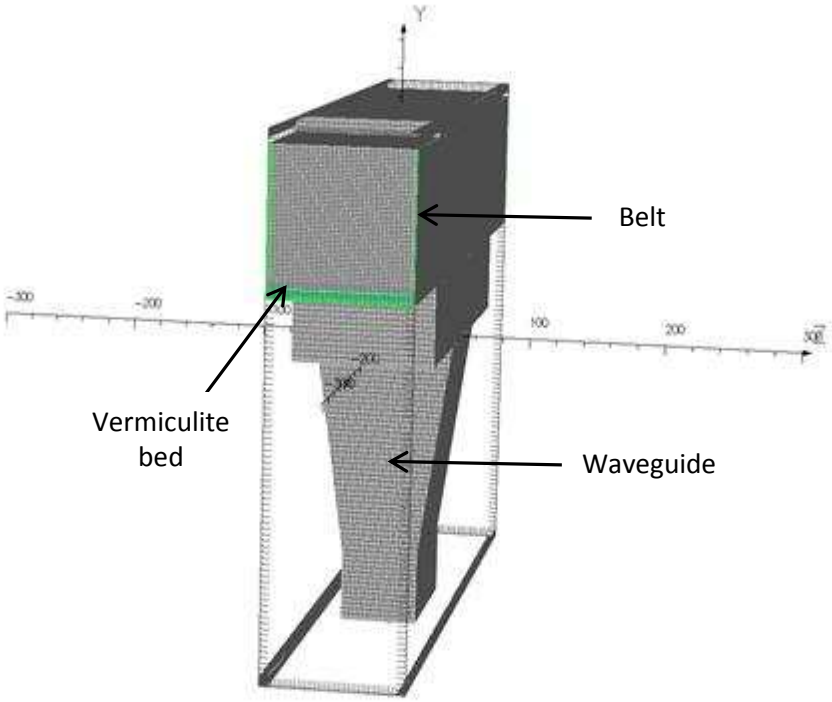

Figure 5-1: Model of the applicator with fine cubic mesh applied over it for the purposes of the FDTD simulation.

An input microwave power of 30 kW at 2450 MHz, which was the highest available power at 2450 MHz, was used for the simulation. This is to obtain the sufficient high power density requirement for vermiculite exfoliation and to identify any high field concentrations that could lead to arcing. The dielectric constant and loss factor of vermiculite measured at 2450 MHz are 2.87 and 0.18 respectively, and these were used for modelling the microwave cavity. The belt used in conveying the vermiculite through the applicator is a silicone coated glass fibre belt supplied by Biscor Belting, UK. The values of dielectric constant and loss factor of the belt material are 3 and 0.05 respectively. The dielectric properties of the conveyor belt material showed that the material of the conveyor belt used in this project is transparent to microwave energy because of its low loss factor. Therefore, it allows the microwave energy to be transmitted directly and interacts with only the interlayer water of the vermiculite, which is the microwave absorber phase of the target material. The total number of the cells

simulated by using an Intel Xenon Processor E5507 is 2046220 with minimum mesh cell size of 1.87 x 1 x 1 mm and a time step of 1.9 x 10^{-3} ns. The simulations (125000 iterations) take about 3 hours. In this design, walls of the applicator were simulated as a perfect electric conductor that supports total reflection of the microwave energy at these boundaries. The FDTD method theoretically has quadratic convergence. The data of the simulations were analysed in MATLAB.

Figure 5-2 presents the average Electric field distribution in a vermiculite-loaded applicator. The applicator is 165 mm high and 300 mm long. The model domain of the applicator is shown in Figure 5-3.

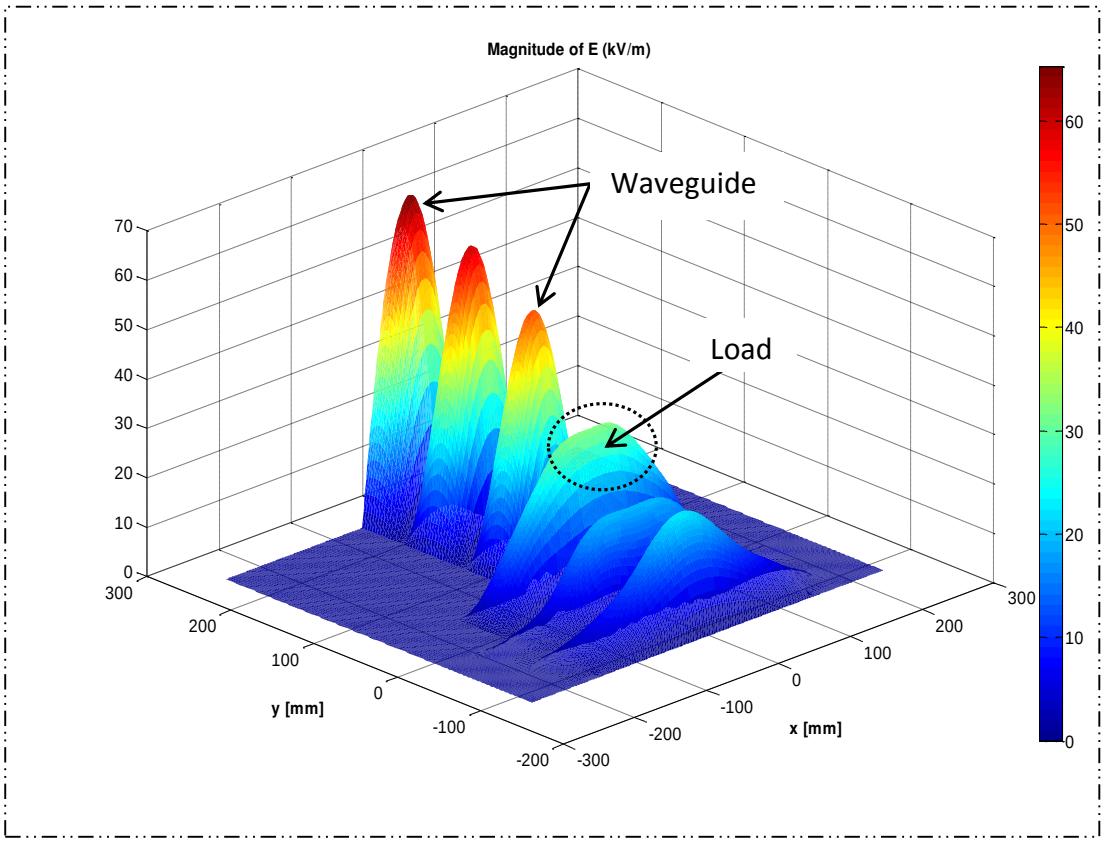

Figure 5-2: The E-field distribution in the resonant tunnel applicator. The blue colour shows a region with low electric field distribution and red colour indicates region with higher field strength. The electric field in the load is represented as the region with the dotted ring

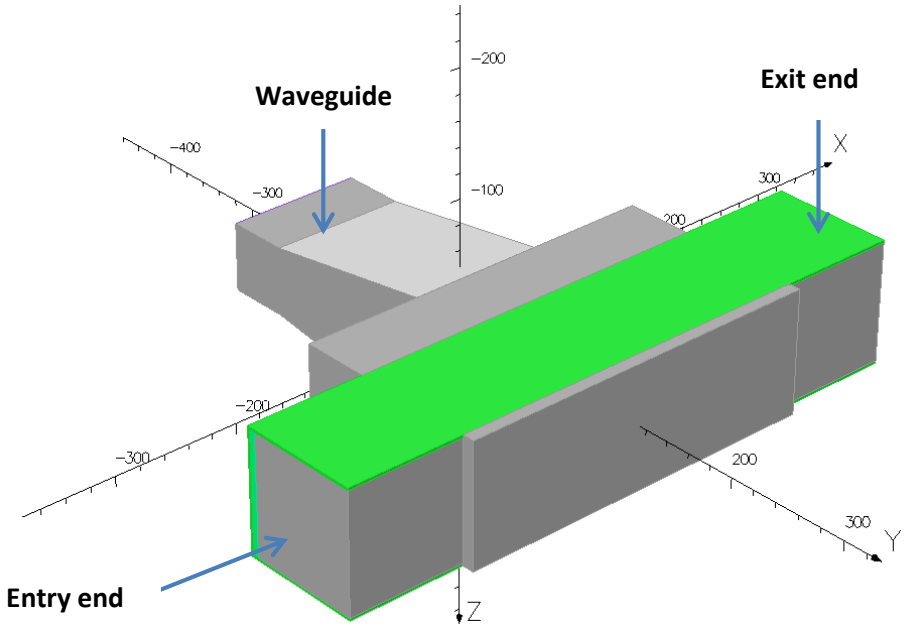

Figure 5-3: Model domain of the applicator designed for vermiculite exfoliation

It is evident from the 3D view of the electric field distribution that there is a reduction in the amplitude of the E-field as it propagates from the waveguide feed to the cavity. The reduction in the electric field as it transit the cavity from the waveguide is unsurprising and is due to the increase in the physical size of the system as the electromagnetic wave travels from the small waveguide to the larger cavity. Therefore, the larger cavity volumes relative to the waveguide is associated with its lower E-field strength for the same propagating microwave power. According to the electric field distribution shown in Figure 6-2, the average electric field intensity in the load is about 35 kV/m. The power density distribution in the applicator loaded with vermiculite is presented in Figure 5-4. The power density distribution shown in Figure 5-4 is across the path of the flow of the vermiculite through the applicator as shown in Figure 5-5. The applicator shown in Figure 5-5 was stepped so as to high obtain a high power density at the cavity centre.

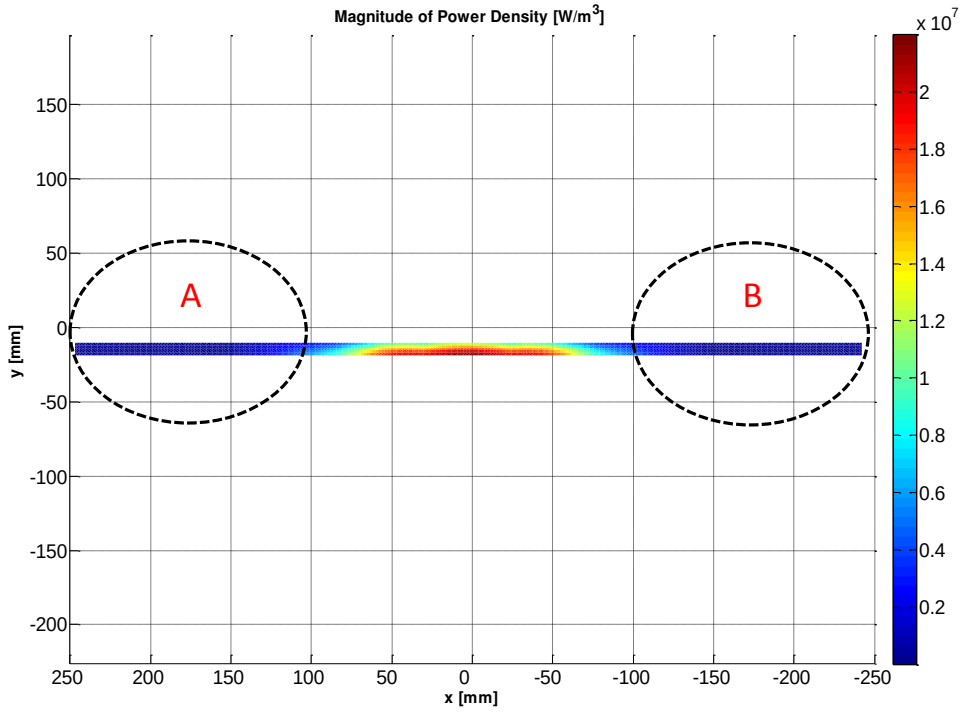

Figure 5-4: Power density in the vermiculite load in resonant tunnel applicator. The blue colour signifies low power density while the red colour represents high power density region

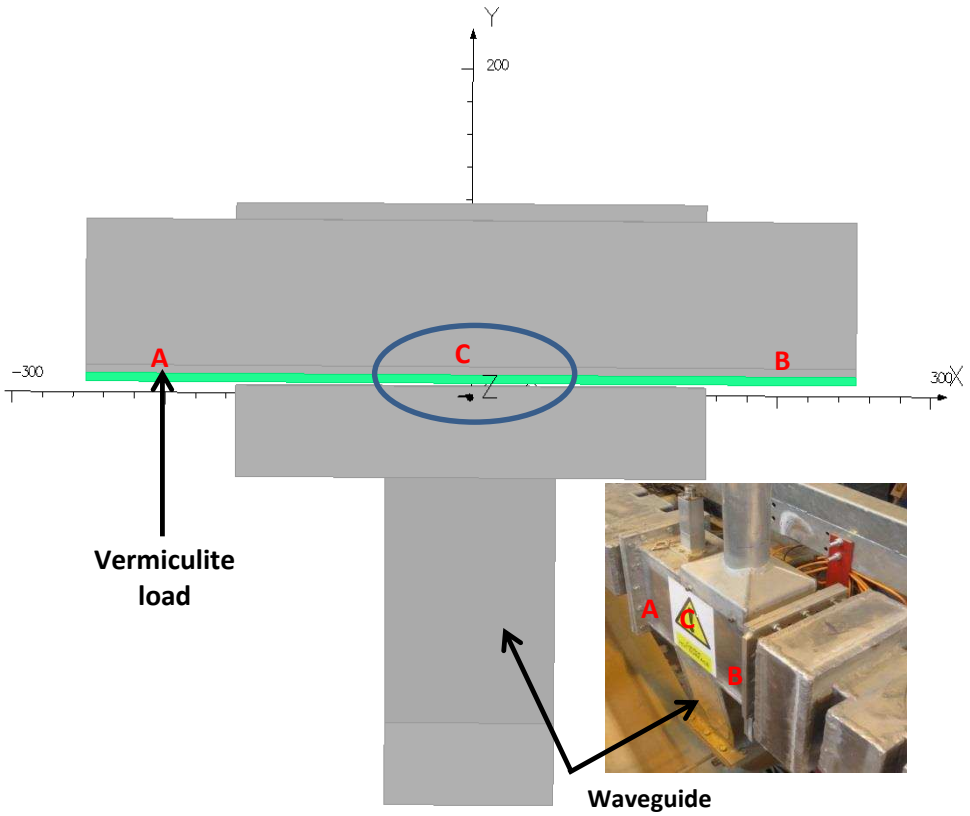

Figure 5-5: Microwave applicator with vermiculite load. An area *marked 'A' and 'B'* signifies the input and exit ends of the applicator respectively and they experience low power *density. The area marked 'C' is at the centre of* the applicator and this is the region of high power density.

Microwave power is dissipated as the vermiculite interacts with the incident microwave energy. The results of the electromagnetic simulation shown in Figure 5-4 show that a maximum average power density of about 2.2 x 10^7 W/m^3 was obtained at the cavity centre, which is the region labelled 'C' in Figure 5-5 for a 5 mm vermiculite bed. The areas labelled 'A' and 'B' in Figure 6-5 represent the regions labelled as 'A' and 'B' in Figure 5-4 respectively. These signify the regions of low power density as shown in Figure 5-4. The value of power density was computed taking into account only the bulk dielectric properties of the material as the actual dielectric properties of the vermiculite interlayer water phase is not known due to the difficulty of measuring the dielectric properties of the vermiculite interlayer water. It is challenging to simulate the electric field and the power density in the vermiculite interlayer water phase because it is difficult to construct the model, as the interlayer water dimensions are extremely small. Assuming that the loss factor of the vermiculite interlayer water is between 13 and 20, which are the measured loss factor for distilled water and ionic water at 25 °C (Meredith, 1998), the loss factor of the silicate is zero and the same electric field of 35 kV/m is in the interlayer water. Therefore, the actual value of power density in the interlayer water is expected to be as high as 2.5 x 10^9 W/m^3 when calculated from the power density equation (Equation 3-16).

A combination of reflective and resistive chokes were designed by the electromagnetic experts at the National Centre for Industrial Microwave Processing (NCIMP) using Concerto software (Concerto, 2006). These chokes were designed to allow continuous operation to take place and prevent microwave leakage below the restricted standard of below 5 mW/cm^2 for both 2450 MHz and 896 MHz over an exposure time of 30s, both measured at a distance of 5 cm from the equipment (BSI, 2011). The methodology used for the choke design and the results obtained are reported in appendix 4. To ensure compliance with safety standards each choke structure was tested and the design models validated prior to use. In each case, the simulations were found to be accurate.

5.2.1 Experimental Procedure for Vermiculite Exfoliation

Figure 5-6 shows a schematic of the microwave system used for the vermiculite exfoliation at 2.45 GHz. The system is made up of different components which enable efficient and safe processing of vermiculite material. The raw vermiculite is loaded into the hopper (labelled as 'a' in Figure 5-6) which is connected to the feeder (labelled as 'b' in Figure 5-6). The rate of delivering of the raw vermiculite into the continuously moving conveyor belt (labelled as 'c') is controlled by the automatic vibratory feeder control and chokes are situated at both ends of the system. The microwave energy entering the cavity through the waveguide (shown as 'h') interacts with the vermiculite as it passes through the cavity (labelled as 'g' in Figure 5-6).

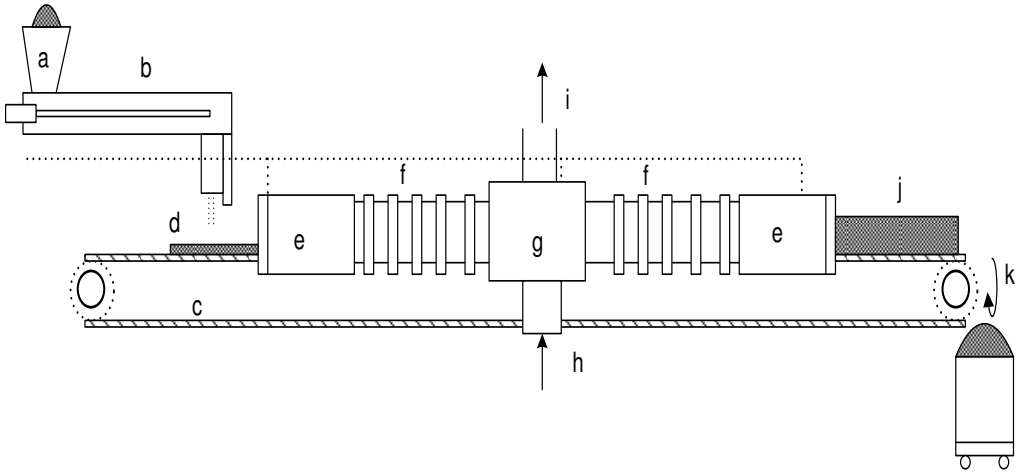

Figure 5-6 : Industrial Microwave Vermiculite Exfoliation rig (2.45 GHz) (a) hopper, (b) feeder, (c) conveyor belt , (d) crude vermiculite, (e) resistive choke section (f) reflective choke section, (g) microwave applicator (heating zone), (h) microwave from generator entering the applicator, (i) to dust and gas extractor, (j) exfoliated vermiculite and (k) discharged end.

To ensure safe processing of the vermiculite material, an arc detector is incorporated at the upper end of the microwave cavity and at both opening ends of the system. A microwave leakage detector is used to scan the two open ends of the system and other leakage potential areas for any microwave leakage. The raw vermiculite material is delivered to the microwave transparent silicon coated glass fibre conveyor belt 'c', which continuously passes the untreated vermiculite through the area of high microwave field ('g') where the processing occurs. A microwave generator manufactured by Sairem, of France, delivering a maximum microwave power of 15 kW at 2.45 GHz was used for the

experiment. Representative samples used for the tests were loaded into the hopper, and continuously moved through the system on the conveyor belt. An automatic 3-stub tuner was used to match the impedance of the microwave source and transmission line to that of the load. The matching was performed to obtain a minimum reflected power and thus maximise the proportion of applied microwave energy absorbed by the load. This therefore improves the heating efficiency of the process. Processed samples used for the system performance were collected at the outlet (l) as shown in Figure 5-6. The system performance was determined in terms of the bulk density of the products. Lower bulk density of exfoliated product signifies better performance of the system because the target of the vermiculite processing industry is to exfoliate vermiculite to a density below the TVA standard for various applications. Exfoliated product above the TVA density ranges are classified as poorly exfoliated product.

The system performance was studied by using two size classifications sourced from South Africa, Australia, Brazil and China. The superfine size grade (ranges from 0.355 mm to 1 mm) was obtained from South Africa and Australia while the medium size grade (ranges from 1.4 mm to 4.0 mm) was obtained from Brazil and China. Table 5-1 presents the industrial specification for particle size and bulk density of exfoliated vermiculite product as set by The Vermiculite Association (TVA) (The Vermiculite Association, 2011).

Table 5-1: Particle size and bulk density of TVA specification for industrial exfoliated vermiculite (The Vermiculite Association, 2011)

Grade	Particle size (mm)	Bulk density (kg/m^3)
Micron	0.5-1	90-160
Superfine	1-2	80-144
Fine	2-4	75-112
Medium	4-8	72-90
Large	8-16	64-85

Two litre-measuring cylinders were used to determine the bulk density of the exfoliated vermiculite. The weight of the empty measuring cylinder was determined and representative samples of processed vermiculite were collected directly from the production stream for 30 seconds at each microwave power

and throughput. The collected samples were then immediately transferred into the measuring cylinder by means of scoop to prevent moisture re-absorption. The segregation of the particles was avoided by discharging the sample from a height not above 50mm from the top of the cylinder. The mass of the measuring cylinder and its contents were then measured. This was repeated three times for a fresh sample of the same grade of vermiculite exfoliated at the same microwave power and throughput. The mass of samples collected for 30s at specified powers and throughputs was determined, and the effective bulk density was calculated from Equation 5-1.

$$\text{Bulk density}\,(\text{kg}/\text{m}^3) = \frac{\text{Mass of exfoliated sample collected}}{\text{Volume of exfoliated sample collected}} \qquad \text{Equation 5-1}$$

5.2.2 Results and Discussion

The throughput of raw vermiculite moving through the applicator determines the bed depth, interacting mass and the volume of material in the applicator as does the belt speed. For the pilot scale system, the throughput of the vermiculite was varied by using a vibratory feeder, which allows control over the feedstock bed depth when combined with a moving belt conveyor.

5.2.2.1 Bulk Density Performance of Exfoliated Vermiculite

Figure 5-7 shows the graph of bulk density versus the throughput of both South African and Australian vermiculite, processed at microwave power of 15 kW from throughput 53 kg/h to 126 kg/h. Although the simulation of the cavity was performed at 2450 MHz and 30 kW but the microwave generator used for the vermiculite exfoliation only supports a maximum of 15 kW microwave power. Figure 5-7 shows the mean of three experimental repeats of exfoliation tests for each vermiculite sample.

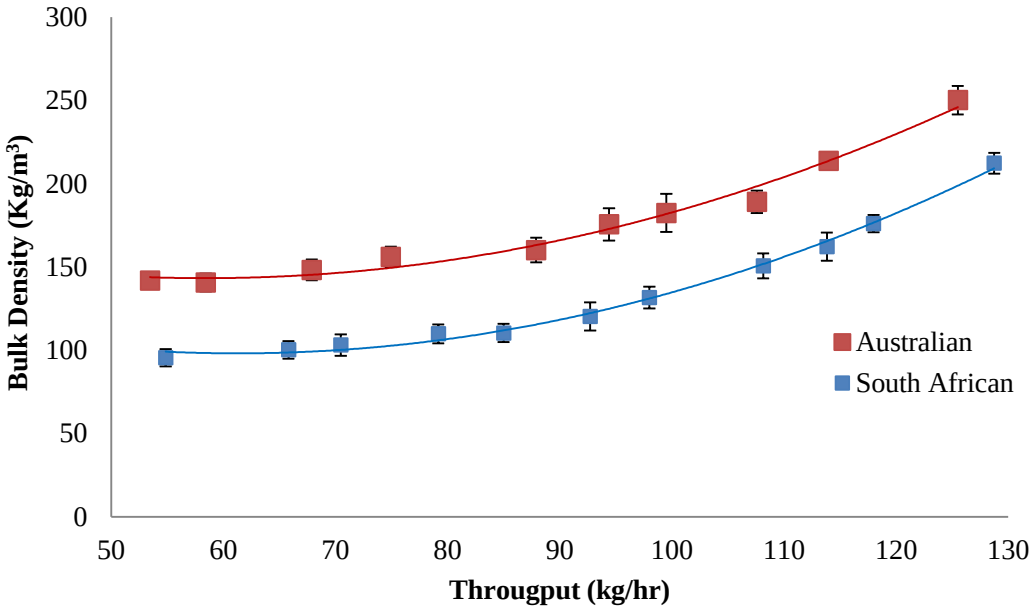

Figure 5-7: Mean Performance (bulk density) vs throughput of pilot scale of vermiculite exfoliation system operating at 2.45 GH and 15 kW.

The bulk density of the Australian vermiculite varies from 141 kg/m^3 to 250 kg/m^3 within the measured throughputs while that of the South African vermiculite varies from bulk density of 95 kg/m^3 to 212 kg/m^3. The comparison of the exfoliation performances of the two samples demonstrates that the South African sample yields a lower bulk density than the Australian sample when both samples were subjected to the same operating conditions. It is evident from the results that only the South African sample exhibits a bulk density within the TVA standard for superfine grade (Table 5-1) between 55 kg/h and 98 kg/h but the bulk densities of the Australian sample within the processed throughput are higher than the TVA standard (Table 5-1). To achieve lower bulk density products of the exfoliated form of the Australian sample within these throughputs, higher microwave power will be required. This will increase the electric field intensity and the power density available for the vermiculite exfoliation. Figure 5-8 shows the bulk density performance versus throughput of Brazilian and Chinese vermiculite processed between throughput of 73 kg/h and 132 kg/h.

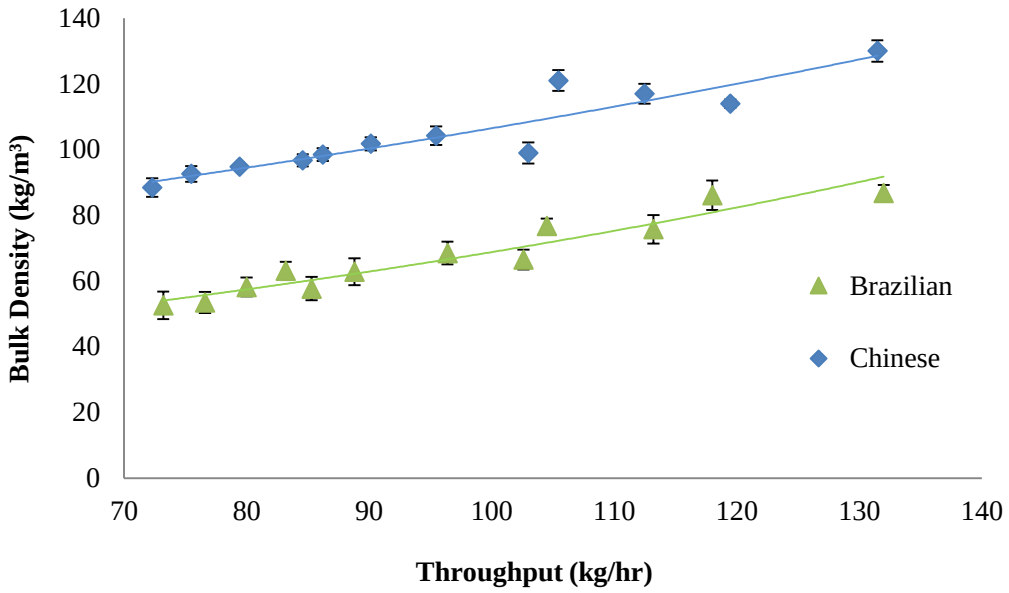

Figure 5-8: Mean performance (bulk density) vs throughput of industrial microwave vermiculite exfoliation system operating at 2.45 GHz and 15 kW

Within these measured throughputs between 73 kg/h and 132 kg/h, the bulk density of the Brazilian sample varies from 52 kg/m^3 to 86 kg/m^3 while that of the Chinese sample varies from 72 kg/m^3 to 130 kg/m^3. The comparison of the exfoliation performance of the Brazilian and the Chinese samples, which are of the same size specifications, shows that the Brazilian sample yields a lower bulk density than the Chinese sample when processed at the same microwave power and mass throughput. Figure 5-8 shows that within the limit of the throughput used, the Brazilian sample exfoliated to a bulk densities far below the TVA standard for the medium grade (Table 5-1). In the case of the Chinese sample, the exfoliated products obtained within these throughputs are higher than the TVA specification. This implies that higher electric field intensity and power density will be required by the Chinese sample to achieve exfoliated products with bulk densities within the TVA specifications, when processed between 73 kg/h and 132 kg/h. This can be achieved by increasing the microwave power generated from the microwave generator, although ultimately this is limited by dielectric breakdown of air, which causes arcing in the system.

5.2.2.2 Effect of Throughput on Degree of Exfoliation

The results shown in Figure 5-7 show that a lower bulk density for the processed vermiculite is obtained at lower throughputs, for both samples at a specific

microwave power. Similarly, for the exfoliation performance of the Chinese and Brazilian vermiculite sample shown in Figure 5-8, lower bulk density of the exfoliated vermiculite products is obtained at lower throughput. This is not surprising because the lower the throughput the higher the energy dose and thus the greater the expansion and the lower the product bulk density.

According to the TVA standard shown in Table 5-1, the industrial specification for superfine grade requires bulk densities of 80-144 kg/m^3 for treated material. The bulk densities obtained for the South African sample between processed throughputs of 55-108 kg/h are far below the industrial specification approved by TVA. Only the samples processed at 53 kg/h and 68 kg/h for the Australian sample are within the industrial specification. For the Brazilian medium grade sample, the bulk densities obtained between throughputs of 73-132 kg/h are far below the industrial specifications. In the case of the Chinese sample, which is also a medium grade, only exfoliation at 73 kg/h is within the TVA standard. For all the samples tested at 15 kW, enhanced yields of exfoliated products can be produced only at lower throughputs and it is demonstrated that it is possible to generate material product, which has lower bulk densities than the industrial specification. Therefore, to achieve exfoliated products of Chinese and Australian samples within the TVA specifications at the measured throughput requires increasing the microwave power to over 25 kW.

5.2.2.3 Effect of Energy and Cavity Power on Degree of Exfoliation

The total energy consumed for the exfoliation of the vermiculite sample was calculated by Equation 5-2.

$$\text{Energy consumed (kWh/t)} = \frac{\text{Microwave power applied (kW)}}{\text{Mass flowrate (t/h)}} \qquad \text{Equation 5-2}$$

The effect of total energy input on the degree of exfoliation of the South African sample is shown in Figure 5-9 and Figure 5-10.

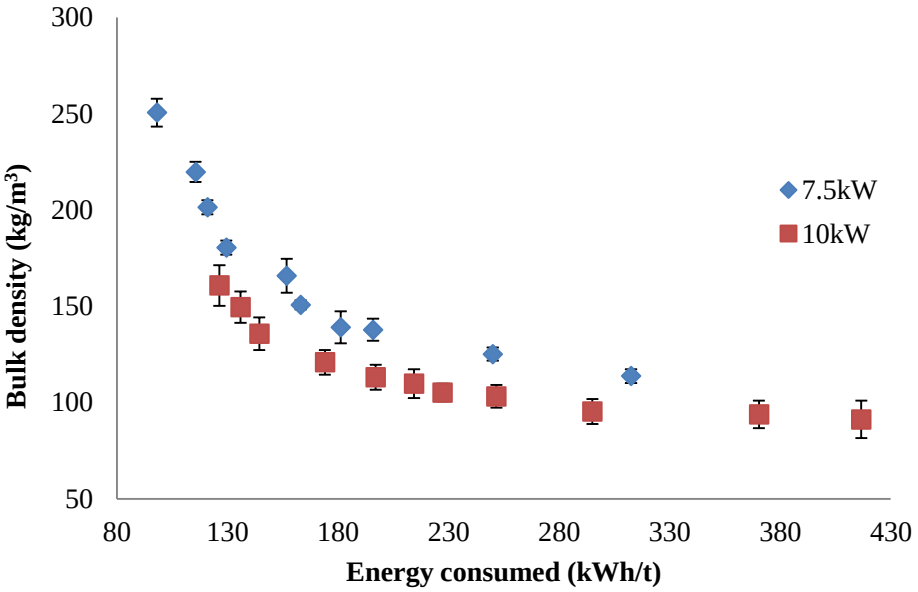

Figure 5-9: Effect of total energy consumed on the degree of exfoliation at 7.5 kW and 10 kW for a South African vermiculite sample

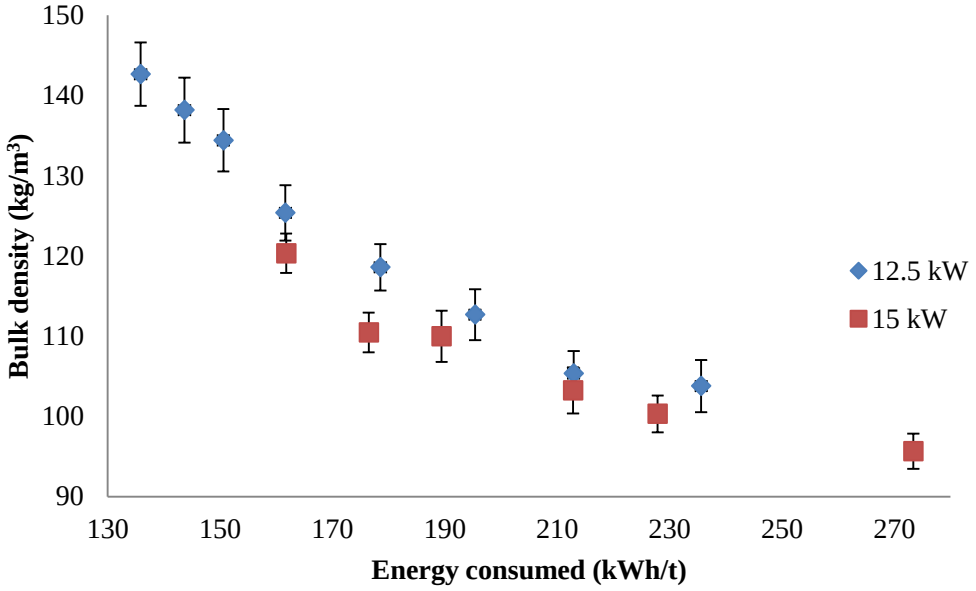

Figure 5-10: Effect of total energy consumed on the degree of exfoliation at 12.5 kW and 15 kW on the South African sample

The results demonstrated that the bulk density of the exfoliated product decreases with an increase in energy input during vermiculite exfoliation. This may be due to either an Increase in the microwave power or a decrease in the mass flow rate of raw vermiculite. Therefore, for commercial processing of vermiculite, a compromise must be reached to either process at a very low

throughput or increase the microwave power, in order to obtain exfoliated product within or far lower than the TVA bulk density specification (Table 5-1).

The effect of microwave power supplied into the cavity upon the degree of exfoliation was investigated by varying the microwave power from 7.5 kW to 15 kW for both South African and Australian superfine grades. Figure 5-11 shows the effect of microwave power on the degree of exfoliation of South African and Australian vermiculite.

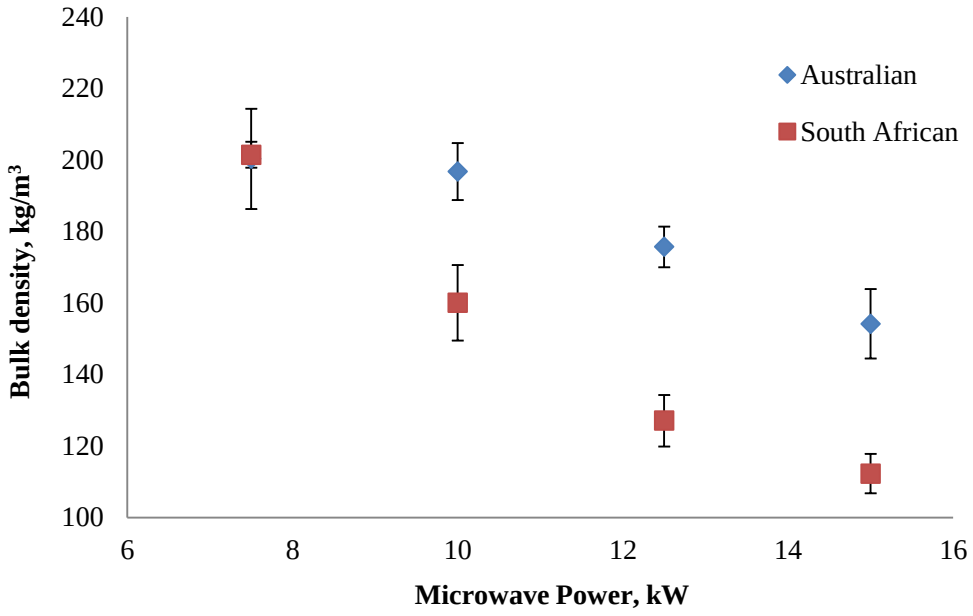

Figure 5-11: Effect of microwave power on the degree of exfoliation of South African and Australian samples processed at constant energy input of 135 kWh/t.

It is shown in Figure 5-11 that the bulk density of the processed vermiculite at the same energy input decreases with an increase in microwave power. This means that the quality of the products with respect to the TVA bulk density specification increases with an increase in the microwave power. This is almost certainly due to an increase in the electric field strength as the microwave power supplied to the cavity increases, and hence more energy is supplied to the vermiculite interlayer water, which is the microwave absorber phase. It was also observed that high degree of exfoliation in terms of the product bulk density was obtained in the South African sample when compared to the Australian sample.

5.2.2.4 Effect of Vermiculite Geological Source on Degree of Exfoliation

The geological source of minerals determines their physical and chemical properties such as chemical composition, moisture content, specific heat capacity and their dielectric properties. These properties dictate materials response to a specific processing methodology (Basset, 1963, Rao and Chernyshova, 2011, Bulelwa et al., 2013).

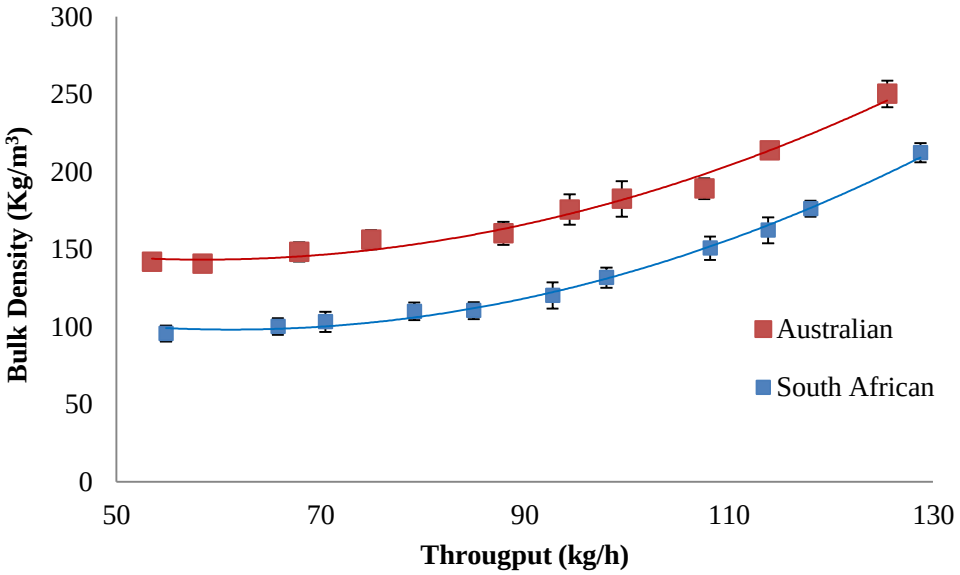

Figure 5-12: Effect of the geographic location on bulk density of exfoliated vermiculite processed at 15 kW.

Figure 5-12 shows a plot of the bulk density versus throughput for Australian and South African vermiculite, processed under the same conditions. The exfoliating performance of the two samples was compared because both are superfine grade. It is evident from Figure 5-12 that the South African sample produced a lower bulk density than the Australian sample at all measured throughputs.

Figure 5-13 shows the performance plot of Brazilian and Chinese samples, which are both medium grade vermiculite. Both samples were processed at 15 KW from throughputs 73 kg/h to 132 kg/h. The results show that the Brazilian sample has a lower bulk density at all the measured throughputs compared to that of the Chinese sample. The variations in the exfoliation performances of the different vermiculite samples can be related to the variations in the interlayer

water content, interlayer cations, chemical composition, and dielectric properties (Ernst et al., 1958, Huo et al., 2012).

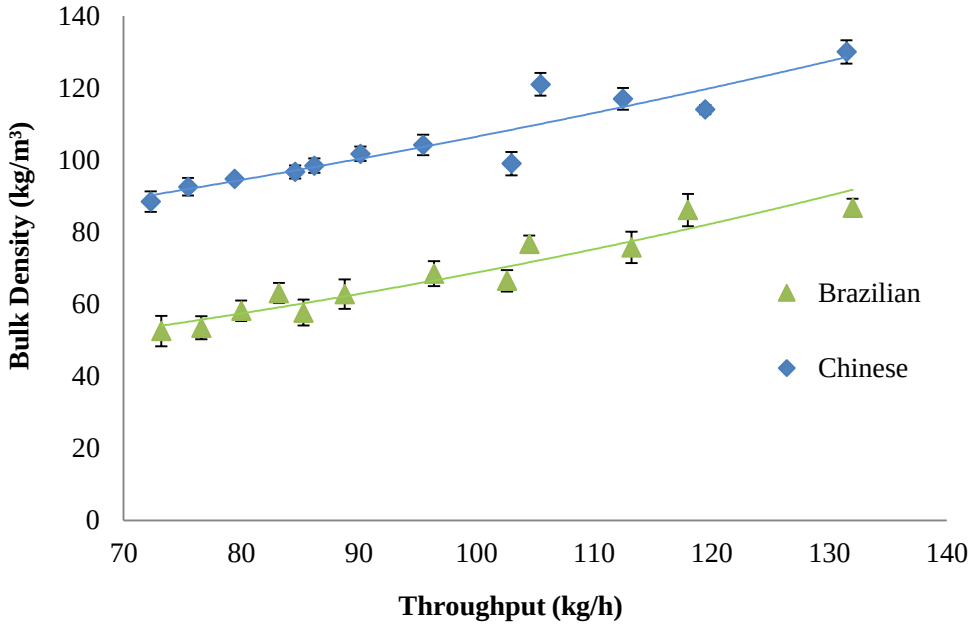

Figure 5-13: Effect of geographical location on bulk density of exfoliated vermiculite

Microwave heating parameters such as power density, heating rate and penetration depth depend on the dielectric properties of materials, which is a function of factors such as temperature, frequency, material chemical composition and moisture content present in the heated material. The dielectric properties of these vermiculite samples have been presented earlier in Chapter 4 to be influenced by their interlayer water. The higher amount of interlayer water contents of South African and Brazilian samples compared to that of Australian and Chinese samples is reflected in their higher values of dielectric constant and loss factor. The variations in the exfoliation behaviour of the different vermiculite sample from the different geographical locations can be explained by their mineralogical variations as discussed earlier in Chapter 4. Brazilian vermiculite, which has the same size range as Chinese vermiculite was found to be pure vermiculite according to the MLA (Figure 4-10) and XRD results discussed in section 4.4.1.3 of this thesis. This sample was also shown by the TGA test to contain higher water content (free and bound water) than the Chinese sample. The higher proportion of pure vermiculite in the Brazilian sample as opposed to that of Chinese sample, which is predominantly hydrobiotite, led to its higher degree of exfoliation in the microwave process.

Similarly, higher water content in the South African sample than the Australian sample influences the higher degree of exfoliation of the South African sample. It can be concluded from the exfoliation tests carried out using the pilot scale that the degree of vermiculite exfoliation is directly related to the mineralogy and vermiculite water content is a dominant factor that influences the exfoliation in a microwave process (Obut et al., 2003, Marcos and Rodríguez, 2010a). The pure vermiculite shows higher exfoliation degree than the impure vermiculite (Mortensen, 2006).

5.2.3 Findings from the Pilot Scale

The pilot scale system has been shown to successfully exfoliate two size classifications of raw vermiculite from Australia, Brazil, China and South Africa. It was found that degree of vermiculite exfoliation is fundamentally power density and energy driven. Feedstock throughput and vermiculite mineralogy, which is a function of the mine geology are other factors that influence the exfoliation process. Although, vermiculite mineralogy is a natural property and a parameter that cannot be controlled during the process design, the understanding gives us information about the performance of vermiculite from different deposit to microwave heating. The pilot scale results also showed that exfoliated vermiculite could be produced at a bulk density far below the TVA industrial specifications shown in Table 5-1. This could be achieved by either increasing the microwave power in order to increase the power density in the interlayer water, which is the microwave-heated phase, or controlling the feedstock throughput.

5.3 Scale up of a Continuous Microwave Exfoliator

It is evident from the results from the pilot scale tests that it was possible to successfully exfoliate vermiculite ores from four source locations, however, the system is throughput limited because the bulk density of the products increases with an increase in throughput. In addition, maximum microwave power of 30 kW is available for the pilot scale at 2.45 GHz. The results of the pilot scale system ultimately give an understanding of the route to the system scale up by considering a microwave system using an applicator designed at the available

lower ISM frequency and operated by high power microwave generator (100 kW).

The basis of scale up for the microwave exfoliator system is to increase the throughput of the exfoliated product (with bulk density within TVA specifications) to a level comparable with that of the commercial conventional system. For example, Torbed Service Limited. (1997) claims that their conventional systems named Torbed 1000 and Torbed 400, which are fuelled by oil or natural gas produce an exfoliated product at a throughputs between 1.4-2t/h and 0.2-0.25t/h for Torbed 1000 and Torbed 400 respectively. From a processing point of view, achieving a sufficiently high throughput in the microwave exfoliator entails increasing the width of the microwave cavity or reducing the residence time by increasing the belt speed. The main challenge of increasing the cavity width, however, is the reduction in the power density in a larger volume of the cavity. This can be overcome by increasing the microwave power, which therefore leads to an increase in the power density in the cavity volume and the available energy.

This section discusses the methodology used to design the microwave cavity, which was designed to operate at the industrially allocated frequency of 896 MHz (Meredith, 1998, Gupta and Eugene, 2007) and produce an optimum throughput of exfoliated vermiculite. Also discussed in this section are the challenges of the system scale up. Finally, the system commissioning and performance are discussed.

5.3.1 Consideration for System Scale-up

The key parameters for scale up of any microwave system are dielectric properties, the operating frequency (Bowman et al., 2008, Mehdizadeh, 2010), and nature of the material (solid or liquid) (Mehdizadeh, 2010). The dielectric properties of a material depend upon factors such as moisture content, temperature and frequency (Meredith, 1998, Metaxas and Meredith, 1983), but its variations with frequency are more significant for the applicator design when changing frequency. For example in this project, we are scaling up from a pilot scale operating at 2450 MHz to a scale up system operating at 896 MHz. The

results of the dielectric property measurements on the Australian, Brazilian, Chinese and South African samples (discussed in Chapter 4 of this thesis) showed that the values of both dielectric constant and loss factor vary with frequency. These variations can potentially have a significant influence on the penetration depth, heating rate and the produced power density.

The penetration depth of the wave into the material are greater at lower ISM frequency such as 896 MHz used in the UK than at higher ISM frequency such as 2450 MHz (Meredith, 1998). For example, Table 5-2 shows the penetration depth calculated by Equation 3-8 at 910 MHz and 2470 MHz respectively. The results show that the penetration depth at 910 MHz is higher than the value at 2470 MHz for the four vermiculite samples used in this project.

Table 5-2: Penetration depth of vermiculite at 910 MHz and 2470 MHz

Sample	Penetration depth (m) @ 910 MHz	Penetration depth (m) @ 2470 MHz
Australian	0.44	0.15
South African	0.30	0.14
Chinese	0.49	0.24
Brazilian	0.26	0.08

There are two possible options for scale up of the microwave system for vermiculite exfoliation. The first option is to use the cavity dimension of the pilot scale system operating at 2450 MHz by processing at a vermiculite bed depth higher than 5mm used for the simulation of the pilot scale or increasing the cavity geometry in order to increase the product throughput. The challenges of increasing the vermiculite bed in the pilot scale system or increasing the cavity of the pilot scale system are low power density and energy presented to the sample as the volume of the feedstock is increased and uneven heating of feedstock. The second possible option for scaling up the microwave exfoliator is to design a scaled up cavity operating at lower ISM frequency (896 MHz) by using the ratio of the wavelength between 896 MHz and 2450 MHz. This option requires the installation of a high power microwave generator (maximum power up to 100 kW) in order to achieve high power density in the large volume cavity.

The second option of changing to a lower frequency was used in this work to design a scale up system operating at 896 MHz. This frequency was chosen, as it is the only choice available at a lower ISM frequency. Due to the higher wavelength at this frequency compared to at 2450 MHz, it is possible to simulate and design a larger volume cavity. However, the shortfalls of this system are a higher microwave power requirement to maintain the same power density and energy requirement as the 2450 MHz system. There is possibility of experiencing arcing in this system due to the build-up of electric field because of the generation of higher electric fields by using high microwave power (Meredith, 1998). Also, according to the power density equation (Equation 3-6), the power density is directly proportional to the frequency, therefore higher electric field intensity will be required by the 896 MHz microwave system in order to compensate for the lower frequency compared to the 2450 MHz system.

Another challenge of the system scale up is the issue of electromagnetic compatibility (EMC) at 896 MHz (Catalá-Civera et al., 2006). The 896 MHz used for the scaled up system is close to the range of frequency used for broadcasting and global system of mobile communication (GSM) (GSM mobile phone channel 30 uses 896 MHz). Therefore, operating the vermiculite exfoliation system at this frequency is subject to control legislation in the United Kingdom (OFCOM, 2013). Within a frequency range close to 896 MHz, the disturbance and interference with communication instruments generally occurs even at a much lower emission level and the EMC limits are much tighter than health and safety (H & S) (Mehdizadeh, 2010). Therefore, choke design for the system requires more consideration. In addition, this frequency is only peculiar to the UK; therefore, provision must be made for the mitigation of the microwave emission to zero or non-detectable level. The EMC restricted standard is 5 mW/cm^2 for both 2450 MHz and 896 MHz over an exposure time of 30s, both measured at a distance of 5 cm from the equipment (BSI, 2011). Choke systems (both reflective and absorptive) were incorporated at the entry and the exit of the continuous system to prevent the emission of microwave energy to the surroundings to below health and safety and electromagnetic compatibility standards (BSI, 2011). The choke was tested and found to be good in mitigating the emission of electromagnetic waves. The methodology used for

the chokes design and the results obtained are reported in appendix 3. Lastly, higher plant footprint and energy are required for the scaled up system and, therefore, increases the capital cost compared to the pilot scale.

5.3.2 Microwave cavity for the 896 MHz System

Apart from the throughput limitation of the pilot scale system discussed earlier in section 5.2 the obtained results from the system only give a little understanding of the route to scale up at 896 MHz. This is due to the non-linearity of the dielectric properties of vermiculite with frequency. Figure 5-14 shows the variation of dielectric constant of South African and Australian samples with frequency while Figure 5-15 shows the variation of dielectric constant of Brazilian and Chinese samples with frequency.

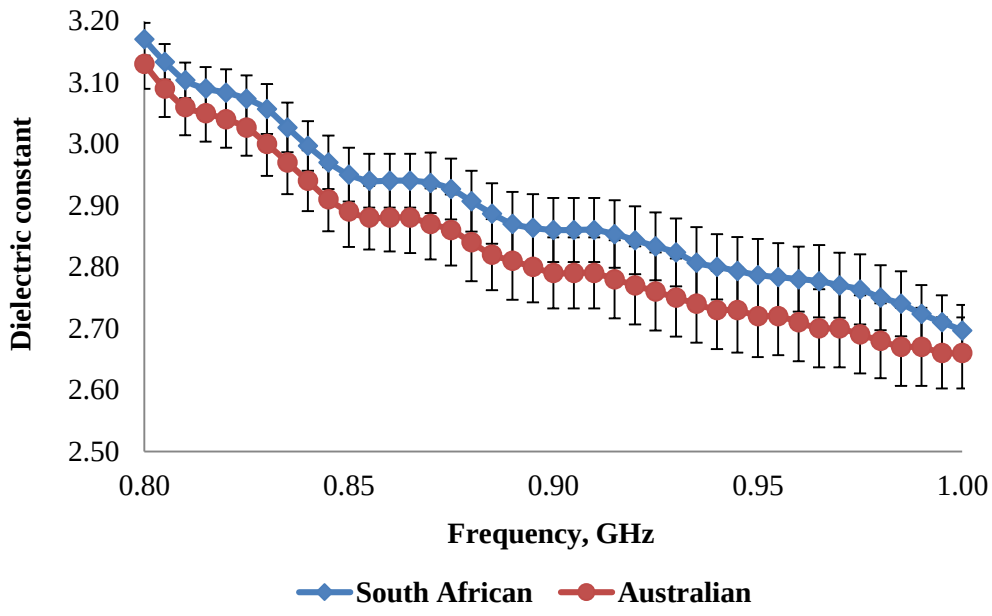

Figure 5-14: Variation of dielectric constant of South African and Australian samples with frequency

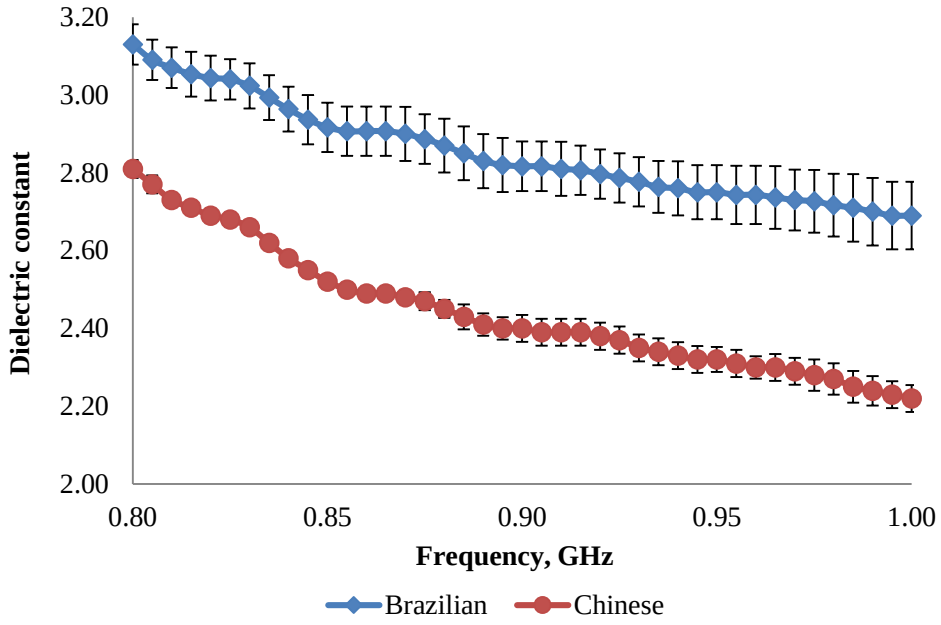

Figure 5-15: Variation of dielectric constant Brazilian and Chinese samples with frequency

Likewise, Figure 5-16 shows the variation of loss factor of the South African and Australian samples with frequency while that of Brazilian and Chinese vermiculite is presented in Figure 5-17. These results have been discussed in detail in Chapter 4 of this thesis.

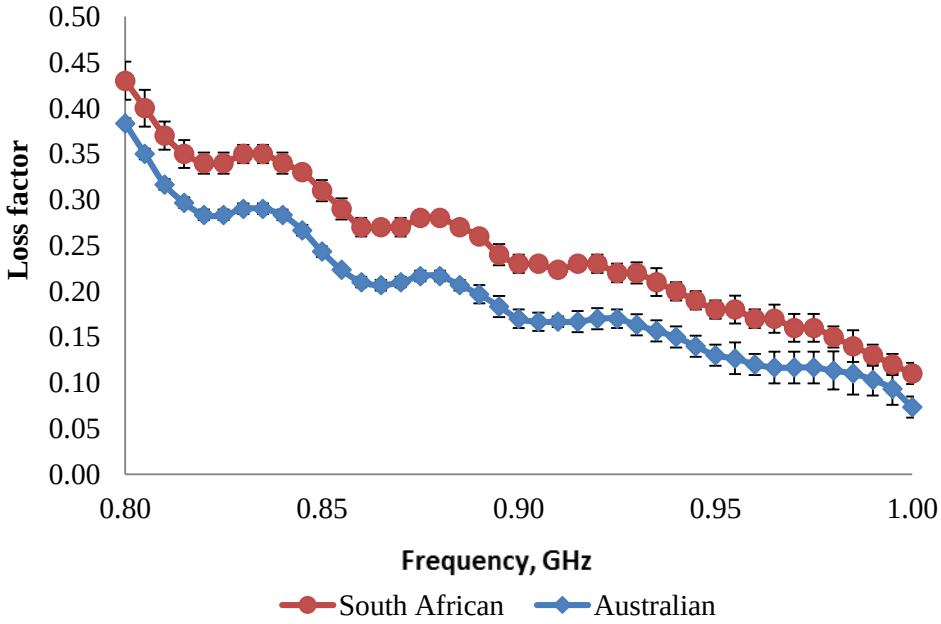

Figure 5-16: Variation of loss factor of South African and Australian samples with frequency

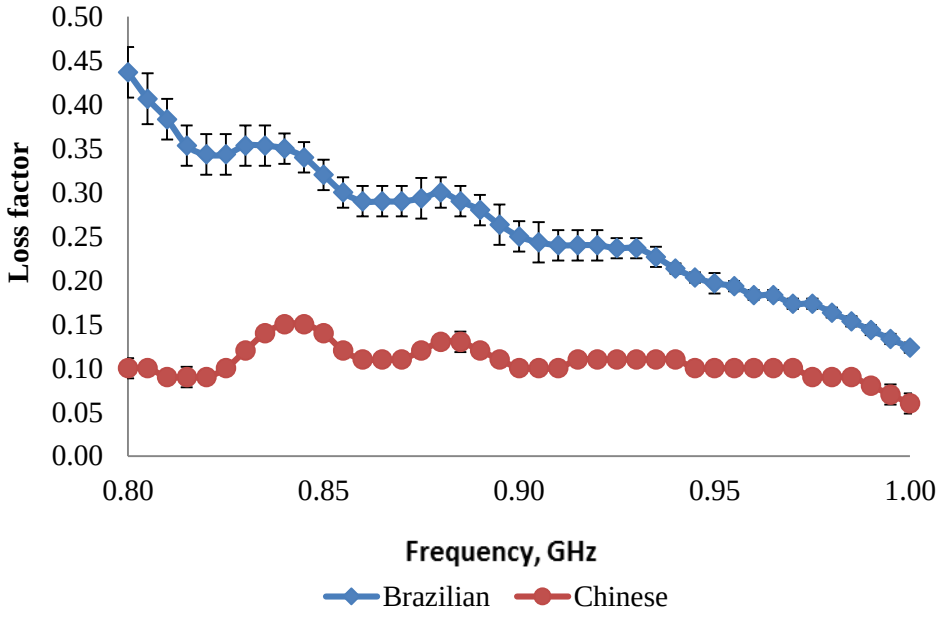

Figure 5-17: Variation of loss factor of Brazilian and Chinese samples with frequency

Similar to the pilot scale, the performance of the applicator designed for the scale up system was evaluated with the use of FDTD numerical technique (Taflove et al., 2005). Also for the purpose of the simulation of the applicator, a commercial package known as CONCERTO® supplied by COBHAM was used (Cobham, 2012). Procedure discussed earlier in section 5.2 was used for simulating the cavity and the walls of the cavity were assumed to be made of a perfect electric conductor and were used as the boundaries this design.

Figure 5-18 shows the model of the applicator with a fine mesh applied over it. For the purposes of the simulation, the dielectric properties of vermiculite measured at 896 MHz were extracted. Dielectric constant was taken as 2.97 and loss factor as 0.17. The simulation was made at 896 MHz and with a microwave power of 100 kW. This power was chosen for the simulation, as this is the maximum available at 896 MHz. This is to obtain sufficient high power density requirement for vermiculite exfoliation and to identify any high field concentrations that could lead to arcing.

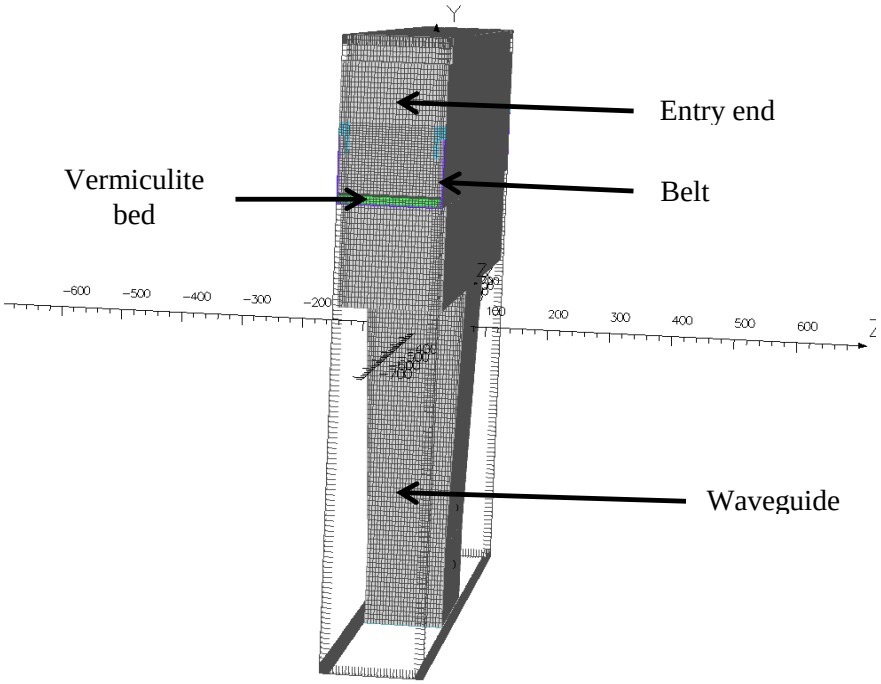

Figure 5-18: Model of the applicator with fine mesh over it for the purposes of the FDTD simulation

Figure 5-19 presents the structure of the designed resonant tunnel cavity used for the scale up system. It has three apertures: the one at its base end is connected to the feed waveguide. The other two apertures are at the input and the output ends that allow the movement of the conveyor belt for the continuous passage of feedstock through the cavity.

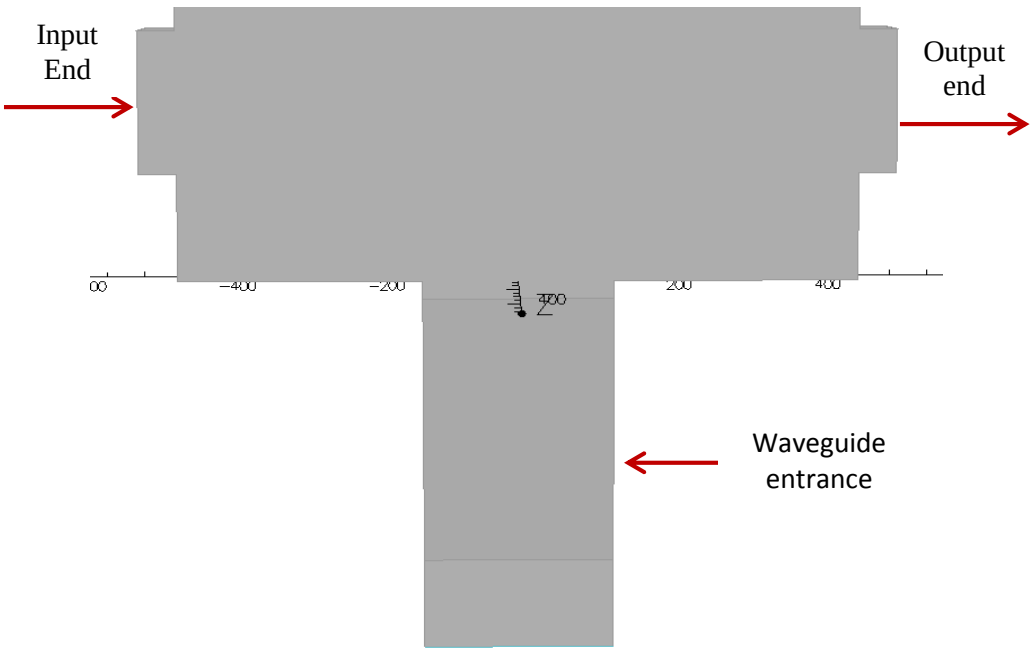

Figure 5-19: Schematic of the internal structure of the cavity showing the input end, the output end and the connector end to the waveguide.

Figure 5-20 depicts the electric field distribution in the cross-section of the empty applicator, which is the applicator without the conveyor belt and vermiculite load.

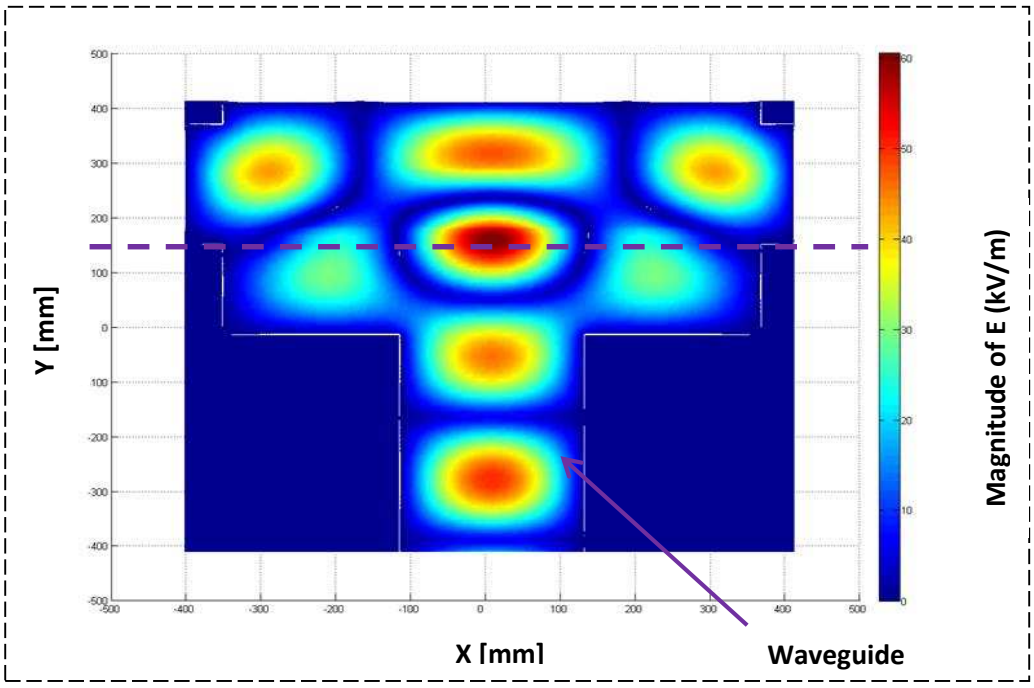

Figure 5-20: The Electric field pattern in the 896 MHz vermiculite exfoliator system

The dotted line that passes through the input and output ends of the applicator represents the path of the conveyor belt, which transports the vermiculite through the applicator. It is evident from Figure 5-20 that the cavity supports a well-defined electric field. There are numbers of hotspots and this is due to the large geometry of the cavity (Luo, 2007). The highest peak of electric field intensity (of about 60 kV/m) is located at the centre of the cavity and directly in the path of the conveyor belt.

When the loaded vermiculite applicator was simulated, the load changed the configuration of the electric field distribution. Figure 5-21 shows the model domain of the applicator for vermiculite exfoliation at 896 MHZ. The X-axis shows the input and output ends view of the cavity. Y-axis shows the region from the waveguide up to the top of the cavity and the Z-axis represents the width of the cavity and the waveguide

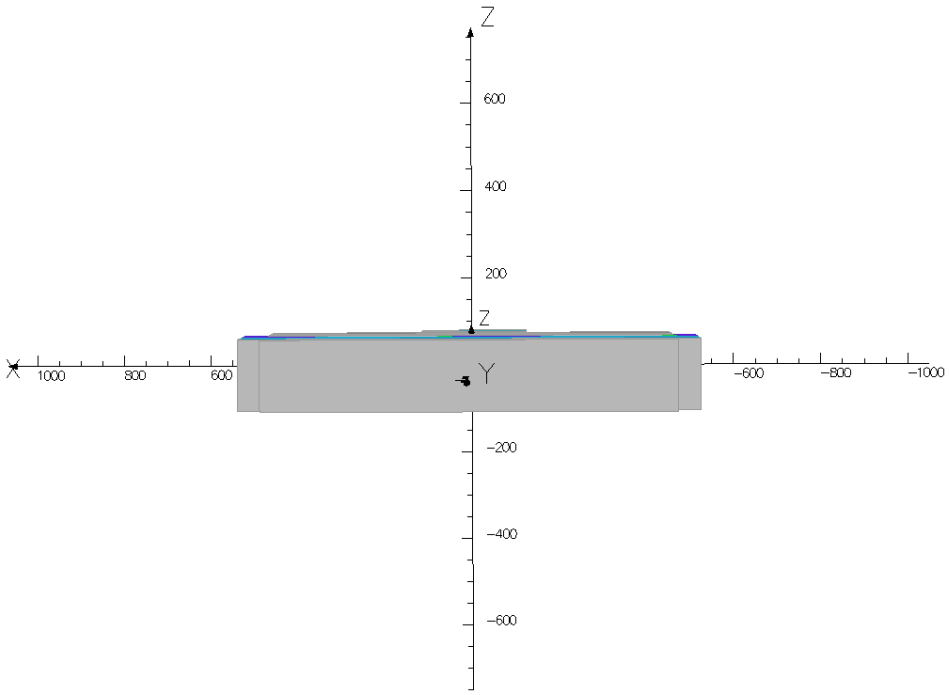

Figure 5-21: Model domain of the 896 MHz cavity for vermiculite exfoliation

Figure 5-22 presents the electric field distribution across the vermiculite load from the input to the output ends of the applicator. This is the view corresponding to the x-axis in Figure 5-21 and the conveyor belt with the vermiculite load travels horizontally along this path. According to Figure 5-22, the two regions (labelled A and B) blue colour on the extreme left and right signify the region with low electric field distribution. Region 'C' with red colouration represents the centre of the cavity that directly links to the waveguide section.

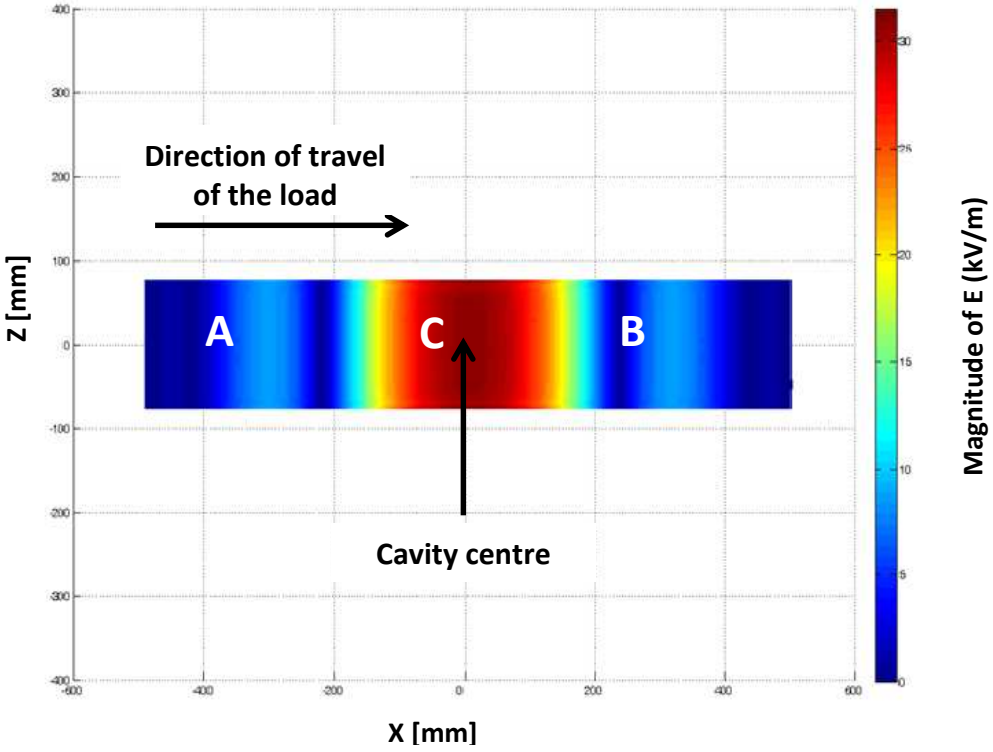

Figure 5-22: Electric field intensity in the vermiculite load as simulated. Regions in red and blue colours are regions of high and low electric field intensity respectively

The result of electric field distribution in a loaded cavity shown in Figure 5-22 shows that the intensity of the electric field in region labelled 'C' (cavity centre), which signifies the location where maximum exfoliation of the load takes place is about 35 kV/m. Comparison of Figure 5-20, which represents the electric field distribution in an empty cavity, and that of Figure 5-22 which represents the electric field distribution in a loaded applicator, shows that electric field intensity in the vermiculite-loaded applicator reduced. This is due to the decrease of the quality factor of the applicator because of the introduction of the load (raw vermiculite). This is as a result of the dissipation of electric field as heat by the water phase in the vermiculite material. The quality factor is a measure of power dissipation in a resonant circuit or applicator (Mehdizadeh, 2010). The intensity of the electric field in the load at the centre of the cavity is about 35 kV/m (Figure 5-22) compared to 60kV/m obtained at same location in an empty applicator (Figure 5-20).

Following the same model domain shown in Figure 5-21, the simulated power density (W/m^3) along the cavity section is shown in Figure 5-23. The simulated

result shows that maximum power density in the load (region C) is over $2.2x10^7$ W/m^3 at the centre of the cavity.

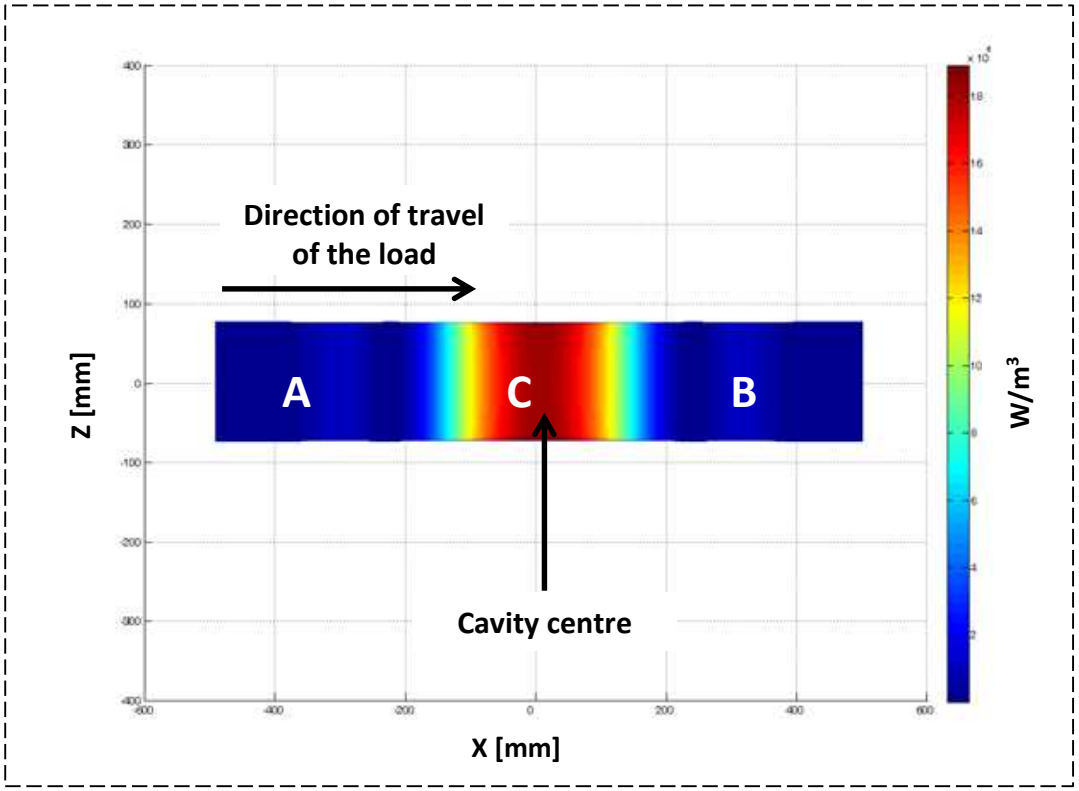

Figure 5-23: The simulated power density in the vermiculite load

The regions labelled 'A' and 'B' in Figure 5-23 are marked with low power density about $0.2x10^7$ W/m^3. It is apparent that the power density is uniform at the centre of the applicator and the continuous movement of the vermiculite through the load will enable homogenous heating. It is important to state that the power density shown in Figure 5-23 is the bulk power density of the vermiculite, but the power density in the interlayer water where most of the energy is dissipated will be higher than $2.2x10^7$ W/m^3. Interlayer water is assumed to have higher loss factor between 13-20 than the bulk vermiculite with loss factor about 0.17.

The comparison of the electric field distribution in the cavity used for the pilot scale (2450 MHz system) shown in Figure 5-2 and that of the scale up system (896 MHz) shown in Figure 5-22 shows that both applicators have similar field pattern. The maximum electric fields intensity and power density presented to the vermiculite load in both applicators are of similar magnitude despite using

microwave power 3 times higher in the 896 MHz system. However, homogenous power density was obtained in the 896 MHz system (Figure 5-23) while the power density in the pilot scale system (2450 MHz) is higher below the load.

5.3.3 Microwave Processing and Sampling Analysis

All microwave exfoliation tests were carried out with a microwave system capable of processing vermiculite continuously at 896 MHz and with a maximum microwave power of 100 kW. The system is a scaled up version of the pilot scale system shown in Figure 5-6. Microwave energy was supplied using a microwave generator manufactured by e2v Technologies Plc, Great Britain. The applicator consists of a tunnel, which allows a conveyor belt to pass through it. Similar to the pilot scale system, it has both reflective and resistive choke sections at both ends to prevent leakage of microwave to the immediate environment. The samples used for the tests were loaded into a feed hopper and fed into the microwave-heating cavity through a silicon coated fibreglass conveyor belt. Fitted and fixed at both ends of the tunnel are magnetic separators. These were used to remove rust and magnetic materials in the vermiculite samples as these might cause arcing in the microwave cavity. The throughput and bed thickness of the crude vermiculite travelling through the applicator was controlled by varying the vibration of the feeder system attached to the hopper. Belt speed was kept constant at 0.07m/s throughout the exfoliation tests.

Microwave energy was fed perpendicularly from the base of the cavity into the vermiculite sample passing through it and the moisture and dust generated within the cavity were removed by a system of vacuum extraction. An automatic 3-stub tuner was used to match the impedance of the microwave generator and the transmission line to the cavity in order to maximise the efficiency of transfer of microwave energy. The 3-stub tuner was used because of its simplicity and ability to match all load admittances (Pozar, 2012, Collin, 2001). The dummy load in the circulator, which protects the magnetron from excessive reflected power that can subsequently damage it, absorbed any reflected power. Exfoliated samples used for the performance tests were collected at the

discharge end of the tunnel. The mass and throughputs of sample collected for 30s at each microwave power used were determined. One of the errors associated with the sampling technique used is the issue of compaction of the vermiculite sample during measurement and this was reduced measuring each collected sample at least 3 times and avoid tapping of the measuring cylinder. Segregation of the exfoliated and non-exfoliated vermiculite in the collected sample is another source of error and this was eliminated by collecting a large volume of sample for measurement. The volume of the collected sample was measured by controlled transfer of the sample into a 5 litre-measuring cylinder without compaction and breakage. The bulk density of the collected and exfoliated sample was then obtained from Equation 5-1.

5.3.4 Experimental Test Matrix Design

The parameter factors used for the system optimisation were microwave power (kW) and throughput (Kg/h) of raw vermiculite. The product bulk density (Equation 5-1), which is the system performance indicator, was set as the dependent output response and the energy consumed was calculated by Equation 5-2. Other calculated parameters such as throughput, which is the hourly mass of feed and the volumetric volume of exfoliated product, are expressed as Equation 5-3 and Equation 5-4 respectively.

$$\text{Throughput}\,(\text{kg}/\text{h}) = \frac{\text{Mass of feed collected}}{\text{total time taken for sample collection}} \qquad \text{Equation 5-3}$$

$$\text{Volumetric flow rate}\,(\text{m}^3/\text{h}) = \frac{\text{Volume of exfoliated sample}}{\text{Total time taken}} \qquad \text{Equation 5-4}$$

Considering the results of the test work of the pilot scale system and the energy requirement for obtaining exfoliated product within the TVA standard, the processing was carried out at three microwave powers of 70, 80 and 90 kW at feedstock throughputs from 320 kg/h to 870 kg/h.

5.3.5 Results and Discussion

5.3.5.1 Exfoliation Performance of Vermiculite Minerals

Figure 5-24 shows the relationship between bulk densities (kg/m^3) of the exfoliated product of South African vermiculite versus the throughputs in kg/h. The results show that a product with a lower density is obtained at lower throughput. As the microwave power is increased from 70 kW to 90 kW, the bulk density of exfoliated product decreased.

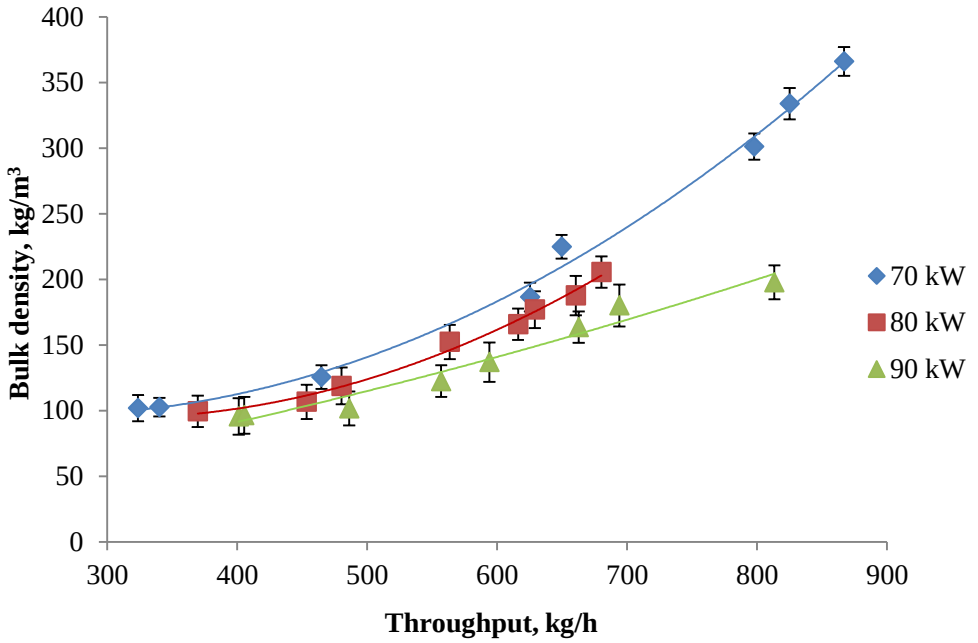

Figure 5-24: Mean performance curve (Bulk density) vs throughput for South African vermiculite using 896 MHz system.

Lower product bulk density obtained with decreasing throughput is due to the availability of a higher proportion of energy for heating the interlayer water at lower throughput. For example, Figure 5-25 shows the results of South African vermiculite processed at 80 kW from 369 kg/h to 680 kg/h. The results show that the bulk density of the product decreased as the total energy consumed increased. This implies that lower bulk density of the product can be obtained by decreasing the feed throughput to increase the available energy for heating the interlayer water of vermiculite.

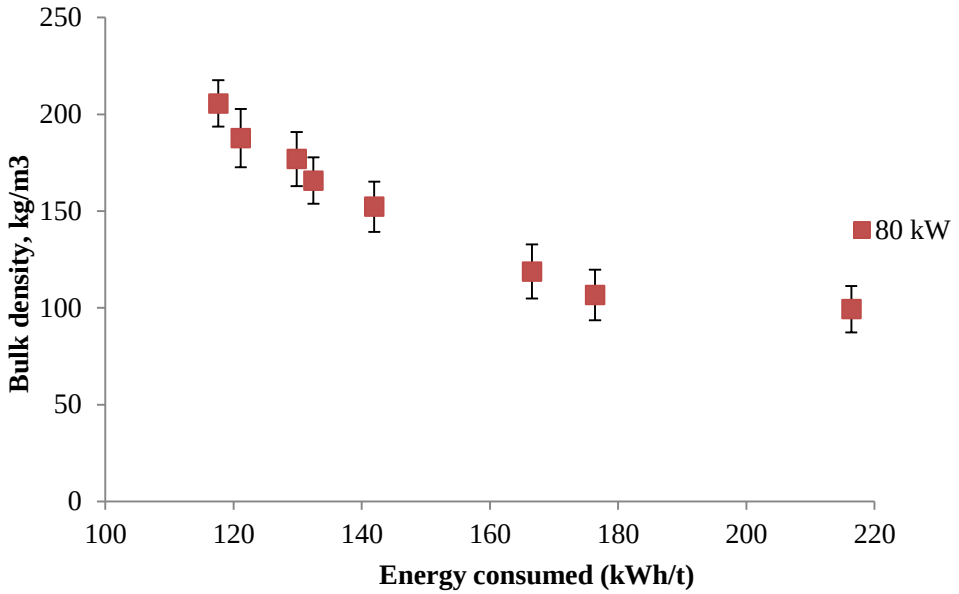

Figure 5-25: Effect of total energy consumed on the degree of exfoliation at 80 kW for a South African vermiculite sample

Comparative analysis of the bulk density of product obtained at 70, 80 and 90kW (Figure 5-24) showed that the highest microwave power produced lowest bulk density exfoliated product. This is because of higher power density available in the applicator for heating the vermiculite interlayer water at higher microwave power.

Figure 5-26 shows the volumetric flowrate of exfoliated product at 70, 80 and 90 kW versus mass throughput (kg/h). This result can be used as a tool for maximizing the profitability of microwave exfoliation of vermiculite. Raw vermiculite is usually bought in mass while the exfoliated product is sold on a volume basis. Therefore, making a greater volume of exfoliated product using less feedstock is more profitable.

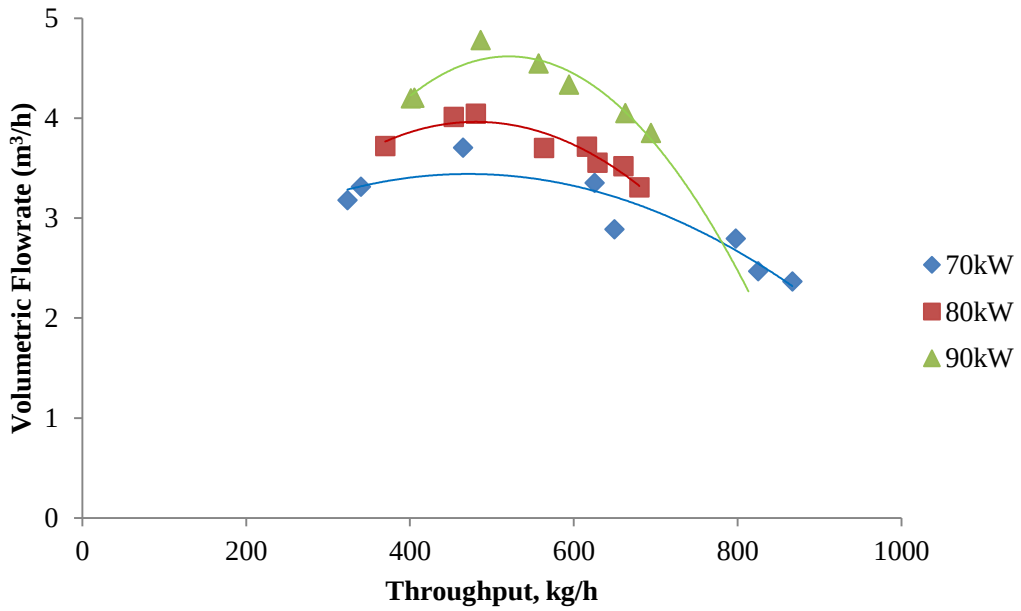

Figure 5-26: Volumetric flowrate vs mass throughput for superfine grade of South African vermiculite using a continuous treatment system operating at 896 MHz

Between mass throughputs of 460 kg/h to 490 kg/h, the maximum volumetric throughputs of over 3.7 m^3/h, 4.0 m^3/h and 4.8 m^3/h were produced at 70, 80 and 90 kW respectively at a bulk density below the TVA specification. As expected, a lower volumetric throughput was obtained for processing carried out at 80 and 70 kW. At a mass throughput of about 490 kg/h, a product with a volumetric flow rate of 4.8 m^3/h was produced at 90 kW, and this product has a bulk density of 9 5kg/m^3. This shows that this product is below the TVA specification.

A trade-off must be reached between the reduction of the product bulk density far below the TVA specification or operating at a product bulk density within the TVA standard. Bulk density below the TVA specification can be obtained by processing at a very low mass throughput and volumetric flowrate while the product with bulk density within the TVA standard can be produced by increasing the volumetric flowrate and mass throughput. However, this may depend on the final applications of the product and process economy.

The statistical analysis software 'Minitab' (Minitab 17, 2010) was employed in this work to study the process window of South African vermiculite processed at 90kW from a throughput between 400 kg/h to 820 kg/h. The process window

shows the response of bulk density of the product to the different combinations of flowrate and energy input. Figure 5-27 shows a 2-D contour plot of process window obtained for superfine grade of South African vermiculite at 90 kW. This result presents the impacts of mass flowrate and energy consumption on the bulk density of the product. The energy consumed was calculated from Equation 5-2. The 2-D contour plot shows that the areas marked A, B and C are above the TVA bulk density specification for superfine grade (80-144 kg/m^3). Areas labelled 1, 2 are within the TVA specification and the bulk density contour area marked 3 is below 100 kg/m^3.

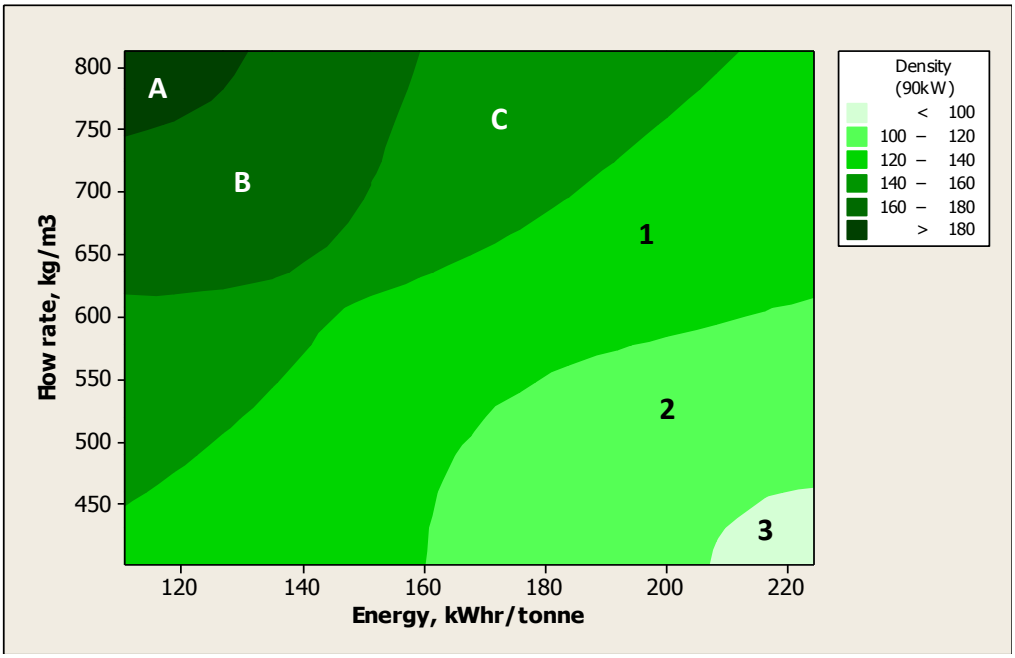

Figure 5-27: Contour plot showing bulk density response to flow rate and energy interactions for South African vermiculite

Analysis of the contour plot shows that the product below 100 kg/m^3 can be obtained by consuming microwave energy between 210-220 kWh/t with a throughput below 450 kg/h (area marked 3 on the plot). The system is capable of operating at a throughput of above 700 kg/h producing exfoliated product with density within the TVA specification for South African superfine as shown in the area marked '1', and consuming energy within the range of 190-220 kWh/tonne. The processing windows labelled 1, 2 and 3 produced exfoliated vermiculite within the TVA standard, but at different bulk densities and energy. The best window to operate depends on the final application of the exfoliated vermiculite. For lightweight concrete application, processing window 2 or 3 will

be more preferable to processing window 1 because of the lower buck density of the exfoliated vermiculite produced.

5.3.5.2 Effects of Particle Size on Vermiculite Exfoliation

Obut et al. (2003) reported that coarser particles are more suitable for microwave exfoliation and Marcos and Rodriguez (2010) found it was challenging expanding flakes between 1-3mm^2. The two authors processed the raw vermiculite in a batch system using a domestic multimode cavity operating at 2.45 GHz with a maximum operating power of 1300 W, however, the present work used a continuous system with a resonant cavity operating at 896 MHz and with a maximum power of 100 kW. It is therefore important to investigate whether the limitations of the work of the two aforementioned authors to exfoliate finer grades are due to a particle size effect or the power density generated in the interlayer water. This was investigated by subjecting superfine (0.355 mm to 1.0 mm size range) and fine (0.710 mm to 2.0 mm size range) grades of South African vermiculite to the same microwave power of 70 kW under the same operating conditions. The expansion ratio of vermiculite is calculated as the ratio of the bulk density of raw vermiculite to that of exfoliated vermiculite.

Figure 5-28 shows a graph of expansion ratio versus throughput for fine and superfine grades of South African vermiculite.

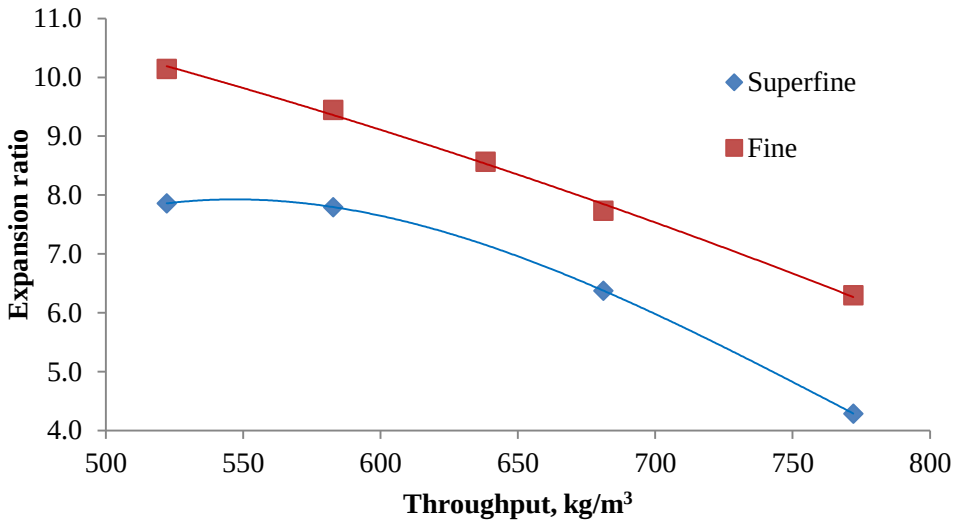

Figure 5-28: Effect of particle size on exfoliation performance of two grades of the South African vermiculite at 70 kW

It can be seen from Figure 5-28 that at all of the measured throughputs, the finer grade with the higher particle size range achieved a higher expansion ratio for the exfoliated product than the superfine grade, although the raw minerals of both samples have the same moisture content.

The lower exfoliation ratio obtained in the lower size grades is due to the reduction in the distance of the interlayer water to the free space, which allows the rapid escape of the interlayer water from the vermiculite structure when converted to steam. The pressure builds up within the individual flake structure as a result of the intense heating of the interlayer water by microwave energy is not sufficient to create a force required to rapidly separate the silicate structure further apart. As the distance is less in the smaller particles, it is easier for the moisture to escape and therefore the expansion of the silicate structure is reduced. This is reflected in Figure 5-29, which shows the influence of energy consumed on the bulk density of both fine and superfine grades of the South African vermiculite.

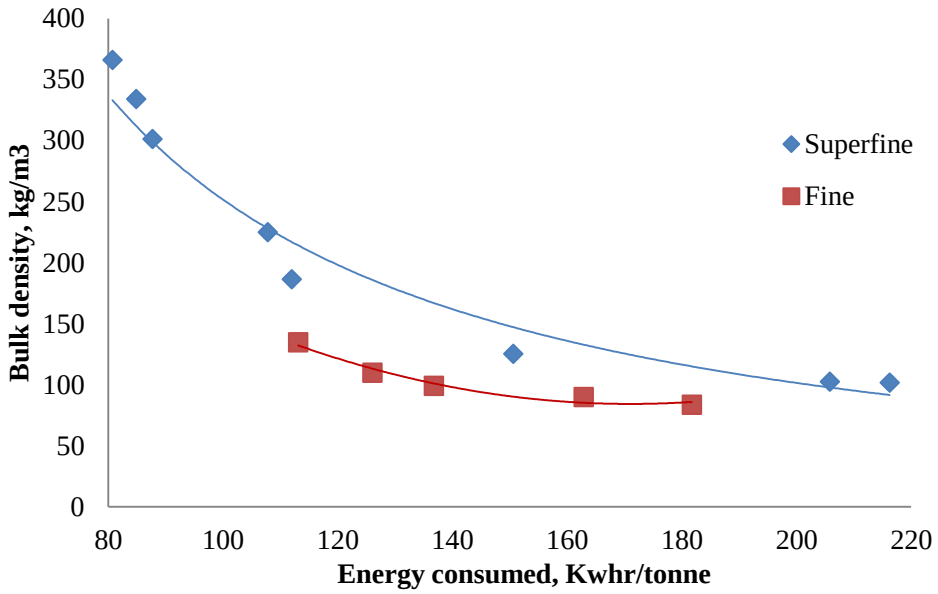

Figure 5-29: Performance indicator (Bulk density) vs energy consumed at 70 kW

Figure 5-29 shows that a lower energy input is required by fine grade vermiculite to achieve the TVA specification compared to superfine grade. This is because the larger distance to free space in the fine grade vermiculite gives room for the packet of steam produced within the silicate structure as a result of intense heating by microwave energy to have sufficient time to build up sufficient

pressure within the vermiculite silicate structure. In the case of the superfine grade, the produced steam escape easily out of the vermiculite structure due to lower distance required by the vaporised interlayer water to escape out of the vermiculite and low pressure is build up within the vermiculite structure. Therefore, higher power density will be needed to heat the interlayer water in the smaller flakes more rapidly to obtained bulk density below the TVA standard. This possibility of exfoliating finer grades of vermiculite to the industrial bulk density specifications compared to the use of batch domestic microwave oven(Marcos and Rodríguez, 2010a) in which there is a limitation in terms of expanding vermiculite flakes below 1-3mm^2 is one of the many benefits of the high power continuous microwave system for exfoliating vermiculite.

5.3.5.3 Comparison of 896 MHz and 2450 MHz Systems

The performance of the pilot scale system operating at a microwave frequency of 2450 MHz was compared to that of larger scale-up system operating at a microwave frequency of 896 MHz. Figure 5-30 shows the plots of bulk density against the energy consumed by both the pilot scale and larger scale-up systems. The plot of the 2450 system MHz represents the data of processing carried out at 15 kW from a throughput of 55 kg/h to 129 kg/h while that of 896 MHz system represents the data of processing carried out at 80 kW from a mass flowrate of 370 kg/h to 700 kg/h.

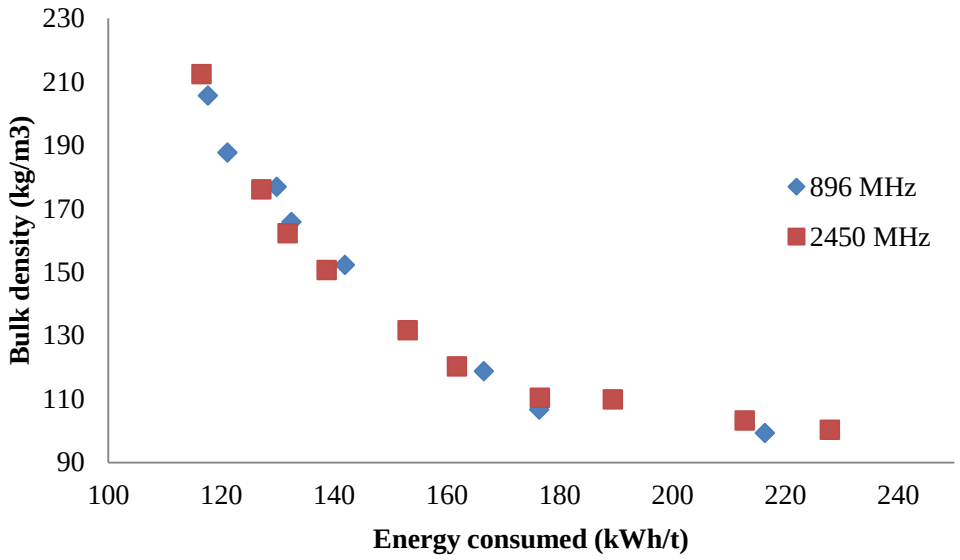

Figure 5-30: comparison of pilot scale system (2450 MHz) and larger scale (896 MHz) systems

Figure 5-30 shows that within the measured throughputs for both 896 MHz system operated at 80 kW and the 2450 MHz system operated at 15 kW, an exfoliated product of similar bulk densities were produced when energy consumed for processing is about 116 kWh/t to 230 kWh/t. Within these measurements limit, the degree of exfoliation of vermiculite by the 896 MHz system is from 4.6 to 9.6 while the degree of exfoliation of vermiculite by the 2450 MHz system is from 4.5 to 9.5. The 896 MHz system requires higher microwave power compared to the 2450 MHz system but it can be concluded that the efficiency of the 896 MHz system is higher than that of 2450 MHz system because with the same amount of energy consumed by both system. The 896 MHz was able to exfoliate higher throughput of vermiculite than that of 2450 MHz system (about 5 times).

5.3.5.4 Mechanism of Microwave Exfoliation of Vermiculite

Many researchers have tried to explain the mechanism of thermal exfoliation of vermiculite (Midgley and Midgley, 1960, Gruner, 1934b, Justo et al., 1989, Obut et al., 2003), and it has been generally agreed that the thermal exfoliation of vermiculite is due to the rapid production of steam as a result of heating of the interlayer water in the vermiculite structure. The intense pressure built up by the steam then pushes apart the vermiculite silicate layer. It was also reported that hydrobiotite exfoliates with a higher degree of expansion than true vermiculite (Midgley and Midgley, 1960, Gruner, 1934b, Justo et al., 1989, Hillier et al., 2013). This observation of a higher degree of exfoliation by hydrobiotite than pure vermiculite is in contrast to the observations made in the present work where the exfoliation was based on vermiculite heating under electromagnetic fields. The results obtained in this work showed that the Brazilian vermiculite, which is a pure form of vermiculite, shows a higher degree of exfoliation than the Chinese vermiculite, which is predominantly hydrobiotite. The difference in the exfoliation behaviour of vermiculite minerals to conventional and microwave heating may be explained by the difference in their exfoliation mechanisms.

Hillier et al. (2013) in their recent research on the mechanism of vermiculite exfoliation associated, the higher degree of exfoliation in mixed layer

vermiculite minerals (such as hydrobiotite and hydrophlogopite) when heated conventionally to their polyphase structure. It was explained that their polyphase structure inhibits the escape of the heated interlayer water, thereby creating higher pressures in order to cause a higher degree of exfoliation than that of pure vermiculite. This explanation may not be applicable to the microwave heated vermiculite since its silicate layer is transparent to the microwave energy but the interlayer water molecules, which are the microwave absorbent phase is the main factor for the microwave exfoliation process. Bulk vermiculite has low dielectric properties as discussed in Chapter 4. These low dielectric values mean vermiculite mineral is effectively transparent to microwave energy. Due to the selective heating advantage of microwave energy, it was possible to selectively heat the microwave absorber, which is the interlayer water phase in the vermiculite structure.

The reason for its exfoliation by microwave energy despite its apparent transparent nature can be explained when the alumino-silicate and the interlayer water phases are considered microscopically. When vermiculite ore passes through an electric field region, the electric field is diffracted at the boundary between the transparent silicate layer and the interlayer water surrounded by hydrated cations. The trapped interlayer water molecules retain their polar properties and have a complex permittivity higher than that of the silicate layer ($\varepsilon^*_{water} > \varepsilon^*_{silicate}$). The heat generated within the interlayer space of the vermiculite structure then transforms the interlayer water phase to steam, which subsequently builds up high pressure that separates the vermiculite layer structure causing expansion (Kupfer, 2005, Sihvola, 2000, Hilhorst et al., 2000). As discussed in section 5.3.5.2, when the particle size decreases, it becomes easier for the steam to escape from within the layers due to the reduced distance from the interlayer space to the silicate layer and this makes exfoliation of smaller grades more challenging, especially for the conventional system. Therefore, a higher power density is required in the interlayer water phase to exfoliate the smaller size ranges than the larger ones. It can be concluded that the main heating mechanisms of microwave vermiculite exfoliation are dipolar polarisation due to the inherent interlayer water and ionic conduction due to the presence of the interlayer cations but the dipolar polarisation effect may be

regarded as the dominant mechanism because the degree of exfoliation is directly proportional to the total interlayer water content.

5.3.5.5 Benefits of Microwave Processing of Vermiculite

One of the main significant benefits of microwave exfoliation of vermiculite over conventional heating is the obvious energy savings benefits (<220 kWh/t) realized through selective heating compared to the conventional heating that requires about 1 MWh/t (Andronova, 2007, Torbed Service Limited., 1997). Some of the other benefits that may be possible from microwave exfoliation of vermiculite include; significantly lower product temperature as the maximum temperature of the product recorded when vermiculite was processed using 896 MHz at a microwave power of 90 kW was below 350 °C. Due to the installation of dust extraction system, the dust emission is reduced and there is reduced noise compared to the conventional system because there is no rubbing together of the equipment parts. The reduced dust emission and noise improve the working conditions and health and safety.

5.4 Conclusions

This study has demonstrated that vermiculite minerals can be exfoliated using a continuous microwave system designed to operate at 2450 MHz for the pilot scale and 896 MHz for the scale up. A microwave exfoliator with two apertures and functioning choke systems to eliminate the emission of electromagnetic waves to the immediate surroundings was simulated and designed. The measured dielectric properties of vermiculite were used for the simulation. The system designed for operating at the two frequencies (pilot scale, 2450 MHz and the scale up, 896 MHz) allows continuous passage of feedstock through the applicator (microwave heating zone) with the aid of a microwave transparent conveyor belt.

The pilot scale system operating at 2.45 GHz was used for testing the exfoliation performance of vermiculite minerals from Australia, Brazil, China and South Africa using a Sairem microwave generator with a maximum microwave power of 15 kW. The results obtained from the pilots scale system demonstrated that microwave energy could be used for the exfoliation of vermiculite. The quality

of exfoliated vermiculite is measured in terms of the bulk density. The lower the bulk density of the exfoliated vermiculite produced, the higher the quality of that product. It was observed that the degree of vermiculite exfoliation is a function of factors such as microwave power density, energy input, material throughput and the mineralogy of the vermiculite samples. There is an inverse relationship between the product bulk density and the feedstock throughput. This means that a lower product bulk density is produced as the material throughput is decreased, and this is due to the availability of higher doses of energy to the material volume as the throughput is decreased.

A higher degree of vermiculite exfoliation was also obtained as the power density is increased by increasing the microwave power. In addition, higher degree of vermiculite exfoliation was recorded by vermiculite sample with higher vermiculite mineral and moisture content than those with higher hydrobiotite content and lower moisture content. This implies that pure vermiculite shows higher interaction with microwave energy due to the higher free interlayer water content. The results also showed that the vermiculite exfoliation requires energy input less than 220 kWh/t to achieve an exfoliated product below the TVA bulk density specification. Ultimately, it was observed that the pilot scale system is throughput limited because of the size limitation of the applicator at 2450 MHz and the limitation of maximum available microwave power of 30 kW at this frequency. However, the pilot scale system gives understanding of the route to the system scale up.

The scale up system was designed to operate at higher throughput by using the available lower ISM frequency of 896 MHz. At this frequency, it was possible to increase the dimensions of the cavity by the ratio of wavelength between 896 MHz and 2450 MHz and the designed system requires a higher microwave power for generating high electric field and power density sufficient for rapid heating of the vermiculite interlayer water. The scale up system operating at 896 MHz was supplied with microwave energy by a microwave generator (Maximum 100 kW) manufactured by e2v Technologies Plc, Great Britain. This was used to test the exfoliation performance of the superfine and fine grades of South African vermiculite. The exfoliation results obtained from the scale up system demonstrated that the system is capable of operating at a volumetric

throughput over 4 m^3/h for a superfine grade of the South African sample and has potential of producing higher volumetric throughput for larger grade because higher degrees of exfoliation was obtained from the coarser feedstock than the finer grade.

The mechanism of microwave exfoliation of vermiculite can be explained as the rapid heating of the vermiculite interlayer water, which builds up a high pressure that pushes apart the vermiculite silicate structure. Moisture content and the purity of the vermiculite minerals influence the degree of microwave exfoliation of vermiculite. Unlike the previous works carried out by conventional heating where it was reported that hydrobiotite and hydrophlogopite minerals exfoliated with higher degrees than pure vermiculite mineral, the results of the present work proved that pure vermiculite material exfoliates with a higher degree of exfoliation than hydrophlogopite and hydrobiotite when subjected to high power microwave energy. This is due to the rapid selective heating of only the interlayer water in the vermiculite structure when under the influence of electric field.

CHAPTER SIX
COMPARATIVE ANALYSIS OF ENERGY AND CARBON FOOTPRINT OF CONVENTIONAL AND MICROWAVE VERMICULITE EXFOLIATION PROCESSES

6.1 Introduction

It was shown in Chapter 2 that conventional exfoliation of vermiculite by natural gas or oil-fired furnaces emit greenhouse gases and other hazardous pollutants. In addition, the process requires energy inputs above 1.2G GJ/t due to the poor heat transfer properties of the vermiculite material. Work within this thesis has already demonstrated significant exfoliation of vermiculite through microwave heating at much lower energy input than conventional systems. However, to get an overall picture of the environmental benefits of microwave technology in this application, it is required to take a more holistic view of the process through a life cycle analysis model. Such models enable comparison of the sustainability of both microwave and conventional processing techniques as a function of energy consumption and environmental emissions (Durucan et al., 2006, Norgate and Haque, 2010).

Life cycle analysis (LCA), is a standardized methodology used to assess the material input, emissions, energy flow and associated environmental impacts through a process or product life cycle from "cradle to grave" (Pardo and Zufía, 2012, Hospido et al., 2010, Norgate and Haque, 2013). This method has previously been used for energy and environmental impact assessments for different mining and mineral processing projects, which is why it was chosen for this application. These include, ore sorting (Norgate and Haque, 2013), copper production (Memary et al., 2012, Ayres et al., 2002), smelting of sulphides (Golonka and Brennan, 1996), aluminium ore extraction and processing (Hake et al., 1998), and lead and zinc smelting (Xueyi et al., 2002). However, most published work involving LCA does not consider a complete cradle to grave analysis due to limited time, insufficient data and poor understanding of the entire process (Liu and Müller, 2012, Durucan et al., 2006, Swart and Dewulf, 2013).

The cradle to grave, life cycle assessment for mineral processing is divided into four different stages: raw materials extraction, manufacturing or processing,

utilisation and disposal of used products. For each stage in the life cycle analysis, the flow of materials and energy as inputs as well as emissions and waste, (the outputs), are calculated. The assessment of the environmental impact of each of the phases gives the overall impact of the process (Hospido et al., 2010, Durucan et al., 2006).

Figure 6-1 shows the comprehensive flow diagram for vermiculite processing, starting from the mining stage of the vermiculite ore to the storage of the exfoliated product. Open pit mining method is normally used for mining vermiculite ore as it is typically found in open pit mines. The mined ore is then transported to the mill or processing plant where it is stored and it is then fed into a series of unit operations, which make up primary processing. Screening is carried out to remove the waste rock greater than 1.6 cm and then blending occurs as the material is conveyed to the mill feed bin prior to being split into different fractions by wet screening ahead of gravity concentration. The concentrated ore is dried between 120 °C to 480 °C to reduce the surface moisture from about 15 % to less than 6 %. Primarily processed vermiculite ore is then transported to the exfoliation plant for final processing into industrial usable form (NPI, 1999, Marinshaw, 1995). The exfoliation process is an important stage of vermiculite processing as the raw feedstock is transformed to an inert material with low density, which is industrially used for different applications, such as fire retardant, agriculture and horticulture, and lightweight concrete (Muiambo et al., 2010, Justo et al., 1989).

It is important to quantify the emissions of particulate matter (PM and PM_{10}) in each processing stage (Marinshaw, 1995). Particulate matter or particulates are microscopic solid or liquid suspended in air as pollutants. During drying and conventional exfoliation stages, in addition to the emission of particulate matter, there are emissions of gaseous pollutants such as carbon monoxide (CO), carbon dioxide (CO_2), nitrogen oxides (NO_X) and sulphur oxides (SO_X) generated as a result of combustion (Marinshaw, 1995, NPI, 1999). For vermiculite exfoliation irrespective of the processing technique used, the emission limit of particulate matter is set to be 50 mg/m^3 (US EPA, 1998), therefore, this standard should be

used as a benchmark during the design and commissioning of the vermiculite exfoliator.

The life cycle assessment discussed in this chapter is limited only to that of the exfoliation stage of vermiculite ore highlighted in Figure 6-1. This is because the exfoliation stage is the only process that will change because of a different exfoliation technique being employed in the present project**.** The rest of the stages, from mining to the storage of exfoliated product are identical for both conventional and microwave exfoliation. The comparative life cycle analysis of microwave exfoliation and conventional exfoliation of vermiculite by direct heating in oil and gas vertical furnace was carried out with respect to energy consumption, production cost and the environmental impacts.

6.2 Life Cycle Analysis Standards and Guidelines

Several different standard and protocols have been developed by public and private organisations for carrying out a credible and comparable life cycle analysis. Examples of these are the International Organisation for Standardisation (ISO) standards (ISO 14040 and ISO 14044), and International Reference Life Cycle Data System (ILCD) designed by the European commission. Others are Greenhouse Gas Protocol (GHG Protocol) developed by the World Resources Institute (WRI) and the World Business Council for Sustainable Development (WBSCSD) and The Publicly Available Specification 2050:2008 prepared by the British Standard Institution (BSI) (ISO 14040, 2006, ISO 14044, 2006, PAS 2050, 2011, Marc-Andree et al., 2012, WBCSD, 2013). Many of these standards are continually being updated to improve and design a new perspective on the life cycle assessment.

The present study was performed in accordance with the LCA standards designed by the International Organisation for Standardization (ISO) and the British Standards Institution (BSI), which are the two most commonly used standards. The ISO 14040 (principles and framework), ISO 14044 (Requirements and guidelines) and PAS2050 are the three series of standards used in this work (ISO 14040, 2006, ISO 14044, 2006, PAS 2050, 2011).

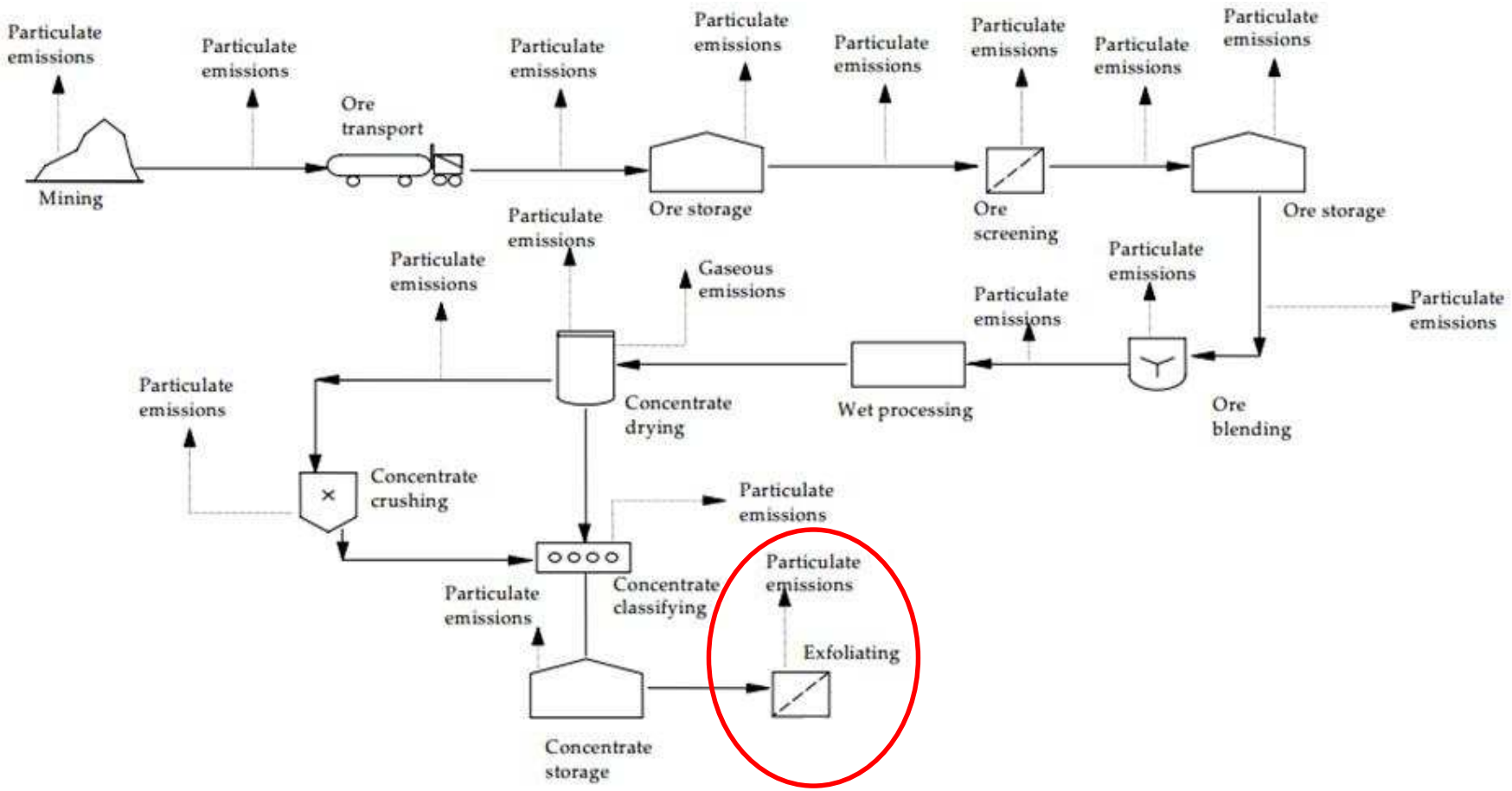

Figure 6-1: Process flowsheet for vermiculite processing from mining stage for storage of exfoliated product (NPI, 1999)

6.3 Methodology Used for Performing the Life Cycle Analysis

The life cycle analysis presented in this section follows the ISO and BSI procedural framework for performing life cycle assessment (LCA) as given in the ISO 14040, ISO 14044 and PAS2050 series. The two frameworks are divided into four phases (Figure 6-2). They are; goals and scope definition, life cycle inventory analysis, life cycle impact assessment and Interpretation of results (ISO 14040, 2006, ISO 14044, 2006, PAS 2050, 2011). The comparative life cycle assessment carried out in this work followed these four standard steps.

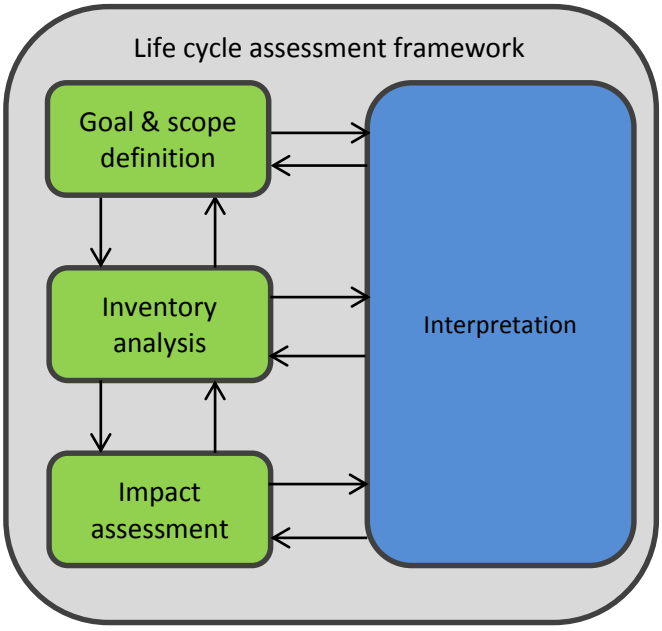

Figure 6-2: Phases of life cycle assessment framework (ISO 14040, 2006)

6.3.1 Life cycle Analysis Software Selection

Over thirty software tools are available for carrying out life cycle analysis of a process or product. These software tools vary in their stage of development, language, use, availability, and flexibility. Some popular tools are SimaPro (Pre, 2011), CCaLC (The University of Manchester, 2007), LCAD, KCL-ECO GABI and PEMS. This work used CCaLC, which is an Excel software designed to work under macro environment. This LCA calculator was developed by the carbon calculation team at The University of Manchester (The University of Manchester, 2007). It was chosen to be used for this work because of the robustness of its impact assessment, its flexibility and free accessibility (The

University of Manchester, 2007). In addition, in contrast to other life cycle analysis software where the users have to develop the systematic process of the task, CCaLC has an inbuilt systematic process as shown in Figure 6-3. This makes it very easy to be used by non-expert and offers different levels of complexity to users of different levels of experience.

CCaLC is an Excel macro based application and allows quick, reliable, and easy estimation of environmental impacts of a process or product. Its development follows the ISO 14044 and PAS2050 LCA standard (ISO 14044, 2006, PAS 2050, 2011), and it is capable of estimating environmental impacts, which include carbon footprint (global warming potential), water footprint, ozone layer depletion potential, acidification potential, human toxicity potential, photochemical smog, and hypertrophication. A carbon footprint, which is the estimate of the climate change impact due to emission of greenhouse gases (Ercin and Hoekstra, 2012), is the most important environmental impacts considered in this work. This is because the vermiculite exfoliation process only has a direct impact on the greenhouse gases emissions, as a result of burning of fossil fuel (oil or natural gas) for conventional exfoliation and the use of electrical power for both conventional and microwave exfoliation processes.

This tool has three databases relating to environmental impact. The CCaLC database consists of publicly available data inbuilt into the tool; this contains data related to global warming and other environmental impacts. The Ecoinvent database owned by the Ecoinvent centre, Zurich, contains comprehensive data included in the CCaLC tool, and consist consistent and up-to-date Life Cycle Inventory (LCI) data, while the CCaLC users can create the user database to suit their purpose. Generally included in the CCaLC databases are the carbon footprint of materials, which includes agricultural products, biomass, energy supply, construction and packaging materials. Vermiculite, which is the material of interest to this work, is grouped under the construction materials. Also included is the comprehensive information about the carbon footprint index (kg CO2 eq/kWh) of different form of available energy. This life cycle analysis tool has been used by various researcher for conducting the life cycle analysis of the production of food materials (Iriarte et al., 2014, Djekic et al., Whittaker et al.,

2013), impact assessment of freshwater (Jeswani and Azapagic, 2011), LCA of recycling of PVC material (Stichnothe and Azapagic, 2013) and industrial productions (Karjalainen, 2013).

In calculating the carbon footprint of any process using CCaLC, the user inputs the data of the materials used, the quantity of energy consumed and the waste generated, into the excel macro. Moreover, the user can include any inventory data in their process that is not included in the database. The results of the calculated carbon footprint are obtained either in numerical or graphical form depending on the user choice. In the present work, the data of the quantity of vermiculite processed and the energy consumed by the system were input into the program.

6.3.2 Goal and Scope Definition

Goal and scope definition provide the basic process being examined. The objective of this study is to determine and compare the energy consumption and environmental impacts associated with microwave and conventional exfoliation of vermiculite. The results of this study could be used to ascertain the more efficient technique between the two processes in terms of energy consumption and overall environmental impacts (carbon footprint). In addition, this study gives quantification of the environmental effect, energy cost and social implications of shifting from conventional vermiculite processing to microwave processing.

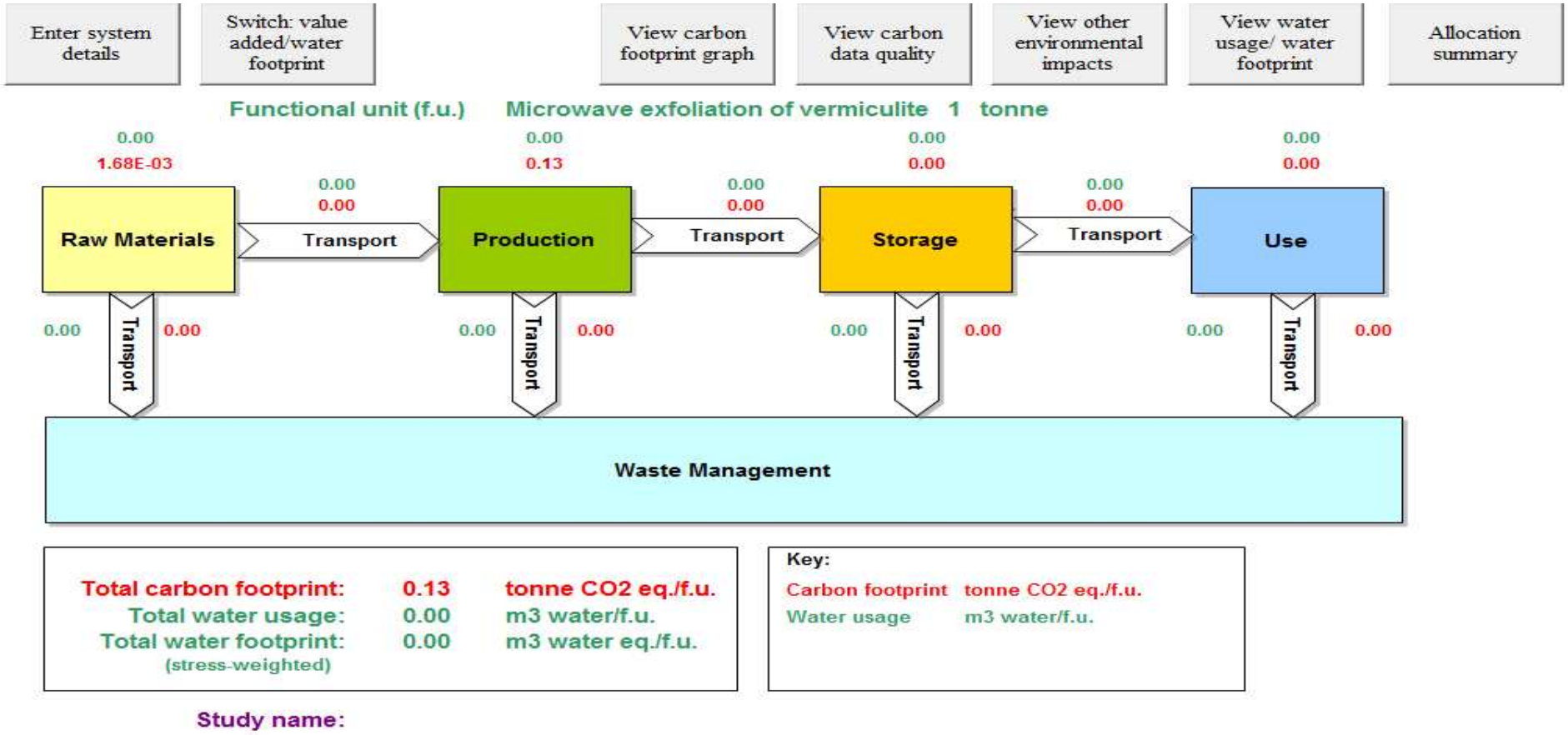

Figure 6-3: An In-built system of CCaLC showing the raw materials, production stage, storage and uses.

6.3.2.1 Conventional Exfoliation Process

As described in Chapter 2, conventional thermal exfoliation of vermiculite uses a vertical or rotary furnace systems fuelled by natural gas or oil. Figure 6-4 shows the process diagram for conventional exfoliation with vermiculite ore as the input material. The furnace is directly powered by oil or natural gas, while the peripheral equipment is operated by electricity. In this system, vermiculite ore is fed continuously into the furnace where it has direct contact with a large volume of high velocity heated gas and flame produced from the combustion of oil or natural gas (Kogel et al., 2006, Torbed Service Limited., 1997). The fume emitted as a result of fuel combustion and the dust collected in the dust extraction system during the conventional exfoliation are much higher in size and capacity than that of the microwave system.

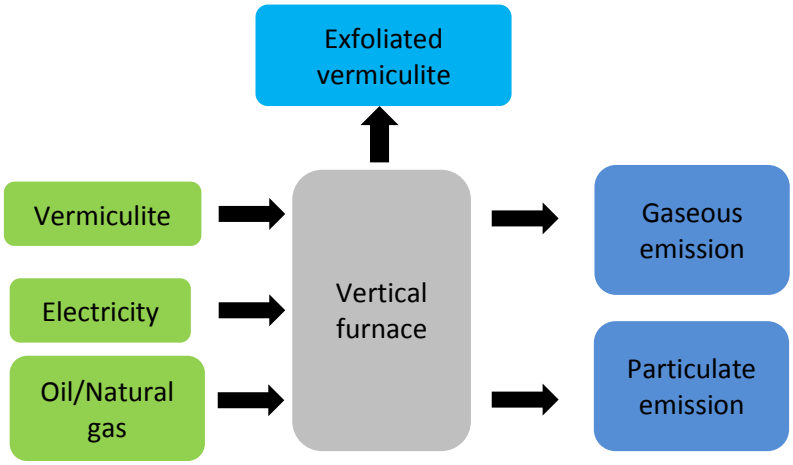

Figure 6-4: Conventional exfoliation process diagram showing the material and energy input and the associated particulate and gaseous emissions

The exfoliation occurs between the process temperature of 850 °C to 1200 °C for a period up to 8 seconds or less (NPI, 1999, Torbed Service Limited., 1997, Marinshaw, 1995, Kogel et al., 2006). There is a high loss of energy in this type of system because of the transfer of heat from the insulating surface of the vermiculite to the interlayer space that contains the interlayer water. In addition to energy losses, there is emission of particulate matter and gaseous pollutants, which includes carbon monoxide (CO), carbon dioxide (CO_2), nitrogen oxides (NO_X), and sulphur oxides (SO_X) generated from the combustion of natural gas and oil. In the vertical exfoliator, the exfoliated vermiculite is removed from the

furnace through the furnace top section by the upward flow of large volumes of air. Due to the large volume of heated air required for vermiculite exfoliation, high cost of fuel will be required for the operation and the dust recovery equipment may be large and expensive.

The recently developed thermal exfoliator (Torbed 400 and 1000) designed by Torftech Limited, UK, incorporates fluidised bed and cyclone technologies. They operate by the continuous contact between hot flames (1250 °C) and vermiculite ore. Torbed Ltd designed two exfoliation reactors, Torbed 400 (max 0.25 t/h) and Torbed 1000 (max 2 t/h) for exfoliating vermiculite. Both reactors operate by the burning of either oil or natural gas (Torbed Service Limited., 1997).

6.3.2.2 Microwave Exfoliation Process

Figure 6-5 shows the process diagram for the microwave exfoliator. The engineering design of this system was discussed in Chapter 5. In contrast to conventional exfoliation, microwave exfoliation occurs by the selective interaction of the electromagnetic waves with the interlayer water molecules. This overcomes the problem of energy loss across the temperature gradient.

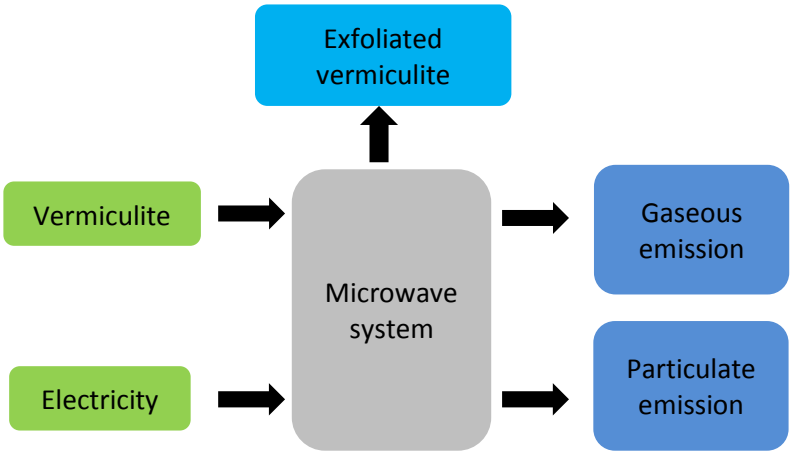

Figure 6-5: Microwave exfoliation process diagram showing the material and energy input and the associated particulate emissions

In addition to this advantage, the only energy input to the microwave system is from electricity and there is no emission of gaseous pollutants since there is no combustion of fossil fuels. The particulate emissions are reduced to a minimum because the vermiculite ore continuously flows through an enclosed tunnel. Due to better understanding of the material handling, a sophisticated extraction

system was installed to collect dust from the dust emission spots. Mixtures of water vapour and dust generated in the microwave-heating cavity during the exfoliation process are also extracted away from the microwave-heating zone. The exfoliation temperature measured by the infrared thermocouple showed a maximum temperature of 350 °C, for the exfoliation of South African grade vermiculite at microwave power of 80 kW and throughput of 700 kg/h. Therefore, the products were collected under this temperature as the experimental test matrixes were carried out below this microwave power.

6.3.2.3 Functional Unit

The functional unit, which is the main unit any life cycle assessment is built upon, must be defined before life cycle analysis of a product is carried out. The function of the two systems described in this work is the continuous exfoliation of vermiculite ores from different geological locations. Therefore, both the inputs and outputs in the life cycle inventory stage of this work were expressed relative to the functional unit, which is 1 tonne of vermiculite ore processed.

6.3.2.4 System Boundary

The processing of vermiculite from open pit mining up to the storage of the exfoliated product has a complex multiphase process flowsheet as shown in Figure 6-1 (NPI, 1999), and the system boundary for the LCA carried out in this study is well defined. Since this work is limited only to the exfoliation stage of the vermiculite ore using microwave energy and conventional heating, the comparative life cycle assessment studied in this work only focuses on the exfoliation stage highlighted in Figure 6-1. The stages outside the boundary such as mining, ore transportation and storage, screening and storage, blending, concentrate drying and concentrate classifying were not taken into account in this study. The boundaries of the study are crossed when the vermiculite ore is fed into the vertical furnace and microwave applicator in the case of conventional exfoliation and microwave exfoliation respectively, and finishes when the exfoliated vermiculite is collected from the discharge. The environmental impacts of the bagging process are not considered because of limited data. The life cycle assessment carried out in this work compares the environmental impacts of two processing techniques (conventional and

microwave exfoliation of vermiculite) based on the carbon footprint and the process economy.

6.3.2.5 Data Quality

All the input data used in this life cycle analysis were collected from three different sources and were introduced as inputs into the LCA software (The University of Manchester, 2007):

1. The primary data for microwave processing were collected from the continuous full scale running of the commercial scale-up system, operating at 896 MHz and a maximum power of 100 kW. The data used for this analysis was obtained for a test carried out at 70 kW as this gives a product density below the TVA standard. The value of maximum energy consumed by the system in achieving commercial throughput was obtained from the performance curve of density (kg/m^3) against the energy power consumption shown in Chapter 5.
2. The data used for the conventional exfoliation (industry) were obtained through personal communication with colleague at the Vermiculite Association meeting (The Vermiculite Association, 2011).
3. The data for a more energy efficient but still conventionally heated vermiculite exfoliator designed by the Torftech group (named Torbed exfoliator in this work) were obtained via the internet (Torbed Service Limited., 1997).

6.3.3 Life Cycle Inventory (LCI)

The life cycle inventory, which is the second stage of life cycle analysis, provides the basis for life cycle assessment. This is the phase where the input and output data associated with a process and product are collected. It includes data collection and data analysis. A good life cycle inventory should be quantitative, replicable, detailed and useful (Ciambrone, 1997). The inventories used in this work include the material (vermiculite ore) and the energy (natural gas and electricity) used in the exfoliation process. The energy characterisation parameters (natural gas inputs and electricity used) were used to calculate the carbon footprint which was the indicator used in this work as the basis of comparison.

6.3.3.1 Data Collection and Analysis

Table 6-1 gives the summary of the data collected and inserted as inputs into the CCaLC software used for the life cycle assessment.

Table 6-1: Energy consumed and process temperature of microwave and conventional exfoliation

	Microwave exfoliator	Industrial exfoliator	Torbed exfoliator
Vermiculite ore (Tonne)	1	1	1
Total energy (kWh/t)	180-220	800[1] 300[2]	347-472[1] 428[2]
Exfoliation temperature	350 °C	Up to 85 0°C	850 °C-1200 °C

(1: Energy for heating furnace, 2: Electricity for peripheral equipment (Torbed Service Limited., 1997)

The results discussed earlier in Chapter 5 showed that the continuous microwave exfoliator operating at 896 MHz had an energy consumption of between 180-220 kWh/t at a throughput up to 800 kg/h. The results obtained during exfoliation of South African superfine grade vermiculite were used because it is a representative of the vermiculite grades in terms of processing performance and demand. A maximum energy of 220 kWh/t obtained during the system testing was used to quantify the worst-case environmental impact of microwave exfoliation.

The available information obtained from the industrial conventional exfoliation (named industrial exfoliator in this work) using natural gas fired furnace, showed that 800 kWh/t was used for heating the furnace and average of 300 kWh/t expended on electricity to power peripheral dust extraction equipment. The information about the energy requirements of Torbed Exfoliator were obtained from the Torftech website as of July 2014. The available information showed that Torbed exfoliating system used between 347-472 kWh/t for heating the furnace for vermiculite exfoliation. About 80 kWh/t of electricity was used to operate the peripheral equipment. It was also claimed that the system has a

dedicated cooler unit that cools the exfoliated product from 1200 °C to 35 °C. Energy required for cooling 1 tonne of exfoliated vermiculite down to 35°C is calculated as 1258 MJ (348 kW/h) from Equation 6-1: Where 'M' is the mass of exfoliated vermiculite (1000 kg), 'C' is the vermiculite specific heat capacity (1080 J/kgK) (The Vermiculite Association, 2011) and 'θ' the change in temperature (1165 °C). Therefore, 428 kW/h of electrical energy is required to operate the system.

$$Q = MC\theta \qquad \text{Equation 6-1}$$

Both conventional exfoliation systems studied in this work were assumed to emit the same amount of particle matter (PM10), 0.32 kg/t, when compared to similar vertical furnaces (Marinshaw, 1995, NPI, 1999).

According to the available information on the carbon footprint index, for different energy in the CCaLC databases, the overall contribution of electricity to the carbon footprint varies depending on the electricity production mix of the country used for the analysis. In addition, the type of natural gas and oil used in a country where the life cycle analysis is carried out also influences the life cycle assessment results. For simplicity, only the UK electricity production mix was used in this work and the heavy oil used for firing industrial furnaces in Europe was also used for the analysis. The natural gas used in the UK for heating furnaces up to 100 kW was used for the furnace heating.

6.4 Life Cycle Impact Assessment

At this phase of life cycle assessment, the materials/energy flows and the associated emissions identified and collected during the life cycle inventory analysis stage, are translated to their potential human and ecological effects. The Ecoinvent database in the CCaLC macro was used to determine the environmental impact of the processed material (vermiculite ore) and energy (electricity for both microwave and conventional exfoliation, and natural gas and fuel oil for conventional exfoliations only). The carbon footprint is the main environmental impact this study focuses on. The impacts are presented with respect to the functional unit earlier defined.

6.5 Interpretation of Results and Discussions

6.5.1 Life Cycle Energy Analysis

The increase in the cost of fuel (oil and natural gas) and the subsequent negative environmental impact from the emission of greenhouse gases has been the major concerns of using the conventional thermal exfoliation system. Energy saving and minimum environmental effects are thought to be the main drivers for switching to microwave energy for the exfoliation of vermiculite minerals. Figure 6-6 shows the average energy consumed in exfoliating a tonne of vermiculite ore by microwave and conventional thermal exfoliators (Industrial and Torbed systems).

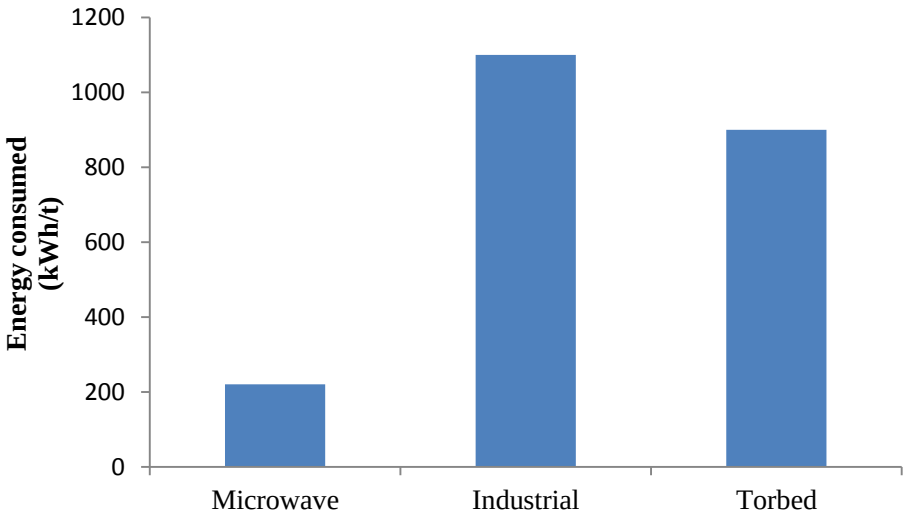

Figure 6-6: Energy analysis of the different exfoliation methods studied

Figure 6-6 shows that the microwave exfoliation system consumed the lowest amount of energy (220 kWh/t) compared to the two conventional systems, which consumed about 1100 kWh/t and 900 kWh/t respectively. The results indicate that microwave system gives 80 % and 75 % energy savings over the industrial and Torbed systems respectively. Since the conventional technique depends directly on the burning of natural gas or oil in a vertical furnace, its operation and operating cost will be influenced by the increase in the price of natural gas and oil frequently caused by the instability in the oil producing nations (Toft, 2011, Le and Chang, 2013). Although, microwave heating depends directly on the cost of electricity, (which may also fluctuate) the higher cost of electricity

will be offset by factors such as, reduction in the total energy consumption, lower heating temperature compared to conventional thermal system and resultant improved quality of product. In addition, there is no need for warming up and cooling down time, as microwave heating is operated with instantaneous on and off power.

6.5.2 Global Warming Potential (GWP)

The main objective of conducting this life cycle assessment was to identify, quantify and compare the environmental impacts of the microwave and conventional exfoliation techniques discussed in sections 6.3.2.1 and 6.3.2.2. The results of the carbon footprint, which is an indicator used to determine the overall global warming potential are discussed in this section. The carbon footprint analysis measures the greenhouse gas emissions of a product life cycle. This includes both direct and indirect emissions from the handling of raw materials, transportation, production, use and disposal (Weidema et al., 2008).

Global warming and reduction of carbon emission is the world top policy on environmental management today (IPCC, 2007), therefore the design and shifting to industrial process that is energy efficient and environmentally friendly is significant. The carbon footprint analysis carried out in this work is only limited to the process involved in the exfoliation of vermiculite. Therefore, microwave and conventional thermal exfoliation (Industrial and Torbed systems) of vermiculite were compared in terms of their overall carbon emissions, which is an indicator used for global warming potential of a system. The global warming potential (GWP) is defined as the amount of heat traps by greenhouse gas (GHG) comparable to the same amount of carbon dioxide (IPCC, 2007). The expression of the environmental impact of a process in terms of GWP allows the comparison of the greenhouse gases to each other and their impacts are normalised and presented numerically as carbon equivalents. For example, carbon dioxide, nitrous oxide and methane have a GWP of 1, 298 and 25 respectively, as considered for a 100-year period (Guinee et al., 2001, IPCC, 2007).

It is sufficient to interpret the results of the carbon footprint of these systems as CO_2 equivalents per product since the exfoliated vermiculite produced from the three exfoliation systems (microwave, industrial and Torbed) have the same monetary value (Weidema et al., 2008). The formulation used by the CCaLC in calculating the carbon footprint from the three energy sources used for vermiculite exfoliation and the raw materials (vermiculite ore) is given as Equation 6-2. Where CF represents the estimated carbon footprint, cf_i is the carbon footprint per kWh of energy used or per kg of material while m_i is the total energy consumed (kWh) or total mass of processed materials.

$$CF = \sum_i cf_i \times m_i \qquad \text{Equation 6-2}$$

The cf_i values for different forms of energy and materials are available in the CCaLC database. The values for electricity, oil and natural used for the carbon footprint calculations in this work are given in Table 6-2 and the quantity of energy used for the exfoliation of 1 tonne of vermiculite was used as the input in CCaLC for the carbon footprint modelling.

Table 6-2: Carbon footprint per kWh of energy used

Energy	**Cf_i (kg CO2 eq./kWh)**	**Source**
Electricity mix UK	0.58	Ecoinvent
Natural gas for furnace	0.26	Ecoinvent
Fuel oil	0.33	Ecoinvent

Figure 6-7 shows the results of carbon footprint (global warming potential) analysis of the microwave exfoliation system and conventional thermal exfoliation (Industrial and Torbed systems) as modelled by CCaLC. In the results shown in Figure 6-7, the microwave system was directly powered by electricity while the industrial and Torbed systems were fuelled by natural gas.

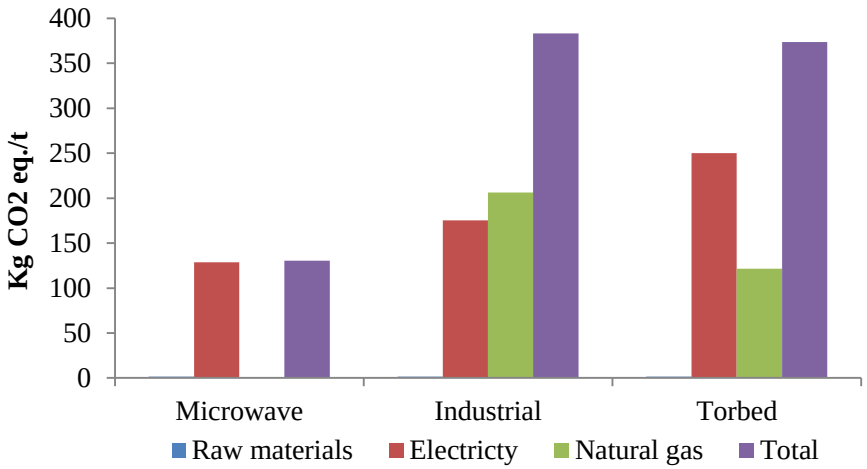

Figure 6-7: Life cycle CO_2 emission for microwave and conventional thermal exfoliation using natural gas for furnace heating

The calculated carbon footprints correlate directly to the quantity of energy used for both microwave and conventional thermal exfoliation processes. For the microwave processing, about 1.68 kg CO_2 eq./tonne was produced from the raw material and this is insignificant when compared to the energy contribution which is about 98.7% (128.61 kg CO_2 eq./tonne) of the total carbon footprint generated by this process. Similar to the microwave exfoliation, both conventional techniques produced about 1.68 kg CO_2 eq./tonne during the handling of raw vermiculite. The energy contribution of carbon footprint during the exfoliation stage in the industrial system is about 381.61kg CO_2 eq./tonne, which is over 99 % of the total carbon footprint generated.

The Torbed exfoliator also produced a total carbon footprint of 373.56 kg CO_2 eq./tonne and similar to the industrial system, 99 % of the total carbon footprint is generated from the burning of natural gas and the use of electricity. The results showed that the main hot spot for global warming potential during vermiculite exfoliation is from the usage of electricity for microwave exfoliation and the combination of electricity and natural gas in the conventional exfoliation process. The raw material (Vermiculite) is not a major contributor to the carbon footprint in both microwave and conventional thermal exfoliation processes, when the system boundary is limited to the vermiculite exfoliation process.

Figure 6-8 shows the results of the carbon footprint when the industrial and Torbed exfoliator were fuelled by oil.

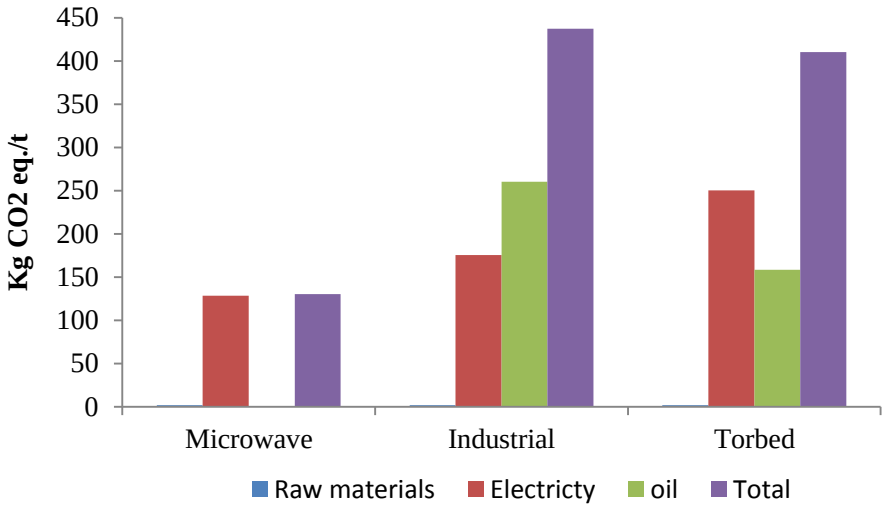

Figure 6-8: Life cycle CO_2 emission for microwave and conventional thermal exfoliation using oil for furnace heating

In this case, about 437.23 kg CO_2 eq./tonne was produced by the industrial system while the Torbed exfoliator generated about 410.38 kg CO_2 eq./tonne. The life cycle energy characterisation of the industrial and Torbed systems is made up of contributions from electricity used for operating the peripheral equipment and the gas or oil used for heating the furnace. The selection of either natural gas or oil for heating the furnace for the industrial and Torbed exfoliator may influence the overall carbon emissions. Figure 6-9 and Figure 6-10 show the individual contribution of natural gas and oil to the GHG emissions for the two systems.

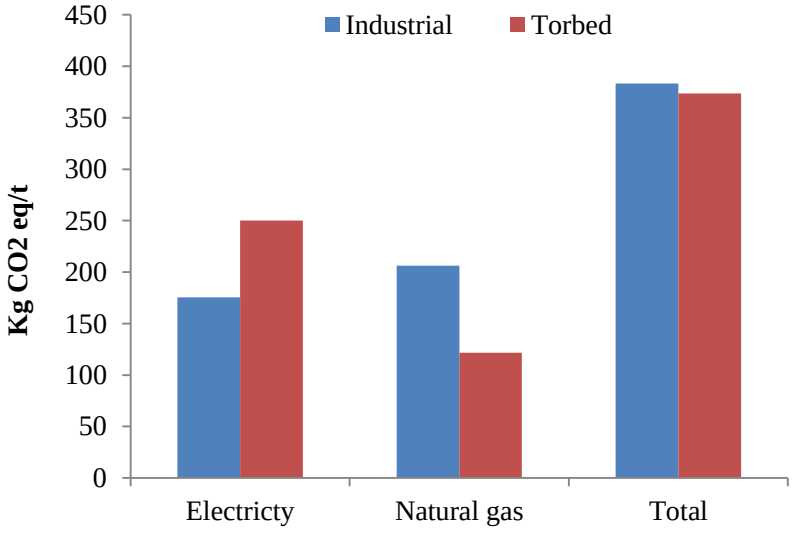

Figure 6-9: Life cycle CO_2 emission contributed by electricity and gas in conventional thermal exfoliation

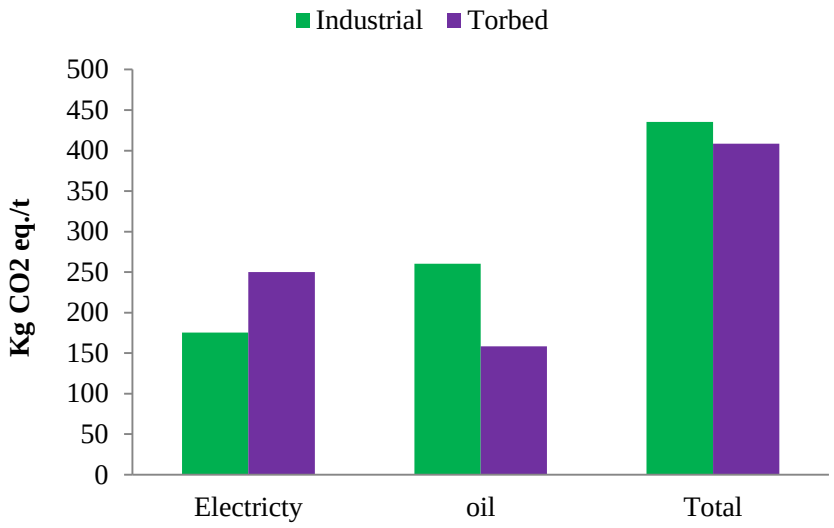

Figure 6-10: Life cycle CO_2 emission contributed by electricity and oil in conventional thermal exfoliation

When natural gas is used to fuel the industrial system, a total of 383.29 kg CO_2 eq./tonne of GHG is generated with about 54% and 46% of the total GHG generated from natural gas and electricity respectively (Figure 6-9). A total of 435.55 kg CO_2 eq./tonne of GHG is generated when the industrial system is fuelled by oil and the contribution of oil to the total emission is about 60%. The Torbed exfoliator generated about 373.55 kg CO_2 eq./tonne (33% from natural gas and 67% from electricity) and 408.75 kg CO_2 eq./tonne (38% from oil and 62% from electricity) when the system is fuelled by natural gas and oil respectively. The higher proportion of carbon emissions being associated with electricity usage in the Torbed system is the high energy required for cooling the exfoliated vermiculite from a process temperature of 1200 °C to 35 °C. This is not required in the microwave system as the product is collected at a lower temperature. There is a little difference of only about 2.5 % and 6.1 % respectively between the total estimated carbon footprint for the industrial and Torbed exfoliator when natural gas and oil are used to heat the furnace. The usage of oil rather than natural gas for heating the furnace increases the overall carbon emissions for both the industrial and Torbed exfoliator by about 14% and 9% respectively. This indicates that oil driven furnace has higher environmental impacts than the gas driven vermiculite furnace.

Assuming that both the microwave and conventional thermal (Industrial and Torbed) exfoliators are to be continuously operated for 8 hours per day to

exfoliate vermiculite at the rate of 1 tonne per hour, the estimated annual environmental impact when the systems are operated for average of 250 days per year is shown in Figure 6-11

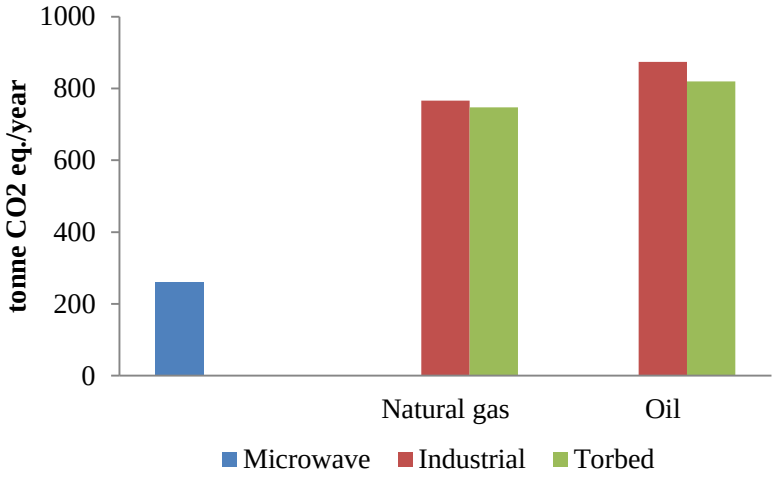

Figure 6-11: Annual carbon footprint impact from vermiculite exfoliation

The annual estimation of carbon footprint for microwave exfoliation is about 260 tonne CO2 eq/year. The industrial and Torbed systems recorded about 766 tonne CO2 eq./year and 747 tonne CO2 eq./year, respectively, when natural gas is used for the processing, while 874 tonne CO2 eq./year and 820 tonne CO2 eq./year are recorded when the furnace is heated by oil. It is evident from the life cycle analysis carried out in this work (Figure 6-7 to Figure 6-11) that the use microwave energy for vermiculite exfoliation has the lowest value of carbon emission per tonne of vermiculite processed. It gives a carbon footprint reduction of about 66 % and 65 % over the industrial and Torbed exfoliator respectively, when natural gas is used for the furnace heating, and about 70 % and 68 % carbon footprint savings respectively when oil is employed for the furnace heating.

This indicates that the conventional thermal exfoliation process has a higher environmental impact when compared with microwave exfoliation. Therefore, shifting to microwave energy driven system for vermiculite exfoliation rather than employing the conventional system that depends on the burning of natural gas or oil will have a positive impact on the climate change.

6.5.3 Comparative Cost Analysis of Microwave and Conventional Exfoliation

Aside from the carbon saving, energy reduction is another factor considered in transferring to a new system for industrial processing, as this will definitely have a positive effect on the profit margin. The annual energy costs of running the microwave, industrial and Torbed exfoliators were calculated, assuming the systems were operated for an average of 8 hours per day over a period of 250 days per year. The present UK cost of electricity, gas and fuel oil as at December 2013 were used for the calculation. The price of electricity, gas and fuel were given as £0.0883 per kWh, £0.0288 per kWh and £0.5795 per litre.

About 68 litres and 37 litres of fuel oil are required to heat the industrial and the Torbed furnaces respectively. These quantities are needed to achieve energy of 800 kWh and 428 kWh required for exfoliating 1 tonne of vermiculite by the industrial and the Torbed furnaces respectively. Assume that the total energy was used for heating the interlayer water. Therefore, it means that about 136,000 and 74,000 litres of fuel oil will be needed annually by the two systems respectively, for vermiculite exfoliation. The annual energy requirements and cost of energy were calculated using the values of energy consumed by the systems in processing 1tonne of the material (Table 6-3).

Table 6-3: Cost analysis of vermiculite exfoliation by the microwave and conventional thermal exfoliation systems

System	Electricity (MWh/yr)	Gas (MWh/yr)	Oil (MWh/yr)	Annual Total cost (£)
Microwave	440			38,852
Industrial [1]	600	1600		99,172
Industrial [2]	600		1600	131,792
Torbed [1]	944	856		102,837
Torbed [2]	944		856	118,467

1: Furnace heated by gas, 2: Furnace heated by Oil

The annual costs of energy needed to operate the three systems are shown in Table 6-3. The results showed that using microwave system for vermiculite exfoliation saves annual energy cost of between £60,000-£93,000 over the

industrial system and between £64,000-£79,000 over the Torbed system. This indicates that shifting to the microwave system for vermiculite exfoliation has potential of saving a huge cost of energy over the conventional thermal exfoliation systems. Other advantages of microwave system over the conventional systems are processing efficiency, reduced floor space and minimised labour cost.

6.6 Conclusions

Comparative life cycle analysis of vermiculite exfoliation using microwave heating and conventional heating systems was undertaken in this chapter. The life cycle analysis was implemented in accordance with the available LCA frameworks by the International Organisation for Standardisation (The ISO 14040: principles and framework and ISO 14044: Requirements and guidelines) and British standards institution (PAS2050). The LCA calculation software tool, CCaLC, designed by the carbon calculation team at the University of Manchester was used for the life cycle assessment. The quantities of energy required by the microwave, industrial and Torbed systems for achieving The Vermiculite Association (TVA) density standard were used as the inputs for calculating global warming potential. The comparative cost analysis of the three systems was also carried out.

The energy consumed by the three systems for exfoliating 1 tonne of vermiculite were 220 kWh/t, 1100 kWh/t and 900 kWh/t for microwave, Industrial and Torbed exfoliators respectively. The modelled carbon footprint for the microwave, industrial, and Torbed systems are 130.29 kg CO_2 eq./t, 383.29 kg CO2 eq./t and 373.56 kg CO2 eq./t respectively. The microwave system gives an energy savings of about 80% and 75% over industrial and Torbed Exfoliators respectively. It also gives a carbon footprint saving potential of about 66% and 65% over the industrial and Torbed exfoliator respectively. The annual energy cost analysis carried out also shows that the microwave system saves an energy cost between £60,000-£93,000 over the industrial system and between £64,000-£79,000 over the Torbed system. Therefore the adoption of microwave technology for vermiculite exfoliation will be advantageous in terms of cost of operating energy and overall environmental impact.

CHAPTER SEVEN
CONCLUSIONS AND FURTHER WORK

7.1 Conclusions

Vermiculite is a 2.1 phyllosilicate clay mineral that has been used for many decades in the expanded form for agriculture and horticulture, construction, insulation and for other industrial applications such as for drilling mud, paints and brake pads. Vermiculite expansion occurs when the trapped interlayer water molecules within the structure are rapidly heated at high temperatures of between 870-1100 °C leading to the mechanical separation of the silicate layers. A critical literature review in the field of vermiculite processing has shown that chemical and conventional thermal exfoliation techniques are the two prominent exfoliation methodologies. The chemical exfoliation method uses chemicals such as H_2O_2 and weak electrolytes. This exfoliation method is limited to laboratory scale and there are no reports of such techniques being used for exfoliation at a commercial level. Despite being the state of the art the industrial thermal exfoliation of vermiculite by oil and gas furnaces is unsustainable for vermiculite processing due to high environmental impact, large energy requirement (greater than 1 GJ/t), poor process control, and emissions of dust and particulate matter (PM<10μm).

Due to the sustainability limitations of both chemical and conventional methods of vermiculite exfoliation, some researchers have employed the selective heating advantage of microwave energy for vermiculite exfoliation. The little body of published work which considers the application of microwave energy for vermiculite exfoliation has typically focused on the use of domestic microwave ovens (2.45 GHz, power below 1200 W), which produce heterogeneous distributions of electric field and uneven heating of the feedstock due to the creation of multiple hotspots and low power density. Few attempts have ever been made to scale up microwave processing of vermiculite and there are no previous reports of a continuous high electric field based vermiculite exfoliation system at microwave energy inputs of greater than 15 kW. This may be due to the little attention given to understanding the interaction of microwave energy with such minerals.

The work reported in this thesis demonstrated the application of a continuous microwave system designed at 2450 MHz for a pilot scale system operating at maximum microwave power of 30 kW and a scaled up system designed to operate at 896 MHz and a maximum power of 100 kW.

The fundamentals of microwave interaction with vermiculite were investigated by conducting dielectric and mineralogical characterisations of vermiculite minerals from different geological locations.

7.1.1 Mineralogical Characterisation of Vermiculite

In order to understand the relationship between vermiculite chemical composition and microwave induced exfoliation, X-ray diffraction (XRD) analysis was carried out to identify and characterised the different vermiculite samples. This test gave information about the different mineral phases present in the different vermiculite samples. Mineral liberation analysis was also carried out on the vermiculite samples from different geological areas in order to quantify the different mineral phases present in the analysed vermiculite samples. The results of a quantitative analysis of mineral composition of vermiculites from Australia, Brazil, China and South Africa using the mineral liberation analysis (MLA) and X-ray diffraction analysis (XRD) showed that the Chinese, Australian and South African sample are predominantly hydrobiotite but Chinese has the highest amount of hydrobiotite. The Brazilian sample was the most pure form of vermiculite of all the tested samples. Thermogravimetric analysis (TGA) identified three different types of water network in the vermiculite structures and these were grouped as free water, bound water and high temperature hydroxyl water. The Brazilian sample had the highest interlayer water (free and bound water) content followed by the South African sample. It was concluded that the total interlayer water content in vermiculite is directly related to the chemical composition and subsequently to the ability to be exfoliated in an applied microwave field.

7.1.2 Dielectric Characterisations of Vermiculite

Cavity perturbation and waveguide techniques were used for measuring the dielectric properties of all of the vermiculite samples. The results demonstrated that both dielectric constant and loss factor of such materials are a function of factors, which include; bulk density, temperature, mineralogy and frequency. All of the characterised vermiculite samples showed a decrease in dielectric constant with frequency due to the lagging of the interlayer molecules (interlayer water and cations) behind the applied electric field. It was also observed that the measured dielectric properties (both ε' and ε'') increase with an increase in bulk density. Of all the samples measured, the Brazilian sample had the highest dielectric properties. The highest dielectric properties were related to the highest interlayer water and pure vermiculite content.

A method based on the linear functions of the dielectric constant and loss factor versus bulk density of air-particle mixtures was used in this thesis to estimate the complex permittivity (ε' and ε'') of the solid vermiculite from the measurements of ε' and ε'' of the pulverised form over a range of bulk densities. This was performed to determine the actual values of dielectric properties of vermiculite flakes and the results will allow accurate simulation and modelling of the material in the cavity. For all of the vermiculite samples tested with mixing rules and graphical extrapolations, the linear relationship of $\sqrt{\varepsilon'}$ against bulk density, CRIM and modified Bruggeman-Hanai mixing rules give the closest estimation of dielectric constant to the Goldschmidt mixing rule. For the loss factor estimation, there was an agreement between the linear relationships of $(\varepsilon'')^{1/2}$, $(\varepsilon''+e)^{1/2}$ with bulk density and the estimated loss factor are consistent with that obtained from CRIM, Goldschmidt and modified Bruggeman-Hanai mixing rules. Dielectric properties of solid form of vermiculite from these geological locations need to be measured for comparison.

7.1.3 Microwave Exfoliation Tests of Vermiculite Minerals

Experimental investigations into the microwave exfoliation of vermiculite has shown that a continuous microwave system can be used for the high throughput

exfoliation of vermiculite at lower energy inputs (< 220 kWh/t) than those used in conventional thermal exfoliation plants that require energy inputs typically of over 1 MWh/t. The microwave system used for the exfoliation tests in this project has two apertures that allow easy passage of a microwave transparent conveyor belt with the feedstock. Functioning chokes systems incorporated at both ends eliminate the emission of electromagnetic waves to the immediate surroundings. A pilot scale system operating at 2.45 GHz (maximum 30 kW generator) and a scaled up system operating at 896 MHz (maximum 100 kW) were used for the exfoliation tests. The exfoliation results showed that the degree of expansion is a function of factors such as microwave power density, energy input, material throughput and the mineralogy of the vermiculite samples. A lower product bulk density was produced as the material throughput was decreased due to the increase of the energy input. A higher degree of vermiculite exfoliation was also obtained as the power density is increased in the heated phase by increasing the microwave power. In addition, the highest degree of exfoliation was recorded by the Brazilian sample, which also had the highest free water content. The exfoliation results obtained from the scaled up system demonstrated that the system is capable of operating at a volumetric throughput over 4 m^3/h for superfine grade obtained from the South Africa. It also has a potential of producing higher volumetric throughputs for the larger grade than the conventional systems because higher degrees of exfoliation were obtained from the coarser feedstock than the finer grades.

7.1.4 Comparative Analysis of Microwave and Conventional Exfoliation Methods

The life cycle analysis (LCA) calculation software tool, CCaLC, developed by the carbon calculation team at The University of Manchester was used for life cycle assessment in this project. The quantities of energy required by the microwave, an industrial rotary furnace and a Torbed system (considered current state of the art industrially in terms of energy efficiency) for achieving The Vermiculite Association (TVA) density standard are used as the inputs for calculating global warming potential. The energy consumed by the three systems for exfoliating 1 tonne of vermiculite were 220 kWh/t, 1100 kWh/t and 900

kWh/t for microwave, Industrial and Torbed exfoliators respectively. The results showed that the microwave system can potentially give an energy saving in the order of 80% and 75% over conventional furnace technology and Torbed exfoliators respectively and a carbon footprint saving potential in the order of 65%. It was concluded that transitioning to a microwave based system for the exfoliation of vermiculite will saves an annual energy cost between £60,000-£93,000 over the industrial system and between £64,000-£79,000 over the Torbed system.

7.2 Future Work

This research investigated the fundamental interaction of electromagnetic waves with vermiculite from different geological locations. The mechanisms of microwave exfoliation of vermiculite were studied and the factors influencing microwave exfoliation investigated. The pilot and larger scaled up systems were commissioned and used for testing the exfoliation behaviour of the vermiculite materials from Australia, Brazil, China and South Africa. The success recorded in the application of microwave energy for vermiculite exfoliation can be applied for the expansion of other expandable minerals such as perlite and expanded clay. The recommended further work to be carried out are explained as below.

Similar to the experimental programme carried out in this work, there is a need to understand the fundamental of interaction of microwave energy with perlite and expanded clay. This will involve using mineralogical characterisation techniques such as X-ray diffraction analyses to identify the different mineral phases present in these minerals, mineral liberation analysis (MLA) to quantify the identified the mineral phases and to characterise the texture of the identified minerals. Since the presence of water in these minerals is the major factor that dictates how they interact with microwave energy, thermogravimetric analysis would be used to characterise and quantify the different water networks in these minerals. Extensive measurements of dielectric properties of these minerals would be carried out at ISM frequencies. The results of these measurements will give information about the interaction of these materials with microwave energy

and the obtained data can be used to design special heating cavity and choke systems for their processing.

The potential of using the designed microwave system for the expansion of other expandable minerals such as perlite and expanded clay will be carried out and the factors affecting their degree of exfoliation will be studied in order to understand the optimum conditions required for their processing. In addition to these, it is recommended as a further worker to investigate and consider how microwave technology could be used to process the forms of vermiculite, which are less responsive in the system developed for this project.

References

A.C METAXAS AND R.J. MEREDITH 1983. Industrial Microwave Heating, London, The Institution of Engineering and Technology.

AL-HARAHSHEH, M., KINGMAN, S. & BRADSHAW, S. 2006a. Scale up possibilities for microwave leaching of chalcopyrite in ferric sulphate. International Journal of Mineral Processing, 80**,** 198-204.

AL-HARAHSHEH, M. & KINGMAN, S. W. 2004. Microwave assisted leaching - a review. Hydrometallurgy, 73**,** 189-203.

AMANKWAH, R. K. & OFORI-SARPONG, G. 2011. Microwave heating of gold ores for enhanced grindability and cyanide amenability. Minerals Engineering, 24**,** 541-544.

AMANKWAH, R. K., PICKLES, C. A. & YEN, W. T. 2005. Gold recovery by microwave augmented ashing of waste activated carbon. Minerals Engineering, 18**,** 517-526.

ANDRES, U. 1996. Dielectric separation of minerals. Journal of Electrostatics, 37**,** 227-248.

ANDRONOVA, V. I. 2007. A Study of the Crystalline Structure of Vermiculite from the Tebinbulak Deposit. Refractories and Industrial Ceramics, 48**,** 91-95.

ANJOS, D. I. F., FONTGALLAND, G. & R.S.C. FREIRE 2011. Vermiculite dielectric constant measurement using a volumetric water content probe. IEEE**,** 1-5.

ASAMI, K. 2002. Characterisation of heterogeneous systems by dielectric spectroscopy. Progress in Polymer Science, 27**,** 1617-1659.

ATOMIC ENERGY OF CANADA LIMITED 1990. Microwave and minerals: Industrial mineral background paper. Ontario: Energy, mines and resource, Canada.

AYRES, R. U., AYRES, L. W. & RÅDE, I. 2002. The Life Cycle of Copper, its Co-Products and By-Products. France: Centre for the Management of Environmental Resources INSEAD.

BAKER-JARVIS, J., JANEZIC, M. D., JOHN H. GROSVENOR, J. & GEYER, R. G. 1993. Transmission/Reflection and short-circuit line methods for measuring permittivity and permeability. In: NATIONAL INSTITUTE OF STANDARDS AND TECHNOLOGY (ed.). Colorado: U.S. Government printing office.

BALLANTYNE, G. R. & HOLTHAM, P. N. 2010. Application of dielectrophoresis for the separation of minerals. Minerals Engineering, 23**,** 350-358.

BASSET, W. A. 1963. The Geology of Vermiculite Occurences. Clays and Clays Minerals, 10**,** 61-93.

BASSETT , W. A. 1959. Origin of the vermiculite deposit at Libby, Montana. American Minerals, 44**,** 282-299.

BEHARI, J. 2005. Microwave dielectric behavior of wet soil, New Delhi, Anamaya Publishers.

BELRHITI, M. D., BRI, S., NAKHELI, A., HADDAD, M. & MAMOUNI, A. 2012. Dielectric constant determination of liquid using rectangular waveguide structure combined with EM simulation Journal of material and environmental science, 3**,** 575-584.

BERCK, P., LEVY, A. & CHOWDHURY, K. 2012. An analysis of the world's environment and population dynamics with varying carrying capacity, concerns and skepticism. Ecological Economics, 73**,** 103-112.

BERGAMELLI, F., IANNELLI, M., A, J., MARAFIE & MOSELEY, J. D. 2010. A commercial continuous flow microwave reactor evaluated for scale-up. Organic Process Research & Development, 14**,** 926-930.

BERGAYA, F., THENG, B. K. G. & LAGALY, G. (1st eds.) 2006. Handbook of clay science, Elsevier, Oxford.

BERGMAN, R., SWENSON, J., BORJESSON, L. & JACOBSSON, P. 2000. Dielectric study of superccoled 2D water in a vermiculite clay. Journal of Chemical Physics, 113**,** 1-7.

BERTRAND PERIO, M.-J. D., AND JACK HAMELIN 1998. Ecofriendly Fast Batch Synthesis of Dioxolanes, Dithiolanes, and Oxathiolanes without Solvent under Microwave Irradiation. Organic Process Research & Development, 2**,** 428-430.

BEYER, J. & REICHENBACH, H. G. V. 2002. An extended revision of the interlayer structures of one- and two- layer hydrates of Na- vermiculite. Clay Minerals, 37**,** 157-168.

BÖTTCHER, C. J. F. 1945. The dielectric constant of crystalline powders. Recueil des Travaux Chimiques des Pays-Bas, 64**,** 47-51.

BOWMAN, M. D., HOLCOMB, J. L., KOMOS, C. M., LEADBEATER, N. E. & WILLIAMS, V. A. 2008. Approaches for scale-up of microwave-promoted reactions. Organic Process Research & Development, 12**,** 41-57.

BOWS, J. R. 2000. A classification system for microwave heating of food. International Journal of Food Science & Technology, 35**,** 417-430.

BOYARSKII, D. A., TIKHONOV, V. V. & KOMAROVA, N. Y. 2002. Model of Dielectric Constant of Bound Water in Soil for Applications of Microwave Remote Sensing. Progress in Electromagnetics Research, 35**,** 251-269.

BOYER, R. 2002. Interactive concepts in biochemistry [Online]. Available: http://www.wiley.com/college/boyer/0470003790/reviews/pH/ph_water.htm [Accessed 12/11/2013].

BRADSHAW, S., LOUW, W., MERWE, C. V. D., READER, H., KINGMAN, S., CELUCH, M. & KIJEWSKA, W. 2007. Techno-economic considerations in the commercial microwave processing of mineral ores. Journal of Microwave Power and Electromagnetic Energy, 40**,** 228-240.

BRADSHAW, S. M., WYK, E. J. V. & DE, J. B. S. 1998. Microwave heating principles and the application to the regeneration of granular activated carbon. The Journal of the South African Institute of Mining and Metarlurgy**,** 201-212.

BRANDLEY, W. F. & SERRRATOSA, J. M. 1960. A Discussion of the Water Content of Vermiculite. Proceeding of the 7th National Clay Conference. New York: Pergamon Press.

BRAZIL MINERIOS 2011. Presentation: TVA meeting-london. TVA.

BRICHAK, J. R., GARDNER, C. G., HIPP, J. E. & VICTOR, J. M. 1974. High dielectric constantmicrowave probes for sensing soil moisture. Proceeding IEEE, 62**,** 93-98.

BRINDLEY, G. W. 1951. Structural Mineralogy of Clays. Clays and Clays Technology**,** 33-43.

BROWN, G. 1961. The X-Ray Identification and Crystal Structures of Clay Minerals, London, Jarold and Sons Ltd.

BROWN, T. J., SHAW, R. A., BIDE, T., RAYCRAFT, E. R. & WALTERS, A. S. 2013. World mineral production 2007-2011. In: National Environment Research Council (1st ed.) First ed. keyworth, Nottingham: British Geological Survey.

BS EN 55103 2012. Electromagnetic compatibility-product family standard for audio, video, audio-visual and entertainmen, lightning control and apparatus for professional use. UK.

BS EN 60519-6 2011. Specifications for safety in industrial microwave heating equipment. London: British Standard Institution.

BULELWA, N., SAEED, F. & DEE, B. 2013. The effect of phyllosilicate minerals on mineral processing industry. International Journal of Mineral Processing 125**,** 149-156.

C. OLIVER KAPPE, A. S., DORIS DALLINGER 2012. Microwaves in organic and medicinal chemistry, Germany, Wiley-VCH.

CABALLERO, E. D., BELENGUER, A., ESTEBAN, H. & BORIA, V. E. 2013. Thru-reflect-line calibration for substrate integrated waveguide devices with tapered microstrip transitions. Electronics Letters, 49**,** 1-2.
CAMELIA, G., SAMI, G., EDWARD, H. G., EDWARD, H. G., BEN, S. J. H. & MINGOS, M. P. D. 1998. Dielectric parameters relevant to microwave dielectric heating. Chemical Society Reviews, 27**,** 213-224.
CAMPOS, A., MORENO, S. & MOLINA, R. 2009. Characteristics of Vermiculite by XRD and Spectroscopic Techniques. Earth Science Resources, 13**,** 17.
CAPLAIN, P., FUZELLIER, H., HUDRY, D., JULIAA, J.-F., LEFRANCOIS, M. & REINERT, L. 2009. Method for making a highly exfoliated vermiculite without using any organic binder or additive for forming the same. USA patent application PCT/EP2008/056329.
CARRERA, G. D. & MACK, A. 2010. Sustainability assessment of energy technologies via social indicators: Results of a survey among European energy experts. Energy Policy, 38**,** 1030-1039.
CARSLAW, H. S. & JAEGER, J. C. 1959. Conduction of heats in solids, Oxford, Oxford University Press.
CARVALHO, N. B. & SCHREURS, D. 2013. Microwave and wireless measurement techniques, Cambridge, Cambridge University Press.
CATALÁ-CIVERA, J. M., SOTO, P., BORIA, V. E., BALBASTRE, J. & REYES, E. D. L. 2006. Design Parameters of Multiple Reactive Chokes for open Ports in Microwave Heating Systems. In: WILLERT-PORADA, M. (ed.) Advances in Microwave and Radio Frequency Processing. Springer Berlin Heidelberg.
CHAN, T. V. C. T. & READER, H. C. 2000. Understanding Microwave Heating Cavities, London, Artech House, INC.
CHAO, S.-H. 1985. Measurements of Microwave Conductivity and Dielectric Constant by the Cavity Perturbation Method and Their Errors. IEEE, Microwave theory and techniques, 3**,** 519-526.
CHEMICAL MINE WORLD. 2004. Uses of Vermiculite [Online]. Tehran, Iran. Available: http://biz-chemical.com/contact%20us.htm [Accessed 20/06/2011].
CHEN, L. F., ONG, C. K. & NEO, C. P. 2004. Microwave electronics: Measurement and materials characterisation, Chichester, John Wilwy & Sons.
CHEN, T. T., DUTRIZAC, J. E., HAQUE, K. E., WYSLOUZIL, W. & KASHYAP, S. 1984b. The relative transparency of minerals to microwave radiation. Canadian Metallurgical Quarterly, 23**,** 349-351.
CHEN, Y. & OR, D. 2006. Effects of Maxwell-Wagner polarization on soil complex dielectric permittivity under variable temperature and electrical conductivity. Water resources research, 42**,** 1-14.
CHURCH, R. H., WEBB, W. E. & SALSMAN, J. B. 1988. Dielectric properties of low-loss minerals. Alabama: Bureau of Mines.
CIAMBRONE, D. F. 1997. Environmental life cycle analysis, Florida, CRC Press LLC.
CISPR 1990. Radio disturbance and immunity measuring apparatus and methods: Part 1. In: INTERFERENCE, I. S. C. O. R. (ed.) 16.
CLARK, D. E., FOLZ, D. C., FOLGAR, C. E. & MAHMOUD, M. M. 2005. Microwave Solution for Ceramic Engineers, Ohio, The American Society.
CLARK, D. E., FOLZ, D. C. & WEST, J. K. 2000. Processing Minerals with Microwave Energy. Materials Science and Engineering, A**,** 153-158.
CLARK, D. E. & SUTTON, W. H. 1996. Microwave processing of materials. Annual Review Material Science, 26**,** 299-331.
CLARKE, R. N., GREGORY, A. P., CANNELL, D., PATRICK, M., WYLIE, S., YOUNG, I. & HILL, G. 2003. A guide to the characterisation of dielectric materials at RF and microwave frequencies. GB: Institute of Measurement and Control / National Physical Laboratory.
CLAYTRON, P. R. 2006. Introduction to Electromagnetic Compactibility, New Jersey, John Wiley & Sons, Inc.

CLEGG, W. 1998. Crystal structure determination, Oxford, Oxford University Press.
COBHAM 2012. Concerto 7.5: High Frequency Electromagnetic Design Software. 7.5R2 ed. Wimborne, UK.
COLLIN, R. E. 2001. Foundation for microwave engineering, New York, IEEE Press.
CONCERTO 2006. Quickwave simulator reference guide.
CORDIER, D. J. 2010. Mineral Commodity Summaries 2010. In: INTERIOR, U. S. D. O. T. & SURVEY, U. S. G. (eds.). Washington: United States Government Printing Office.
CORONEL, P., TRUONG, V.-D., SIMUNOVIC, J., SANDEEP, K. P. & CARTWRIGHT, G. D. 2005. Aseptic Processing of Sweet Potato Purees Using a Continuous Flow Microwave System. Journal of Food Science, 70**,** E531-E536.
COSENZA, P. & TABBAGH, A. 2004. Electromagnetic determination of clay water content: role of the microporosity. Applied Clay Science, 26**,** 21-36.
CROWSON, P. 2001. Statistics and Analyses of the World's Minerals Industry, Kent, UK, Mining Journal Books Ltd.
CURRIE, K. L., KNUTSON, J. & TEMBY, P. A. 1992. The Mud Tank carbonatite complex, central Australia —an example of metasomatism at mid-crustal levels. Contributions to Mineralogy and Petrology, 109**,** 326-339.
DAS, S., MUKHOPADHYAY, A. K., DATTA, S. & BASU, D. 2008. Prospects of microwave processing: An overview. Bull. Mater. Sci, 32**,** 1-13.
DATTA, A. K. & ANANTHESWARAN, R. C. (eds.) 2001. Handbook of microwave technology for food application, New York: Marcel Dekker.
DATTA, A. K., SUNMU, G. & RAGHAVAN, G. S. V. 2005. Dielectric Properties of Foods. In: RAO, M. A., RIZVI, S. S. H. & DATTA, A. K. (eds.) Engineering Properties of Foods, Third Edition. 3rd ed. Florida: CRC Press.
DE LA HOZ, A., ALCÁZAR, J., CARRILLO, J., HERRERO, M. A., MUÑOZ, J. D. M., PRIETO, P., DE CÓZAR, A. & DIAZ-ORTIZ, A. 2011. Reproducibility and Scalability of Microwave-Assisted Reactions.
DEER, W. A., HOWIE, R. A. & ZUSSMAN, J. 1964. Rock-forming minerals, London, Longmans.
DEER, W. A., HOWIE, R. A. & ZUSSMAN, J. 1966. An introduction to the rock-forming minerals, London, Longmans, Green and Co.
DEMIRSKYI, D., AGRAWAL, D. & RAGULYA, A. 2010. Densification kinetics of powdered copper under single-mode and multimode microwave sintering. Materials Letters, 64**,** 1433-1436.
DIBBEN, D. C. 1995. Numerical and experimental modelling of microwave applicators. PhD, University of Cambridge.
DIBBEN, D. C. & METAXAS, R. 1996. Time domain finite element analysis of multimode microwave applicators. IEEE Transaction on Magnetics, 32**,** 942-945.
DINNEBIER, R. E. & BILLINGE, S. J. L. (eds.) 2008. Powder diffraction: Theory and practice, Cambridge: The Royal Society of Chemistry.
DJEKIC, I., MIOCINOVIC, J., TOMASEVIC, I., SMIGIC, N. & TOMIC, N. Environmental life-cycle assessment of various dairy products. Journal of Cleaner Production.
DODDS, C., DIMITRAKIS, G. & KINGMAN, S. 2010. Microwave Processing of Feedstock, Such as Exfoliating Vermiculite and other Minerlas, and Treating Contaminated Materials. PCT/GB2009/051744.
DONOVAN, S., KLEIN, O., HOLCZER, M. & GRUNER, G. 1993. Microwave cavity perturbation technique: Part II:Experimental scheme. International Journal of infrared and millimeter waves, 14**,** 3459-2487.
DUBE, D. C. & PARSHAD, R. 1969. Study of Bottcher formula for dielectric correlation between powder and bulk Journal of Physics and applied Physics, 3**,** 677-684.

DURUCAN, S., KORRE, A. & MUNOZ-MELENDEZ, G. 2006. Mining life cycle modelling: a cradle-to-gate approach to environmental management in the minerals industry. Journal of Cleaner Production, 14**,** 1057-1070.

EBARA, H., INOUE, T. & HASHIMOTO, O. 2006. Measurement method of complex permittivity and permeability for a powdered material using a waveguide in microwave band. Science and Technology of Advanced Materials, 7**,** 77-83.

ELLENBERGER, J., VANDU, C. O. & KRISHNA, R. 2006. Vibration-induced granular segregation in a pseudo-2D column: The (reverse) Brazil nut effect. Powder Technology, 164**,** 168-173.

ELLIOT, J. 2011. Global vermiculite price soar on tight supply. Available: http://www.indmin.com/Article/2835972/Global-vermiculite-prices-soar-on-tight-supply.html [Accessed 10/04/2013].

ENGEN, G. F. & HOER, C. A. 1979. "Thru-Reflect-Line": An improved technique for calibrating the dual six-port automatic network analyser. IEEE Transactions on Microwave Theory and Techniques, 27**,** 987-993.

ERCIN, A. E. & HOEKSTRA, A. Y. 2012. Carbon and Water Footprints Concepts, Methodologies and Policy Responses. In: PROGRAMME, U. N. W. W. A. (ed.). France: United Nations Educational, Scientific and Cultural Organization.

ERNST, W. S., HAVENS, I. F. & WILSON, H. H. 1958. Effects of the Exchangeable Ion on the Dehydration Properties of Vermiculite. Journal of the American Ceramic Society, 41**,** 238-241

EROL UCGUL & GIRGIN, I. 2002. Chemical Exfoliation Characteristics of Karakoc Phlogopite in Hydrogen Peroxide Solution. Turkish Journal of Chemistry, 26**,** 431-439.

ESSINGTON, M. E. 2004. Soil and water chemistry: An integrative approach, Washington, D.C., CRC Press.

EVANS, A., STREZOV, V. & EVANS, T. J. 2009. Assessment of sustainability indicators for renewable energy technologies. Renewable and Sustainable Energy Reviews, 13**,** 1082-1088.

FANDRICH, R., GU, Y., BURROWS, D. & MOELLER, K. 2007. Modern SEM-based mineral liberation analysis. International Journal of Mineral Processing, 84**,** 310-320.

FEI 2013. MLA Dataview. 3.1.3.612 ed. Hillsboro.

FERNA'NDEZ, Y., ARENILLAS, A. & MENE'NDEZ, J. A. 2011. Microwave Heating Applied to Pyrolysis In: GRUNDAS, S. (ed.) Advances in Induction and Microwave Heating of Mineral and Organic Materials. Spain: InTech.

FIGUEROA, G., MOELLER, K., BUHOT, M., GLOY, G. & HABERLAH, D. Advanced discrimination of Hematite and magnetite by automated mineralogy. In: BROEKMANS, M. A. T. M., ed. 10th International Congress for Applied Mineralogy, 2011 Trondheim, Norway. Springer, 197-204.

FOLDVARI, M. 1991. Measurement of different water species in minerals by means of thermal derivatography. In: SMYKATZ, W. & WARNE, S. S. J. (eds.) Lecture notes in earth science.

FÖLDVÁRI, M. 2011. Handbook of thermogravimetric system of minerals and its use in geological practice, Hungary, Geological Institute of Hungary.

FONTGALLAND, G., BARBIN, S. E. & ANJOS, D. I. F. Use of TDR to Determine the Dielectric Constant of Vermiculite. PIERS Proceedings, August 18-21 2009 Moscow, Russia. 722-725.

FRANK, D. & EDMOND, L. 2001. Feasibility for identifying mineralogical and geochemical tracers for vermiculite ore deposits. Seattle, WA: United States Environmental Protection Agency

FREDRIK LEHMANN, Å. P., KRISTINA LUTHMAN 2003. Efficient large scale microwave assisted Mannich reactions using substituted acetophenones. Molecular Diversity, 7**,** 145-152.

FROHLICH, H. 1958. Theory of dielectrics: dielectric constant and dielectric loss, Oxford, Oxford University Press.
GEORGE, E. Z. 1960. Production of exfoliated vermiculite. USA patent application.
GEYER, R. G. 1990. Dielectric characterization and reference materials. Washington: National Institute of standard and technology.
GIACOMINO, A., MALANDRINO, M., ABOLLINO, O., VELAYUTHAM, M., CHINNATHANGAVEL, T. & MENTASTI, E. 2010. An approach for arsenic in a contaminated soil: Speciation, fractionation, extraction and effluent decontamination. Environmental Pollution, 158**,** 416-423.
GILLOTT .J.E. 1987. Clay in Engineering Geology, New York, Elsevier Publishing Company.
GOLONKA, K. A. & BRENNAN, D. J. 1996. Application of life cycle assessment to process selection for pollutant treatment: A case study of sulphur dioxide emission from Australian metallurgical smelters. Institution of Chemical Engineers, 74**,** 105-109.
GONCHARENKO, A. V. 2003. Generalisation of the Bruggeman equation and a concept of shape-distributed particle composites. The American Physical Society, 68**,** 1-13.
GOVERNMENT OF INDIA 2012. Indian Minerals Yearbook 2011 (Part-II). In: MINISTRIES OF MINES (ed.). Nagpur.
GRAF, H., REICHENBACH, V. & BEYER, J. 1994. Dehydration and Rehydration of Vermiculit: I. Phlogopitic MG- Vermiculite. Clay Minerals, 29**,** 327-340.
GRANTT, J. P., CLARKE, R. N., SYMM, G. T. & SPYROU, N. M. 1989. A critical study of the openended coaxial line sensor technique for RF and microwave complex permittivity measurements. J. Phys. E: Sci. Instrum., 22**,** 757-770.
GREENACRE, N. R. 1996. Measurement of the high temperature dielectric properties of ceramic at microwave frequencies. PhD, University of Notiingham.
GREGORY, A. P. & CLARKE, R. N. 2006. A review of RF and microwave techniques for dielectric measurements on polar liquid. Transaction on dielectric and electrical insulations, 13**,** 727-743.
GRIM, R. E. 1968. Clay Mineralogy, New York, McGraw-Hill
GRUNER, J. W. 1934a. The structures of the vermiculite and their collapse by dehydration. Journal of the mineralogical society of America, 19**,** 557.
GRUNER, J. W. 1934b. Vermiculite and Hydrobiotite Structure. American Mineralogist, 19**,** 557-575.
GU, Y. 2003. Automated Scanning Electron Microscope Based Mineral Liberation Analysis: An Introduction to JKMRC/FEI Mineral Liberation Analyser. Journal of Minerals & Materials Characterisation & Engineering, 2**,** 33-41.
GUAN, D., CHENG, M., WANG, Y. & TANG, J. 2004. Dielectric properties of mashed potatoes relevant to microwave and radio-frequency pasteurization and sterilization processes. Food engineering and physical properties, 69**,** 31-37.
GUINEE, J. B., HUPPES, G., SLEESWIJK, A. W., BRUIJN, H. D., DUIN, R. V. & HUIJBREGTS, M. A. J. 2001. Life cycle assessment: An operational guide to the ISO standards (Part 2b). Netherlands.
GUO, C., JIN, C., JIN-HUI, P. & RUN-DONG, W. 2010. Green evaluation of microwave assisted leaching process of high titanium slag on life cycle assessment. Trans. Nonferrous Met. Soc. China, 20**,** 198-204.
GUPTA, M. & EUGENE, W. W. L. 2007. Microwave and Metals, Singapore 129809, John and Wiley and sons (Asia).
GY, P. M. 1979. Sampling of particulate materials theory and practice, Amsterdam, Elsevier scientific publishing company.
HAHN, D. W. & OZISIK, N. M. 2012. Heat conduction, New Jersey, John Wiley & Sons.

HAKE, J.-F., LANDWEHR, U. & SCHREIBER, A. 1998. Integrated analysis of metallic resource flows. The International Journal of Life Cycle Assessment, 3**,** 182-183.

HALLIKAINEN, M. T., DOBSON, M. C., ULABY, F. T., EL-RAYES, M. A. & WU, L.-K. 1985. Microwave Dielectric Behaviour of Wet Soil-Part 1:Empirical Models and Experimental Observations. IEEE TRANSACTION ON GEOSCIENCE AND REMOTE SENSING, GE-23**,** 25-33.

HAMMOND, G. P. 2004. Engineering Sustainability: thermodynamics, energy systems, and the environment. International Journal of Energy Research, 28**,** 613-639.

HAQUE, K. E. 1999. Microwave energy for mineral treatment processes—a brief review. International Journal of Mineral Processing, 57**,** 1-24.

HARRAZ, H. Z. & HAMDY, M. M. 2010. Interstratified vermiculite-mica in the gneiss-metapelite-serpentinite rocks at Hafafit area, Southern Eastern Desert, Egypt: From metasomatism to weathering. Journal of African Earth Sciences, 58**,** 305-320.

HARRISON, P. T. C., LEVY, L. S., PATRICK, G., PIGOTT, G. H. & SMITH2, L. L. 1997. Comparative Hazards of Chrysotile Asbestos and Its Substitutes: A European Perspective. Environmental Health Perspectives, 107**,** 607-611.

HASAR, U. C. 2010. Unique permittivity determination of low loss dielectric materials from transmission measurements at microwave frequencies. Progress in Electromagnetics Research, 107**,** 31-46.

HASSLER, Y. & JOHANSEN, L. Microwave heating of fused quartz to high temperatures in the fabrication process of optical fibres. Proceeding of the 18th European Microwave Conference, 1988 Madrid, Spain. 613-618.

HASTED, J. B. 1973. Water, Dielectrics, Electric Properties, New York, Chapman and Hall

HAYES, J. C. & PALATINE. 1958. Method of Exfoliating Vermiculite. U.S.A patent application. 1962.

HENDRICK, S. B. & JEFFERSON, M. E. 1938. Crystal Structure of Vermiculites and Mixed Vermiculite-Chlorites. American Minerals . 23**,** 851-863.

HILHORST, M. A., DIRSKEN, C., KAMPERS, F. W. H. & FEDDES, R. A. 2000. New Dielectric Mixture Equation for Porous Materials Based on Depolarization Factors. Soil Sci. Soc. Am. J.**,** 1581-1587.

HILLIER, S., MARWA, E. M. M. & RICE, C. M. 2013. On the mechanism of exfoliation of 'Vermiculite'. Clay minerals, 48**,** 563-582.

HIPPEL, A. R. V. 1954. Dielectrics and Waves, Massachusetts, John Wiley and Sons.

HOEKSTRA, P. & DELANEY, A. 1974. Dielectric properties of soils at UHF and microwave frequencies. Journal of geophysical research, 79**,** 1699-1708.

HOSPIDO, A., DAVIS, J., BERLIN, J. & SONESSON, U. 2010. A review of methodological issues affecting LCA of novel food products. International journal of life cycle assessment, 15**,** 44-52.

HOUGARDY, J., SERATOSA, J. M., STONE, W. & OLPHEN, H. V. 1970. Interlayer water in vermiculite: thermodynamics properties, packing density, nuclear pulse resonance, and infra-red absorption. Spec. Discuss. Faraday Soc., 1**,** 187-193.

HOZ, A. D. L., ALCÁZAR, J., CARRILLO, J., HERRERO, M. A., MUÑOZ, J. D. M., PRIETO, P., CÓZAR, A. D. & DIAZ-ORTIZ, A. 2011. Reproducibility and Scalability of Microwave-Assisted Reactions. In: CHANDRA, D. U. (ed.) Microwave Heating. Croatia: InTech.

HUA YIXIN. & CHUNPENG, L. 1996. Heating Rate of Minerals and Compound in Microwave Field. Transactions of NFsoc, 6**,** 6.

HUANGA, Z., GOTOHB, M. & HIROSE, Y. 2009. Improving sinterability of ceramics using hybrid microwave heating. journal of materials processing technology, 209**,** 2446-2452.

HUO, X., WU, L., LIAO, L., XIA, Z. & WANG, L. 2012. The effect of interlayer cations on the expansion of vermiculite. Powder Technology, 224**,** 241-246.

ICNIRP 2009. Guidelines for limiting exposure to time-varying electric, magnetic, and electromagnetic fields (Up to 300 GHz). Health Physics Society, 97**,** 257-259.

INTERNATIONAL COMMISSION ON NON-IONIZING RADIATION PROTECTION (ICNIRP) 1998. Guidelines for limiting exposure to time-varying electric, magnetic, and electromagnetic fields (up to 300 GHz). Health Physics, 74**,** 494-523.

IPCC 2007. Climate change 2007:Mitigation of climate change. In: METZ, B., DAVIDSON, O., BOSCH, P., DAVE, R. & MEYER, L. (eds.) Fourth Assessment Report of the Intergovernmental Panel on Climate Change. Canada: Intergovernmental Panel on Climate Change.

IRIARTE, A., ALMEIDA, M. G. & VILLALOBOS, P. 2014. Carbon footprint of premium quality export bananas: Case study in Ecuador, the world's largest exporter. Science of The Total Environment, 472**,** 1082-1088.

ISO 14040 2006. Environmental management-life cycle assessment-principles and framework.

ISO 14044 2006. Environmental management -- Life cycle assessment -- Requirements and guidelines.

ISO 14044 2006. Environmental management-Life cycle assessment-Requirements and guidelines. International organisation for standardization.

J. CLEOPHAX, M. L., A. LOUPY, A. PETIT 2000. Application of Focused Microwaves to the Scale-Up of Solvent-Free Organic Reactions. Organic Process Research & Development 4**,** 498-504.

JADE 6.5 2003. Software package for XRD analysis. 6.5 ed. Livermore, CA: Material Data Inc.

JANEK, M., MATEJDES, M., SZOCS, V., BUGAR, I., GAAL, A., VELIC, D. & DARMO, J. 2010. Dielectric properties of micaceous clays determined by tetrahertz time-domain spectroscopy. Philosophical Magazine, 90**,** 2399-2413.

JEBBOR, N., BRI, S., SÀNCHEZ, A. M. & CHAIBI, M. 2013. A microwave measurement method for complex permittivity determination of dielectric materials at Ku-Band Physics and Technical Sciences, 1**,** 6-9.

JENKINST, S., HODGETTSS, T. E., CLARKE, R. N. & PREECE, A. W. 1989. Dielectric measurements on reference liquids using automatic network analysers and calculable geometries. Meas. Sci. Technol., 1**,** 691-702.

JESWANI, H. K. & AZAPAGIC, A. 2011. Water footprint: methodologies and a case study for assessing the impacts of water use. Journal of Cleaner Production, 19**,** 1288-1299.

JINKAI, X. 1990. Dielectric properties of minerals and their applications in microwave remote sensing. Chinese Journal of Geochemistry, 9**,** 169-177.

JKMRC 2004. MLA System User Operating Manual Mode. Australia: Julius Kruttschnitt Mineral Research Centre.

JOHN, O. M. & RONALD, P. C. 2003. Historical Review of RF Exposure Standards and the International Committee on Electromagnetic Safety (ICES). Bioelectromagnetics Supplement**,** 7-16.

JOKOVIC, V., RIZMANOSKI, V., DJORDJEVIC, N. & MORRISON, R. 2014. FDTD simulation of microwave heating of variable feed. Minerals Engineering, 59**,** 12-16.

JONES, D. A., LELYVELD, T. P., MAVROFIDIS, S. D., KINGMAN, S. W. & MILES, N. J. 2002. Microwave heating applications in environmental engineering--a review. Resources, Conservation and Recycling, 34**,** 75-90.

JONES, M. P. 1987. Applied mineralogy: A quantitative approach, Oxford, Alden Press.

JUSTO, A., MAQUEDA, C., PEREZ-RODRÍGUEZ, J. L. & MORILLO, E. 1989. Expansibility of some vermiculites. Applied Clay Science, 4**,** 509-519.

JUSTO, A., PE'REZ-RODRI'GUEZ, J. L. & P.J. SANCHEZ-SOTO 1993. Thermal Study of Vermiculite and Mica-Vermiculite Interstratifications. Journal of Thermal Analysis, 40**,** 59-65.

KARJALAINEN, P. 2013. The carbon footprint of the Finnish beverage industry for year 2000-2012 as calculated with CCaLC. Master's thesis, University of Helsinki.

KAUR, N., SINGH, M., SINGH, A., AWASTHI, A. M. & SINGH, L. 2012. Dielectric relaxation spectroscopy of phlogopite mica. Physica B: Condensed Matter, 407**,** 4489–4494.

KAVIRATNA, P. D. & PINNAVAIA, T. J., SCHROEDER, P. A. 1996. Dielectric properties of smectite clays. Journal of Physics and Chemistry of Solids, 57**,** 1897-1906.

KEHAL, M., REINERT, L. & DUCLAUX, L. 2010. Characterization and boron adsorption capacity of vermiculite modified by thermal shock or H2O2 reaction and/or sonication. Applied Clay Science, 48**,** 561-568.

KELLENERS, T. J. & VERMA, A. K. 2010. Measured and Modelled Dielectric properties of Soils at 50 Megahertz. Soil Physiscs, 74**,** 744-752.

KENNEDY, B. A. (ed.) 1990. Surface mining, Baltimore, Maryland: Port City Press.

KENT, M. 1977. Complex permittivity of fish meal: a general discussion of temperature, density and moisture dependence Journal of Microwave Power, 12**,** 341-345.

KINGMAN, S. W. & ROWSON, N. A. 1998. Microwave treatment of minerals-a review. Minerals Engineering, 11**,** 1081-1087.

KINGMAN, S. W., VORSTER, W. & ROWSON, N. A. 2000. The influence of mineralogy on microwave assisted grinding. Minerals Engineering, 13**,** 313-327.

KIRCHHOFF, M. M. 2003. Promoting green engineering through green chemistry. Environmental Science Technology**,** 5349-5353.

KITCHEN, R. 1993. RF and Microwave radiation safety handbook, Oxford, Butterworth-Heinemann.

KLEIN, A. 1981. Microwave determination of moisture in coal-comparison of attenuation and phase measurement. Journal of Microwave Power and Electromagnetic Energy, 16**,** 289-304.

KNOLL, M. D. 1996. A petrophysical basis for ground-penetrating radar and very early time electromagnetics, electrical properties of sand-clay mixtures. PhD, University of British Columbia.

KOBUSHESHE, J. 2010. Microwave enhanced processing of ores. PhD, The University of Nottingham.

KOGEL, J. E., TRIVEDI, N. C., BARKER, J. M. & KRUKOWSKI, S. T. (eds.) 2006. Industrial minerals and rock: commodities, markets and uses, Colorado: Society for mining, metallurgy, and exploration.

KOLEINI, S. M. J. & BARANI, K. 2012. Microwave heating applications in mineral processing. In: CAO, W. (ed.) The development and application of microwave heating. InTech.

KOMAROV, V., WANG, S. & TANG, J. 2005a. Permittivity and Measurement. In: J., T. (ed.) Encyclopedia of RF and Microwave Engineering.

KOUGHNETT, A. L. V. & DUNN, J. G. 1973. Doubly corrugated chokes for microwave heating systems. Journal of Microwave Power, 8**,** 101.

KU, H. S., ELIAS, S. & R, B. J. A. 2001a. Microwave Processing of Materials: Part 1. The Hong Kong Institute of Engineers, 8**,** 31-37.

KU, H. S., SIU, F., SIORES, E., BALL, J. A. R. & BLICBLAU, A. S. 2001b. Applications of Fixed and Variable Frequency Microwave Facilities in Polymeric Materials Processing and Joining. Journal of Material Processing 184-188.

KUMAR, A., VOEVODIN, A. A., PAUL, R., ALTFEDER, I., ZEMLYANOV, D., ZAKHAROV, D. N. & FISHER, T. S. 2013. Nitrogen-doped graphene by microwave plasma chemical vapor deposition. Thin Solid Films, 528**,** 269-273.
KUMAR, P., CORONEL, P., TRUONG, V. D., SIMUNOVIC, J., SWARTZEL, K. R., SANDEEP, K. P. & CARTWRIGHT, G. 2008. Overcoming issues associated with the scale-up of a continuous flow microwave system for aseptic processing of vegetable purees. Food Research International, 41**,** 454-461.
KUPFER, K. 2005. Electromagnetic Aquametry, Weimar, Germany, Springer.
KUSAMA, Y., HASHIMOTO, O. & MAKIDA, M. 2002. Analysis of door seal structure of microwave oven with consideration of higher modes by the FDTD method. Electronics and Communications in Japan, 85**,** 667-673.
LANDAU, L. D. & LIFSHITZ, E. M. 1960. Electrodynamics of continuous media, Oxford, Pergamon press.
LE, T.-H. & CHANG, Y. 2013. Oil price shocks and trade imbalances. Energy Economics, 36**,** 78-96.
LEE, T. 2011. Microwave preparation of raw vermiculite for use in removal of copper ions from aqueous solution. Environmental Technology, 32**,** 1195-1203.
LEONELLI, C., VERONESI, P., DENTI, L., GATTO, A. & IULIANO, L. 2008. Microwave assisted sintering of green metal parts. Journal of Materials Processing Technology, 205**,** 489-496.
LESTER, E. & KINGMAN, S. 2004. The effect of microwave pre-heating on five different coals. Fuel, 83**,** 1941-1947.
LEWIS, D. A., HEDRICK, J. C., LYLE, G. D., WARD, T. C. & MCGRATH, J. E. 1988. Microwave Processing of Polymers. MRS Online Proceedings Library, 124**,** null-null.
LIDSTROM, P., TIERNEY, J., WATHEY, B. & WESTMAN, J. 2001. Microwave assisted organic synthesis-a review. Tetrahedron, 47**,** 9225-9283.
LILL, J. R., INGLE, E. S., LLU, P. S. & PHAM, V. 2007. Microwave assisted proteomics. Mass spectrometry reviews, 26**,** 657-671.
LIN, Q., CHEN, G. & LIU, Y. 2012. Scale-up of microwave heating process for the production of bio-oil from sewage sludge. Journal of Analytical and Applied Pyrolysis, 94**,** 114-119.
LIU, G. & MÜLLER, D. B. 2012. Addressing sustainability in the aluminium industry: a critical review of life cycle assessments. Journal of Cleaner Production, 35**,** 108-117.
LIU, S., FUKUOKA, M. & SAKAI, N. 2013. A finite element model for simulating temperature distributions in rotating food during microwave heating. Journal of Food Engineering, 115**,** 49-62.
LIU, S., OGIWARA, Y., FUKUOKA, M. & SAKAI, N. 2014a. Investigation and modelling of temperature changes in food heated in a flatbed microwave oven. Journal of Food Engineering, 131**,** 142-153.
LIU, S., YU, X., FUKUOKA, M. & SAKAI, N. 2014b. Modelling of fish boiling under microwave irradiation. Journal of Food Engineering, 140**,** 9-18.
LOGSDON, S. D. & LAIRD, D. A. Ranges of Bound Water Properties Associated with a Smectite Clay. Electromagnetic Wave Interaction with Water and Moist Substances, 2003 Rotorua, New Zealand. Industrial Research, Auckland, New Zealand, 23-26.
LOOYENGA, H. 1965. Dielectric constants of heterogeneous mixtures. Physica, 31**,** 401-406.
LOVÁS, M., ZNAMENÁČKOVÁ, I., ZUBRIK, A., KOVÁČOVÁ, M. & DOLINSKÁ, S. 2011. The Application of Microwave Energy in Mineral Processing – a Review. Acta Montanistica Slovaca, 16**,** 137-148.
LUO, J. 2007. Analyses of multimode forming process in a microwave-heating cavity. PIERS Online, 3**,** 801-807.

MACKINNON, A., KINGSTON, P. W. & SPRINGER, J. S. 1989. Vermiculite in the Stanleyville Area, Lanark County, Eastern Ontario. Ontario.
MALANDRINO, M., ABOLLINO, O., GIACOMINO, A., ACETO, M. & MENTASTI, E. 2006. Adsorption of heavy metals on vermiculite: Influence of pH and organic ligands. Journal of Colloid and Interface Science, 299**,** 537-546.
MANTAS, P. Q. 1999. Dielectric response of materials: extension to the Debye model. Journal of the European Ceramic Society, 19**,** 2079-2086.
MARC-ANDREE, W., RANA, P., KIRANA, C., SERENELLA, S. & DAVID, P. 2012. The International Reference Life Cycle Data System (ILCD) Handbook - Towards more sustainable production and consumption for a resource-efficient Europe. Publications Office of the European Union.
MARCOS, C., ARANGO, Y. C. & RODRIGUEZ, I. 2009. X-ray diffraction studies of the thermal behaviour of commercial vermiculites. Applied Clay Science, 42**,** 368-378.
MARCOS, C., ARGUELLES, A., RUIZ-CONDE, A., SANCHEZ-SOTO & BLANCO, J. A. 2003. Study of the dehydration process of vermiculite by applying a vacuum pressure: formation of interstratified phases. Mineralogical Magazine, 67**,** 1253-1268.
MARCOS, C. & RODRÍGUEZ, I. 2010a. Expansibility of vermiculites irradiated with microwaves. Applied Clay Science, 51**,** 33-37.
MARCOS, C. & RODRÍGUEZ, I. 2010b. Expansion behaviour of commercial vermiculites at 1000 °C. Applied Clay Science, 48**,** 492-498.
MARCOS, C. & RODRÍGUEZ, I. 2014. Exfoliation of vermiculites with chemical treatment using hydrogen peroxide and thermal treatment using microwaves. Applied Clay Science, 87**,** 219-227.
MARIAN JANEK, BUGAR, I., LORENC, D., SZOCS, V., VELIC, D. & CHORVAT, D. 2009. Terahertz Time-Domain Spectroscopy of Selected Layered Silicates. Clay and Clay Minerals, 57**,** 416-424.
MARINSHAW, R. 1995. Mineral Product Industry: Vermiculite Processing In: AGENCY, U. S. E. P. (ed.). North Carolina: U.S. Environmental Protection Agency.
MARLAND, S., MERCHANT, A. & ROWSON, N. 2001. Dielectric properties of coal. Fuel, 80**,** 1839-1849.
MARON, N. & MARON, O. 2004. On the mixing rules for astrophysical inhomogeneous grains. Monthly notices of the Royal Astronomical Society, 357**,** 873-880.
MARWA, E. M. M., MEHARG, A. A. & RICE, C. M. 2009. The effect of heating temperature on the properties of vermiculites from Tanzania with respect to potential agronomic applications. Applied Clay Science, 43**,** 376-382.
MAX SUCHER & FOX, J. (eds.) 1963. Handbook of Microwave Measurements, Broklyn: Polytechnic press of the Polytechnic Institute of Broklyn.
MCGILL, S. L., WALKIEWICZ, J. W. & CLARK, A. E. 1995. Microwave heating of chemicals and minerals. USA: United States Department of The Interior.
MCLELLAN, B. C., CORDER, G. D., GIURCO, D. & GREEN, S. 2009. Incorporating sustainable development in the design of mineral processing operations – Review and analysis of current approaches. Journal of Cleaner Production, 17**,** 1414-1425.
MEHDIZADEH, M. 2010. Microwave/Rf applicators and probe for material heating, sensing, and plasma generation, Oxford, William Andrew.
MEMARY, R., GIURCO, D., MUDD, G. & MASON, L. 2012. Life cycle assessment: a time-series analysis of copper. Journal of Cleaner Production, 33**,** 97-108.
MENEZES, R. R., SOUTO, P. M. & KIMINAMI, R. H. G. A. 2007. Microwave hybrid fast sintering of porcelain bodies. Journal of Materials Processing Technology, 190**,** 223-229.

MEREDITH, R. 1998. Engineers' Handbook of Industrial Microwave Heating, London, The Institution of Engineering and Technology.
METAXAS A.C; MEREDITH R.J 1988. Industrial Microwave Heating, Exeter, UK, The Institution of Engineering and Technology.
METAXAS, A. C. 1996. Foundations of electroheat: A unified approach, Chichester, Wiley.
MICHAEL WINDSOR SYMONS. 1997. Method of Preparing an Exfoliated Vermiculite for the Manufacture of Finished Product. U.S.A patent application. March 1999.
MIDGLEY, H. G. & MIDGLEY, C. M. 1960. The mineralogy of some commercial vermiculite. Clay minerals, 4**,** 142-150.
MIKUTTA, R., KLEBER, M., KAISER, K. & JAHN, R. 2005. Review: Organic Matter Removal from Soils using Hydrogen Peroxide, Sodium Hypochlorite, and Dissodium Peroxodisulfate. Social Science Society of America, 69**,** 120-135.
MILOVANOVIĆ, B., DONČOV, N. & JOKOVIĆ, J. 2004. Microwave heating cavities: modelling and analysis. Microwave Review, 10**,** 26-35.
MINGOS, D. M. P. & BAGHURST, D. R. 1991. Applications of microwave dielectric heating to synthetic problems in chemistry. Chem. Soc. Rev., 20**,** 1-47.
MINITAB 17 2010. Minitab statistical software. Minitab Inc.
MONDAL, A., AGRAWAL, D. & UPADHYAYA, A. 2009. Microwave Heating of Pure Copper Powder with varying Particle Size and PoroSity. Journal of Microwave Power and Electromagnetic Energy, 43**,** 1-10.
MOORE, D. M. & REYNOLD, R. C. 1998. X-ray diffraction and the identification and analysis of clay minerals Oxford, Oxford University Press
MORSCHHÄUSER, R., KRULL, M., KAYSER, C., BOBERSKI, C., BIERBAUM, R., PÜSCHNER, P. A., GLASNOV, T. N. & KAPPE, C. O. 2012. Microwave-assisted continuous flow synthesis on industrial scale. Green Process Synthesis, 1**,** 281-290.
MORTENSEN, A. 2006. Concise encyclopedia of composite materials. In: MORTENSEN, A. 2nd ed. Oxford: Elsevier Ltd.
MOSELEY, J. D., LENDEN, P., LOCKWOOD, M., RUDA, K., SHERLOCK, J.P., THOMSON, A. D. & GILDAY, J. P. 2007. A Comparison of Commercial Microwave Reactors for Scale-Up within Process Chemistry. Organic Process Research & Development, 12**,** 30-40.
MOUZDAHIR, Y. E., ELMCHAOURI, A., MAHBOUB, R., GIL, A. & KORILI, S. A. 2009. Synthesis of nano-layered vermiculite of low density by thermal treatment. Powder Technology, 189**,** 2-5.
MUIAMBO, H. F. & FOCKE, W. W. 2013. Ion exchange vermiculites with lower expansion onset temperature. Molecular Crystals Liquid Crystals, 555**,** 65-75.
MUIAMBO, H. F., FOCKE, W. W., ATANASOVA, M., WESTHUIZEN, I. V. D. & TIEDT, L. R. 2010. Thermal properties of sodium-exchanged palabora vermiculite. Applied Clay Science, 50**,** 51-57.
MURPHY, E. J. & MORGAN, S. O. 1937. The dielectric properties of insulating materials. Bell system technical journal, 16**,** 493-512.
MUTYALA, S., FAIRBRIDGE, C., PARÉ, J. R. J., BÉLANGER, J. M. R., NG, S. & HAWKINS, R. Microwave applications to oil sands and petroleum: A review. Fuel Processing Technology, 91**,** 127-135.
MYSORE, D., VIRARAGHAVAN, T. & JIN, Y.C. 2005. Treatment of oily waters using vermiculite. Water Research, 39**,** 2643-2653.
NATIONAL RADIOLOGICAL PROTECTION BOARD (NRPB) 1993. Restriction on Human Exposure to Static and Time Varying Electromagnetic Fields and Radiation. London.
NATIONAL RESEARCH COUNCIL (NRC). 1994. Microwave Processing of Materials. In: NATIONAL MATERIALS ADVISORY BOARD, C. O. E. A. T. S. (ed.). USA: National Academy Press.

NELSON, S., KRASZEWSKI, A. & YOU, T. 1991. Solid and particle material permittivity relationship. Journal of Microwave Power and Electromagnetic Energy, 26**,** 45-51.
NELSON, S., LINDROTH, D. & BLAKE, R. 1989. Dielectric properties of selected and purified minerals at 1 to 22 GHz. International microwave power institute, 24**,** 213-220.
NELSON S.O & YOU T.S 1989. Relationships between Microwave Permittivities of Solids and Pulverised Plastics. Journal of Physics D.: Applied Physics, 23**,** 346-353.
NELSON, S. O. 1991. Dielectric Properties of Agricultural Products: Measurement and Applications. IEEE transaction on electrical insulation, 26**,** 845-898.
NELSON, S. O. Estimation of permittivities of solids from measurements on pulverised or granular materials. In: SUTTON, W. H., BROOKS, M. H. & CHABINSKY, I. J., eds. Progress in Electromagnetics Research, 1992a New York. Elsevier, 231-271.
NELSON, S. O. 1994. Measurement of microwave dielectric properties of particulate materials. Journal of Food Engineering, 21**,** 365-384.
NELSON, S. O. 2005. Density-Permittivity Relationships for Powdered and Granular Materials. IEEE transactions on instrumentation and measurement, 54**,** 2033-2040.
NORGATE, T. & HAQUE, N. 2010. Energy and greenhouse gas impacts of mining and mineral processing operations. Journal of Cleaner Production, 18**,** 266-274.
NORGATE, T. & HAQUE, N. 2013. The greenhouse gas impact of the IPCC and ore-sorting technologies. Minerals Engineering, 42**,** 13-21.
NPI, N. P. I. 1999. Emission estimation technique manual for mining and processing of non-metallic minerals. Australia: National Pollutant Inventory
NRPB 2003. Measurement of Radiation Leakage from Microwave Ovens. In: AGENCY, H. P. (ed.). Oxfordshire.
NRPB 2004. Advice on limiting exposure to electromagnetic fields (0-300GHz). In: BOARD, N. R. P. (ed.). Chilton, Oxfordshire: National Radiological Protection Board.
OBUT, A. & GIRGIN, I. 2002. Hydrogen peroxide exfoliation of vermiculite and phlogopite. Minerals Engineering, 15**,** 683-687.
OBUT, A., GIRGIN, I. & YORUKOGLU, A. 2003. Microwave Exfoliation of Vermiculite and Phlogopite. Clay and Clay Minerals, 51**,** 452-456.
OFCOM 2013. United Kingdom table of radio frequency allocations 9kHz-105GHz.
OGHBAEI, M. & MIRZAEE, O. 2010. Microwave versus conventional sintering: A review of fundamentals, advantages and applications. Journal of Alloys and Compounds, 494**,** 175-189.
ONCU, N. B. & BALCIOGLU, I. A. 2013. Microwave-assisted chemical oxidation of biological waste sludge: Simultaneous micropollutant degradation and sludge solubilization. Bioresource Technology, 146**,** 126-134.
OSEPCHUK, J. M. 2002. Microwave power applications. IEEE Transactions on Microwave Theory and Techniques, 50**,** 975-985.
PALABORA EUROPE. 2009. Expert in Vermiculite [Online]. Surrey, GU2 7YB, UK. Available: http://www.palaboraeurope.co.uk/home.php? [Accessed 20/06/2011 2011].
PARDO, G. & ZUFÍA, J. 2012. Life cycle assessment of food-preservation technologies. Journal of Cleaner Production, 28**,** 198-207.
PAS 2050 2011. How to carbon footprint your products, identify hotspots and reduce emissions in your supply chain. London: British Standards Institution.
PECHARSKY, V. K. & ZAVALIJ, P. Y. 2009. Fundamentals of powder diffraction and structural characterisation of materials, New York, Springer.

PETERSEN, L., DAHL, C. K. & ESBENSEN, K. H. 2004. Representative mass reduction in sampling—a critical survey of techniques and hardware. Chemometrics and Intelligent Laboratory Systems, 74**,** 95-114.

PETERSEN, L., MINKKINEN, P. & ESBENSEN, K. H. 2005. Representative sampling for reliable data analysis: Theory of Sampling. Chemometrics and Intelligent Laboratory Systems, 77**,** 261-277.

PETRUK, W. 2000. Applied mineralogy in the mining industry, Netherland, Elsevier.

PIRAJNO, F., SELTMANN, R. & YANG, Y. 2011. A review of mineral systems and associated tectonic settings of northern Xinjiang, NW China. Geoscience Frontiers, 2**,** 157-185.

PONIZOVSKY, A. A., CHUDINOVA, S. M. & PACHEPSKY, Y. A. 1999. Performance of TDR calibration models as affected by soil texture. Journal of Hydrology, 218**,** 35-43.

POZAR, D. M. 2012. Microwave engineering, USA, John Wiley & Sons.

PRE 2011. Simapro 7.3.3. 7.3.3 ed. Netherlands: Pre Consultants.

QI, S., VAIDHYANATHAN, B. & HUTT, D. 2013. Conventional and microwave-assisted processing of Cu-loaded ICAs for electronic interconnect applications. Journal of Materials Science, 48**,** 7204-7214.

RAJU, G. G. 2003. Dielectric in Electric Fields, New York, Marcel Dekker Inc.

RAO, K. H. & CHERNYSHOVA, I. V. 2011. Challenges in sulphide mineral processing. The Open Mineral Processing Journal, 4**,** 7-13.

REED, S. J. B. 2005. Electron microprobe and scanning electron microscopy in geology, Cambridge, Cambridge University Press.

REEVES, G. M., SIMS, I. & CRIPPS, J. C. (eds.) 2006. Clay materials used in construction, Trowbridge: Cromell Press.

REGALADO, C. M. 2004. A physical interpretation of logarithmic TDR calibration equations of volcanic soils and their solid fraction permittivity based on Lichtenecker's mixing formulae. Geoderma, 123**,** 41-50.

REICHENBACH H. GRAF V. & BEYER, J. 1994. Dehydration and rehydration of vermiculites: I. Phlogopitic M_G-vermiculite. Clay Minerals, 29**,** 327-340.

REYNOLDS J.A & MOUGH J.M 1957. Formulae for Dielectric Constants of Mixtures. Proceeding Physics Society, 70**,** 769-775.

RICHARD C. FERRERO, JONATHAN J. KOLAK, DONALD J. BILLS, ZACHARY H. BOWEN, DANIEL J. CORDIER, TANYA J. GALLEGOS, JAMES R. HEIN, KAREN D. KELLEY, PHILIP H. NELSON, VITO F. NUCCIO, JEANINE M. SCHMIDT & SEAL, R. R. 2013. U.S. Geological Survey energy and minerals science strategy—A resource lifecycle approach. In: INTERIOR, U. S. D. O. T. & SURVEY, U. S. G. (eds.). Virginia: U.S. Geological Survey (USGS).

RIINA K. ARVELA, N. E. L., MICHAEL J. COLLINS 2005. Automated batch scale-up of microwave-promoted Suzuki and Heck coupling reactions in water using ultra-low metal catalyst concentrations. Tetrahedron, 61**,** 9349–9355.

RIO TINTO 2010. Palabora Mining Company: Competent persons report. Phalaborwa.

ROBINSON, D. A., COOPER, J. D. & GARDNER, C. M. K. 2002. Modelling the relative permittivity of soils using soil hygroscopic water content. Journal of Hydrology, 255**,** 39-49.

ROBINSON, J. P., KINGMAN, S. W., LESTER, E. H. & YI, C. 2012. Microwave remediation of hydrocarbon-contaminated soils–scale-up using batch reactors. Separation and Purification Technology, 96**,** 12-19.

ROBINSON, J. P., KINGMAN, S. W., SNAPE, C. E., BARRANCO, R., SHANG, H., BRADLEY, M. S. A. & BRADSHAW, S. M. 2009. Remediation of oil-contaminated drill cuttings using continuous microwave heating. Chemical Engineering Journal, 152**,** 458-463.

ROBINSON, J. P., KINGMAN, S. W., SNAPE, C. E., BRADSHAW, S. M., BRANDLEY, M. S. A., SHANG, H. & BARRANCO, R. 2010. Scale-up and

design of a continuous microwave treatment system for the processing of oil-contaminated drill cuttings. Chemical Engineering Research and Design, 88**,** 146-154.
ROEBUCK, B. D. & GOLDBLITH, S. A. 2006. Dielectric Properties of Carbohydrate-Water Mixtures at Microwave Frequencies. Journal of Food Science, 37**,** 199-204.
RUSCHER, C. H. & GALL, S. 1995. On the polaron-mechanism in iron-bearing trioctahedral phyllosilicates: an investigation of the electrical and optical properties. Phys Chem Minerals, 22**,** 468-478.
RUSCHER, C. H. & GALL, S. 1997. Dielectric properties of iron-bearing trioctahedral phyllosilicates. Physical chemistry minerals, 24**,** 365-373.
RUTHRUFF, R. F. 1967. Vermiculite and Hydrobiotite. The American Mineralogist, 52**,** 478-484.
SAHOO, B. K., DE, S. & MEIKAP, B. C. 2011. Improvement of grinding characteristics of Indian coal by microwave pre-treatment. Fuel Processing Technology, 92**,** 1920-1928.
SAKIEWICZ, P., NOWOSIELSKI, R., PILARCZYK, W., GOŁOMBEK, K. & LUTYŃSKI, M. 2011. Selected properties of the halloysite as a component of geosynthetic clay liners (GCL). Journal of achievements in materials and manufacturing engineering, 48**,** 177-191.
SALSMAN J. B; AND HOLDERFIELD S. P 1994. A Technique for Measuringth the Dielectric Properties of Minerals at Microwave Heating Frequencies Using an Open-Ended Coaxial Line. In: MINES, U. S. D. O. T. I. B. O. (ed.). Washington
SANZ, J., HERRERO, C. P. & SERRATOSA, J. M. 2006. Arrangement and mobility of water in vermiculite hydrates followed by 'H NMR spectroscopy. Journal of Phys. Chem., 110**,** 7813-7819.
SATEESH, M., CRAIG, F., JOCELYN, J. R. P., JACQUELINE, M. R. B., SIAUW, N. & RANDALL, H. 2010. Microwave applications to oil sands and petroleum: A review. Fuel Processing Technology, 91**,** 127-135.
SCHOEMAN, J. J. 1989. Mica and Vermiculite in South Africa. Journal of South Africa Inst. Miner. Metall, 89**,** 1-12.
SCHUBERT, H. & REGIER, M. (eds.) 2005. The microwave processing of foods, Cambridge, UK: Woodhead publishing Limited.
SCHUMACHER, B. A., SHINES, K. C. & PAPP, M. L. 1990. A comparison of soil sample homogenisation techniques. In: (EPA), E. M. S. L. (ed.). Las Vegas: EPA.
SEABORN, D. J. & JAMESON, G. J. 1976. Some ion exchange properties of exfoliated vermiculite. Hydrometallurgy, 2**,** 141-155.
SENGWA R.J & SONI A. Density Dependence Complex Dielectric Constant of Pulversied Limestone-Coal Mixture at 10.1GHz. International Conference on Microwave, 2008 China. IEEE.
SHAHEEN, M. S., EL-MASSRY, K. F., EL-GHORAB, A. H. & ANJUM, F. M. 2012. Microwave Applications in Thermal Food Processing. In: CAO, W. (ed.) The Development and Application of Microwave Heating. INTECH.
SHARIF, S. 1995. Chemical and mineral composition of dust and its effect on the dielectric constant. IEEE TRANSACTION ON GEOSCIENCE AND REMOTE SENSING, 33**,** 353-359.
SHEEN, J. 2009. Measurements of microwave dielectric properties by an amended cavity perturbation technique. Measurement, 42**,** 57-61.
SHEEN, J. & HONG, Z. W. 2010. Microwave Measurements of Dielectric Constants by Exponential and Logarithmic Mixture Equations. Progress in Electromagnetic Research**,** 13-26.
SHEEN, J., MAO, W. L. & LIU, W. 2007. Study on the Measurement Techniques of Microwave Dielectric Properties. NST**,** 349-352.

SIDDIQUI, M. N., REDHWI, H. H. & ACHILIAS, D. S. 2012. Recycling of poly (ethylene terephthalate) waste through methanolic pyrolysis in a microwave reactor. Journal of Analytical and Applied Pyrolysis, 98**,** 214-220.
SIHVOLA, A. 2000. Electromagnetic mixing formulas and applications, London, The institution of Electrical Engineers.
SIHVOLA, A. 2000 (a). Mixing Rule with Complex Dielectric Coefficients. Subsurface Sensing Technologies and Applications, 1**,** 22.
SKLYAREVICH V; AND SHEVELEV M. 2006. A method of expanding mineral ores using microwave radiation. USA patent application PCT/US2005/030741.
SOBBY, A. & CHAOUKI, J. 2010. Microwave assisted biorefinery. Chemical Engineering Transaction, 19**,** 25-32.
SOSA-MORALES, M. E., VALERIO-JUNCO, L., LÓPEZ-MALO, A. & GARCÍA, H. S. 2010. Dielectric properties of foods: Reported data in the 21st Century and their potential applications. LWT - Food Science and Technology, 43**,** 1169-1179.
STEER, M. B. 2010. Microwave and RF design: A system approach, Raleigh, SciTech Publishing, Inc.
STERLING, D. 2013. Identifying opportunities to reduce the consumption of energy across mining and processing plants. Australia: Schneider Electric.
STICHNOTHE, H. & AZAPAGIC, A. 2013. Life cycle assessment of recycling PVC window frames. Resources, Conservation and Recycling, 71**,** 40-47.
STRAND, P. R. & STEWART, O. F. 1983. Vermiculite: Industrial Rocks and Minerals, New York, Society of Mining Engineers.
STUERGA, D. 2006. Microwave-material interactions and dielectric properties, key ingredients for mastery of chemical microwave processes. In: LOUPY, A. (ed.) Microwave in organic synthesis. Weinheim: WILEY-VCH.
STUERGA, D. & GAILLARD, P. 1996. Microwave heating as a new way to induce localised enhancements of reaction rate. Non-isothermal and heterogeneous kinetics. Tetrahedron, 52**,** 5505-5510.
SULLIVAN, D. M. 2000. Electromagnetic simulation using the FDTD method, New York, IEEE Press.
SUN, B., HUANG, J., WANG, C. & ZHANG, J. 2005a. Genesis and metallogenic model of a super-large vermiculite deposit, Qieganbulak, Xinjiang, China. Mineral deposit research: Meeting the global challenge. Berlin: Springer.
SUN, X., HWANG, J.-Y., HUANG, X., LI, B. & SHI, S. 2005b. Effects of Microwave on Molten Metals with Low Melting Temperatures. Journal of Minerals & Materials Characterisation & Engineering, 4**,** 107-112.
SUNDBERG, M., RISMAN, P. O., KILDAL, P. S. & OHLSSON, T. 1996. Analysis and design of industrial microwave ovens using the finite difference time domain method. Journal of Microwave Power and Electromagnetic Energy, 31**,** 142-157.
SUQUET, H., CHEVALIER, S., MARCILLY, C. & BARTHOMEUF, D. 1991. Preparation of porous materials by chemical activation of the llano vermiculite. Clay Minerals, 26**,** 49-60.
SUTTON, W. H. Microwave processing of ceramics-an overview. Microwave processing of materials III-Materials Research Society Symposium Proceedings. , 1992 Pittsburg. Materials Research Society, 3-20.
SUZUKI, M., WADA, N., HINES, D. R. & WHITTINGHAM, M. S. 1987. Hydrations states and phase transitions in vermiculite intercalation compounds. Physical Review B, 36**,** 2851.
SWAIN, M. J., JAMES, S. J. & SWAIN, M. V. L. 2008. Effect of power output reduction of domestic microwave ovens after continuous (intermittent) use on food temperature after reheating. Journal of Food Engineering, 87**,** 11-15.

SWART, P. & DEWULF, J. 2013. Quantifying the impacts of primary metal resource use in life cycle assessment based on recent mining data. Resources, Conservation and Recycling, 73**,** 180-187.
T. MICHAEL BARNARD, G. S. V., AND MICHAEL J. COLLINS, JR 2006. Scale-Up of the Green Synthesis of Azacycloalkanes and Isoindolines under Microwave Irradiation. Organic Process Research & Development, 10**,** 1233-1237.
TAFLOVE, A., SUSAN, C. & HAGNESS 2005. Computational Electrodynamics: The finite difference time domain method. Artech House, Boston, Mass.
TANG, J., HAO, F. & LAU, M. 2002. Microwave heating in food processing. In: YANG, X. H. & TANGS, J. (eds.) Advanced in Bioprocessing Engineering Singapore: Word Scientific Ltd.
TANNER, A. O. 2013. 2011 Minerals Yearbook: Vermiculite. In: U.S. DEPARTMENT OF THE INTERIOR; & U.S. GEOLOGICAL SURVEY (ed.). U.S. Geological Survey.
TASSINARI, M. M. L., KAHN, H. & RATTI, G. 2001. Process mineralogy studies of Corrego do Garimpo REE ore, catalao-I alkaline complex, Goias, Brazil. Minerals Engineering, 14**,** 1609-1617.
TAYLOR, M., ATRI, B. S., MINHAS, S. & TEA, I. 2005. Evaluserve Analysis: Developments in Microwave Chemistry. London.
TERIGAR, B. G., BALASUBRAMANIAN, S., SABLIOV, C. M., LIMA, M. & BOLDOR, D. 2011. Soybean and rice bran oil extraction in a continuous microwave system: From laboratory- to pilot-scale. Journal of Food Engineering, 104**,** 208-217.
THE COOPERATIVE SOIL SURVEY. 2013. Soil Texture - Physical Properties [Online]. Available: http://soils.missouri.edu/tutorial/page8.asp.
THE UNIVERSITY OF MANCHESTER 2007. Carbon calculations over the life cycle of industrial activities. CCaLc 3.1 ed. Manchester: The University of Manchester.
THE VERMICULITE ASSOCIATION. 2011. The World of Vermiculite [Online]. Hampshire, GU35 9LU, United Kingdom. Available: http://www.vermiculite.org/ [Accessed 20/06/2011 2011].
THOSTENSON, E. T. & CHOU, T. W. 1999. Microwave processing: fundamentals and applications. Composites Part A: Applied Science and Manufacturing, 30**,** 1055-1071.
TIERNEY, J. P. & LINDSTROM, P. (eds.) 2005. Microwave Assisted Organic Synthesis, Oxford: Blackwell Publishing Ltd.
TINGA, W. & XI, W. 1993. Design of a new high-temperature dielectrometer system. International microwave power institute, 28**,** 93-103.
TOFT, P. 2011. Intrastate conflict in oil producing states: A threat to global oil supply? Energy Policy, 39**,** 7265-7274.
TOMA N. GLASNOV, C. O. K. 2007. Microwave-Assisted Synthesis under Continuous-Flow Conditions. Macromolecular Rapid Communications, 28**,** 395-410.
TORBED SERVICE LIMITED. 1997. Vermiculite Exfoliation [Online]. Reading, UK. Available: http://www.torbedservices.co.uk/facts/28vermiculite.pdf [Accessed 21/06/2011 2011].
TSINTZOU, G. P., ANTONAKOU, E. V. & ACHILIAS, D. S. 2012. Environmentally friendly chemical recycling of poly(bisphenol-A carbonate) through phase transfer-catalysed alkaline hydrolysis under microwave irradiation. Journal of Hazardous Materials, 241–242**,** 137-145.
TSUJI, M., HASHIMOTO, M., KUBOKAWA, Y. & TSUJI, T. 2005. Microwave-assisted synthesis of metallic nanostructure in solution. Chemical European Journal, 11**,** 440-452.

ULABY, F. T., BENGAL, T. H., DOBSON, M. C., EAST, J. R., GARVIN, J. B. & EVANS, D. L. 1990. Microwave dielectric properties of dry rocks. IEEE GEOSCIENCE AND REMOTE SENSING, 28**,** 325-336.

UNITED NATIONS 2013. World population prospects: The 2012 Revision : Key findings and advance tables In: AFFAIRS, D. O. E. A. S. (ed.). New York.

US EPA 1998. Compilation of air pollutant emission factors. In: STANDARDS, O. O. A. A. R. O. O. A. Q. P. A. (ed.) Fourth Edition ed. North Carolina: United States Environmental Protection Agency

VAIDHYANATHAN, B., ANNAPOORANI, K., BINNER, J. & RAGHAVENDRA, R. 2010a. Microwave Sintering of Multilayer Integrated Passive Devices. Journal of the American Ceramic Society, 93**,** 2274-2280.

VAIDHYANATHAN, B., ANNAPOORANI, K., BINNER, J. G. P. & RAGHAVENDRA, R. 2010b. Microwave Assisted Large Scale Sintering of Multilayer Electroceramic Devices. Advanced Processing and Manufacturing Technologies for Structural and Multifunctional Materials III. John Wiley & Sons, Inc.

VELDE, B. 1992. Introduction to Clay Minerals, London, Chapman and Hall.

VENKATESH, M. S. & RAGHAVAN, G. S. V. 2004. An Overview of Microwave Processing and Dielectric Properties of Agri-food Materials. Biosystems Engineering, 88**,** 1-18.

VENKATESH, M. S. & RAGHAVAN, G. V. S. 2005. An overview of dielectric properties measuring techniques. Canadian Biosystems Engineering 47**,** 15-30.

VONGPRADUBCHAI, S. & RATTANADECHO, P. 2009. The microwave processing of wood using a continuous microwave belt drier. Chemical Engineering and Processing, 48**,** 997-1003.

VORSTER, W. 2001. The effect of microwave radiation on mineral processing. PhD, The University of Birmingham.

VORSTER, W., ROWSON, N. A. & KINGMAN, S. W. 2001. The effect of microwave radiation upon the processing of Neves Corvo copper ore. International Journal of Mineral Processing, 63**,** 29-44.

WADA, T. & OSAKA. 1973. Method for the Expansion of Vermiculite. U.S.A patent application 41/61560.

WALKER, G. F. 1949. Water Layers in Vermiculite. Journal of Nature, 163**,** 726-727.

WALKER, J. F. 1961. Vermiculite Minerals, "The X-ray Identification and Crystal Structures of Clay Minerals," London, Mineralogical Society of Great Britian.

WALKER, J. F. & GARRETT, W. G. 1967. Chemical Exfoliation of Vermiculite and the Production of Colloidal Dispersion. Science, 156**,** 385-387.

WALKIEWICZ, J. W., KAZONICH, G. & MCGILL, S. L. 1988. Microwave heating characteristics of selected minerals and compounds. Minerals and Metallurgical Pocessing**,** 39-42.

WANG H; LU S 2003. A new approach to electrification of powdered minerals by electron beam radiation. Journal of mining science, 39**,** 405-409.

WANG, Y. & AFSAR, M. N. 2003. Measurement of complex permittivity of liquids using waveguide techniques. Progress In Electromagnetics Research, 42**,** 131-142.

WBCSD 2013. Greenhouse Gas Protocol. USA: World business council for sustainable development.

WEAVER, C. E. 1956. The distribution and identification of mixed-layer clays in sedimentary rocks. American mineralogists, 41**,** 202-221.

WEBB, W. E. & CHURCH, R. H. 1986. Measurement of dielectric properties of minerals at microwave frequencies. Alabama: United State Department of The Interior.

WEIDEMA, B. P., THRANE, M., CHRISTENSEN, P., SCHMIDT, J. & LØKKE, S. 2008. Carbon Footprint: A Catalyst for Life Cycle Assessment? Journal of Industrial Ecology, 12**,** 1-6.

WHITTAKER, C., MCMANUS, M. C. & SMITH, P. 2013. A comparison of carbon accounting tools for arable crops in the United Kingdom. Environmental Modelling & Software, 46**,** 228-239.

WHITTAKER G. 1994 & 2007. A Basic Introduction to Microwave Chemistry [Online]. Available: http://www.tan-delta.com/basics.html 2011].

WILLS, B. A. & NAPIER-MUNN, T. J. 2006. Mineral Processing Technology: An Introduction to the Practical Aspects of Ore Treatment and Mineral Recovery, Oxford, GB, Butterworth-Heinemann (Elsevier).

XUEYI, G., SONGWEN, X., XIAO, X., QIHOU, L. & RYOICHI, Y. 2002. LCA case study for lead and zinc production by an imperial smelting process in china a brief presentation. The International Journal of Life Cycle Assessment, 7**,** 276-276.

YARLAGADDA, K. D. V. P. & CHUAN, C. T. 1998. An investigation into welding of engineering thermoplastics using focused microwave energy. Journal of Materials Processing Technology, 74**,** 199-212.

YE, H.-M., LI, X.-H. & LAN, Z.-W. 2013. Geochemical and Sr–Nd–Hf–O–C isotopic constraints on the origin of the Neoproterozoic Qieganbulake ultramafic–carbonatite complex from the Tarim Block, Northwest China. Lithos, 182–183**,** 150-164.

YOSHIKAWA, N. 2011. Recent studies on fundamentals and application of microwave processing of materials. In: GRUNDAS, S. (ed.) Advances in induction and microwave heating of minerla and organic materials. In-Tech.

YOUNG, J. 2013. MA 28351 "Mud Tank". Melbourne: Davenport Resources Limited.

ZHAO, M., TONGJIANG, P., YONGGUANG, X. & WEI, Y. 2010. Preparation of Expanding Vermiculite by Chemical and Microwave Methods. Advanced Material Research, 96**,** 155-160.

ZLOTORZYNSKI, A. 1995. The Application of Microwave Radiation to Analytical and Environmental Chemistry. Critical Reviews in Analytical Chemistry, 25**,** 43-76.

APPENDIX 1

XRD Patterns of measured vermiculite and identified minerals

XRD Pattern of Brazilian Sample

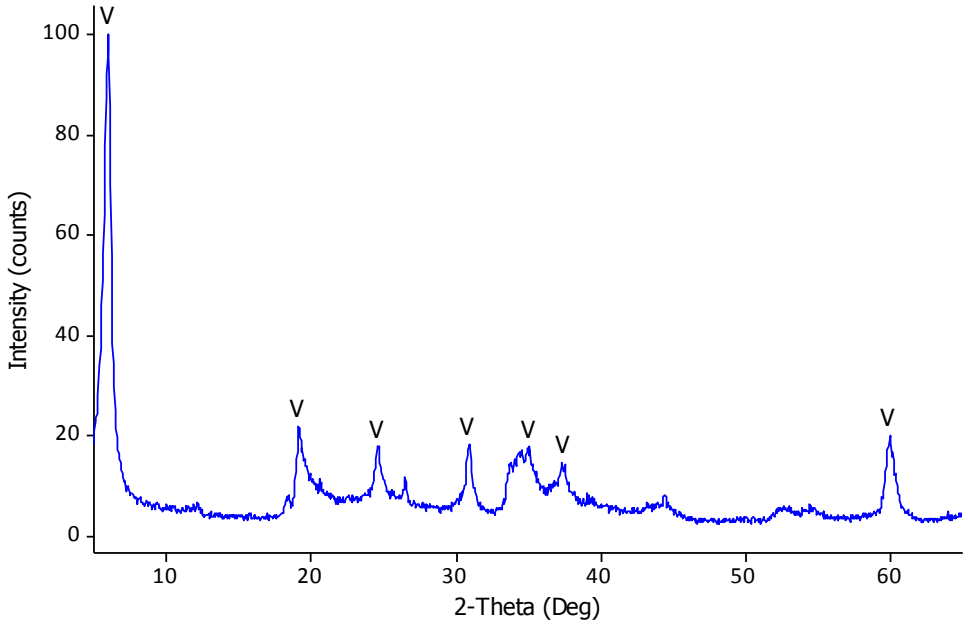

XRD Pattern of Chinese Sample

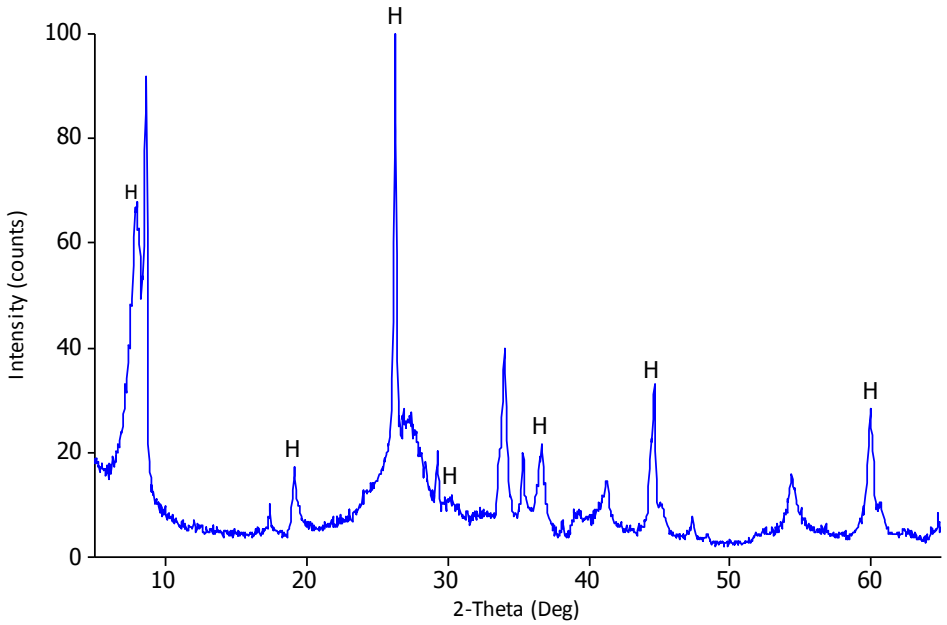

XRD Pattern of Australian Sample

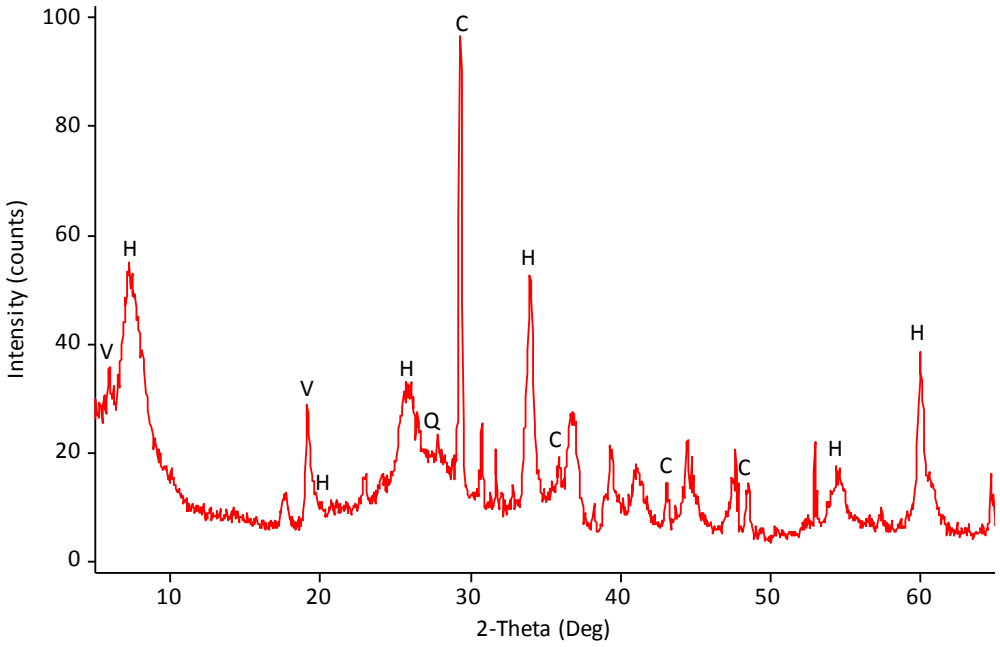

XRD Pattern of South African Sample

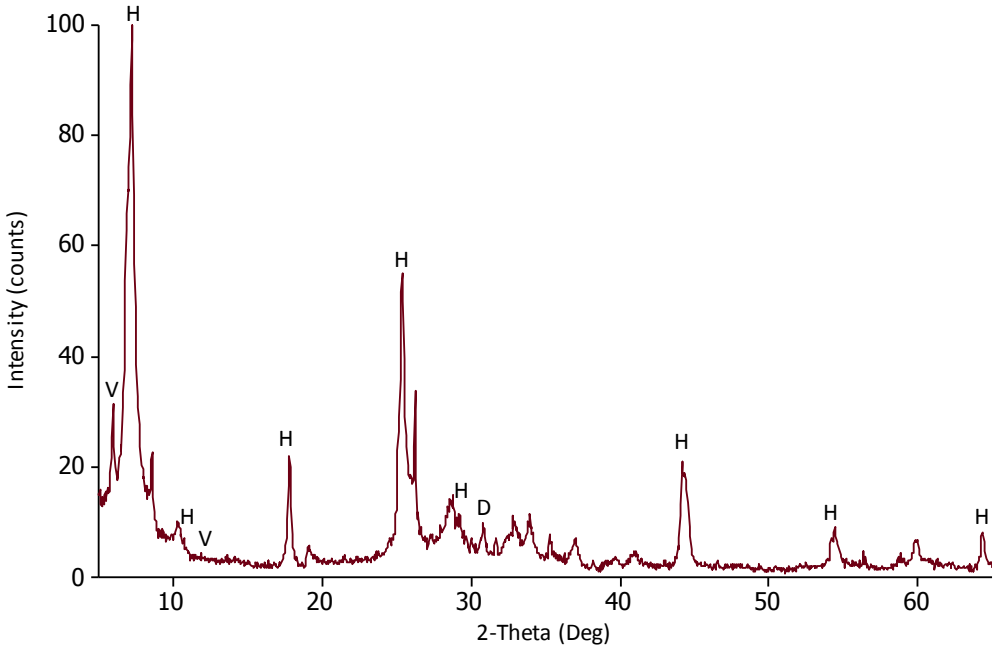

XRD Pattern of Apatite

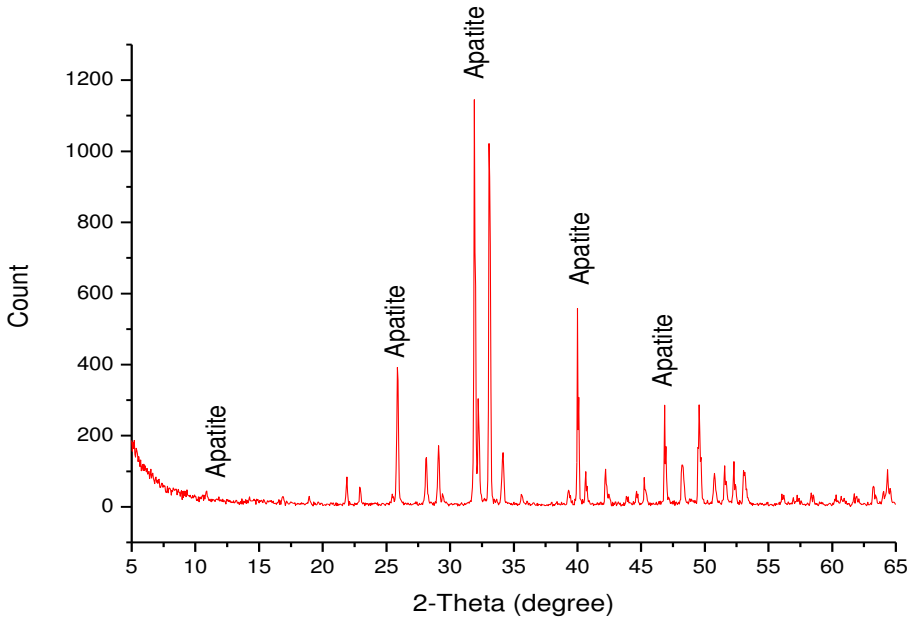

XRD Pattern of Augite

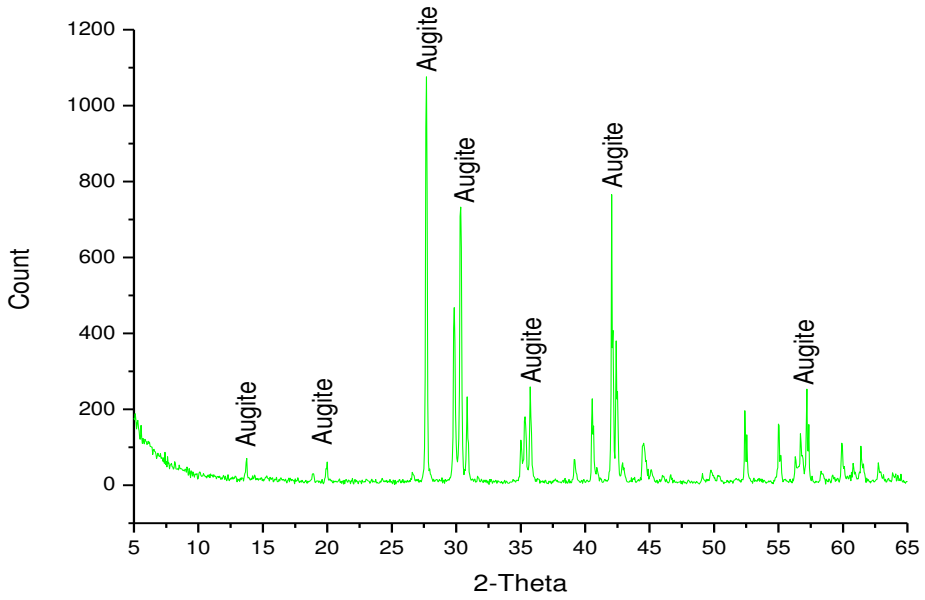

XRD Pattern of Hydrobiotite

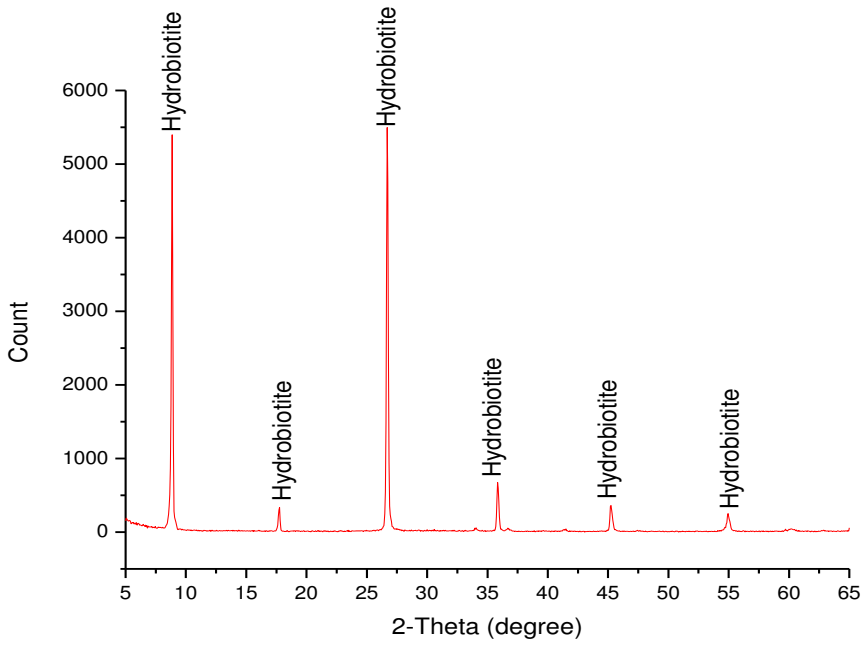

XRD Pattern of Dolomite

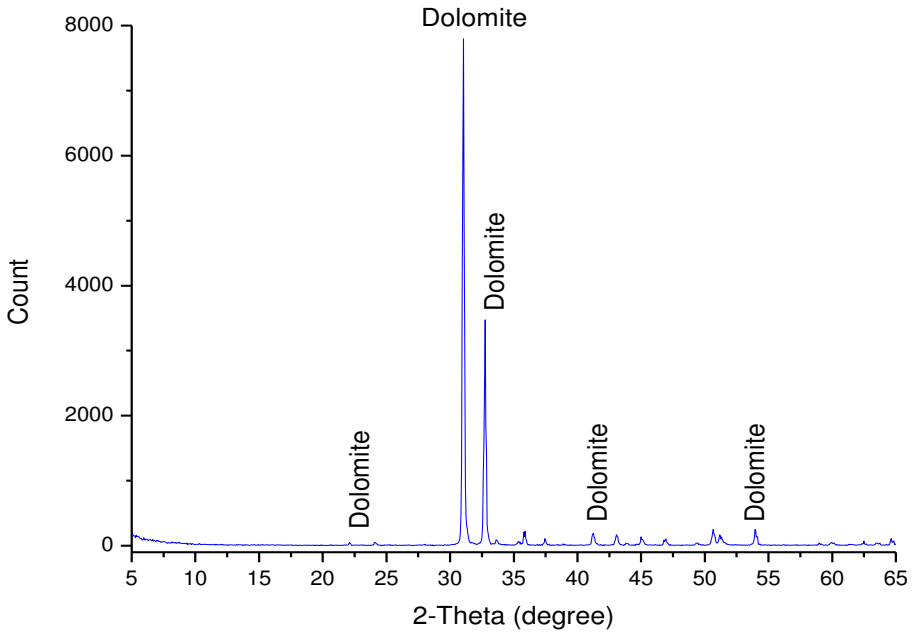

XRD Pattern of Albite

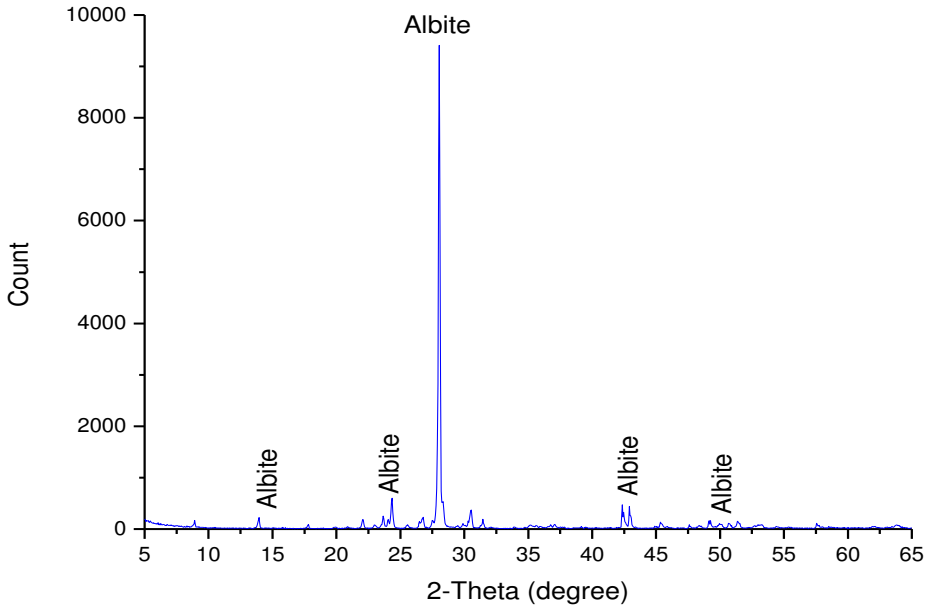

XRD Pattern of Ilmenite

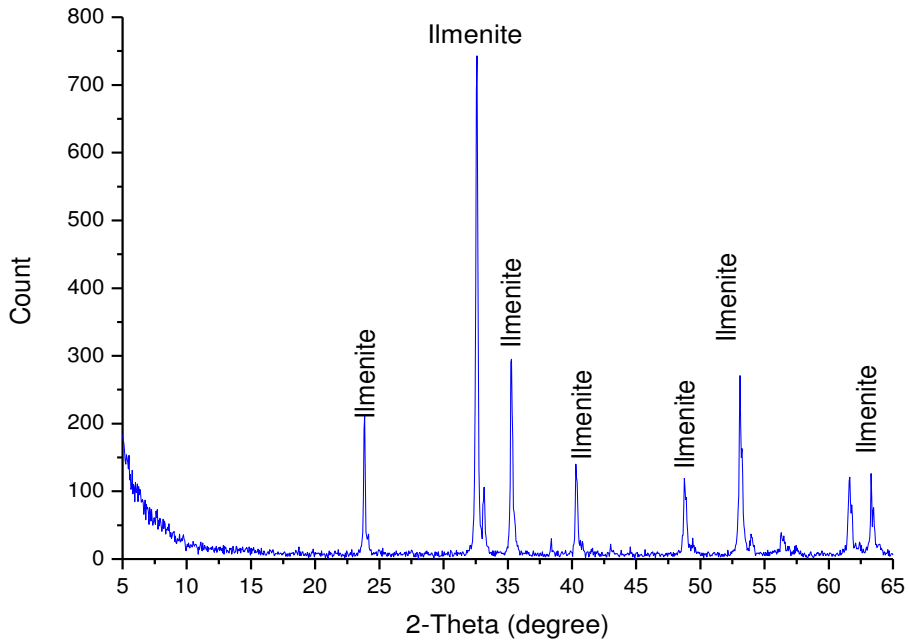

XRD Pattern of Magnetite

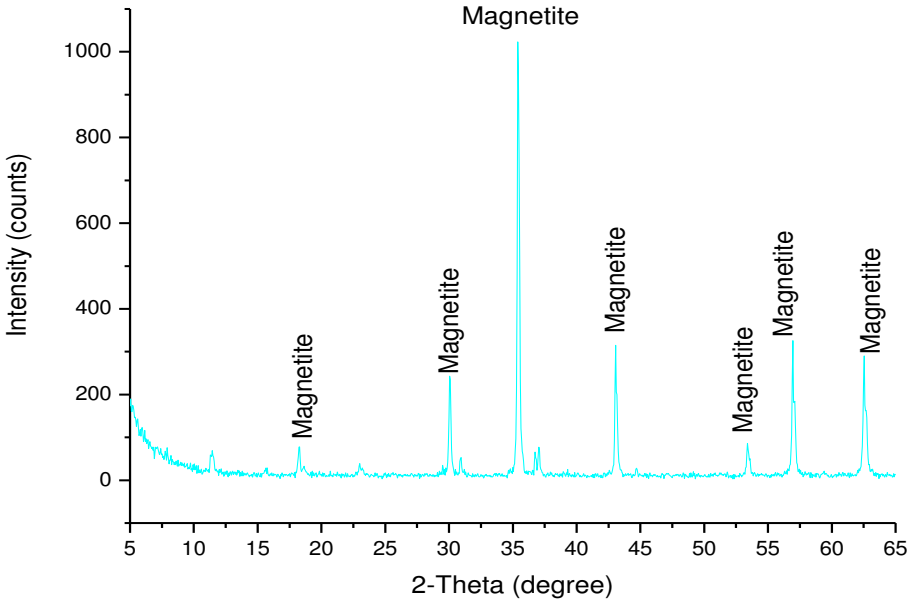

XRD Pattern of Quartz

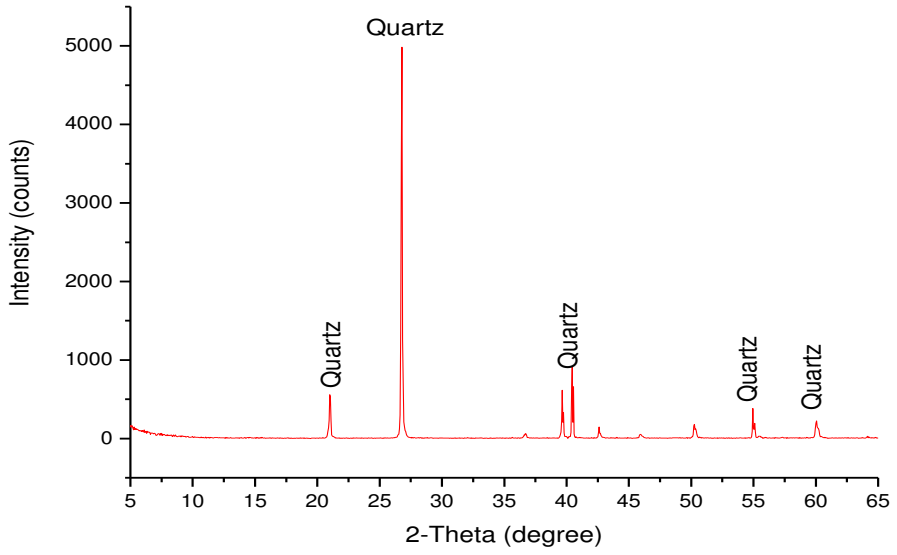

APPENDIX 2

Dielectric Properties of Vermiculite and Associated Minerals

Dielectric Properties of Identified Minerals by Mineral Liberation Analysis

Mineral	Freq. (MHz)	ε'+jε''	ε'+jε''	ε'+jε''	ε'+jε''
Apatite		1.73g/cm³	1.82g/cm³	2.113g/cm³	2.15g/cm³
	934	3.36+j0.013	3.42+j0.014	4.22+j0.017	4.26+j0.018
	2143	3.36+j0.005	3.46+j0.007	4.17+j0.009	4.22+j0.010
Augite		1.72g/cm³	1.91g/cm³	2.19g/cm³	2.26g/cm³
	934	2.72+j0.017	3.00+j0.023	3.33+j0.024	3.51+j0.027
	2143	2.45+j0.007	2.74+j0.008	3.13+j0.010	3.24+j0.013
Dolomite		1.54g/cm³	1.73g/cm³	1.91g/cm³	2.03g/cm³
	934	2.84+j0.013	3.03+j0.013	3.20+j0.013	3.35+j0.013
	2143	2.85+j0.016	3.06+j0.020	3.28+j0.021	3.47+j0.022
Magnetite		2.16g/cm³	2.40g/cm³	2.64g/cm³	2.80g/cm³
	934	6.39+j0.044	7.44+j0.058	8.48+j0.070	9.17+j0.081
	2143	6.52+j0.052	7.59+j0.070	8.64+j0.086	9.35+j0.098
Titanite		1.90g/cm³	2.30g/cm³	2.40g/cm³	2.50g/cm³
	934	4.34+j0.011	5.62+j0.015	5.86+j0.017	6.28+j0.018
	2143	4.42+j0.013	5.71+j0.018	5.95+j0.018	6.37+j0.020
Quartz		1.32g/cm³	1.38g/cm³	1.44g/cm³	1.78g/cm³
	934	2.15+j0.004	2.21+j0.009	2.25+j0.014	2.54+j0.040
	2143	2.17+j0.005	2.23+j0.006	2.27+j0.007	2.56+j0.020
Hydrobiotite		0.96g/cm³	1.02g/cm³	1.25g/cm³	1.42g/cm³
	934	1.71+j0.022	1.77+j0.023	1.94+j0.029	2.12+j0.035
	2143	1.70+j0.013	1.77+j0.014	1.93+j0.018	2.12+j0.022

Dielectric Properties of South African Sample (superfine) as measured by waveguide technique

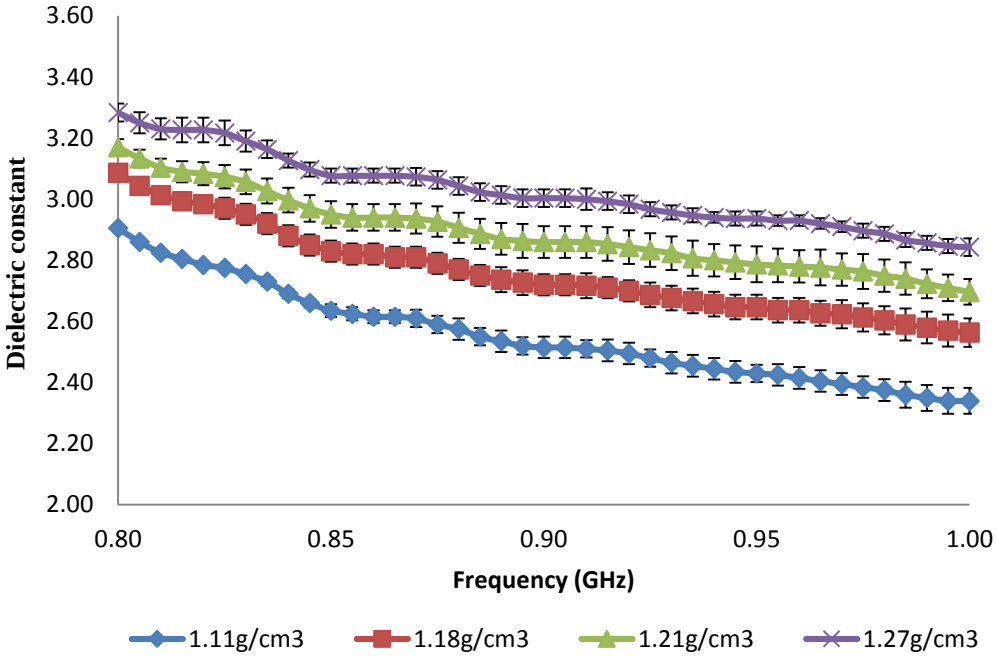

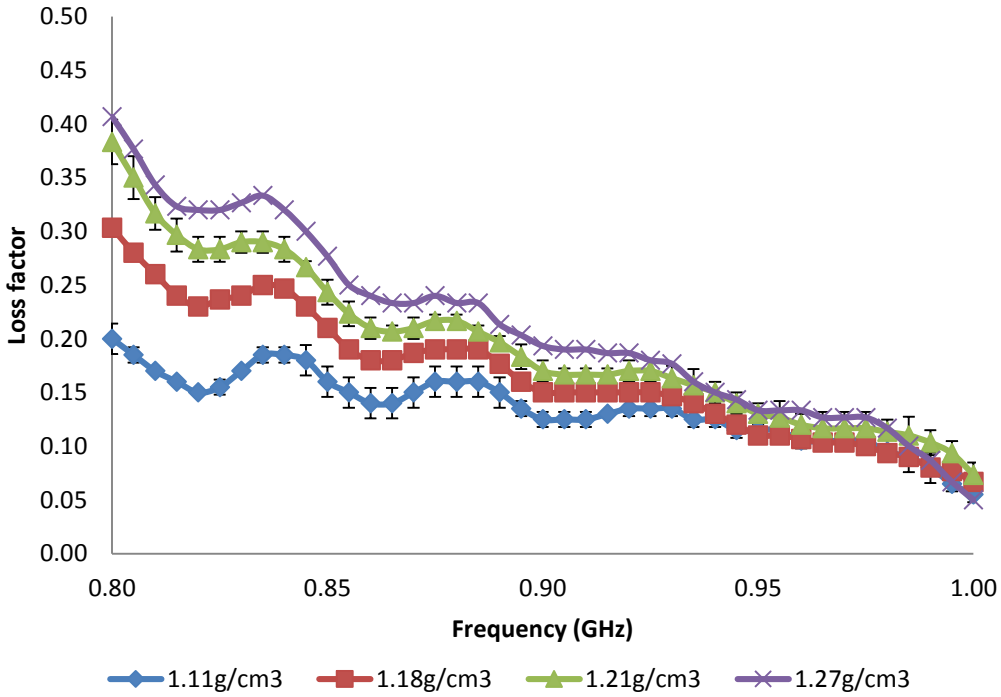

Dielectric Properties of Australian Sample (superfine) as measured by waveguide technique

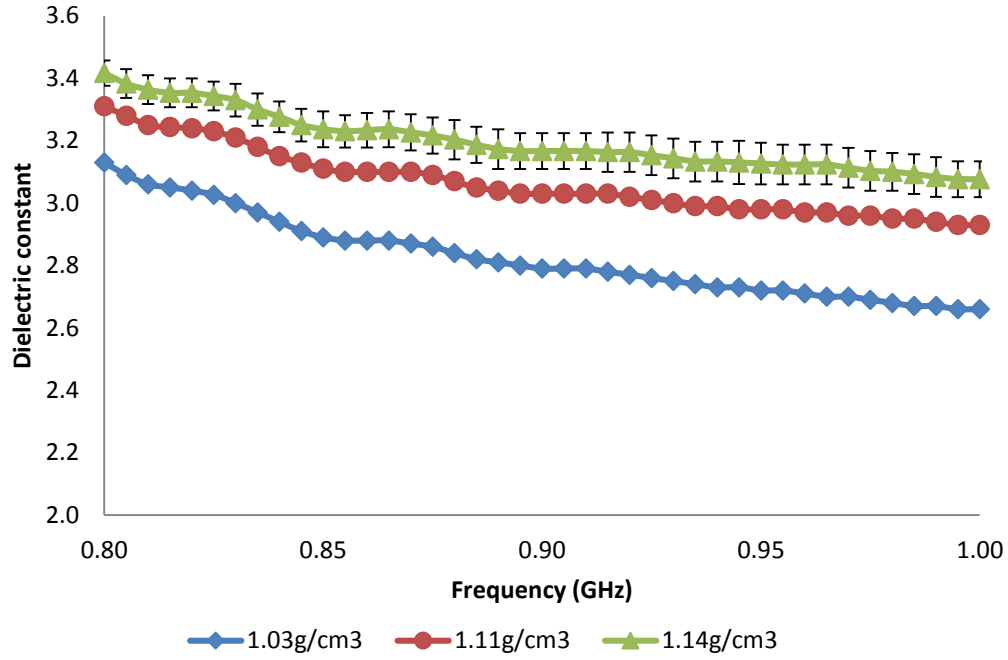

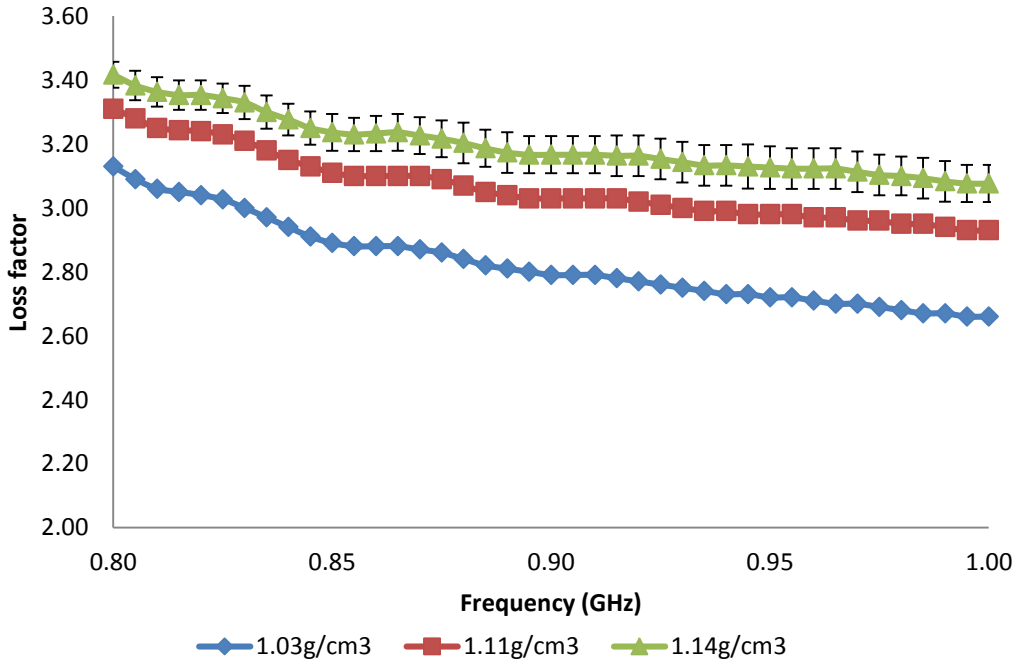

Dielectric Properties of Brazilian Sample (Medium) as measured by waveguide technique

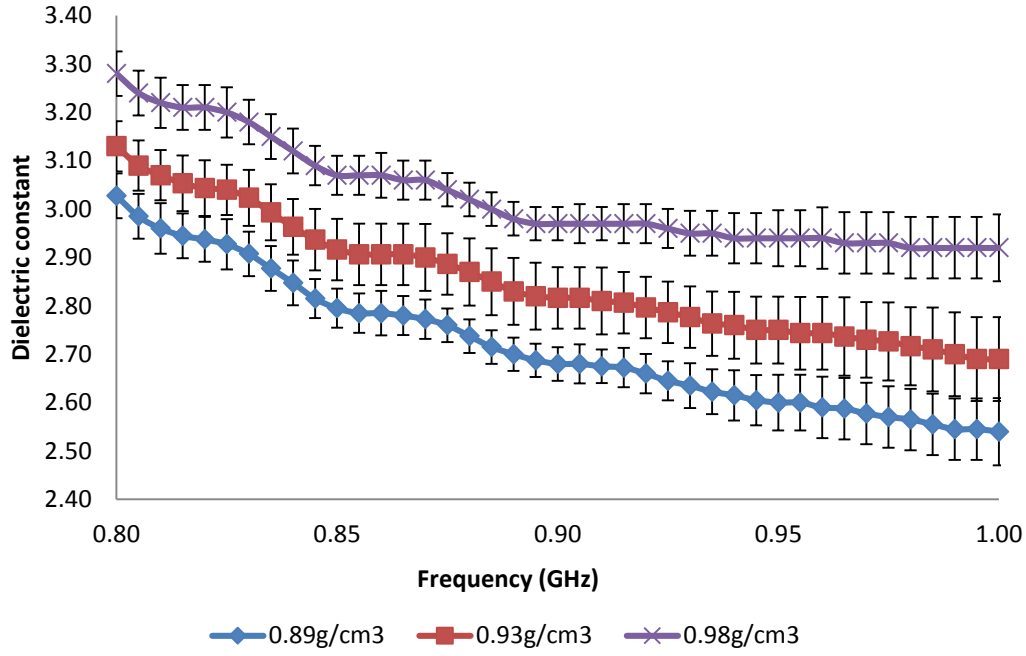

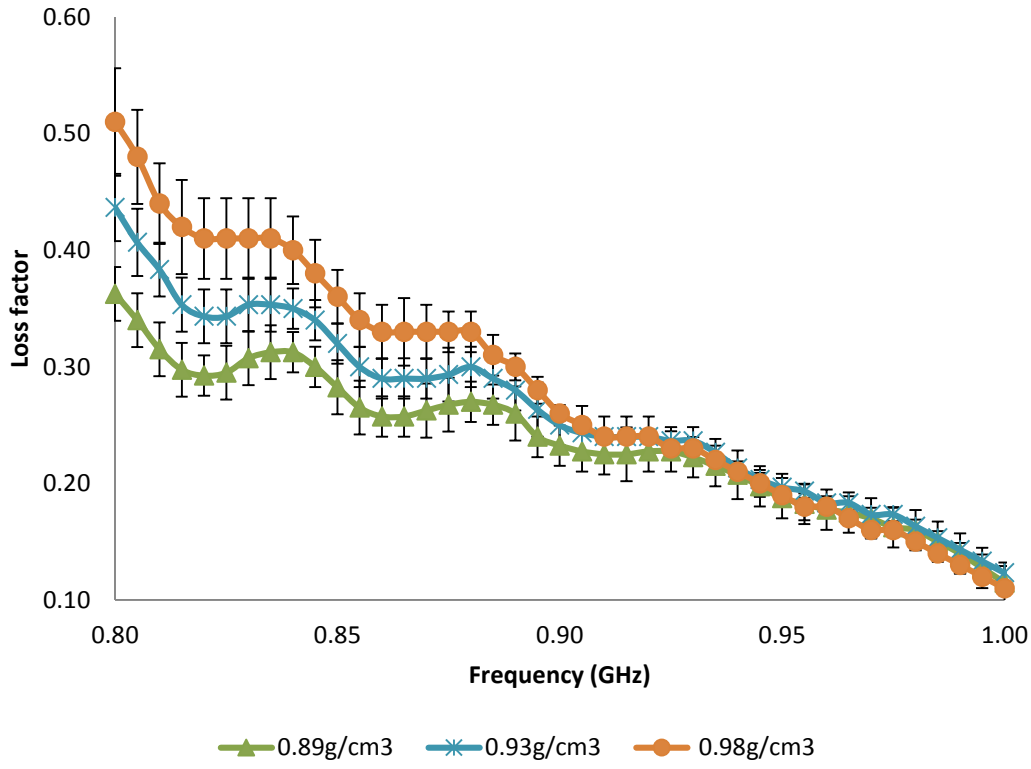

Dielectric Properties of Chinese Sample (Medium) as measured by waveguide technique

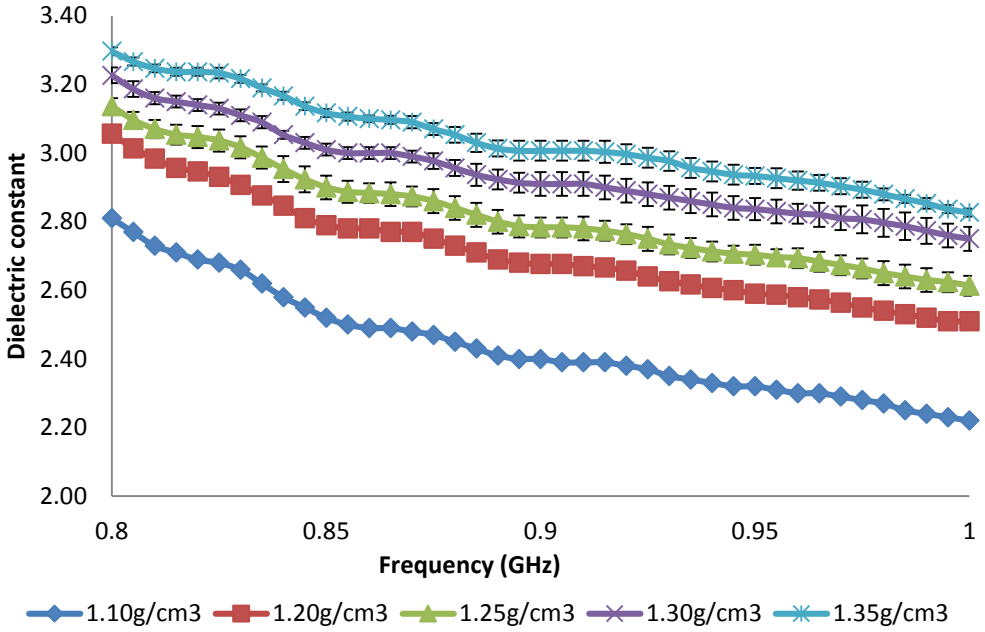

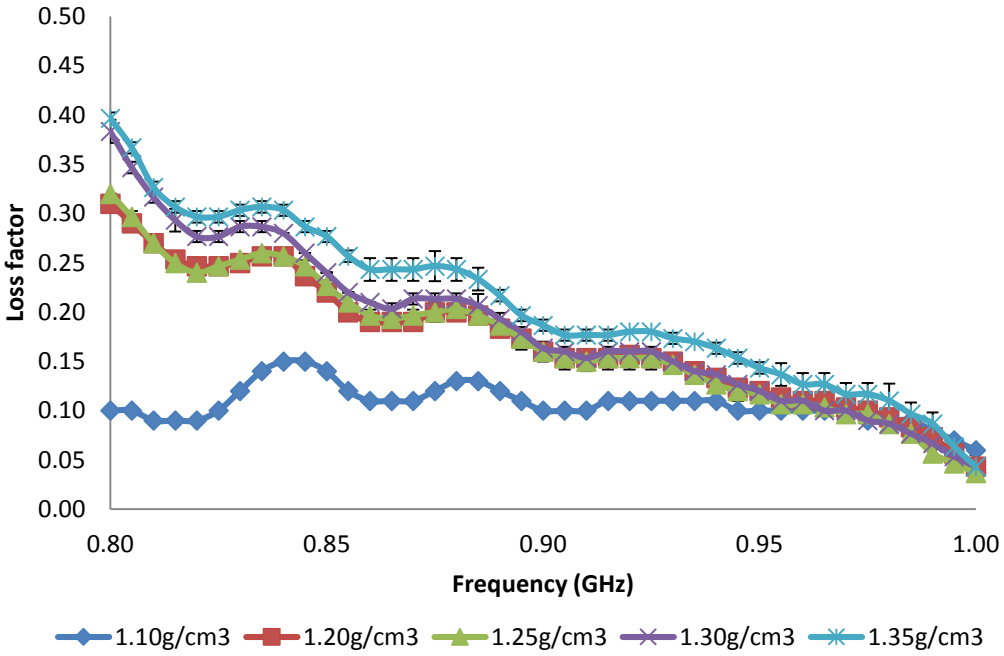

APPENDIX 3

Theoretical estimation of dielectric properties of vermiculite

A.3.1 Theoretical estimation of permittivity of vermiculite

Plots of dielectric constant and loss factor for each pulverised sample versus bulk density of vermiculite samples from Australia, Brazil, China and South Africa were used for the graphical extrapolation of both dielectric constant and loss factor for the solid form of vermiculite. For the South African sample, the measured dielectric constant and loss factor of the pulverised sample at 934 MHz and 2143 MHZ and bulk densities of 0.84 g/cm^3-1.42 g/cm^3 are shown in Figure A:3-1 and Figure A:3-2 respectively.

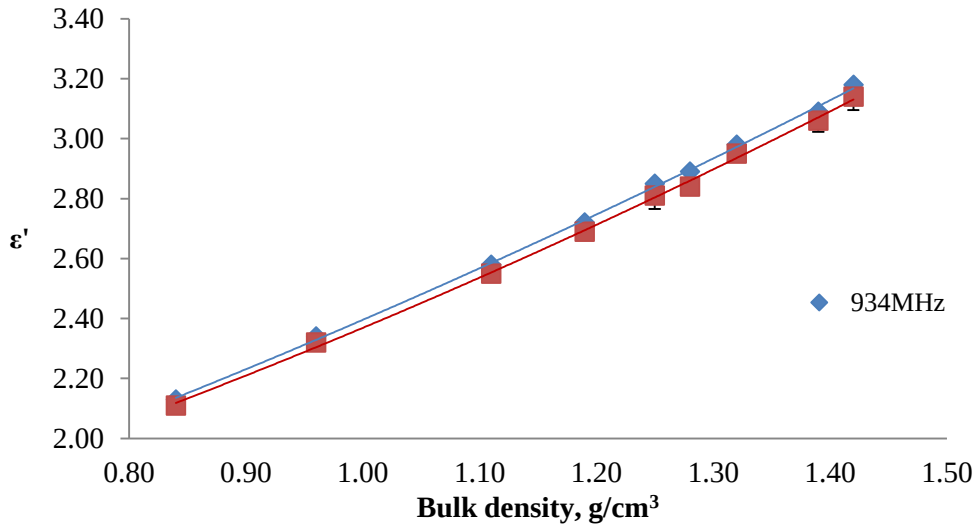

Figure A:3-1: Second order polynomial regression curve of dielectric constant (934 and 2143 MHz) of pulverised South African sample against bulk density.

The dielectric constant and loss factors are repeatable as shown by the small error bars in Figure A:3-1 and Figure A:3-2. A second order polynomial regression curve, is the best line of fit obtained with a regression coefficient higher than 0.99, for both measurements and at the two frequencies. This agrees with results published in the literature for different materials (Nelson, 1992b, Kent, 1977, Nelson et al., 1989). The regression equations obtained for both dielectric constant and loss factor are also consistent with Equation 4-13 and Equation 4-14 respectively. This indicates that the measured vermiculite is an air-particle mixture of needles or random inclusions (Asami, 2002).

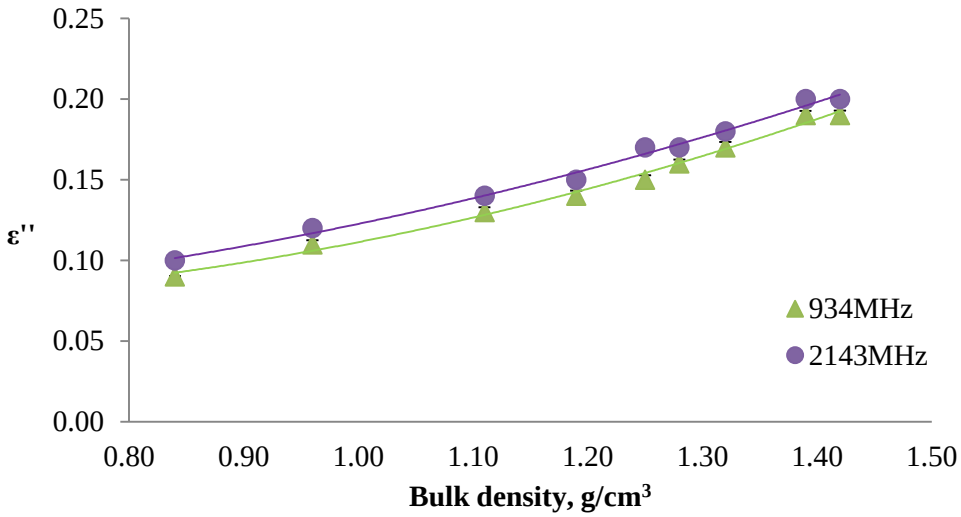

Figure A:3-2: Second order polynomial regression curve of loss factor (934 and 2143 MHz) of pulverised South African vermiculite against bulk density

The coefficients of the second order polynomial were obtained for both dielectric constant and loss factor curves. They were then used to estimate the dielectric constant and loss factor of the solid form of the South African sample at its measured particle density of 2.71 g/cm^3.

The same procedure was performed on dielectric constant and loss factor data for pulverised Australian, Brazilian and Chinese samples measured over a range of bulk densities in order to estimate both the dielectric constant and loss factor of their solid forms. The second order polynomial curves of dielectric constant and loss factor versus bulk density of the Australian sample are shown in Figure A:3-3 and Figure A:3-4 respectively. Figure A:3-5 and Figure A:3-6 present data for the Brazilian sample while FigureA:3-7 and Figure A:3-8 show data for the Chinese sample.

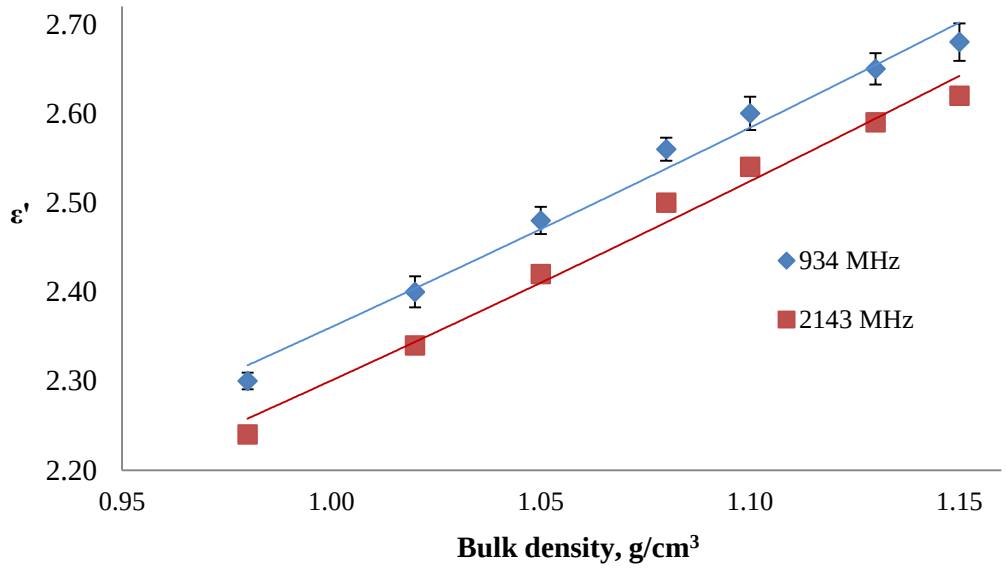

Figure A:3-3: Second order polynomial regression curve of dielectric constant (934 and 2143 MHz) of Australian sample against bulk density.

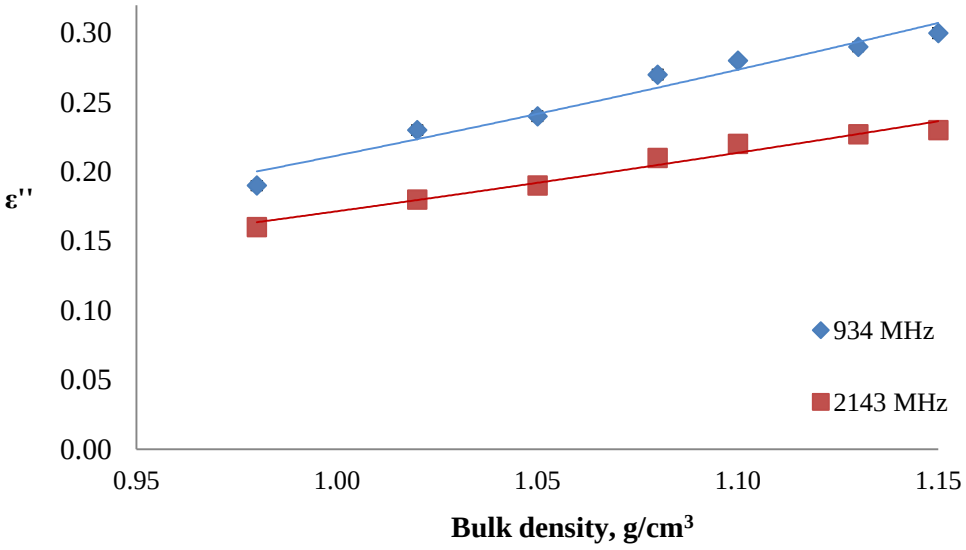

Figure A:3-4: Second order polynomial regression curve of loss factor (934 and 2143 MHz) of pulverised Australian sample against density

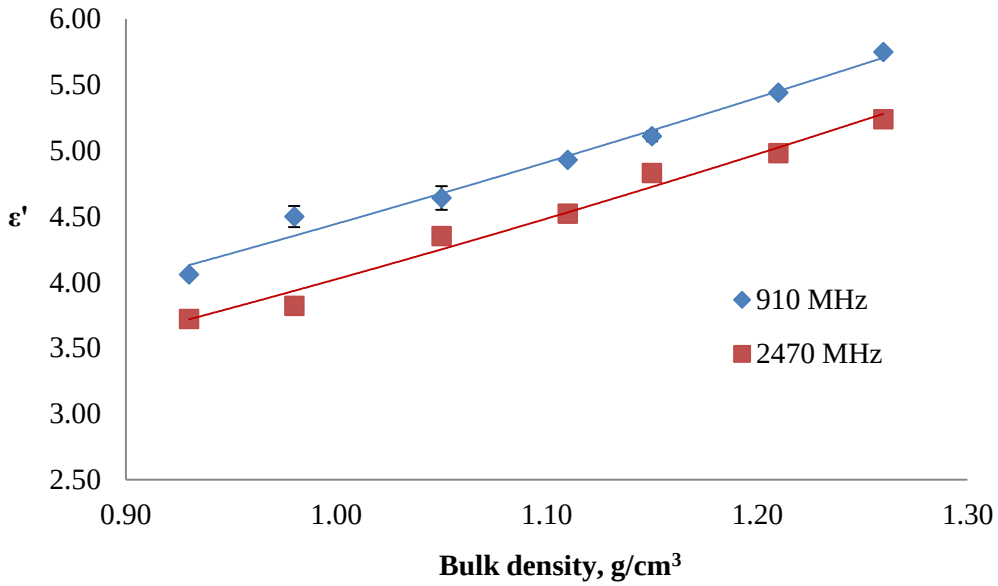

Figure A:3-5: Second order polynomial regression curve of dielectric constant (910 and 2470 MHz) of Brazilian pulverised vermiculite against bulk density.

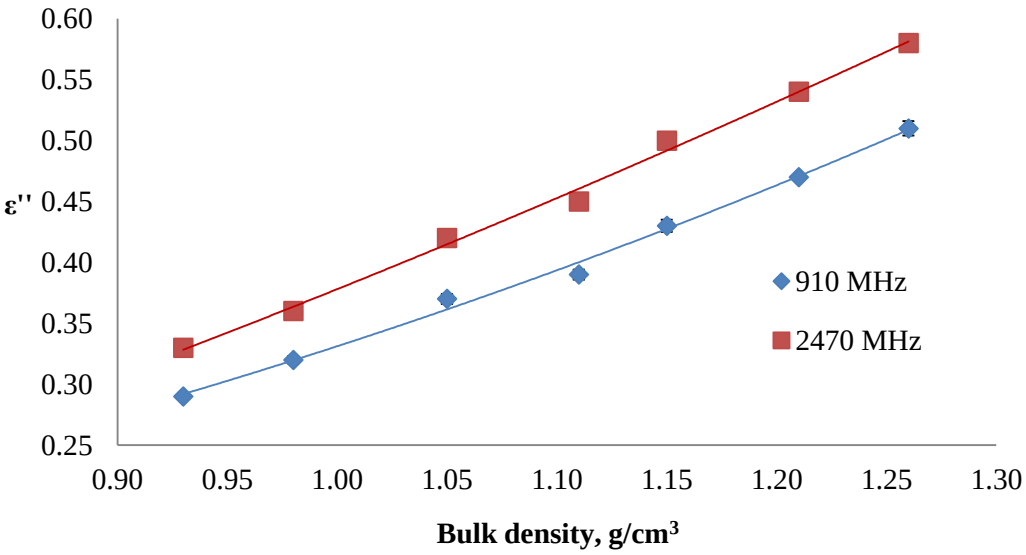

Figure A:3-6: Second order polynomial regression curve of loss factor (910 and 2470 MHz) of pulverised Brazilian sample against bulk density

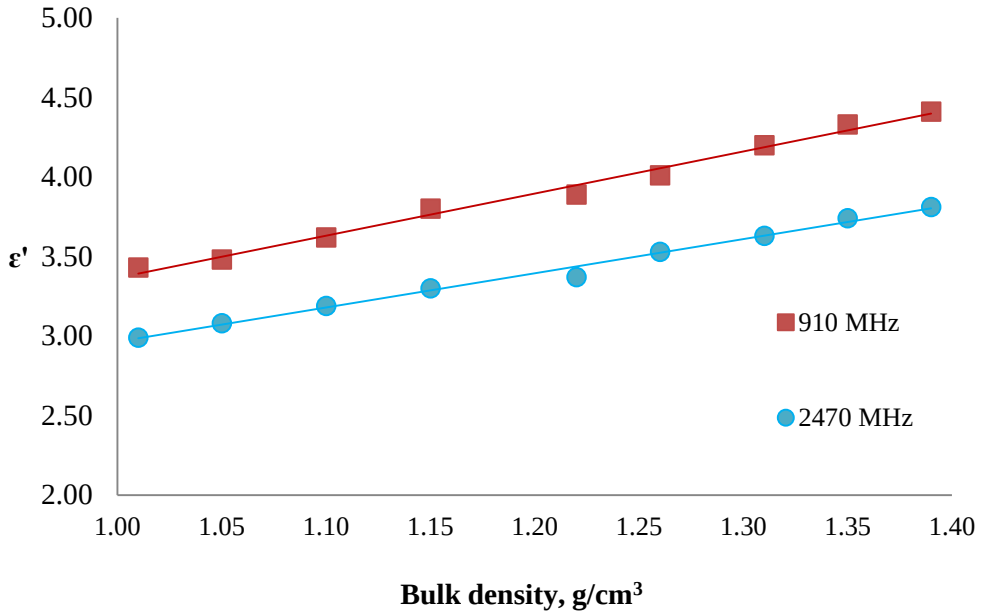

Figure A:3-7: Second order polynomial regression curve of dielectric constant (910 and 2470 MHz) of pulverised Chinese sample against bulk density

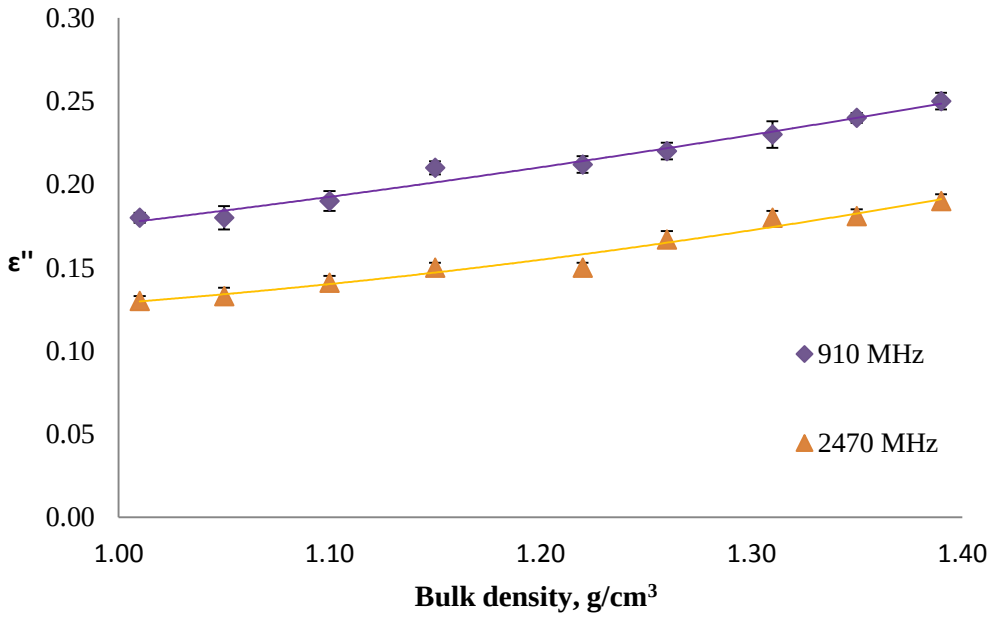

Figure A:3-8: Second order polynomial regression curve of loss factor (910 and 2470 MHz) of pulverised Chinese vermiculite against its bulk density

It is also possible to use linear extrapolation to estimate the dielectric constant of a solid material from the linear relationships of square root and cube root of measured dielectric constant of its pulverised form versus the bulk density. These are consistent with Equation 4-15. Figure A:3-9 and Figure A:3-10

respectively show the linear relationships of both square root and cube root of the measured dielectric constant of South African sample to bulk density.

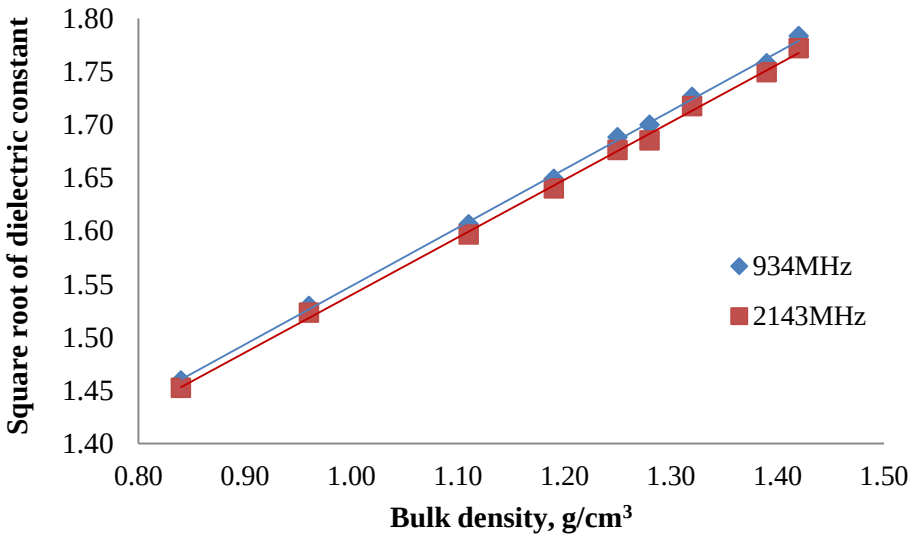

Figure A:3-9: Linear relationship of between $\sqrt{\varepsilon'}$ of South African sample with bulk density

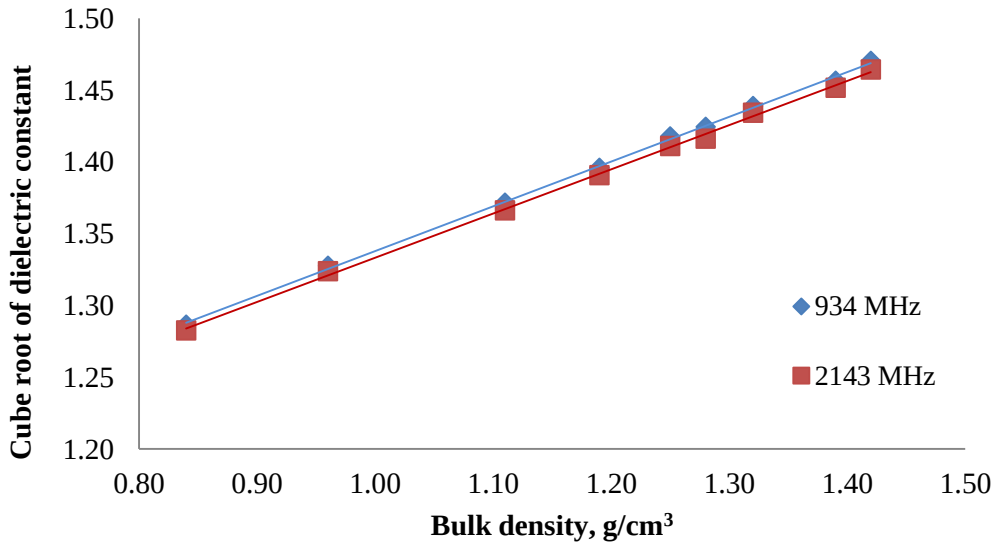

Figure A:3-10: Linear relationship between $\sqrt[3]{\varepsilon'}$ of South African sample with bulk density

Similarly, Figure A:3-11 and Figure A:3-12 show the linear relationships of both square root and cube root of the measured dielectric constant for the Australian sample to bulk density. The error bars are small because the results are repeatable.

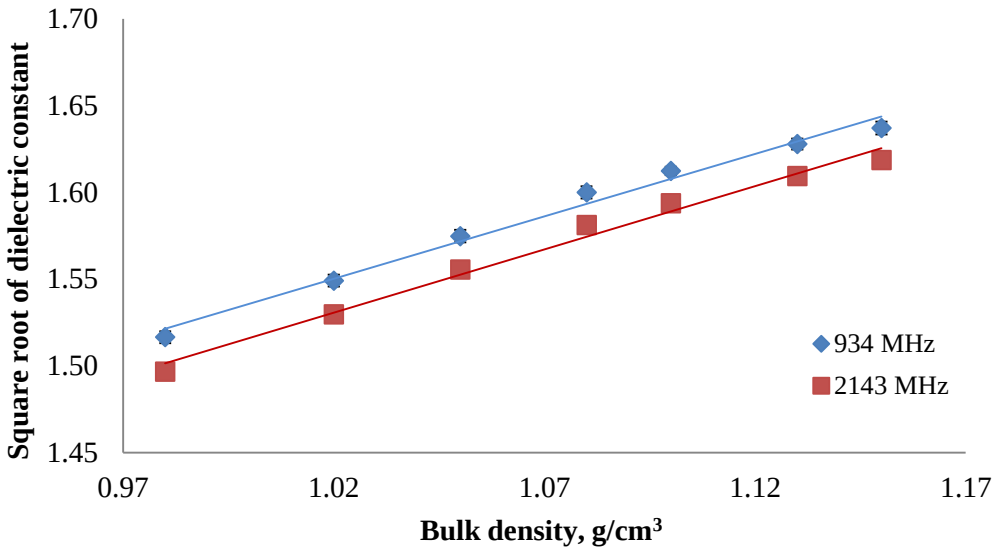

Figure A:3-11: Linear relationship between $\sqrt{\varepsilon'}$ of Australian sample with bulk density

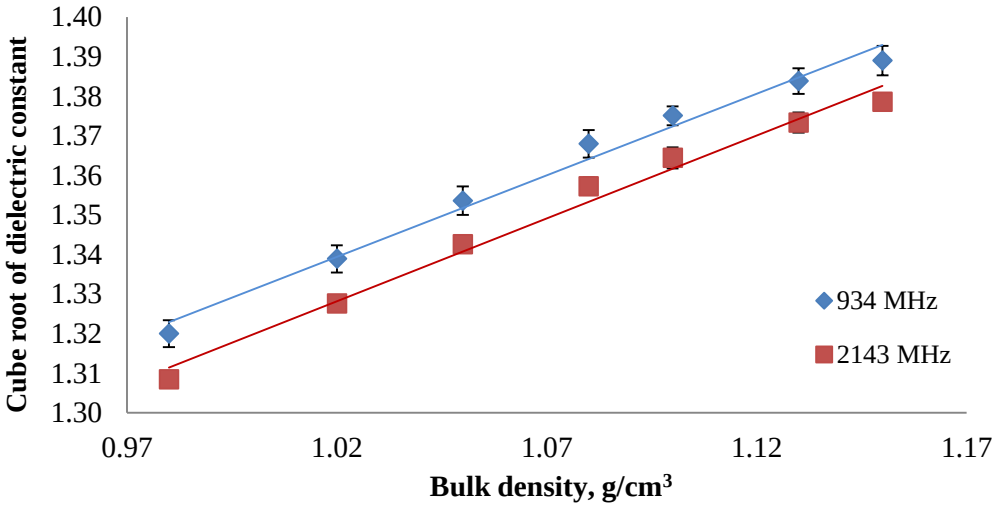

Figure A:3-12: Linear relationship between $\sqrt[3]{\varepsilon'}$ of Australian sample with bulk density

Figure A:3-13 and Figure A:3-14 present the linear relationships of square root and cube root of dielectric constant with density for vermiculite ore from Brazil while Figure A:3-15 and Figure A:3-16 illustrate similar relationships for the Chinese sample.

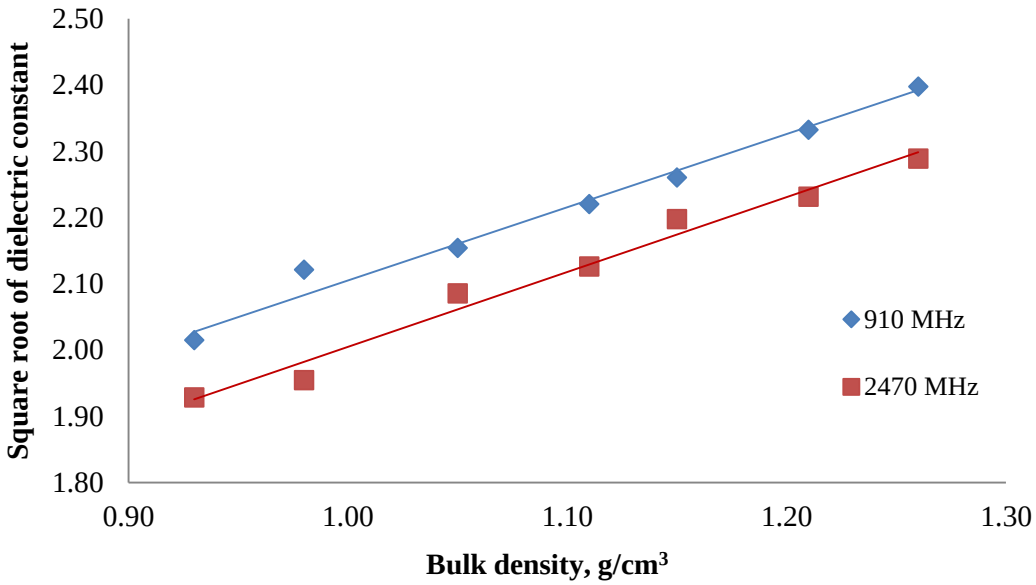

Figure A:3-13: Linear relationship between $\sqrt{\varepsilon'}$ of Brazilian sample with bulk density

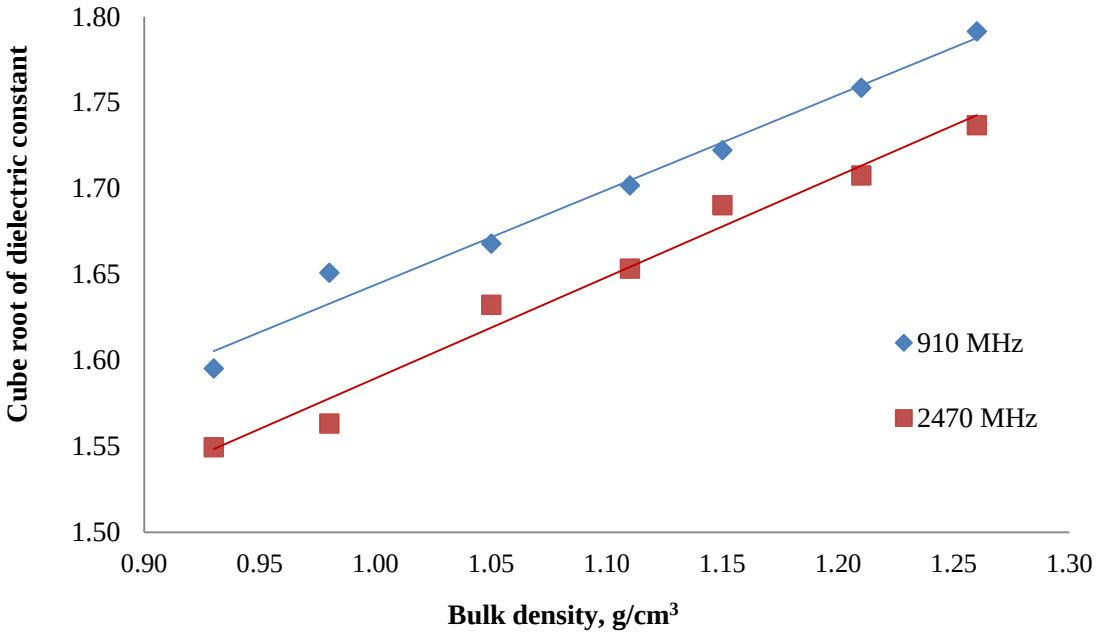

Figure A:3-14: Linear relationship between $\sqrt[3]{\varepsilon'}$ of Brazilian sample with bulk density

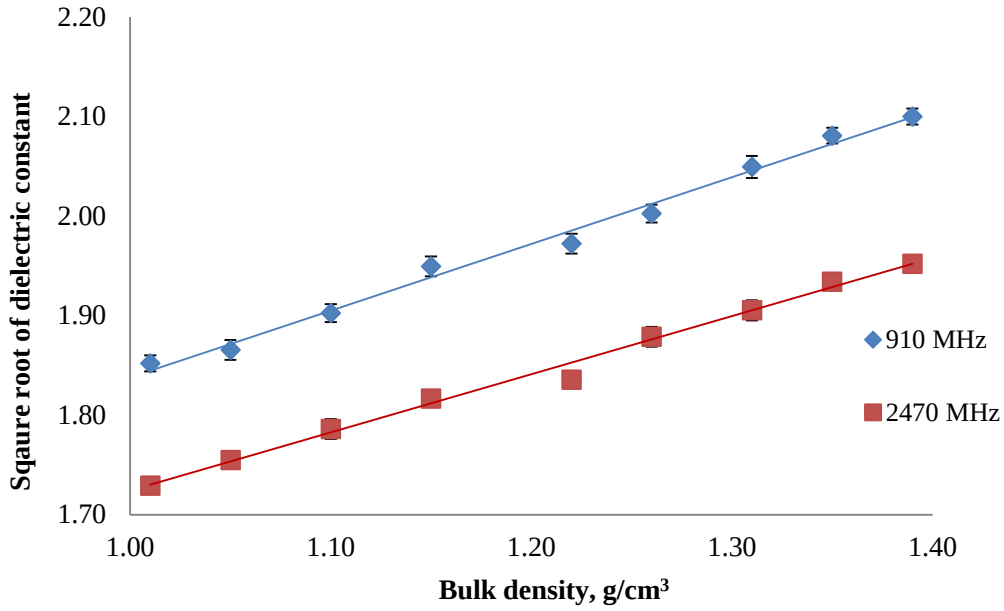

Figure A:3-15: Linear relationship between $\sqrt{\varepsilon'}$ of Chinese sample with bulk density

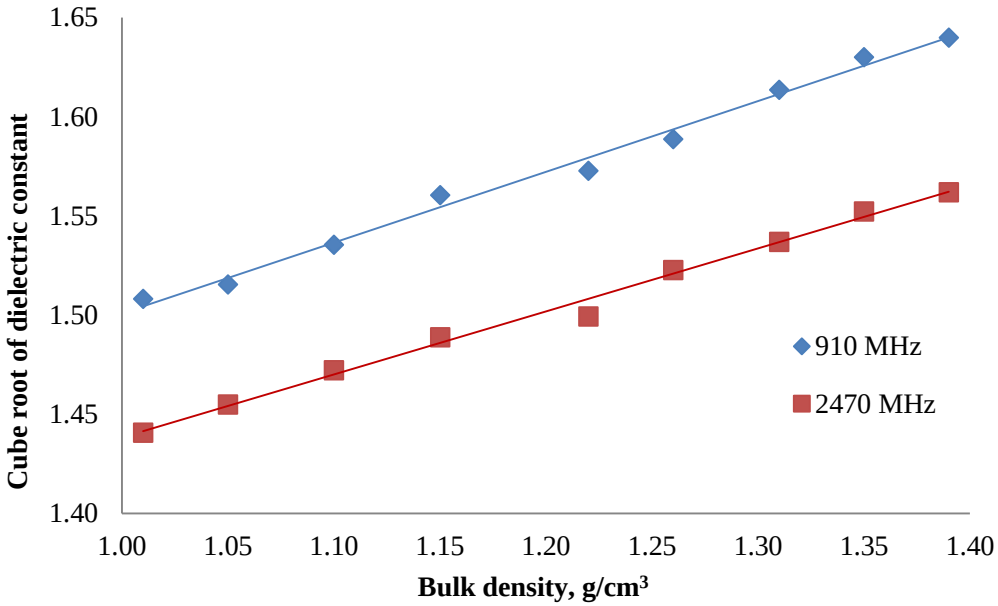

Figure A:3-16: Linear relationship between $\sqrt[3]{\varepsilon'}$ of Chinese sample with bulk density

These relationships were used to estimate the dielectric constant of solid forms of vermiculite from South Africa, Australia, Brazil and China. In these curves, only the data points of the measured ε' and ε'' are shown, as the points ρ=0: ε'=1 and ρ=0: ε''=0, which respectively correspond to the dielectric constant and loss factor of air at zero density were excluded for the purpose of clarity.

The regression analyses of the square root relationships give an intercept closer to '1' than the cube-root curves. This implies that the relationship between the square root of dielectric constant and bulk density may be closer to true linearity and hence will give the best estimation, i.e. closer to the true value. Regression of the square root and cube root curves gives linear equations expressed as Equation A:3-1 and Equation A:3-2 respectively, with regression constants K and K_0, which represent the intercept and slope. The parameter ρ represents the bulk density. These equations are similar to Equation 4-15.

$$\sqrt{\varepsilon'} = K + K_0\rho \qquad \text{Equation A:3-1}$$

$$\sqrt[3]{\varepsilon'} = K + K_0\rho \qquad \text{Equation A:3-2}$$

For the estimation of the loss factor of solid vermiculite, the linear relationships of $\sqrt{\varepsilon''}$ for the measured pulverised vermiculite samples with bulk density were used. Figure A:3-17 to Figure A:3-20 illustrate the relationship of $\sqrt{\varepsilon''}$ for South African, Australian, Brazilian and Chinese samples with bulk density. The loss factor of the solid form was then extrapolated from the curves using the measured particle density.

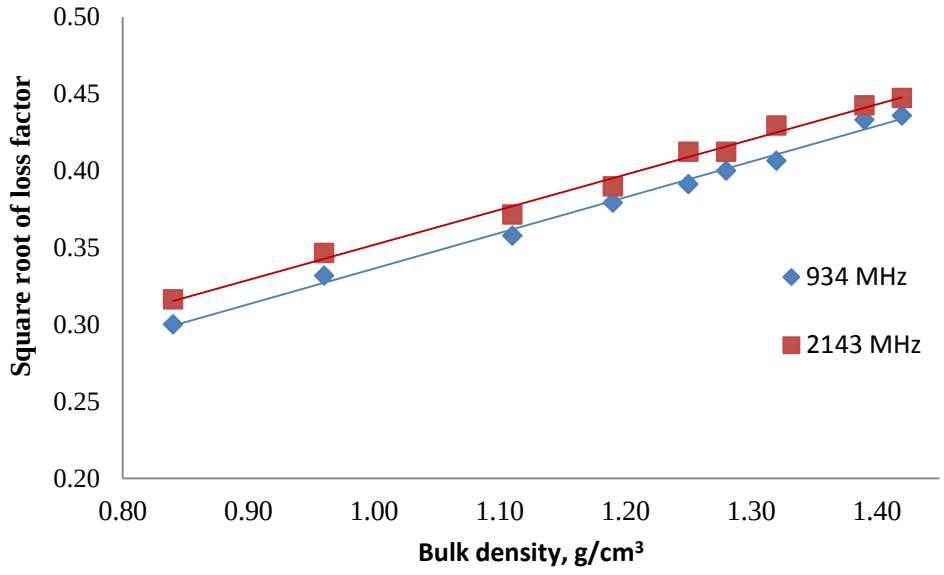

Figure A:3-17: Linear relationship between $\sqrt{\varepsilon''}$ of South African sample and density

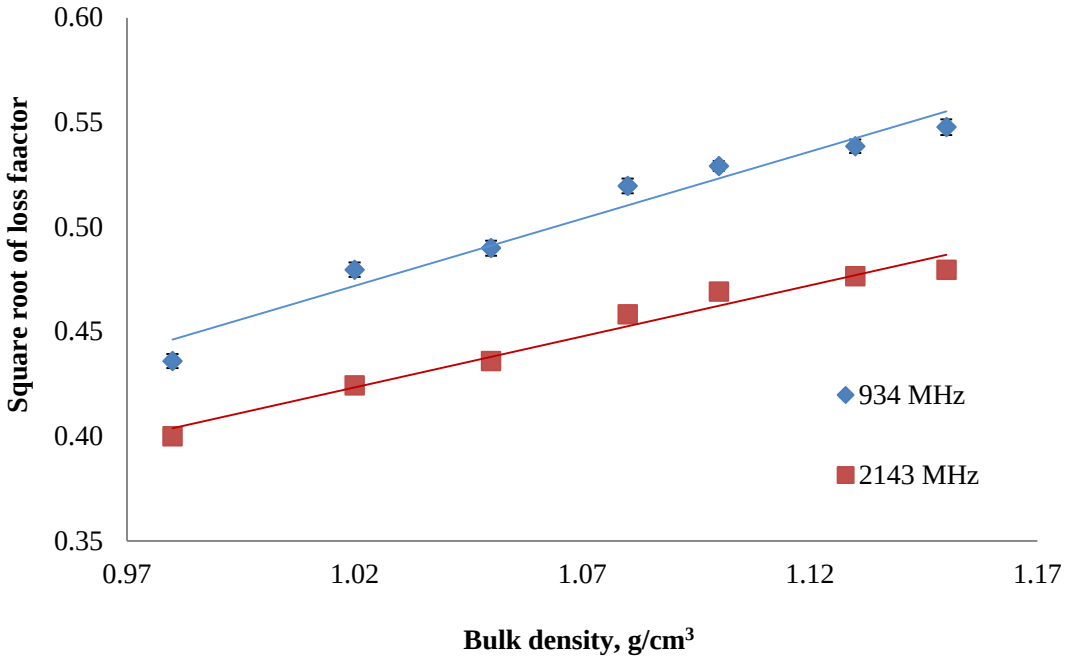

Figure A:3-18: Linear relationship between $\sqrt{\varepsilon''}$ of Australian sample and bulk density

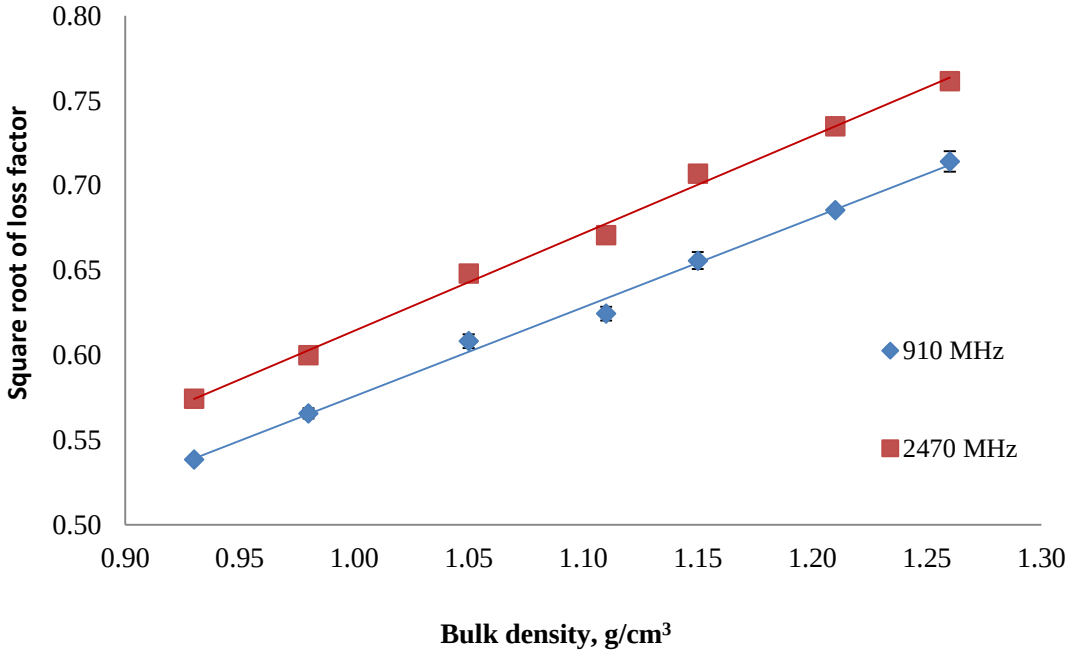

Figure A:3-19: Linear relationship between $\sqrt{\varepsilon''}$ of Brazilian sample and density

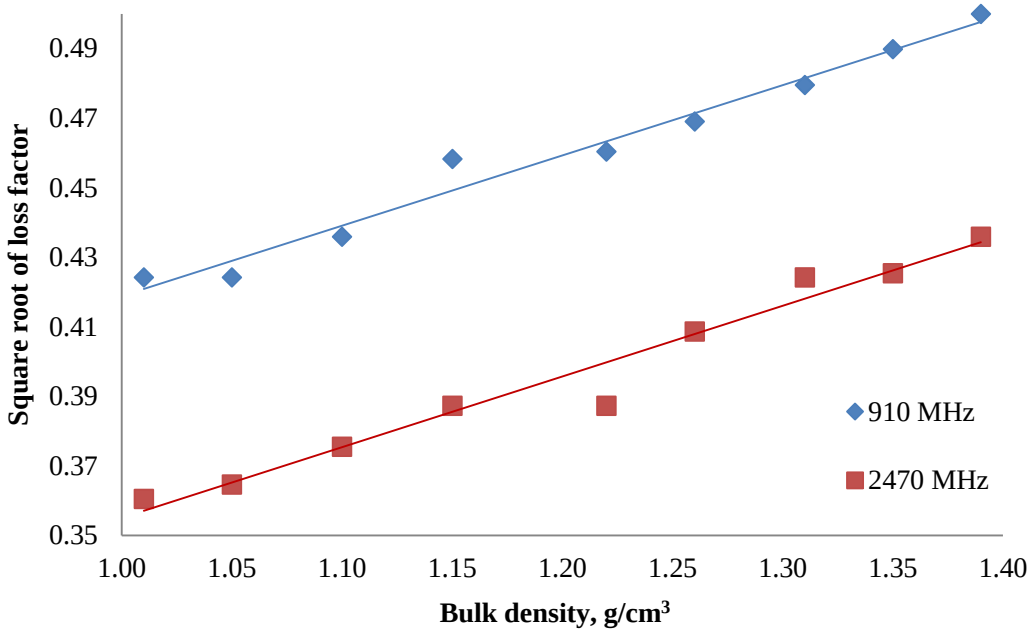

Figure A:3-20: Linear relationship between $\sqrt{\varepsilon''}$ of Chinese sample and density

In addition to using the linear function $\sqrt{\varepsilon''}$ versus bulk density for estimating the loss factor of solid vermiculite, linear regression curves of $(\varepsilon'' + \frac{\delta^2}{4\alpha})$ versus bulk density at the various frequencies were also plotted to estimate the loss factor of the solid materials. This approach was adopted by Nelson S.O and You T.S (1989) to obtain a linear fit for the measured loss factor of pulverised materials over a range of bulk densities. The values of the constant $\frac{\delta^2}{4\alpha}$ (represented as 'e' on the curves for clarity), which is a function of the material under study, were obtained from the second order polynomial curves of loss factor versus bulk density. As expressed in Equation 4-14, these were calculated at all frequencies for South African, Australian, Brazilian and Chinese samples. The calculated values of 'e' at 934 MHz and 2143 MHz for the South African sample are 0.019 and 0.038 respectively, while the calculated values at the same frequencies for Australian samples are 0.017 and 0.003 respectively. Similarly, the calculated values of 'e' for the Brazilian sample at 910 MHz and 2470 MHz are 0.003 and 0.002 respectively, while the calculated values of 'e' for the Chinese sample at 910 MHz and 2470 MHz are 0.81 and 0.09 respectively.

Figure A:3-21 and Figure A:3-22 present the plots of $(\varepsilon''+e)^{1/2}$ versus the bulk density for South African and Australian vermiculite samples respectively at 934 and 2143 MHz.

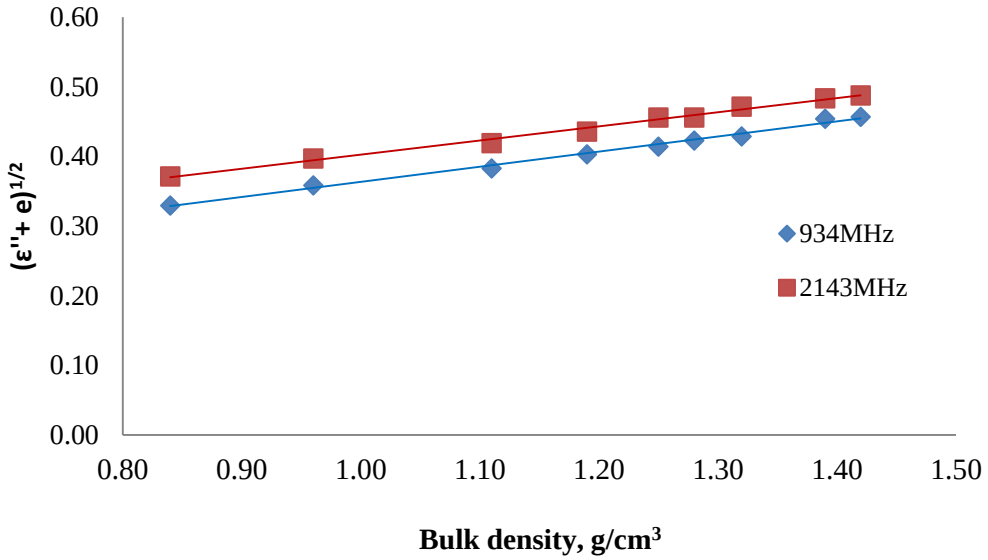

Figure A:3-21: Linear relationship between $(\varepsilon''+e)^{1/2}$ and density for South African sample

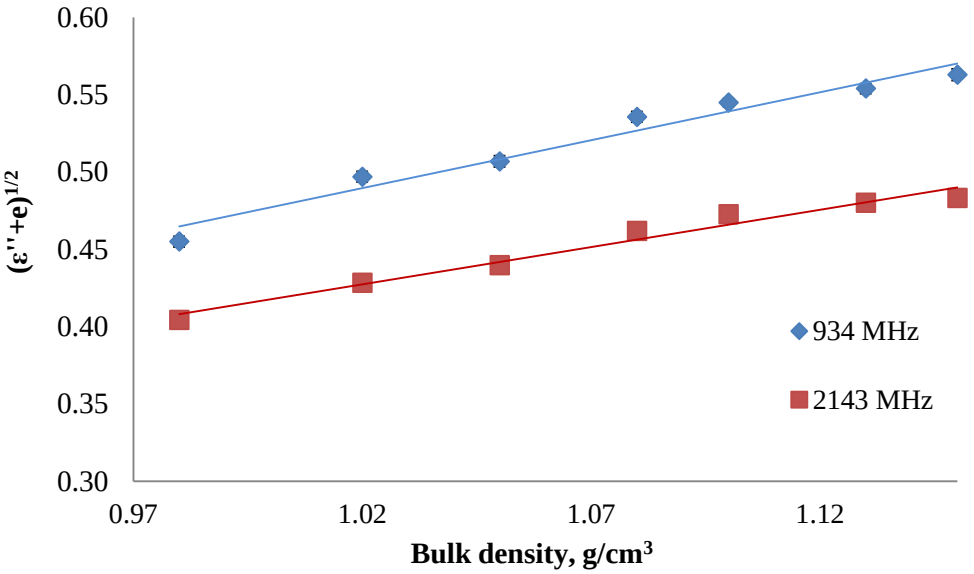

Figure A:3-22: Linear relationship between $(\varepsilon''+e)^{1/2}$ and density for Australian sample

The linear relationships of $(\varepsilon''+e)^{1/2}$ against the bulk density at 910 MHz and 2470 MHz for Brazilian and Chinese vermiculite samples are shown in Figure A:3-23 and Figure A:3-24 respectively.

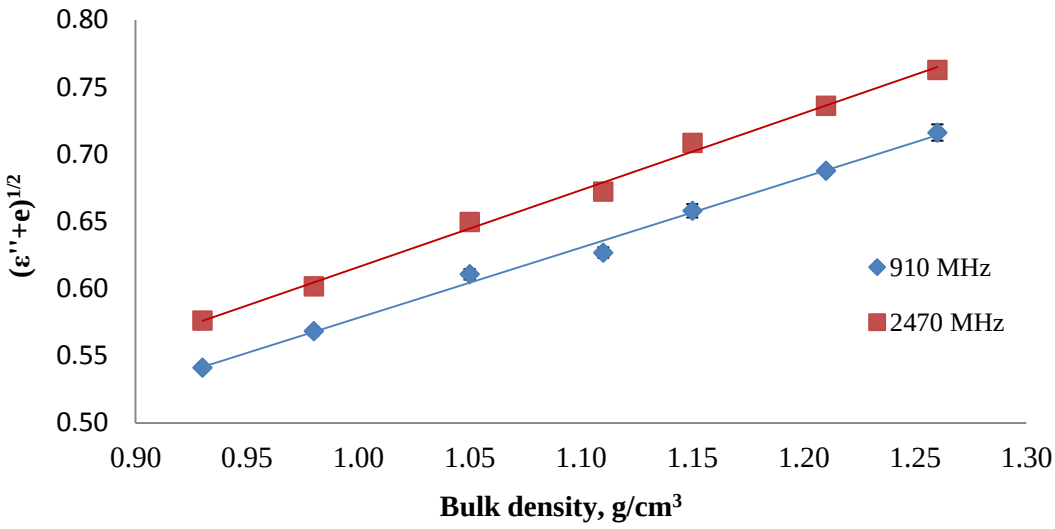

Figure A:3-23: Linear relationship between $(\varepsilon''+e)^{1/2}$ and density for Brazilian sample

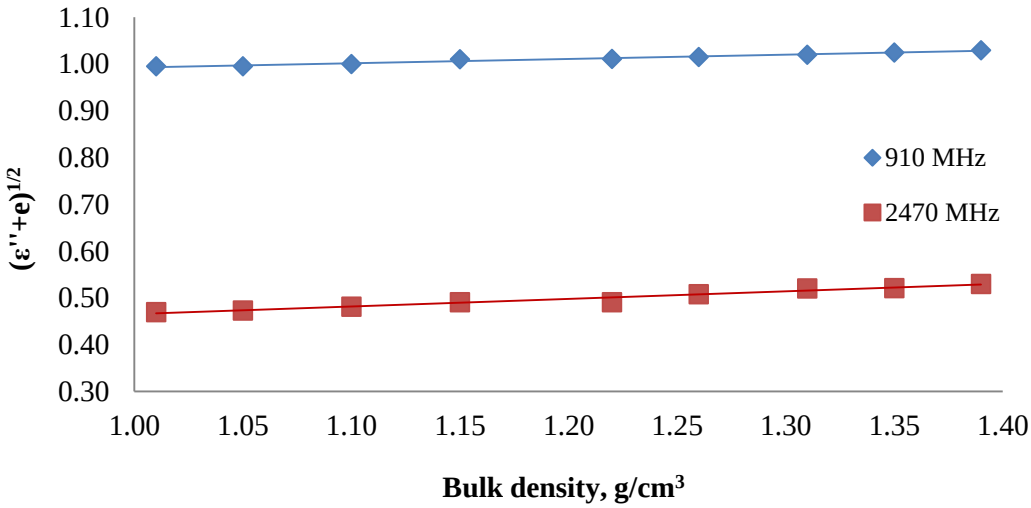

Figure A:3-24: *Linear relationship between* $(\varepsilon''+e)^{1/2}$ and density for Chinese sample

The regression equations of linear curves of Figure A:3-21 to Figure A:3-24 were used for extrapolating the loss factor of the solid forms of South African, Australian, Brazilian and Chinese samples respectively at their particle density.

A.3.2 Regression coefficients used for dielectric property estimation

Table A:3-1 and Table A:3-2 present the regression coefficients for the empirical equations that relate the dielectric constant of the pulverised form of the vermiculite samples to a range of measured bulk densities. The regression models presented are that of the regression coefficients of the second order polynomial and linear relations. These coefficients are consistent with Equation 4-13 and Equation 4-14 discussed earlier in section 4.6.2. They can be used for the estimation of dielectric constant at any density, and they were employed in

this work to estimate the dielectric constant of each vermiculite ore at their particle density, which is equivalent to the dielectric constant of the solid vermiculite material.

Table A:3-*1: Regression coefficient of empirical equations relating ε' of pulverised* vermiculite of South African and Australian samples to bulk density

Regression model	Constant	South African		Australian	
		934 MHz	2143 MHz	934 MHz	2143 MHz
$\varepsilon'=\partial\rho^2+\beta\rho+k$ (Figure 5-1and Figure 5-3 for South African and Australian samples respectively.)	∂ β K R^2	0.3675 0.9493 1.0785 0.9990	0.4301 0.7730 1.1654 0.9987	0.7966 0.5638 1.0112 0.9856	0.8494 0.4511 1.1210 0.9853
$(\varepsilon')^{1/2}=m\rho+k$ (Figure 5-9 and Figure 5-11 for South African and Australian samples respectively.)	m k R^2	0.5495 0.9986 0.9991	0.5418 0.9982 0.9986	0.5520 0.9966 0.9975	0.5348 0.9960 0.9966
$(\varepsilon')^{1/3}=m\rho+k$ Figure 5-10 and Figure 5-12 for South African and Australian samples respectively	m k R^2	0.3119 1.0260 0.9991	0.3081 1.0251 0.9988	0.3383 0.9985 0.9985	0.3285 0.9981 0.9971

Table A:3-2: Regression coefficient of *empirical equations relating ε' of pulverised* vermiculite of Brazilian and Chinese samples to bulk density

Regression model	Constant	Brazilian		Chinese	
		910 MHz	2470 MHz	910 MHz	2470 MHz
$\varepsilon'=\partial\rho^2+\beta\rho+k$ (Figure 5-5 and Figure 5-7 for Brazilian and Chinese samples respectively.)	∂ β K R^2	1.1203 2.3236 1.1200 0.9837	1.4371 1.5862 1.2110 0.9809	1.3692 0.6349 2.6640 0.9928	0.7618 0.3231 1.8979 0.9931
$(\varepsilon')^{1/2}=m\rho+k$ (Figure 5-13 and Figure 5-15 for Brazilian and Chinese samples respectively.)	m k R^2	1.1035 1.0020 0.9987	1.0270 0.9917 0.9974	0.7956 1.0151 0.9967	0.6887 1.0127 0.9969
$(\varepsilon')^{1/3}=m\rho+k$ (Figure 5-14 and Figure 5-16 for Brazilian and Chinese samples respectively.)	m k R^2	0.6294 1.0061 0.9977	0.5895 1.0001 0.9985	0.4644 1.0130 0.9936	0.4078 1.0109 0.9941

The regression coefficients for the empirical equations that relate the loss factor of the pulverised vermiculite samples to the bulk density are illustrated in Table A:3-3 for South African and Australian sample and Table A:3-4 for the Brazilian and Chinese samples. They were applied to estimate the loss factor of the solid form of the measured vermiculite samples. This was carried out by extrapolating the loss factor at the measured particle density of these samples. A Helium pycnometer, which gives a precise measure of true density, was used to determine the particle density of all the vermiculite samples.

Table A:3-*3: Regression coefficient of empirical equations relating ε'' of pulverised vermiculite of* South African and Australian samples to bulk density

Regression model	Constant	South African		Australian	
		910MHz	2470MHz	910MHz	2470MHz
$\varepsilon''=\alpha\rho^2+\delta\rho+k$ (Figure 5-2 and Figure 5-4 for South African and Australian samples respectively)	∂ β K R^2	0.1288 0.1185 0.1010 0.9916	0.1008 0.0533 0.0751 0.9919	0.3704 0.1587 0.1100 0.9623	0.2274 0.0559 0.1201 0.9700
$(\varepsilon'')^{1/2}=m\rho+k$ (Figure 5-17 and Figure 18 for South African and Australian samples respectively)	m k R^2	0.2317 0.1047 0.9931	0.2282 0.1236 0.9925	0.6415 0.1825 0.9616	0.4874 0.0738 0.9724
$(\varepsilon''+e)^{1/2}=(\delta)^{1/2}+(e)^{1/2}$ (Figure 5-21 and Figure 5-22 for South African and Australian samples respectively)	m k R^2	0.2170 0.1463 0.9924	0.2031 0.1993 0.9916	0.6202 0.1430 0.9623	0.4832 0.0655 0.9725

Table A:3-4: Regression *coefficient of empirical equations relating ε'' of pulverised vermiculite of* Brazilian and Chinese samples to bulk density

Regression model	Constant	Brazilian		Chinese	
		910MHz	2470MHz	910MHz	2470MHz
$\varepsilon''=\alpha\rho^2+\delta\rho+k$ (Figure 5-6 and Figure 5-8 for Brazilian and Chinese samples respectively.)	∂ β K R^2	0.3725 0.1587 0.1174 0.9949	0.2155 0.2946 0.1321 0.9956	0.0814 0.0095 0.1045 0.9770	0.1576 0.2167 0.1878 0.9711
$(\varepsilon'')^{1/2}=m\rho+ k$ (Figure 5-19 and Figure 5-20 for Brazilian and Chinese samples respectively.)	m k R^2	0.5243 0.0515 0.9947	0.5738 0.0406 0.9956	0.2021 0.2168 0.9755	0.2031 0.1520 0.9658
$(\varepsilon''+e)^{1/2}=(\delta)^{1/2}+(e)^{1/2}$ (Figure 2-23 and Figure 5-24 for Brazilian and Chinese samples respectively.)	M k R^2	0.5223 0.0561 0.9947	0.5728 0.0436 0.9956	0.0918 0.9007 0.9753	0.1616 0.3039 0.9643

Using the regression models in Table A:3-1 to Table A:3-4, both dielectric constant and loss factor of the solid vermiculite materials were estimated.

Appendix 4

Design of Chokes for Pilot and Larger Scale-up Systems

Design of microwave chokes for the pilot scale system

It is obvious that the apertures at both the input and outs ends of the applicator are the primary sources of microwave emission from the industrial microwave system (Meredith, 1998, Mehdizadeh, 2010, Metaxas and Meredith, 1983, Catalá-Civera et al., 2006). The magnitude of the leakage microwave emission to the surrounding depends on the size of the aperture, and this emitted microwave energy always poses risk to the environment in two ways (Meredith, 1998). The first is the occupational health and safety (OHS) issue on the people in close vicinity, as human body is a good microwave receptor. Interference and disturbance of electronics and communication instruments is the second issue associated to the leakaged microwave energy (Catalá-Civera et al., 2006). The accepted levels for emitted microwave energy are below 10 mW/cm^2 and 5 mW/cm^2 at 2450MHz and 896MHz respectively over an exposure time of 6 minutes (ICNIRP, 1998, NRPB, 2003, NRPB, 1993, BSI, 2011), both measured at a distance of 5 cm from the equipment. In the United Kingdom the National Radiological Protection Board (NRPB) set the specific energy-absorption rate (SAR), which is associated to maximum human body absorption as 0.4 W/kg for both 2450 MHz and 896 MHz (NRPB, 2003, NRPB, 2004). Consequently, operating the continuous microwave system below the emission limit is paramount to this work as there is presence of apertures that are potential route for microwave emission, at both ends of the system. Metaxas and Meredith (1983) suggested that the microwave emission via the apertures may be reduced by restricting the aperture size to less than that of the cut-off waveguide at the operating frequency or restricting the aperture to a rectangle with dimension less than a half wavelength. This latter suggestion would limit the microwave leakage to one plane of polarisation. They also recommended the use of a choking system, which can either absorb the escaping microwave energy or reflected it back into the applicator.

The choke tunnels, which are specialised equipment for controlling and attenuating the microwave energy leakage to acceptable levels are designed and employed in this project. They can be placed into one of two categories: resistive and reflective chokes, based on their method of attenuating the escaping

microwave energy (Metaxas and Meredith, 1983, Mehdizadeh, 2010). The reflective choke, which is also known as the reactive chokes acts as a bandstop microwave filters by introducing a high values of impedance (essentially resistance) at certain frequencies. It creates a high reflection coefficient by using a passive lossless reflector and therefore restricts the propagation of microwaves out of the applicator. Generally, they consist of rectangular corrugated sections made of high conductive metallic materials and their operational characteristics are related to the dimensions and the spacing between the corrugations. Their performance is very sensitive to changes in the dielectric properties of the material under treatment (Mehdizadeh, 2010) and generally do not have broadband response (i.e. perform well within narrow frequency ranges but do not work outside them). Therefore, a great care must be taken when designing this type of choke to allow for the change of dielectric properties of the workload. Due to these limitations on their behaviour, it is important to have several units of these type of chokes connected in series when designing a continuous microwave system. In addition, a resistive, which reduces the emission of microwave energy through the aperture by absorbing the escaping microwave energy, must be combined with the reflective choke in order to maximize the chokes performances.

Resistive chokes utilize highly microwave absorbent materials (lossy materials) such as lossy ferrite and carbon blended with low-permittivity foam i.e. polyurethane. In contrast to reflective chokes their response is broadband and they work across a very wide frequency range (Mehdizadeh, 2010). Their attenuation characteristics are very good and not sensitive to the properties of the processed material. However, they do have the tendency to heat up with high power microwave energy and its attenuation performance decreases as the apertures increased (Meredith, 1998). Therefore, they are used in conjunction with reflective chokes. The reflective chokes are usually positioned close to the applicator and the resistive chokes are normally placed after them (Mehdizadeh, 2010, Metaxas and Meredith, 1983, Meredith, 1998).

A combination of reflective and resistive chokes system designed by the electromagnetism experts in the National Centre for Industrial Microwave Processing (NCIMP) using Concerto software (Concerto, 2006) was used in this

project to attenuate the escaping microwave energy below the emission level stipulated by the National Radiological Protection Board (NRPB) (BSI, 2011). Special care was taken in the design of the choke tunnel with respect to the selection of their dimensions in order to ensure that vermiculite can be conveyed continuously in and out of the applicator via the conveyor belt without any obstruction. Figure A-1 shows the designed chokes with the reflective choke positioned close to the applicator followed by the resistive choke.

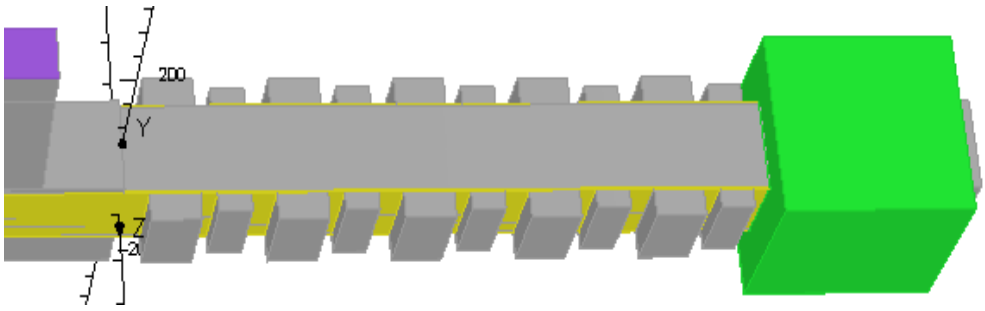

Figure A-1: Detail of the choke used in the current study. The corrugated reflective choke is connected nearest to the applicator followed by the resistive choke (green colour). Note the author of this thesis did not design this

Figure A-2 shows the frequency dependence of the performance of the reflective section of the choke between 2.4GHz to 2.5GHz. The frequency range covers the desired frequency of 2.45GHz. The value of complex permittivity of the material used to generate this data was taken as $\varepsilon^*=5-j1$ (dielectric constant: 5 and loss factor: 1). The complex permittivity used for the simulation was deliberately chosen to be higher than the actual permittivity of vermiculite (dielectric constant of 2.87 and loss factor of 0.18) in order accommodates the extreme condition and to verify the stability of the choke to detuning parameters such as, the presence of high permittivity phases within the sample. It is evident from A-2 that the performance of the reflective choke varies with the operating frequency. In an empty applicator at 2.45GHz, the attenuation is higher than -60db but the value decreases as the load is introduced.

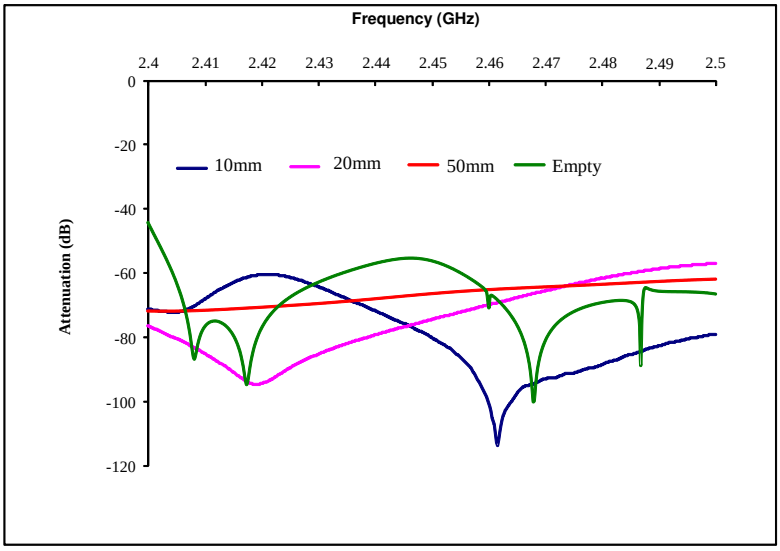

Figure A-2: Attenuation characteristics versus frequency of the reflective choke, used in the present study. The plot shows the results generated during the design phase of the reflective choke both empty and filled with a material of complex permittivity *=5-j1 at different bed heights.

It is also observed that the choke performance reduced for an increasing bed height of the material from 10mmm to 50 mm. However, even at the worst case for the vermiculite bed depth of 50mm, the attenuation introduced by the reflective choke alone is less than -60 dB at 2.45 GHz. The total attenuation achieved by the combination of the reflective and the resistive chokes is expected to be about -80db as the resistive choke produces an attenuation of about -20db. A total attenuation of -80 dB corresponds to a microwave leakage of 0.3 mW (Calculation procedure given in the appendix). This for an aperture of 100 cm^2 corresponds to a radiated value of 0.003 mW/cm^2, which is well below the recommended limit of $10mW/cm^2$. To ensure compliance with safety standards each choke structure was tested and the design models validated prior to use. In each case, the simulations were found to be accurate.

Design of choke for electromagnetic compatibility and safety for the scale up system

As discussed earlier in section in last section, during continuous processing of materials with microwave energy at large scale, the applicator incorporates large apertures, which may cause microwave energy to escape to the environment. The potential hazards from the escaping microwave energy (microwave energy

leakage) from the applicator or from both tunnel open end can be categorised into two groups. The first form of hazard, which falls within the health and safety regime, relates to the direct hazard to the personnel and the people in the immediate environment. The other form of hazard, termed electromagnetic compatibility (EMC) relates to interference of microwave energy which has the potential to cause electromagnetic disturbances of radio and telecommunications, or the malfunctioning of electronic components and equipment (Claytron, 2006). The accepted levels for microwave energy leakage are below 10 mW/cm^2 and 5 mW/cm^2 at 2450MHz and 896MHz respectively over an exposure time of 6 minutes, both measured at a distance of 5 cm from the equipment (NRPB, 2003, Meredith, 1998, BSI, 2011). The EMC standard requirements are stricter than the above limits and vary between different continents and often countries. For example in Europe, the accepted level of microwave energy emissions in the L-band within which the equipment discussed in this work operates is 40 dB (µV/m), measured at 30m from the external walls of the building where the equipment is located (CISPR, 1990, Meredith, 1998, BSI, 2011). Such a requirement demands a total emitted power of 0.3µW (Meredith, 1998), and this equates to about 117 dB for an input power of 100 kW from the microwave generator. Reducing microwave leakage to acceptable level requires the incorporation of several different types of microwave filters and attenuators collectively termed "chokes". Chokes often incorporate a resistive and reflective sections (Meredith, 1998).

The numerical analysis of the chokes system is based on the Finite difference time domain (FDTD) numerical technique (Taflove et al., 2005) from frequency range 800MHz to 1000MHz. A commercial package CONCERTO® supplied by COBHAM was used (Cobham, 2012) for the chokes simulations. In order to implement the FDTD method, a model of designed chokes were created as shown in Figure B-1 and the properties of all the materials together with the boundary conditions are specified. Maxwell's equations were solved for each individual section and the variation with time of the electric and magnetic components of the microwave field are computed.

Figure B-1: Detail of the choke used for the scale up system. The resistive choke is in red colour and is situated at both feed and the discharged ends while the reflective chokes are connected close to the applicator

The choke was simulated in three different steps. Initially, it was simulated when empty, then when it contains only the conveyor belt. Lastly, it was simulated when the vermiculite was loaded on the conveyor belt placed in the choke. This is a representative of the typical process conditions. For the purposes of the simulations the dielectric properties of the belt were taken as $\varepsilon^*=2.68-j0.2$ (dielectric constant: 2.68 and loss factor 0.2), the dielectric properties of the absorbent load within the resistive chokes were taken as $\varepsilon^*=1.5-j1.5$ (dielectric constant:1.5 and loss factor 1.5). The dielectric constant of vermiculite is 2.87 while the loss factor is 0.18.

The designed chokes were connected to the Agilent Network Analyser by means of coax-waveguide transition. The objective of this is to measure the Scattering parameter (S-parameter) within the tested frequency of 800MHz to 1000MHz. Scattering parameters are mathematical matrix used to describe and estimates the propagation of high frequency RF and microwave energy through a multi-port network. For example, in a 2-ports network, S_{11} and S_{22} refer to the input reflection and output reflection coefficient respectively. S_{21} and S_{12} are transmission coefficient and reverse transmission coefficient respectively (Carvalho and Schreurs, 2013). More details and derivation of the two ports network can be found in RF and microwave literature (Carvalho and Schreurs, 2013, Steer, 2010, Pozar, 2012). Since the entire choke structure is effectively a two-port system, the scattering parameter S_{21} (transmission coefficient) can be linked directly to the attenuation level that the choke is producing and thus its performance characteristics. The S_{21} parameter is expressed in dB, therefore a value of -140 dB means that the choke attenuates by 10^{14} times. A negative value of S21 parameter implies that there is a reduction or attenuation of transmitted wave.

The results of the scattering parameters in dB obtained from the simulation of the chokes when operated empty (no belt and no vermiculite), contains conveyor belt only and when loaded with vermiculite sample (bed depth 5mm) are shown in Figure B-2. The results present the S_{21} parameter from 800MHz to 1000MHz.

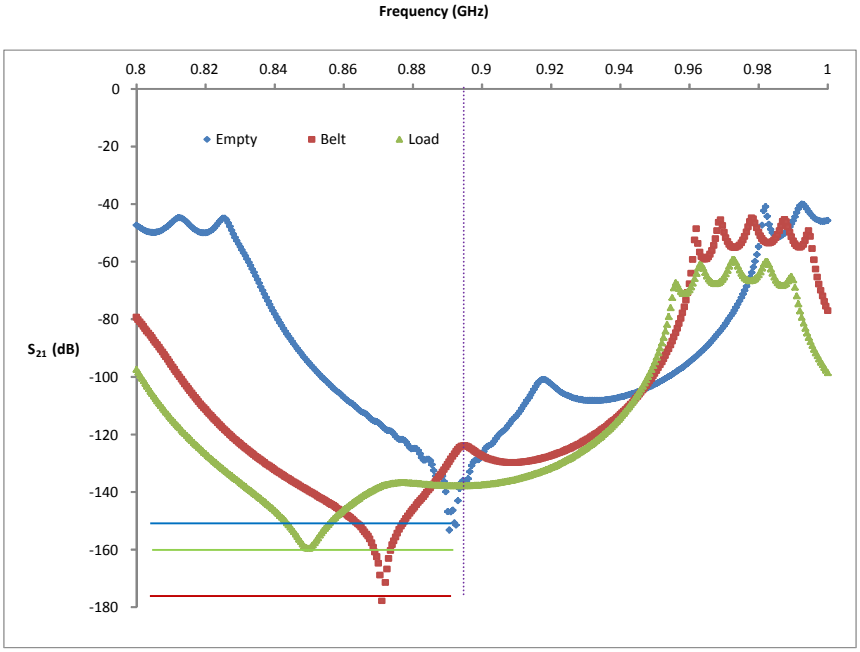

Figure B-2: S_{21} scattering parameters of the choke versus frequency for the three different types of possible operation, totally empty, with belt but unloaded and loaded with a 5mm deep bed of vermiculite.

The values for S_{21} at the frequency of 896 MHz, which is the operating frequency of the microwave generator and the scale up system range from almost -120 dB for the choke loaded with vermiculite to approximately -150 dB for the empty case. For an input power of 100 kW these attenuation values will result to an expected emitted power ranging from 0.0001 μW to 0.1 μW which is below the maximum limit of 0.3 μW set by the legislation.